cidepint

ISSN - 0325 - 4186

CENTRO DE INVESTIGACION Y DESARROLLO
EN TECNOLOGIA DE PINTURAS
CIC - CONICET

ANALES 1994

El Centro de Investigación y Desarrollo en Tecnología de Pinturas es patrocinado actualmente por la Comisión de Investigaciones Científicas de la Provincia de Buenos Aires (CIC) y por el Consejo Nacional de Investigaciones Científicas y Técnicas (CONICET).

Los objetivos fundamentales de su creación fueron los siguientes: obtener nuevos desarrollos tecnológicos relativos a pinturas y revestimientos protectores, particularmente en aquellos aspectos que puedan resultar de mayor interés desde el punto de vista nacional; formar y perfeccionar investigadores y técnicos; y, finalmente, asesorar y prestar asistencia técnica a entidades estatales y privadas, realizar peritajes y efectuar estudios especiales y tareas de control de calidad en los temas de su especialidad.

Desarrolla sus actividades en las siguientes áreas de investigación: estudios electroquímicos aplicados a problemas de corrosión y anticorrosión; análisis electroquímico; propiedades fisicoquímicas de películas de pintura; propiedades protectora de películas de pintura; planta piloto; análisis orgánico; química analítica general, cromatografía e inscrustaciones biológicas.

Durante los últimos treinta años los trabajos realizados se han publicado en diferentes revistas nacionales e internacionales: Anales de la Asociación Química Argentina, Revista de Ingeniería, Revista Latinoamericana de Ingeniería Química y Química Aplicada y Revista del Museo de Ciencias Naturales Bernardino Rivadavia (Argentina); Revista Iberoamericana de Corrosión y Protección (España); Journal of Coatings Technology, Industrial Engineering Chemistry Research, Journal of Solution Chemistry, Journal of Chromatography, Journal of Chromatographic Science, Journal of Colloid and Interface Science y Journal of Physical Chemistry (EE.UU.); Marine Biology, European Coatings Journal (Alemania Occidental); Journal of the Oil and Colour Chemists' Association y Journal of Chemical Technology and Biotechnology (Gran Bretaña); Progress in Organic Coatings (Suiza); Pitture e Vernice (Italia); Revista de la Sociedad Química de México (México); Peintures, Pigments, Vernis y Corrosion-Marine Fouling (Francia).

Otros trabajos han aparecido en Anales y Proccedings de diferentes Congresos Internacionales: Seminario Nacional de Corrosão (Brasil); Protection of Materials in the Sea (India); ACS Organic Coatings and Applied Polymer Science (EE.UU.); Congress on Metallic Corrosion (Brasil, Alemania Occidental, Canadá, India, Italia); Congress on Marine Corrosion and Fouling (Francia, EE.UU., Grecia, España); Congreso Nacional de Corrosión y Protección (España); etc.

CIDEPINT agradece expresamente el apoyo económico que los organismos promotores (Comisión de Investigaciones Científicas de la Provincia de Buenos Aires y Consejo Nacional de Investigaciones Científicas y Técnicas) prestaron para la realización de los trabajos que constituyen el presente volumen.

Editor: CENTRO DE INVESTIGACION Y DESARROLLO EN TECNOLOGIA DE PINTURAS

Dirección: 52 entre 121 y 122
1900 La Plata - Argentina
Teléfonos: (021) 31141/44 y (021) 216214
Fax: 54-21-271537

CIDEPINT-Anales es indizado periódicamente en:

Aquatic Sciences and Fisheries Abstracts (México)
Centre de Documentation CNRS (Francia)
Chemical Abstracts (EE.UU.)
Referativnyi Zhurnal (Rusia)
World Surface Coatings Abstracts (Gran Bretaña)

Diagramación: Prof. Viviana M. Segura

COMITE DE REPRESENTANTES

Comisión de Investigaciones Científicas
de la Provincia de Buenos Aires
(CIC)

Ing. Carlos Mayer (Titular)
Ing. Carlos Gigola (Alterno)

Consejo Nacional de Investigaciones
Científicas y Técnicas
(CONICET)

Dra. Noemí Walsöe de Reca (Titular)
Dr. José María Carella (Alterno)

DIRECTOR

Dr. Vicente J.D. Rascio

SUBDIRECTOR

Ing. Quím. Alejandro R. Di Sarli

JEFES DE AREAS

Ing. Quím. Ricardo A. Armas
a/c Propiedades Fisicoquímicas de Películas de Pintura

Ing. Quím. Juan J. Caprari
Propiedades Protectoras de Películas de Pintura

Dr. Ing. Carlos A. Giúdice
Estudios en Planta Piloto

Dr. Vicente F. Vetere
Estudios Electroquímicos Aplicados a Problemas
de Corrosión y Anticorrosión

Ing. Quím. Alejandro R. Di Sarli
Análisis Electroquímico de Pinturas y Revestimientos

Dr. Javier I. Amalvy
Materiales Poliméricos

Dr. Reynaldo C. Castells
Cromatografía

Tco. Quím. Rodolfo R. Iasi
Absorción Atómica

Ing. Quím. Silvia Zicarelli
Espectrofotometría

Lic. Mirta E. Stupak
Incrustaciones Biológicas

COMENTARIOS DE LA DIRECCION DEL CIDEPINT

La industria de la pintura se encuentra frente al desafío de reducir o eliminar de las formulaciones los componentes orgánicos volátiles (VOC), lo que puede lograrse incrementando la producción de pinturas con alto contenido de sólidos, de pinturas en polvo, de emulsiones diluibles con agua o de pinturas convencionales formuladas con disolventes poco agresivos (p. ej. nuevos productos considerados de baja toxicidad y, en consecuencia, de menor impacto ambiental, tales como ésteres dimetílicos de ácidos orgánicos). Además, algunos pigmentos considerados tóxicos deberán ser reemplazados por otros no objetables desde el punto de vista ecológico.

En EE.UU. y en los restantes países desarrollados, se han implementado Comisiones Técnicas con incumbencia nacional o estatal que establecen regulaciones estrictas de protección ambiental, referidas no sólo a la formulación y aplicación de las pinturas sino también a las operaciones de mantenimiento, donde la preparación por chorreado con abrasivos produce polvos conteniendo no sólo partículas silíceas o metálicas sino también compuestos de plomo, cromo etc. En consecuencia, tanto el sector industrial como los institutos de investigación deberán estar en condiciones de adelantarse al cambio.

Hasta el presente, alrededor del 75 % de los productos que se comercializan han estado constituidos por sistemas clásicos de base solvente. El restante 25 % corresponde fundamentalmente a sistemas acuosos y un muy pequeño porcentaje a productos de alto contenido de sólidos o a pinturas en polvo.

Con vistas a este futuro, dentro de los proyectos del CIDEPINT se ha incluido uno relacionado con pinturas emulsionadas que comprende la síntesis de látices, la cinética y caracterización de la emulsión y, finalmente, su utilización en la formulación de pinturas de alta resistencia. Se estudiará también exhaustivamente el problema desde el punto de vista microbiológico, tanto en el producto envasado como en la película, y se investigará sobre los biocidas más adecuados para lograr la preservación de este tipo de materiales.

En este tomo se incluye, además, una revisión bibliográfica sobre las características de pinturas en polvo y un sistema de cálculo para el diseño de un lecho fluidizado convencional.

También dentro de los proyectos vinculados con aspectos ecológicos, se está tratando de implementar uno dentro del Programa de Cooperación Científica con Iberoamérica 1994-95, cuyo título es "Fisicoquímica de la extracción de impurezas de bajo peso molecular desde poli(acetato de vinilo) utilizando fluidos supercríticos". Sería realizado en forma conjunta entre la Universidad Complutense

de Madrid, la Universidad Nacional de La Plata e investigadores del CIDEPINT. Es un tema relacionado con la residencia de monómeros residuales en películas poliméricas, de su lenta eliminación a la atmósfera circundante y a las características cancerígenas comprobadas o sospechadas en muchos de ellos.

Otros aspectos considerados en los trabajos del presente volumen corresponden a estudios sobre pinturas anticorrosivas y antiincrustantes, incrustaciones biológicas, aplicación de métodos electroquímicos no destructivos para cuantificar la evolución de propiedades tales como permeabilidad al agua, al oxígeno y a los iones en películas de pintura y su influencia sobre los mecanismos y la cinética de las reacciones de corrosión que ocurren en las complejas interfases metal pintado/medio acuoso.

Asimismo, se trabaja en el desarrollo de métodos cromatográficos para determinar propiedades de mezclas líquidas adsorbentes y de métodos analíticos espectrométricos (IR, visible, UV, absorción atómica) para la identificación de materiales poliméricos, pigmentos y disolventes.

Las actividades del CIDEPINT en el período han incluido también la participación en otros proyectos de cooperación científica con el exterior (España, Italia y Méjico) y la publicación de 22 trabajos de investigación en las revistas más prestigiosas relacionadas con corrosión y protección. Un número igual se encuentra en diferentes etapas del proceso de evaluación. Algunos de dichos trabajos fueron publicados también en los Anales del Centro.

En lo relativo a documentación y biblioteca se han efectuado tareas de procesamiento y análisis documental, incluyendo el diseño y formación de bases de datos bibliográficas sobre temas de la especialidad. Se han recibido en el año 21 publicaciones periódicas que cubren los aspectos más importantes en consideración a nivel mundial sobre pinturas, recubrimientos y problemas de corrosión y protección. Se cuenta con un sector que ejecuta tareas de apoyo informático, diseñando e implementando programas de computación destinados a permitir un adecuado manejo de la información por parte de las diferentes áreas de investigación del Centro.

Complementando las tareas de investigación y desarrollo expuestas precedentemente, se han efectuado numerosas acciones de asesoramiento y servicios técnicos a empresas privadas y organismos estatales, provinciales y nacionales.

Dr. Vicente J. D. Rascio
Director del CIDEPINT

INDICE

EVALUATION OF ELECTRICAL AND ELECTROCHEMICAL PARAMETERS FOR PAINTED STEEL/ARTIFICIAL SEA WATER SYSTEMS BY USING EIS

EVALUACION DE LOS PARAMETROS ELECTRICOS Y ELECTROQUIMICOS EN SISTEMAS ACERO PINTADO/AGUA DE MAR ARTIFICIAL UTILIZANDO EIS

V. Ambrosi* **and A. R. Di Sarli****

SUMMARY

The anticorrosive protective properties of metallic substrate/organic coating/electrolyte solution systems were evaluated using an electrochemical impedance technique based on equivalent circuits previously developed. It was emphasized that the classical semi-circumference in the complex plot, which describes the response of a parallel resistive-capacitive circuit, is not real axis centered. This fact makes necessary to consider the organic film and electrochemical double layer capacitance as pseudo-capacitances which depend on a fractional power of the frequency.

Detailed information about the charge transfer resistance, ionic resistance and dielectric capacitance variation at increasing immersion times for naval steel/chlorinated rubber (with different PVC)/artificial sea water systems were analyzed. Parameters thus obtained correlate well with the naval steel/organic coating deterioration with time, also determinated by using corrosion potential measurements and visual assessment.

Keywords: *impedance spectroscopy, coated metal, equivalent circuits, ionic resistance, dielectric capacitance, charge transfer resistance, coating characterization.*

INTRODUCTION

Organic coatings play an important role as anticorrosive agents, establishing not only a **barrier effect** towards the species that may attack the metallic substrate but also the **binder regulates the anticorrosive pigments action**. Nevertheless, as the exposition time increases and as consequence of both degradation and aging effects, the protective properties of these coatings change, specially in the case of submerged structures, buried or exposed to conditions of high atmospheric aggressiveness. It is just in these cases where the continuous film/medium contact favors the water, oxygen and ionic species diffusion towards the metal/coating interface given place to physical, chemical and/or electrochemical interactions which limit the useful lifetime of organic coatings, particularly when the formulation or the painting scheme chosen is not the appropriate one.

---

* Profesional Adjunto de la CIC

** Investigador Independiente de la CIC

Impedance measurements, which consist in the application of a low amplitude alternating electrical signal to system under study, are essentially a transitory or pseudo stationary technique that affords important information without the system need not attained the steady state, requisite that must be fulfilled using methods based on direct current (DC), turning them longer time consuming.

It is important to remark that the DC tests were intensively used since they allow, at first instance, to obtain the kinetic parameters needed for the corrosion rate calculus.

Nevertheless, this technique presents important limitations which, in many cases, can invalidate its employment. Among these ones may be mentioned the difficulty or impossibility to reach the steady state during electrode polarization due to adsorption, passive films formation, diffusing processes or significant ohmic drop phenomena. Likewise, information drawn from potentiostatic or galvanostatic tests only identify the slower processes drawn by the circulating current. The potentiodynamic technique is also questionable because of doubts arising from the swept rate chosen in each case. It must be taken in mind that, electrochemical systems excited by an electrical signal behave similarly to a transmission line made up by passive elements (resistors, capacitors, inductors), whose response is a function of the electrical variation rate. As consequence, the determination of parameters used in corrosion rate calculus could be, in certain cases, rather arbitrary.

The AC tests do not have such a limitations. The supplied information allows that not only the structure of the passive elements network (associated to complex behaviour of metal/organic coating/electrolytic solution (MCE) interfaces) can be deduced but also to interpret their true physicochemical meaning. The more important limitation of this technique is the fact that the time constants of processes taking place in such interface be enough away among them as to avoid overlapping in the impedance spectrum.

The analysis of the impedance/frequency relationship in MCE systems allows to develop equivalent electrical circuits for explaining interfacial processes. Aqueous solutions employed for testing coated metals contain aggressive ions to simulate service conditions. These trials may be accelerated by increasing the ionic concentration and/or the temperature in order to obtain quicker information about both the parameters governing the corrosion processes of metallic specimens and/or the coatings degradation under different environmental conditions.

Measurements carried out on a wide frequency range can provide, at least theoretically, an analytical survey of interfacial processes such as chemical and electrochemical reactions of solvation, adsorption and/or desorption of reaction intermediates and products, natural or forced mass transport, etc. This is because of into an electrode excited with AC only are put into play processes capable to follow changes of the frequency dependent electrical field. By such reason, the most important requirement of this technique is that the time constants of these processes be sufficiently separated one to another as for determining the true physical meaning of each one of the parameters obtained.

A literature review reveals that from the concepts developed by Wolstenholme **[1]**, the assessing of organic coatings protective properties by electrochemical techniques exhibit a marked progress. Leidheiser **[2]** reported an extensive discussion about results obtained with electrical and electrochemical (dielectric capacitance, corrosion potential polarization curves) and mentioned the impedance spectra published by Menges and Schneider **[3]** for coated steels submerged in HNO_3 and by Kendig et al **[4]** for similar systems in HCl solutions. In these spectra, for increasing immersion times it is shown a noticeable increase in the dielectric

capacitance of the coating, development of pores and, in some cases, corrosion phenomena in the metal/polymer interface.

The analysis of papers published by several authors **[5-14]** shows that the majority of the impedance spectra can be interpreted through the general model of equivalent electric circuit of **Fig. 1** where R_s is the ohmic resistance of the solution; C_m is the dielectric capacitance and R_m the ionic resistance of the membrane; C_d, the electrochemical double layer capacitance in the metal/solution (at the base of pores or underneath the membrane); R_t, the charge transfer resistance of the faradaic process in the metal/solution interface and $Z\omega$ is the diffusion impedance (normally called Warburg impedance).

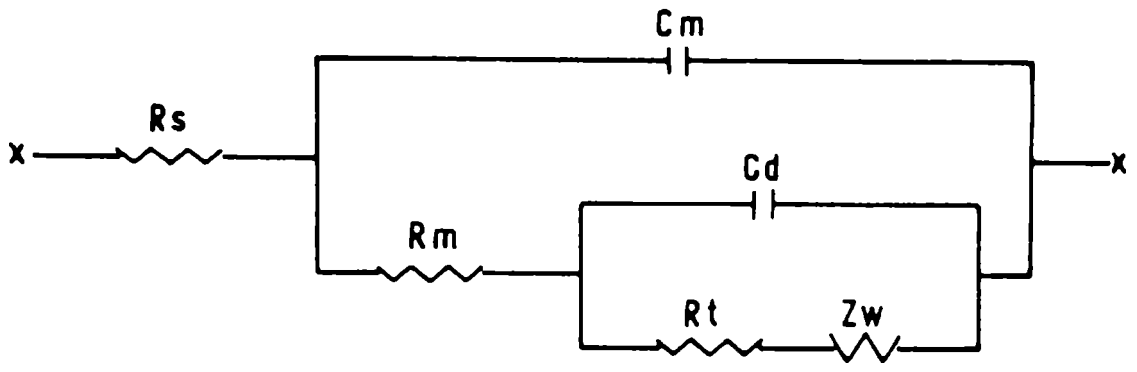

Fig. 1.- Simplified equivalent circuit for a metal/organic coating/electrolyte system

In order to know the value of parameters associated with each element of the model showed in **Fig. 1** it is necessary to measure the impedance within a range of frequencies from e.g. 10^{-3} up to 10^5 Hz. So, if a low frequency is applied, the overall resistance is $R_s + R_m + R_t + Rw$, where Rw is the fraction of diffusion resistance corresponding to such frequency. On the contrary, if the frequency is high enough as to neglect the impedance of C_m front to its parallel circuit, the total resistance will be R_s. Following the same reasoning it is possible to find the resistances $R_s + R_m$ and $R_s + R_m + R_t$ at certain intermediate frequencies, whenever the time constants R_mC_m and R_tC_d differ by a factor ≥ 10 **[15]**.

In determining C_m and C_d values by means of the mathematical model it is proved that both do not are constants but they depend on the applied signal frequency. Capacitance dispersion phenomena in bare electrodes has been considered by various authors **[16, 17]**. Scheider **[18]** attributed such conduct to the fact that heterogeneities at the electrode topography may cause current lines parallels to the electrode surface; therefore, he suggests to replace the capacitor by a ramified RC circuit (type transmission line). From similar studies on coated electrodes may be inferred that the above interpretation would also explain the C_m dispersion since in the membrane there are heterogeneities capable of bring forth current lines tangential to the surface **[19-21]**.

The aim of this paper was to use the AC method described elsewhere **[22]**, with a naval steel/organic coating/artificial sea water system in order to determine some parameters of interest to assess the system evolution with time.

EXPERIMENTAL

SAE 1020 steel plates (20x8x0.2 cm) were used as metallic substrate. The surface was sandblasted to Sa 2 1/2-3 (Swedish Standard SIS 05 59 00/67). The specimens were degreased with toluene and coated with the primers and topcoats whose characteristics and thicknesses are shown in **Table I.**

TABLE I

Composition (g/100 g) and thickness of the experimental paints*

Solid components	1	2	3	4	5
Micaceous iron oxide	41.50	53.50	45.90	59.30	50.00
Barytes	7.00	---	7.60	---	8.20
Micronized talc	3.50	---	3.80	---	4.10
Chlorinated rubber 20cP	33.60	32.70	29.90	28.50	26.40
Chlorinated paraffin 42 %	14.40	13.90	12.80	12.20	11.30
PVC	25.00	25.00	30.00	30.00	35.00
Thickness (μm)	40±5	40±5	40±5	40±5	40±5

* Solvent mixture: Solvesso 100/white spirit, 4/1 ratio by weight.
Castor oil content: 1.0 % by weight on paint.

A Bird applicator was used to apply the organic coatings. The desired film thicknesses were achieved by successive applications, with drying periods of 2 days between each coat. For avoiding contamination with atmospheric dust, the test plates were kept in desiccators at room temperature (20 ± 2 °C). Dry film thickness was measured with an electromagnetic gauge, using a bare sanded plate and standards of known thickness as reference.

On each plate two cylindrical tubes of transparent acrylic were fixed by using an epoxy adhesive in order to get good adhesion to the coated substrate. The geometrical area of each cell exposed for impedance measurements was 28 cm^2.

A large cylinder of graphite axially placed, was used as counter-electrode and a saturated calomel electrode (SCE) as reference. The electrolyte was prepared according to ASTM Standard D 1141-90 with pH 8.25. All the tests were performed at room temperature (20 ± 2° C). All impedance spectra in the frequency range $10^{-3} \leq f \leq 6.5 \times 10^4$ Hz were performed in the potentiostatic mode at the corrosion potential, as a function of the exposure time in the electrolyte solution, using the 1255 Solartron Frequency Analyzer and the 1186 Solartron Electrochemical Interface. Data processing was carried out with an Olivetti PC and a set of programs developed at CIDEPINT **[22]**.

RESULTS AND DISCUSSION

For each experiment carried out at a determined immersion time, a Nyquist diagram (Z_r vs Z_{im}) was done and eventually, for a clearer analysis, also the Bode diagram (log $|Z|$ vs log ω) and the phase diagram (Φ vs log ω). Then, data adjustment was done in the first lace of the complex diagram for finding R_s, R_m and C_m and the coefficient γ (ranging between 0.5 and 1). It takes into account the depression by which the semi-circumference centre is not on the real axes in the complex plane plot **[22]**) of the membrane. Later, the same must be repeated for the second lace in order to calculate R_t, C_d and/or Z_w parameters whenever the corrosion and/or diffusion processes have a significant contribution or be detectable in the experiment.

A way of verifying the accurecy of the adjustment is to plot together the experimental and simulated curves **(Fig. 2)**.

At the present work, sealers were formulated with high chemical inertia pigments because it was very important to obtain formulations with the lowest water permeability as to polarize the cathodic reaction in order to reducing

coating conductivity. The in-flowing water has two effects straight and negatively related with the protective behaviour of polymer films since it not only increases the ionization of polymeric polar groups, and consequently its conductivity, but also the strongly dielectric character of water can modify the intermolecular cohesion forces through its behaviour as plasticizer favoring diffusion processes according to a mechanism by which, initially, the electrolyte come into the membrane developing paths of different depth. In time, when electrolyte reaches the metal/paint interface it allows that corrosion cells can be activated with areas of attack coupled to cathodic regions depolarized by water and oxygen gathered.

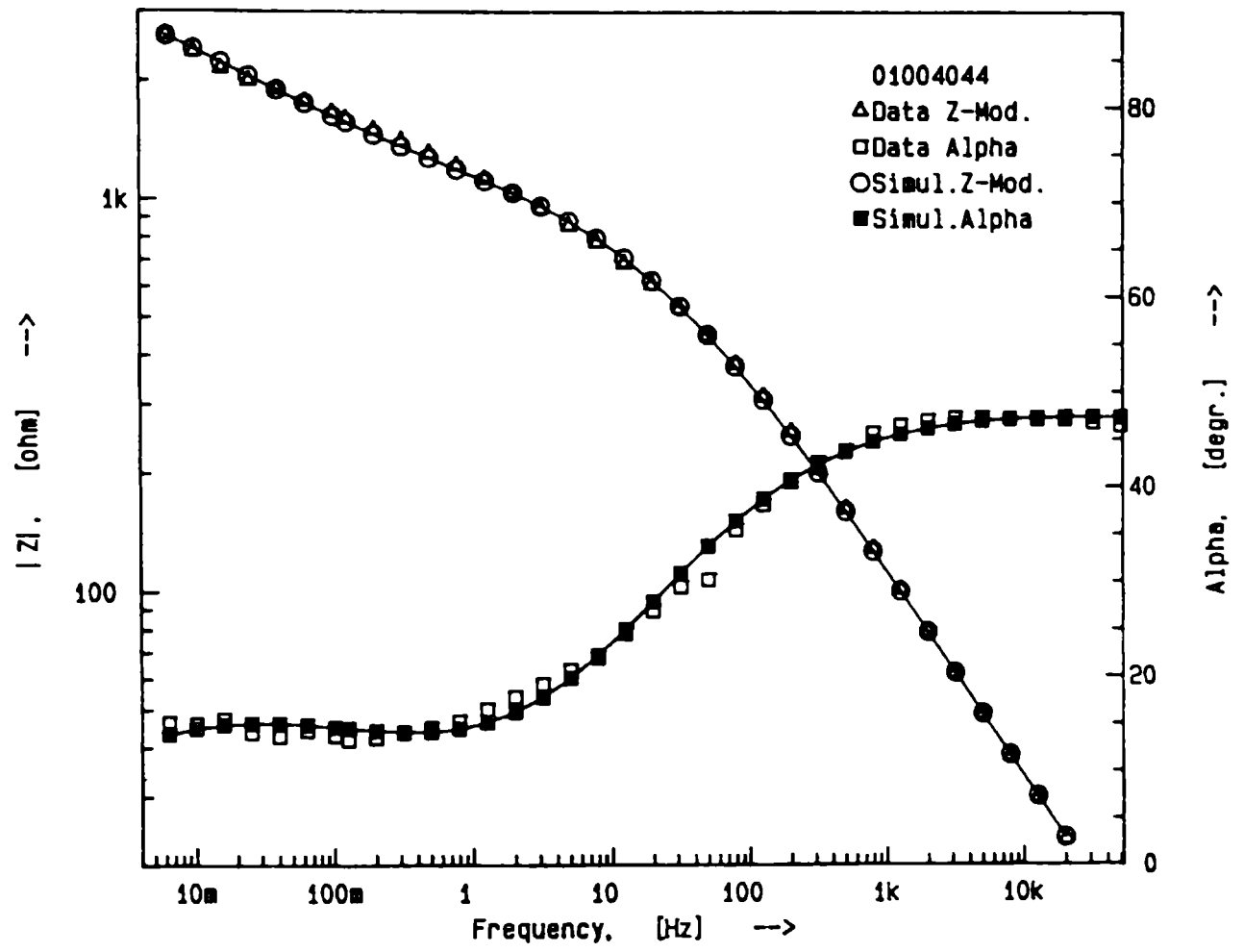

Fig. 2.- Bode diagram + simulated curve

In **Fig. 3-a,** corrosion potentials (E_{corr}) of samples 3 and 4 remain practically constant (between 0.0 and 0.1 V/SCE) during a long period after immersion; E_{corr} for sample 2 was similar to the above, except between 10 and 30 days in which it was approximately 0.15 V/SCE more active. Samples 1 and 5 show a fast displacement of the corrosion potential towards the anodic side from the beginning of immersion.

The plot in **Fig. 3-b** show the dependence of R_t with time for all the samples; in the case of samples type 2, 3 and 4 exhibit higher and more stable values of R_t (ranging between 10^6-10^4 Ωcm^2) than samples of type 1 and 5 (ranging between 10^6-10^2 Ωcm^2).

In addition to knowledge reached from the E_{corr} and R_t values, an important indication about the protective behaviour of coatings is the information given by both ionic resistance R_m (i.e, polymer conductivity) and dielectric capacitance C_m (i.e, the polymer capacity to isolate) changes as a function of immersion time.

The R_m **(Fig.4-a)** and C_m **(Fig.4-b**) evolution show that, although with different rates, the protective properties of all the paints suffered a continuous decrease until 20 days of immersion. Later on, R_m values for samples 2 and 4 tend

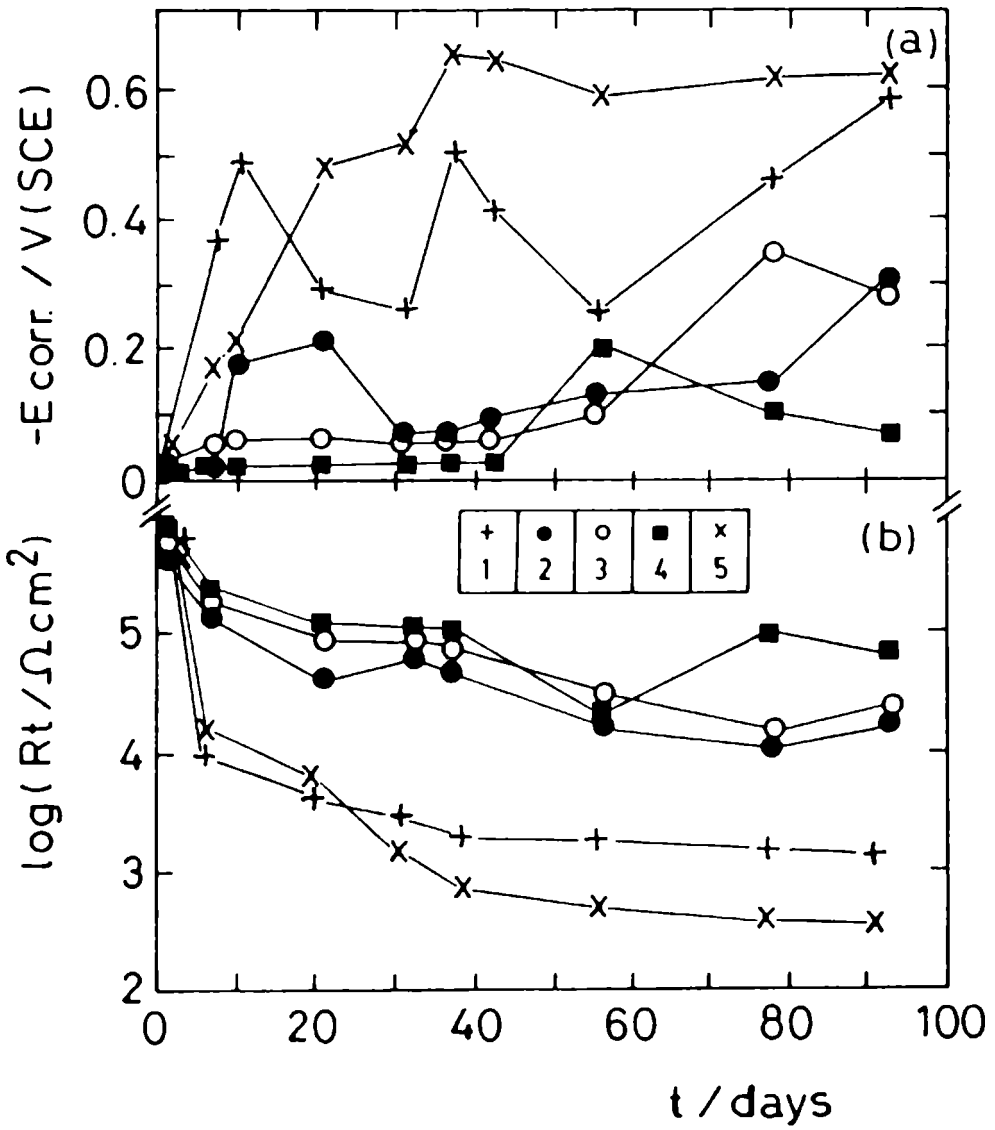

Fig. 3.- a) Corrosion potential (Ecorr) and b) logarithm of charge transfer resistance (Rt) vs immersion time (t) in artificial sea water.

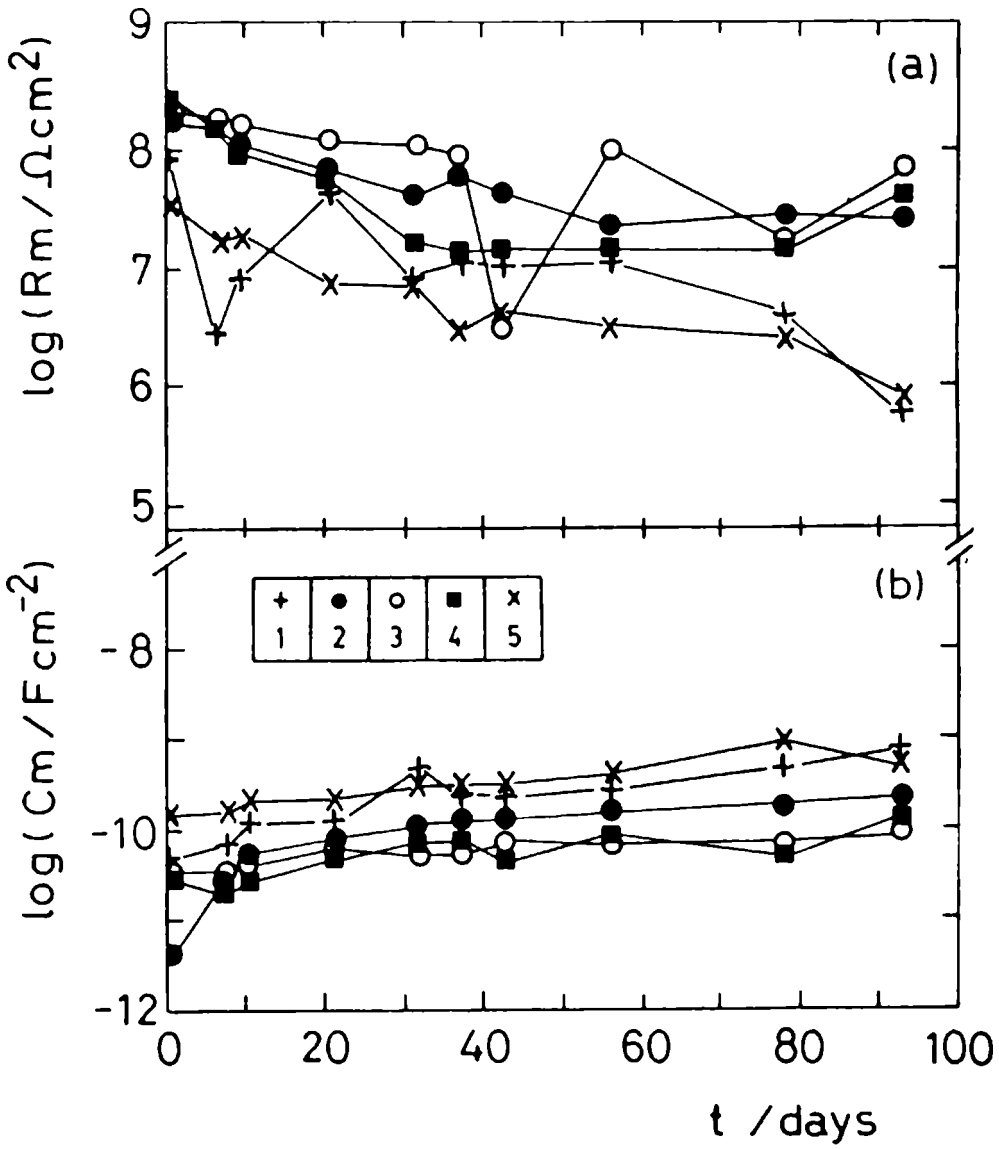

Fig. 4.- a) Logarithm of ionic resistance (Rm) and b) logarithm of dielectric capacitance (Cm) vs immersion time (t) in artificial sea water.

to stabilize at approximately $5x10^7$ and $9.5x10^6$ Ωcm^2, respectively. For sample 3, after 40 days of slow decrease, R_m values start to oscillate within one order of magnitude but remaining highly enough as to keep the protective capacity. On the contrary, from 85 days immersion samples 1 and 5 were considered as poorly protective due to their greater deterioration. Concerning the evolution of the dielectric capacitance C_m, the samples did not show significant variations with values ranging between $5x10^{-9}$ and $4x10^{-8}$ Fcm^{-2} along the whole testing period.

In **Fig. 3-a-b** , the corrosion potential (E_{corr}) and charge transfer resistance (R_t) displacements indicate that starting from more or less similar values, but with a particular kinetic for each coated substrate, all values displaced towards more active ones a short period after immersion in artificial sea water. This movement was almost continuous in samples 1 and 5, pointing out an increasing degree of corrosive activity on metal surface. Such a behaviour in sample 1 was attributed to the fact that micaceous iron oxide concentration could not be enough to reduce significantly the paint permeability, while the bad performance of sample 5 (PVC 35 %) was due to a higher porosity of the organic film since PVC of these samples type was slightly greater than CPVC value (33.9%); In both cases, therefore, a quick increase of metal/electrolyte contact area in the base of pores took place.

It is interesting to observe that in total agreement with this evolution, R_m **(Fig. 4-a)** and C_m **(Fig. 4-b)** describe the behaviour of poorly protective coatings since they showed values extremely low of resistance ($R_m < 10^6$ Ωcm^2) and high of capacitance ($C_m > 10^{-9}$ Fcm^{-2}) which are representative of high permeability to ions and water due to film porosity. Likewise, these agents are able to induce tensile stress in the coating because of gathering of corrosion products, increasing the number of defects and, as consequence, the polymer deterioration rate.

Fairly different behaviour was showed by samples 2, 3 and 4 due to both the magnitude and the relative stability attained by the corrosion potential ($E_{corr} > -0.3$ V/SCE), charge transfer resistance ($R_t \geq 10^4$ Ωcm^2), ionic resistance ($R_m \geq 10^7$ Ωcm^2) and dielectric capacitance ($C_m \leq 10^{-10}$ Fcm^{-2}) values prove that the concentration and size of pigment particles were enough to provide higher barrier effect. The high chemical inertia and low solubility of pigment and resin in the medium considered let to assume that under aggressiveness conditions like to those used in this study a similar or still better protective behaviour could be obtained and kept during longer periods if these paints were only a part of an anticorrosive scheme correctly specified.

In the same way, and particularly from the E_{corr} and R_t values arise that **paints 1 and 2 (PVC 25 %), 3 and 4 (PVC 30 %))** performed in accordance with that established by Bishop and Zobel **[23]** referring to replace part of micaceous iron oxide by inert fillers such as micronized talc and/or barytes, produce a decrease of barrier effect (and therefore of protective capacity) when sealers are used as only coating.

CONCLUSIONS

1.- The general model on which calculus for resistive (R) and capacitive (C) values are based showed to be sufficiently representative, although the unstable behaviour requires to use reference models which take into account dissipative effects which can not be ascribed to the parallel resistance. The coefficient γ has not a precise physical meaning but suggest the replacement of the capacitance by a ramified net (like a transmission line) of RC elements. Up to now, its utility is restricted to keep the primitive concept attributed to the RC parallel equivalent circuit.

2.- The results of electrochemical techniques used to assess the protective behaviour of chlorinated rubber with different pigment volume concentration correlate well with one another and with visual observations.

3.- For sealers based on chlorinated rubber pigmented with micaceous iron oxide a PVC of 30 % was the most adequate to obtain both a high barrier effect and anticorrosive effect.

4.- In replacing 20 % of micaceous iron oxide by barytes or micronized talc the protective capacity was reduced.

ACKNOWLEDGEMENTS

The authors would like to thank the Comisión de Investigaciones Científicas de la Provincia de Buenos Aires (CIC) and the Consejo Nacional de Investigaciones Científicas y Técnicas (CONICET) for financial support of this research.

REFERENCES

[1] Wolstenholme, J.- **Corros. Sci., 13:** 521-530 (1973).

[2] Leidheiser, H. Jr.- **Corrosion Control by Coatings.** Science Press, Princeton, 143 (1979).

[3] Menges, G., Schneider, W.- **Kunststofftechnik, 12:** 265, 316 (1973).

[4] Kendig, M.W., Leidheiser, H. Jr.- **J. Electrochem. Soc., 123:** 982-989 (1976).

[5] Macdonald, A.A., Mc Kubre, M.C.H.- **Electrochemical Impedance Techniques in Corrosion Science, Electrochemical Corrosion Testing.** ASTM STP 727, Florian Mansfeld & Ugo Bertocci Ed., American Soc. for Testing and Materials: 110-149 (1981).

[6] Beaunier, L., Epelboim, I., Lestrade, J.C., Takenouti, H.- **Surf. Techn., 4:** 237-254 (1976).

[7] Szauer, J.- **Progr. Org. Coatings, 10:** 171-183 (1982).

[8] Reinhardt, G., Scheller, O., Hahn, K.- **Plaste und Kautschuk, 22:** 56 (1975).

[9] Scantlebury, J.D., Ho, K.N.- **J. Oil Col. Chem. Assoc., 62:** 89-92 (1979).

[10] Scantlebury, J.D, Sussex, G.A.M.- **Corrosion, Control by Organic Coatings.** Ed. Leidheiser, H. Jr., NACE: 51 (1981).

[11] Callow, L.M., Scantlebury, J.D.- **J. Oil Col. Chem. Assoc., 64:** 83-86; 119-123; 140-143 (1981); **66:** 93-96 (1983).

[12] Potente, H., Brashes, E.- **Adhesion, 11:** 34 (1979).

[13] Piens, M., Verbist, M.- **Corrosion Control by Organic Coatings,** Lehigh University, Bethlehem, Pennsilvanya: 163-177 (1981).

[14] Mansfeld, F., Kendig, M.W., Tsai, S.- **Corrosion, 38:** 478-485(1982).

[15] Walter, G.W.- **J. Electroanal. Chem., 118:** 259-273 (1981).

[16] Cole, K.S., Cole, R.- **J. Chem. Phys., 9**: 341-351 (1941).

[17] De Levie, R.- **Electrochemical response of porous and rough surfaces.** En: **Advances in Electrochemistry and Electrochemical Engineering.** P. Delahay (Ed.), **6**: 329 (1967).

[18] Scheider, H.- **J. Phys. Chem., 79**: 127-135 (1975).

[19] De Levie, R.- **Electrochimica Acta, 9**: 1231-1242 (1964).

[20] Szauer, T., Brandt, A.- **J. Oil Col. Chem. Assoc., 67**(1): 13-15 (1984).

[21] Armas. R., Gervasi, C., Di Sarli, A., Real, S., Vilche, J.- **Corrosion** (NACE), **48**(5), 379 (1992).

[22] Ambrosi, V., Di Sarli, A.R.- **CIDEPINT-Anales**, 81 (1992).

[23] Bishop, D.M., Zobel, F.G.R.- **J. Oil Col. Chem. Assoc., 66**(3): 67-85 (1983).

Nota.- El presente trabajo ha sido remitido para su publicación a Bulletin of Electrochemistry (India).

CORROSION PROTECTION OF STEEL IN ARTIFICIAL SEA WATER USING ZINC RICH ALKYD PAINTS. AN ASSESSMENT OF THE PIGMENT-CONTENT EFFECT BY EIS.

PROTECCION DEL ACERO CONTRA LA CORROSION EN AGUA DE MAR ARTIFICIAL POR MEDIO DE PINTURAS ALQUIDICAS RICAS EN ZINC. EVALUACION DEL EFECTO DEL PVC POR EIS

C.A. Gervasi[1] , A.R. Di Sarli[1]

E. Cavalcanti[2] , O. Ferraz[2]

E.C. Bucharsky[3] , S.G. Real[3] and J.R. Vilche[3]

SUMMARY

The effect of pigment volume concentration (PVC) on the corrosion resistance properties of zinc rich paints (ZRP) has been investigated using electrochemical impedance spectroscopy (EIS) combined with cathodic protective potential measurements. Painted naval steel samples were studied during the exposure to artificial sea water for up to 45 days. ZRP coatings were prepared employing zinc pigment content in the 88-77% concentration range. Results show clearly that samples prepared with PVC values higher than 86 % deteriorated faster than those panels painted using a relatively lower pigment content. The corrosion behaviour of painted steel samples was found to be practically independent of PVC within the 86-78 % range, being the cathodic protection effect still in action after 45 days immersion time due to the fact that these alkyd resin paint coatings behave like a porous active surface layer. Under aggressive conditions similar to those afforded by the artificial sea water, zinc rich alkyd coatings containing PVC values within the 86-78 % range seem to provide longer corrosion protection to steel substrates than other types of ZRP commonly used.

Keywords: *naval steel, corrosion protection, zinc rich alkyd paint, PVC, impedance measurements, cathodic protective potential.*

INTRODUCTION

Primers heavily pigmented with zinc dust have been extensively used in the last two decades for corrosion protection of steel structures in sea water environments. Initially, zinc rich paints (ZRP) with epoxy binders gained

---

[1] CIDEPINT; Miembros de la Carrera del Investigador de la CIC

[2] Instituto Nacional de Tecnología (INT), Brasil

[3] Instituto de Investigaciones Fisicoquímicas Teóricas y Aplicadas (INIFTA), Fac. Cs. Exactas, UNLP

acceptance, whereas both alkaline metal silicates and alkyl silicates became later the most important among the inorganic binders. It is interesting to note that formulations of commercial ZRP currently employed include also different organic binders, like chlorinated rubber, epoxy-esters, polyesters, polyurethanes, and alkyd resins **[1-3]**.

The physicochemical properties of a ZRP are affected by its pigment volume concentration (PVC). Furthermore, there is a critical value of PVC **[4]** above which many of such properties change abruptly, *ie.* blistering and gloss decrease markedly whereas permeability and rusting increase dramatically. In general, data resulting from impedance spectroscopy, open circuit potential (E_{corr}) measurements, steady-state polarization curves and visual assessments have been employed to evaluate the performance of ZRP coatings based on either epoxy or ethyl-silicate binders during the exposure to corrosive media **[5-13]**.

It is commonly accepted that two fundamental protection mechanisms operate in ZRP coatings: *i*) the galvanic protection stage, which requires good electrical contact among the zinc particles themselves as well as between them and the steel substrate; and *ii*) the barrier-like behaviour stage, which is reinforced by the amount and nature of zinc corrosion products leading to promote the formation of a dielectric surface film.

The aim of the present work is to gain deeper insight on the corrosion protection of naval steel in sea water by zinc-rich alkyd paints. Coatings performance was studied from the changes of impedance spectrum and open circuit potential with exposure time in artificial sea water. Results will illustrate the influence of PVC and chlorinated rubber employed in the formulation of this type of ZRP coatings on steel.

EXPERIMENTAL

The experimental set-up was the same as described elsewhere **[12,13]**. SAE 1020 (UNS G10200) steel plates 20x8x0.2 cm were used as metallic substrate. The metal surface was sandblasted to AS 2 1/2-3 degree (SIS Standard 05 59 00/1967). The roughness profile of the steel surface was determined and graphically registered using a Hommel Tester P2-MZ yielding values of 24±3 μm. The sanded plates were degreased with toluene and coated with the paints whose composition is indicated in Table I. A Bird applicator was used to obtain the organic coatings. ZRP film thicknesses were measured with an electromagnetic gauge, employing a bare sanded plate and standards of known thickness as reference. For each paint composition the mean value of six samples measured was 60±5 μm.

On each plate three cylindrical tubes of transparent acrylic were fixed by using an epoxy adhesive to get good adhesion to the coated substrate. The geometrical area for impedance measurements at the corrosion potential was 17.8 cm^2. An axially placed graphite cylinder served as counter-electrode. Potentials were measured and referred to in the text against a saturated calomel electrode (SCE). The electrolyte was artificial sea water prepared in accordance to the ASTM Standard D-1141/90, pH 8.2.

Electrochemical impedance spectroscopy (EIS) measurements in the frequency range 1 mHz $\leq$ f $\leq$ 50 kHz were performed in the potentiostatic mode at the corrosion potential after different exposure times in the electrolyte, using a frequency response analyzer and an electrochemical interface (Solartron, FRA 1250 and EI 1186, respectively), which were integrated with a PC system. For the impedance measurements, an activated Pt probe was coupled to the reference electrode through a 10 μF capacitor to reduce phase shift errors at high frequencies. Detailed descriptions of both hardware arrangement and data

processing have been given elsewhere [14].

TABLE I

Composition of the paints (g/100 g)

Components	Type of ZRP samples			
	1	2	3	4
Zinc	76.92	85.8	78.50	87.7
Alkyd resin (50 % solids)	9.62	8.30	15.89	6.15
Chlorinated rubber	9.62	--	--	--
Toluene	3.84	5.90	5.61	6.15
Total solids	83.64	89.95	86.45	90.78
Zinc content (%) in the dry paint film	91.97	95.39	90.80	96.61

RESULTS AND DISCUSSION

The change of E_{corr} with the exposure time in sea water has been successfully applied **[12,15-17]** as a simple tool for the evaluation of corrosion protection by ZRP coatings due to their conductive nature. The dependence of the corrosion potential (E_{corr}) on immersion time (t) shown in Fig. 1, illustrates about the galvanic protection supplied to naval steel substrates by the alkyd ZRP coatings loaded with different PVC, when immersed in artificial sea water for about 45 days.

Due to the relatively high permeability of ZRP coatings, immediately after immersion of the painted steel panels in the electrolyte E_{corr} is about -1.10 V, a value which lies in the range of the corrosion potential of plain zinc electrodes in sea water **[18]**. This result indicates clearly that necessary conditions to provide initially the galvanic protection are fulfilled in the ZRP coating formulation, which leads to good electrical contact between the zinc particles and the subtrate as well as to an appropriate electrolyte path located between particles and the steel. The gradual shift of E_{corr} to more positive potentials with rising immersion time reveals the progressive loss in galvanic protection effect of ZRP. Thus, at long exposure times E_{corr} reaches the typical value corresponding to the corrosion potential of steel in sea water (-0.65 V). It is worth noting that E_{corr} values recorded for sample 1, which includes chlorinated rubber in its coating formulation, were more negative than those measured for samples 2, 3, and 4, in which a remarkable similar electrochemical behaviour was found. This suggests, in principle, thegreater availability of protective pigment for sample 1 in comparison to the other three samples tested.

Open circuit potential measurements carried out with panels of sample 4 have been interrupted at relatively shorter exposure times in comparison to those performed using samples 1, 2 and 3, since blistering of the coatings were visually

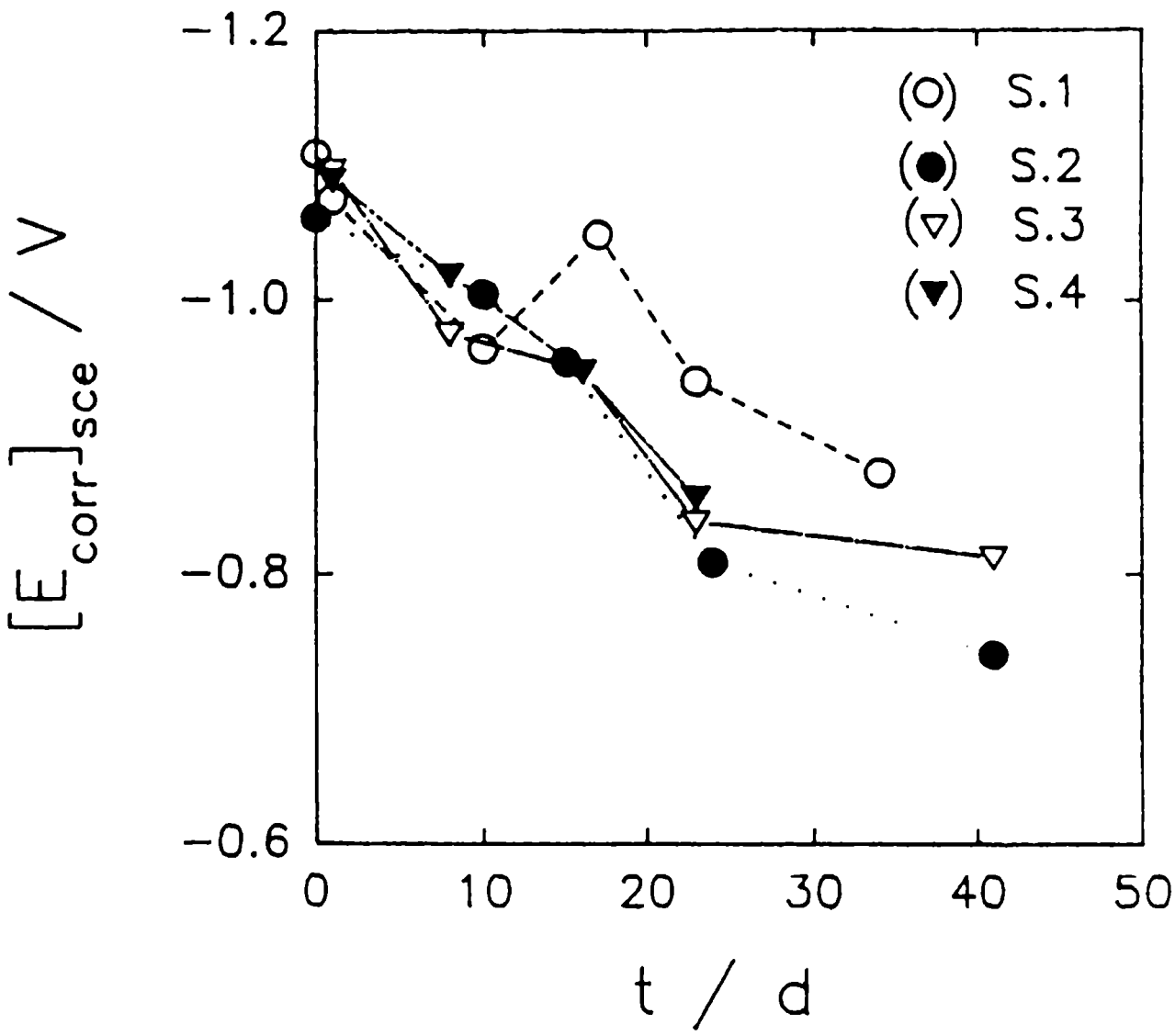

Fig. 1.- Dependence of Ecorr on exposure time in artificial sea water for zinc rich alkyd paint samples 1 to 4 whose compositions are indicated in Table I.

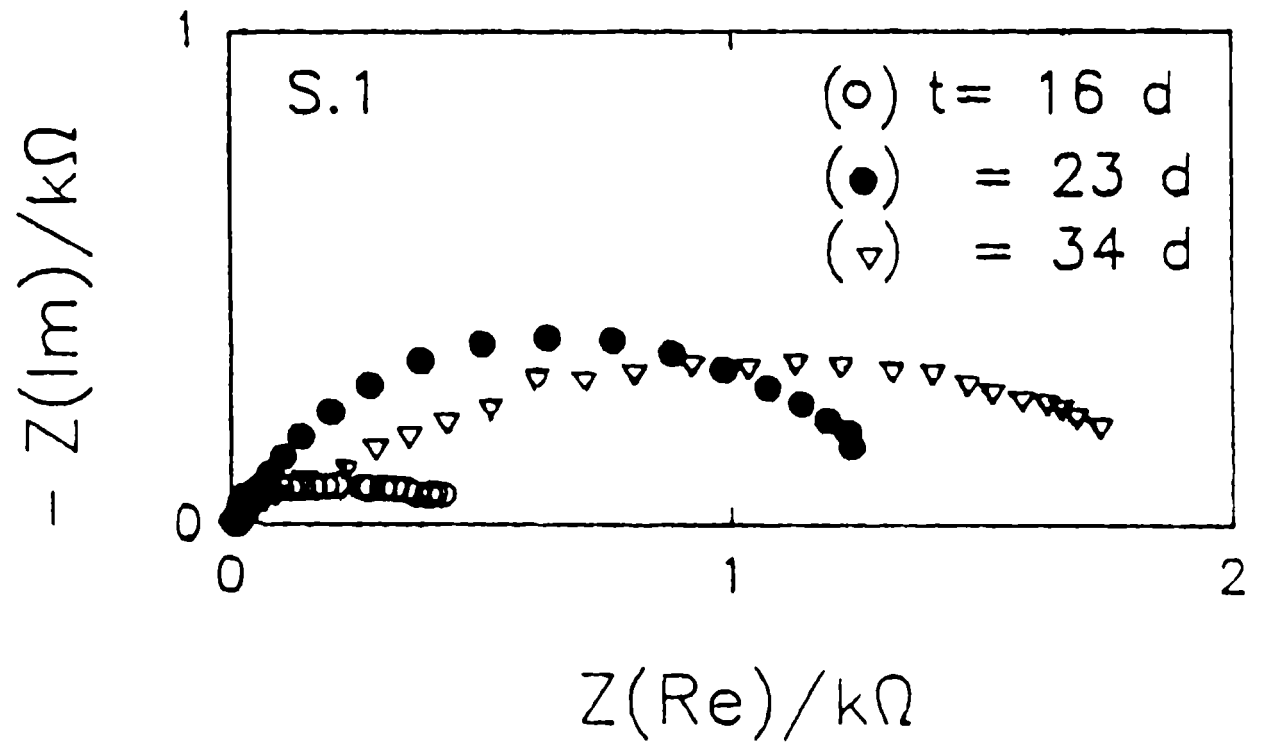

Fig. 2.- Nyquist plots obtained with the alkyd ZRP of sample 1 at different exposure times.

detected. This fact can be explained taking into account that the adhesive properties of a coating diminishes when the vehicle concentration is no sufficient. Accordingly, the higher the vhicle concentration the lower the PVC and concecuently the longer the expected period of durability.

The set of impedance spectra contain valuable informations related to characteristic coating parameters as well as to the charge transfer kinetics of corrosion processes going on extensively through pores and cracks in the ZRP films. Taking into account the dependence of the open circuit potential on immersion time for the coated steel plates (see Fig. 1), corrosion processes can be mainly associated with the pigment anodic dissolution reaction. Typical impedance diagrams obtained at different immersion times for the system naval steel/zinc rich alkyd paint/artificial sea water, are presented in Fig. 2 and 3. It can be clearly seen that the exposure time and the pigment concentration strongly affect the impedance spectra of the ZRP coatings tested in this work. Changes in the coated naval steel/artificial sea water system seem to altered the dynamics of both zinc corrosion and rust formation reactions at prolonged immersion times.

A fairly good description of the experimental impedance diagrams was obtained in terms of transfer function analysis using non-linear fit routines. Because of the complex nature of processes taking place at the coated steel interface it is necessary to derive the appropriate model accounting for the time-dependence of measured impedance for the different samples. It is worth noting that Nyquist diagrams of ZRP coated steel panels often show either one or two capacitive contributions **[11]**. Therefore, the high frequency loop could be related to a charge transfer reaction or to the parallel combined effect of ionic resistance and dielectric capacitance of the insulating layer, whereas the low frequency arc could be associated with either the charge transfer reaction or a diffusion process through a surface layer of finite thickness.

The diffusion tail provokes usually a pronounced curved appearance in the impedance diagram at low frequencies overlapping the capacitive semicircle related to the charge transfer reaction. In the case of ZRP, it is interesting to establish whether the impedance spectrum represents the complex frequency response of an active porous electrode due to the fact that this behaviour can indicate the existence of a high degree of electrical interconnection among the conductive particles of zinc. This favours the galvanic action of the coating providing cathodic protection to the steel substrate. On the contrary, when the coating behaves predominantly like a flat electrode, a low number of conductive particles appear to be in an effective electrical contact. Under these circumstances, the corrosion process takes place being the value of the anodic/cathodic area ratio strongly diminished.

In general, data obtained for the systems naval steel/zinc-rich alkyd paints/artificial sea water suggest that this type of ZRP coatings exhibits a frequency response which resembles those of porous electrodes. This can be probably related to the high PVC used to prepare each sample tested in this work. Likewise, the large majority of pigment particles are in good electrical contact with each other as well as with the substrate. Since at short immersion times the alkyd ZRP is behaving as a coating at the galvanic stage, the corresponding impedance diagrams (Fig. 2 and 3) seem to be associated with the initial corrosion of the zinc particles. The gross flattening of the capacitive contribution can be attributed to a dispersion of time constants due to ZRP coating inhomogeneities whose electrical response can be described by a transmission line model. The low frequency range in such Nyquist plots reveals in some cases an ill-defined diffusion tail.

The chord length pertaining to the high frequency loop in Nyquist diagrams

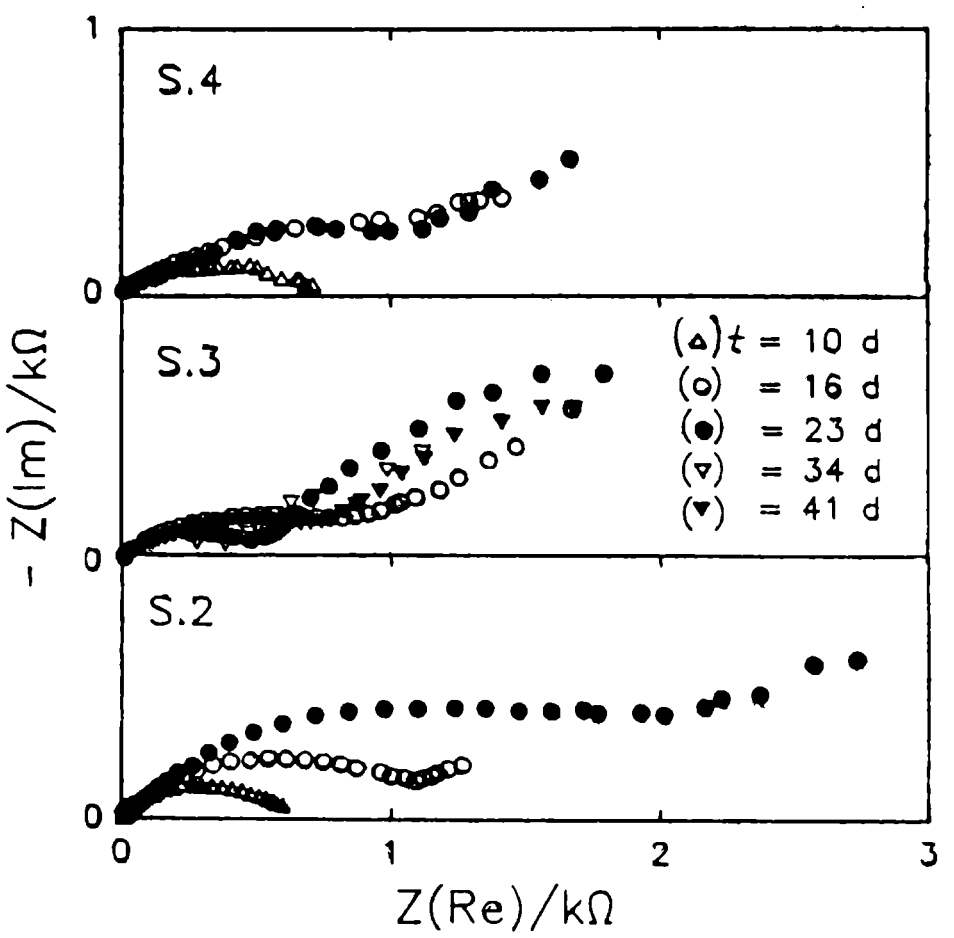

Fig. 3.- Nyquist diagrams for different ZRP coatings: (a) sample 4; (b) sample 3; and (c) sample 2.

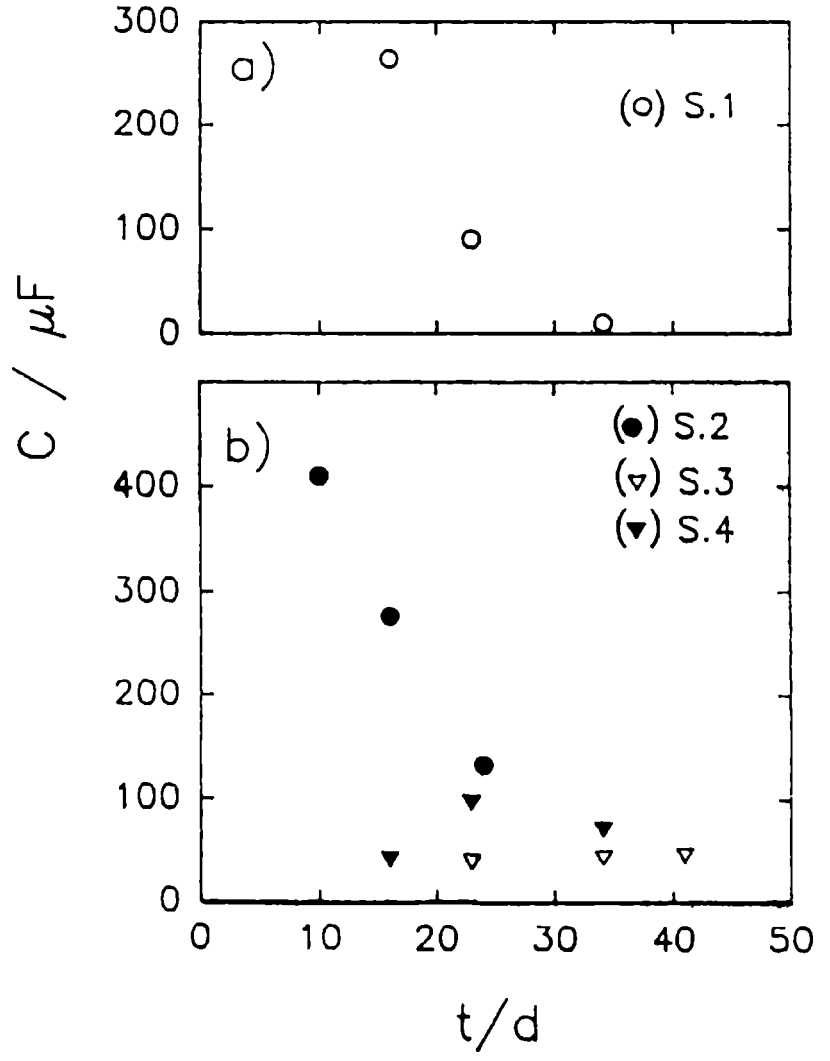

Fig. 4.- Dependence of C on exposure time for different ZRP coatings: (a) sample 1; (b) samples 2, 3, and 4.

tends to increase according to exposure time in sea water. This effect can be related to the formation and accumulation of insoluble corrosion products within the coating (reinforcing the paint barrier effect), whereas small amounts of pigment particles sustain electrical contact among them as well as with the steel sustrate. This result is in agreement with the gradual change of the corrosion potential towards more positive values, as depicted in Fig. 1. However, after prolonged exposure time, such trend may be influenced by perforations of the coating layer causing the deterioration of a protection system which prevailed over the barrier-type effect already enhanced by zinc corrosion products.

Impedance spectra can be analyzed using a non-linear fit routine **[14]** according to the following total transfer function:

$$Z_T(j\omega) = R_\Omega + Z \tag{1}$$

where Z is given by

$$Z^{-1} = CPE^{-1} + \frac{R_c + R_{DO}\,(jS)^{-1/2}\tanh(jS)^{1/2} + R_a}{[R_c + R_{DO}\,(jS)^{-1/2}\tanh(jS)^{1/2}]\,R_a} \tag{2}$$

In eq. (2) the constant phase element, $CPE = [C(j\omega)^{\alpha}]^{-1}$, involves the parameter α whose value was found in the range 0.47-0.54 for all the experiments. It should be noted that $\alpha = 0.5$ corresponds to the special case of active porous electrodes. The resistance R_c is associated with the series combination of the electrolyte resistance inside the pores and the charge transfer resistance of the oxygen reduction reaction. A finite diffusion impedance was considered to account for the transport process involved in the cathodic partial reaction through the coating. The diffusion resistance R_{DO} is the $\omega \rightarrow 0$ limit of a finite-length Warburg impedance $Z_w = R_{DO}(jS)^{-1/2}\tanh(jS)^{1/2}$, where $S = l^2\omega/D$, l and D being the diffusion length and diffusion coefficient, respectively. Accordingly, the lower the value of $l/D^{1/2}$ the sooner the diffusion tail will curve at decreasing frequencies towards the real axis. The resistance R_a is related to the charge transfer resistance of the zinc dissolution process which takes place in parallel with the oxygen reduction reaction.

The dependences of C, R_c, and R_a on exposure time for all samples are given in Fig. 4 to 6, respectively. The decrease of C with increasing time of exposure in the electrolyte (Fig. 4) can be related to the progressive electrical disconnection between the pigment particles due to the accumulation of corrosion products within the pores of the ZRP coating. On the other hand,the gradual increase of the resistance R_c according to exposure time (Fig. 5) can be associated with the continuous build up of zinc corrosion products that gives rise to a decrease of the effective pore radius in the porous coating, while the simultaneous increase of R_a (Fig. 6) is attributed to the decrease of the electrochemical active area of the Zn particles.

Figs. 7 to 9 show the good agreement between experimental results and calculated data. According to the model of eqs. (1) and (2), it is possible to describe the relative contribution of the different processes in impedance diagrams. Thus, the lenth of the high frequency arc chord is determined by the parallel conection of R_c associated with the series combination of the electrolyte resistance inside the pores and the charge transfer resistance of the process

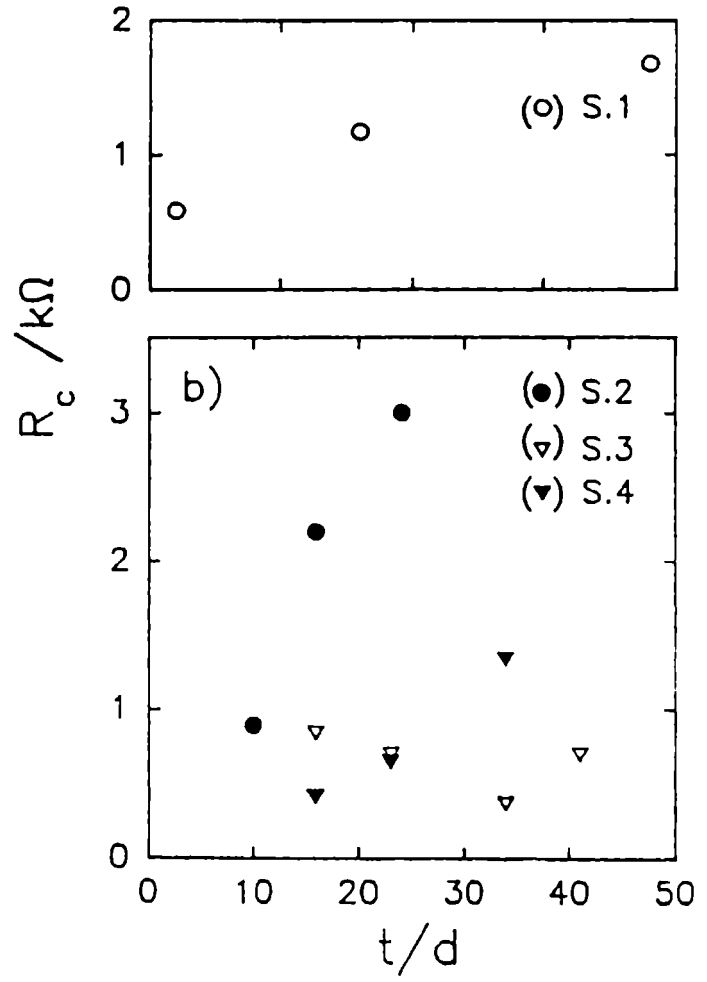

Fig. 5.- Dependence of Rc on exposure time for different ZRP coatings: (a) sample 1; and (b) samples 2, 3, and 4.

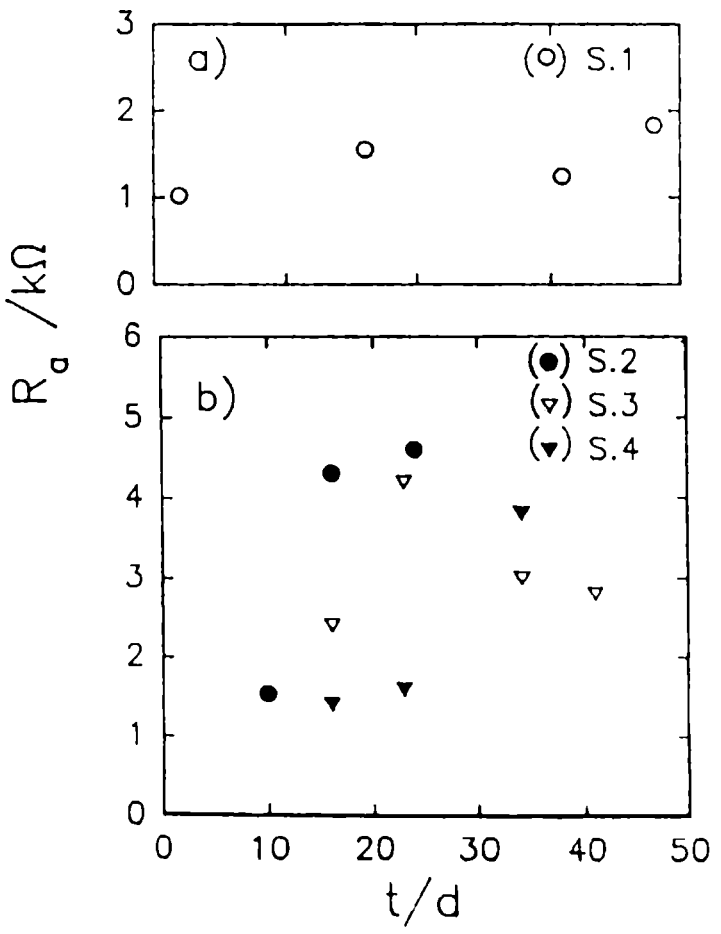

Fig. 6.- Dependence Ra on exposure time for sample 1 (a) and samples 2-4 (b).

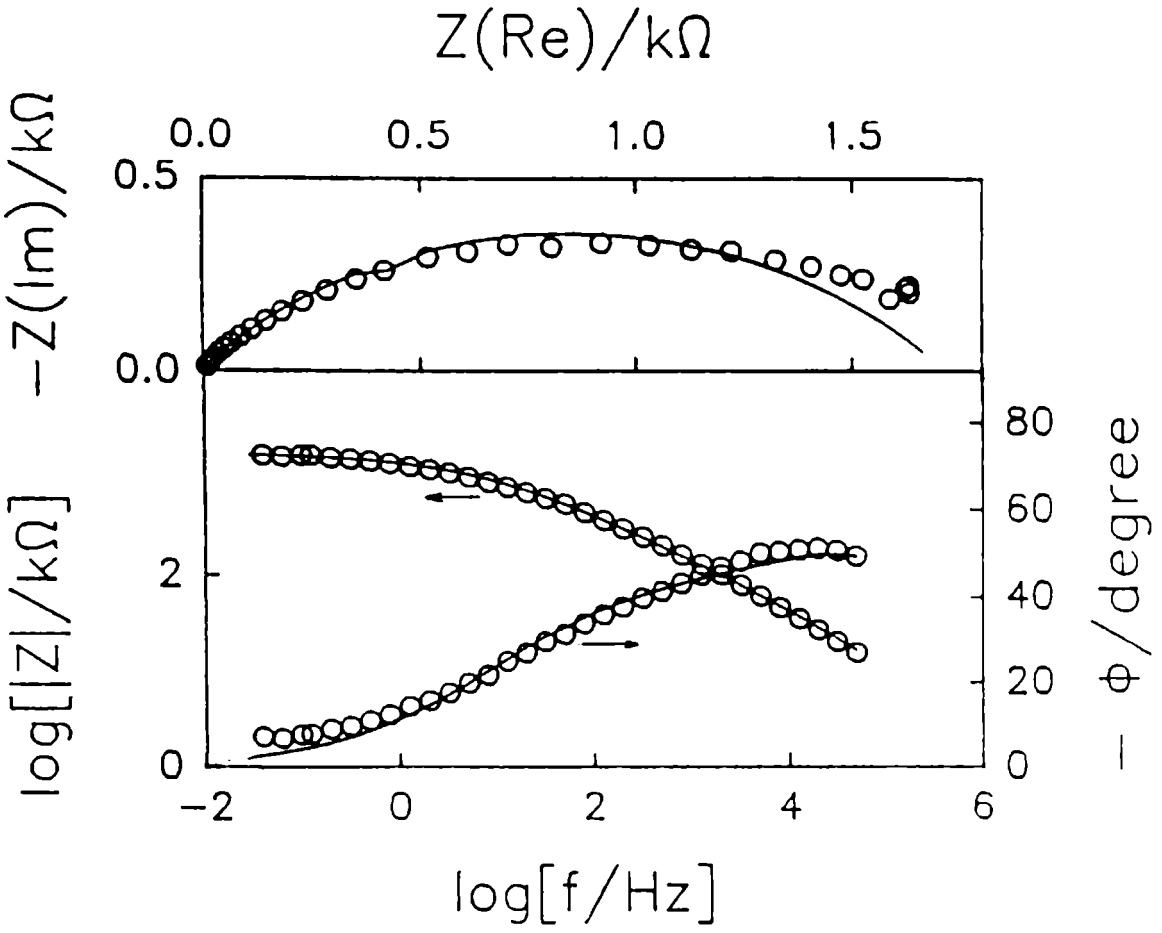

Fig. 7.- Calculated and experimental Nyquist and Bode plots obtained for sample 1 after 34 days immersion time in artificial sea water.

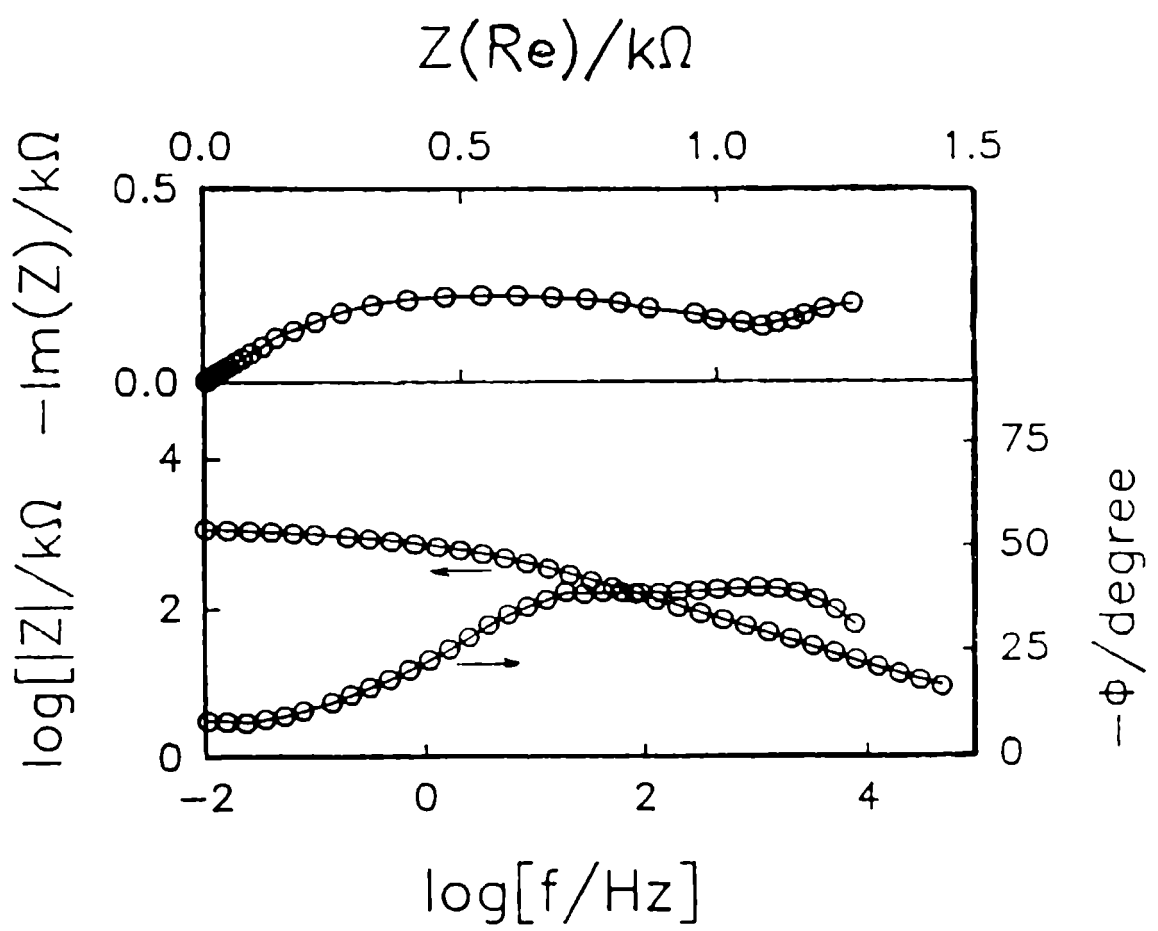

Fig. 8.- Calculated and experimental Nyquist and Bode plots obtained for sample 2 after 15 days immersion time in artificial sea water.

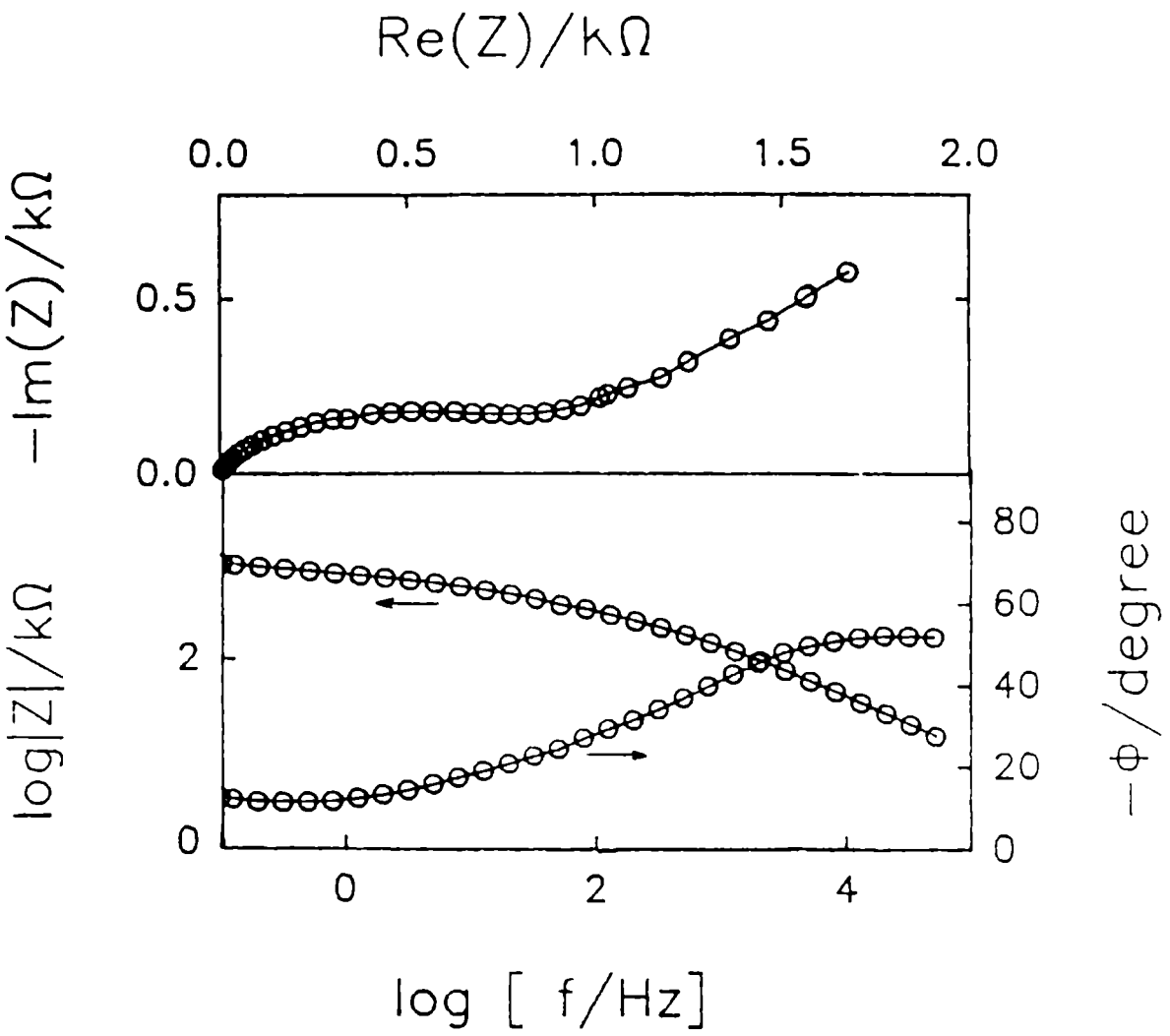

Fig. 9.- Calculated and experimental Nyquist and Bode plots obtained for sample 3 after 16 days immersion time in artificial sea water.

involving the oxygen reduction, and R_a related to the charge transfer resistance of the zinc dissolution process. Similarly, at $\omega \rightarrow 0$ the real part of the impedance includes the sum of R_c and R_{DO} contributions which are in parallel with R_a. Since R_a was found to be smaller than $R_c + R_{DO}$ for all ZRP samples, the real part of the impedance at the lowest frequencies results mainly dominated by the anodic process.

It is worth noting that the increase of the high frequency chord length according to exposure time may be related to a rise in the electrolyte resistance inside the pores and to a decrease in the electrochemical active area generated by the accumulation of corrosion products. On the other hand, the absence of a diffusion tail in the Nyquist diagrams obtained for sample 1 can be explained taking into account the small value of $l/D^{1/2}$.

Data analysis of the whole set of results indicate that the cathodic protection effect given by the ZRP coatings was more effective in the case of the formulation used for sample 1. It should be mentioned that a fairly good cathodic protection effect was still in action for samples 2 and 3 during 41 days immersion time in the aggresive solution. EIS and corrosion potential measurements demonstrated that zinc-rich alkyd paints with PVC levels higher than 86% exhibited a faster coating deterioration in the saline electrolyte, at least from an electrochemical point of view.

CONCLUSIONS

EIS method has provided to be a useful tool to assess the protective behavior of ZRP organic coatings. The impedance spectra have been interpreted using a non-linear fit routineaccording to transfer function analysis.

The zinc rich alkyd coatings tend to act as porous electrode probably because the majority of the metal and the reactive pigment particles maintain the electrical contact among them. Besides, the changes of the capacitance values , the increase of the resistances R_a and R_c, and the appearance of diffusion process with exposure time are attributed to the progressive disconnection of the pigment particles taking place along with the thickening of the zinc corrosion products layer on the same particles.

The relative duration of the cathodic protection effect were similar for samples 1, 2, and 3, although the sample 1 exhibited a relatively faster deterioration. It must be mentioned, however, that the cathodic protection for samples 2 and 3 was still in action even after 41 days of immersion in sea water.

Data obtained from EIS and corrosion potential measurements show that PVC levels higher than 86 % exhibited a faster deterioration in this type of binder when immersed in a very aggressive aqueous medium, at least from an electrochemical point of view.

Acknowledgements

The authors thank the Comisión de Investigaciones Científicas de la Provincia de Buenos Aires (CIC), the Consejo Nacional de Investigaciones Científicas y Técnicas (CONICET) and the Fundación Antorchas of Argentina, and the Instituto Nacional de Tecnología (INT) and the Conselho Nacional de Pesquisas (CNPq) of Brasil, for financial support of this cooperative research work.

REFERENCES

[1] R. Romagnoli and V.Vetere, Corrosion Rev., **10**, 1 (1991).

[2] G. Wranglen, **An Introduction to Corrosion and Protection of Metals**, Inst. for Metallskydd, Stockholm, p. 191 (1972).

[3] C.G. Munger, **Corrosion Prevenntion by Protective Coatings**, Publ. by NACE, 2nd Edition, Houston, p.132 (1986).

[4] W.K. Asbeck and M.van Loo, Ind. Eng. Chem., **41**, 1970 (1949).

[5] T.K. Ross and J. Linghard, Trans. Inst. Metal Finishing, **40**, 186 (1963).

[6] D.S. Newton and F.G. Sampson, J. Oil Col. Chem. Assoc., **48**, 382 (1965).

[7] F. Theiler, Corros. Sci., **14**, 405 (1974).

[8] T.K. Ross and J. Wolstenholme, Corros. Sci., **17**, (341 (1977).

[9] T.Szauer and A. Brawdt, J. Oil Col. Chem. Assoc., **67**, 13 (1984).

[10] S.A. Lindqvist, L. Meszáros and L.Svenson, J. Oil Col. Chem. Assoc., **68**, 10 (1985).

[11] D. Pereira, J.D. Scantlebury, M.G.S. Ferreira and M.C. Almeida, Corros. Sci., **30**, 1135 (1990).

[12] R.A. Armas, C. Gervasi, A. Di Sarli, S.G. Real and J.R. Vilche, Corrosion, **48**, 379 (1992).

[13] S.G. Real, A.C. Elías, C.A. Gervasi, A. Di Sarli and J.R. Vilche, Electrochim. Acta, **38**, 2029 (1993).

[14] E.B. Castro, S.G. Real, R.H. Milocco and J.R. Vilche, Electrochim. Acta, **36**, 117 (1991).

[15] J.E.O. Mayne, J. Iron and Steel Institute, **176**, 140 (1954).

[16] L. Meszáros and S.A. Lindqvist, Proc.EUROCORR'82-Section II, p.147 (1982).

[17] M. Morcillo, R. Barajas, S. Feliú and J.M Bastidas, J. Mat. Sci., **25**, 2441 (1990).

[18] M. Pourbaix, **Atlas d'equilibres èlectrochimiques**, Ganthier-Villars, Paris, p.312 (1963).

[19] G.J. Brug, A.L.G. van den Eeden, M. Sluyters-Rehbach and J.H. Sluyters, J. Electroanal. Chem., **176**, 275 (1984).

Note.- This paper has been accepted for publication in Corrosion Science (Great Britain)

CHARACTERIZATION OF PROTECTIVE PROPERTIES FOR SOME NAVAL STEEL/POLIMERIC COATING/3 % NaCl SOLUTION SYSTEMS BY EIS AND VISUAL ASSESSMENT

CARACTERIZACION DE LAS PROPIEDADES PROTECTORAS EN ALGUNOS SISTEMAS ACERO NAVAL/RECUBRIMIENTO POLIMERICO/SOLUCION 3 % DE NaCl POR MEDIO DE EIS E INSPECCION VISUAL

O. Ferraz[1] , E. Cavalcanti[1] and A.R. Di Sarli[2]

SUMMARY

Electrochemical impedance measurements have been made in 3 % NaCl solution on coated naval steel with alkyd, epoxies, chlorinated rubber and acrylic conventional paints as well as with epoxy-polyamide, ethyl-silicate or alkyd zinc rich paints. Electrochemical impedance measurements have made possible to monitor the uptake of the surrounding aqueous electrolyte into the paint and simultaneously to determine the extent of paint breakdown. Based on corrosion potential and impedance measurements, together with the visual assessment using both the ASTM Standards 610/68 and 714/87, the different paints have been ranked in terms of the effectiveness of their anticorrosive properties in a chloride containing solution. A comparison of visual assessment, corrosion potential and impedance measurements data indicates that the electrochemical impedance technique is a powerful tool for the study of the coated steel behaviour exposed to aggressive aqueous media.

Keywords: *electrochemical impedance, corrosion potential, anticorrosive paints, commercial paints, standardized visual assessment, equivalent circuit.*

INTRODUCTION

Steel products are used in almost all industrial sectors of the economy, ranging from transportation equipment to permanent steel structures. In such metallic substrates, the main purpose of an organic coating is to protect them against an aggressive environment.

The anticorrosive protective properties of these coatings are determined by a complex mechanism which includes the action of different factors:

a) the dielectric properties of the coating;
b) the adhesion of the coating to the substrate;
c) the water, oxygen and ionic coating uptake;
d) the coating formulation;
e) ageing of the coating;
f) intrinsic and extrinsic defects of the coating;

---

1 Instituto Nacional de Tecnología (INT), Brasil

2 CIDEPINT, Miembro de la Carrera del Investigador de la CIC

g) chemical composition and surface pretreatment of the metallic substrate;
h) environmental conditions; and
i) the electrochemical corrosion reactions at the metal/coating interface after permeation of water and oxygen.

Therefore, the protective properties of organic coatings can be attributed to a barrier and to an electrochemical mechanism. As, in general, organic coatings have a high resistance to ionic conductivity, they offer good barrier properties retarding the diffusion of chemical species promoted by the osmotic pressure in the pores and capillaries of the coating, to and from the metal surface.

A painting scheme usually consists of a primer, a sealer and a topcoat. The primer is especially responsible of corrosion protection. In order to prevent adhesion losses for the coating, due to the water molecules arriving at the coating/metal interface as well as to underfilm corrosion taking place, typical barrier pigments are incorporated within the coating. Besides, active pigments in the primer often develop further protective action in addition to the barrier effect when local failures of the organic coating occur. These pigments may protect the metal substrate electrochemically by either a galvanic or a passivating mechanism.

Methods to evaluate with accuracy the relative abilities of painting schemes to provide corrosion protection have not usually been available. However, this situation appears to be changing, particularly with the advent of modern electrochemical techniques. During the last decade, considerable success has been achieved by the use of wide frequency scan electrochemical impedance analysis. Many examples in the literature illustrate the utility of this method with regard to various types of coatings and oxide films on iron and steel **[1-10]**. However, relatively few reports have been published describing results obtained from protective organic paints commercially available.

According to Leidheiser **[11]**, the corrosion potential, in combination with other methods, can also provide information about the mechanism of the reaction and the rate controlling process. He concludes that, in general, the movement of the corrosion potential in the noble direction is indicative of an increasing cathodic/anodic surface area ratio and suggests that the oxygen and water arriving at the metal/coating interface create alkaline conditions (owing to the oxygen reduction reaction) by which delamination may be sufficient as to be of concern. On the contrary, the movement of the corrosion potential in the active (i.e. more negative) direction indicates that the cathodic/anodic areas ratio decreases and, as consequence, the underfilm corrosion process may be significant, denoting the limit of the coating service life.

In the present work, thirteen paint schemes based on organic coatings of commercial grade (acrylic latex, epoxy-polyamide, epoxy-bituminous, alkyd, polyurethane, chlorinated rubber, zinc rich epoxy), with an expected range of anticorrosive protective properties were applied to naval steel sheets and immersed for up to 255 days in 3 % NaCl solution. The painted electrodes were weekly assessed by both electrochemical impedance in the frequency range 65 KHz to 10^{-3} Hz and corrosion potential measurements. The standardized test procedures ASTM D-610/68 and ASTM D-714/87 were also performed in order to assess visually both the rusting and the degree of blistering suffered by the coated steel surfaces.

EXPERIMENTAL

SAE 1020 steel plates (20x8x0.2 cm) were used as metallic substrate. The surface was sandblasted to Swedish Standard SIS 05 59 00/67 Sa 2 1/2 - 3. A

roughness profile of 20 ± 4 μm was obtained. The specimens were degreased with toluene and coated with the primers and topcoats whose characteristics and thicknesses are shown in **Table I**. A Bird applicator was used to apply the organic coatings; the desired film thicknesses were achieved by successive applications, with drying periods of 2 days between each coat. For avoiding contamination with atmospheric dust, the test plates were kept in desiccators at room temperature (20 ± 2 °C). Dry film thickness was measured with an electromagnetic gauge, using a bare sanded plate and standards of known thickness as reference.

TABLE I

Characteristics and thicknesses of the coatings tested

Sample	Anticorrosive primer		Topcoat		Scheme mean thickness
	Paint	Mean thickness μm	Paint	Mean thickness μm	μm
1	Epoxy-Polyamide	35	---	---	35
2	Chlorinated rubber	40	---	---	40
3	Zinc rich epoxy	48	---	---	48
4	---	---	Polyurethane	40	40
5	---	---	Chlorinated		
6	---	---	Alkyd	49	49
7	---	---	Epoxy bituminous	60	60
8	---	---	Epoxy-Polyamide	58	58
9	Acrylic latex	19	Polyurethane	55	74
10	Acrylic latex	19	Hypalon	55	74
11	Acrylic latex	19	Acrylic latex	56	75
12	Epoxy-Polyamide	40	Epoxy-Polyamide	60	100
13	Epoxy-Polyamide	40	Epoxy bituminous	60	100

On each plate two cylindrical tubes of transparent acrylic were fixed by using an epoxy adhesive in order to get good adhesion to the coated substrate. The geometrical area of each cell exposed for impedance measurements was 28 cm^2. A large cylinder of graphite axially placed, was used as counter-electrode and a saturated calomel electrode (SCE) as reference. The electrolyte was 3 % NaCl solution, pH 8.2. All impedance spectra in the frequency range $10^{-3} \leq f \leq 6.5 \times 10^4$ Hz were performed in the potentiostatic mode at the corrosion potential, as a function of the exposure time in the electrolyte solution, using the 1255 Solartron Frequency Analyzer and the 1186 Solartron Electrochemical Interface. Data processing was carried out with an Olivetti PC and a set of programs developed by Boukamp **[12]**.

After immersion, the coatings were assessed weekly with the ASTM Standards D-610/68 and D-714/87 in order to evaluate the degree of rusting and blistering respectively, of the painted steel surfaces, in an attempt to correlate visual observations with electrochemical data.

RESULTS AND DISCUSSION

In spite of the fact that in practice the paints tested are used forming part

of a painting scheme, it was considered interesting to evaluate the protective behaviour of each paint not only within a certain scheme but also individually on steel.

The transport through a polymeric coating is an example of a mixed process where the charge and mass transfer take place at the same time. The ability of a coating to be semipermeable together with, in some cases, its capacity of acting as ionic exchanger complicates the studies of transport through coatings further. On coated steel the corrosion attack initiates at the base of weak points or in mechanically damaged areas of the coating; the remainder metallic surface generally acts as a cathode. In such a case, the corrosion rate depends on: a) the catalytic properties of the substrate for the cathodic reduction reactions take place; b) the coating resistance to the ionic flux and c) the cathodic/anodic surface areas ratio.

The first day after immersion in 3 % NaCl solution, the corrosion potential (Ecorr) for the zinc rich epoxy paint (ZRP)/naval steel system (sample 3) was about - 1.1 V/SCE, confirming that there was electrical contact between the steel substrate and the pigment zinc particles in the primer (Fig. 1-a). The other two anticorrosive primers, epoxy-polyamide (sample 1) and chlorinated rubber (sample 2), pigmented with zinc tetroxychromate (60 % w/w) showed potentials near to - 0.50 V/SCE. This anticorrosive pigment was chosen for its low solubility and the paints were prepared for constant exposure to an aqueous solution. The low solubility added to both the high permeability of the thin primers (like in service) and the high chloride concentration in the electrolyte, lets suppose that the chloride concentration threshold for corrosion starting was surpassed just after immersion, causing the recorded consequences on the potential (and on the impedance and visual assessment as will be seen further on).

These results were quite similar to those obtained for polyurethane (sample 4), chlorinated rubber (sample 5), alkyd (sample 6), Fig. 1-a, and epoxy-bituminous (sample 7) or epoxy-polyamide (sample 8), Fig. 1-b; in this case, the bad results are attributed to the low barrier effect afforded by the topcoats. In return, the much more noble potentials ($\cong$ 0.1 $\pm$ 0.05 V/SCE) exhibited by the steel sheets coated with primer + topcoat paints (samples 9 to 13) at the same exposure time were attributed to the higher barrier effect (i.e., lower permeability to aggressive species) of the thicker coatings.

As the test goes on however, it is evident (except for sample 12) the coated specimens potentials trend to values close to the freely corrosion potential characteristic of uncoated steel under equivalent environmental conditions. Such a trend gives value to the assumption of an increasing electrochemical activity at the metal surface during the test, i.e. no polymeric coating is impenetrable and, therefore, different chemical species can diffuse towards the metal surface with a rate and to an extent determined by the particular physicochemical characteristics of the paint scheme applied.

Impedance spectra contain valuable information about the electrical coating parameters and kinetics of the corrosion processes taking place on the metallic substrate. Due to the dynamic character of rust formation the impedance spectra of coated steel/3 % NaCl solution systems change throughout the exposure time. A fairly good description of the experimental impedance diagrams can be obtained in terms of a transfer function analysis using non-linear fit routines as developed by Boukamp **[12]**; the complex nature of the processes at a coated steel interface makes necessary to derive models that account for the impedance data measured at such interfaces.

Four types of equivalent circuit models have been used in order to explain the impedance data. Initially, when a coated steel contacts with the aqueous

electrolyte there is no solution within the metal/coating interface; therefore, no electrochemical double layer nor faradaic reaction occur and the only information obtained from impedance data must be related with the dielectric properties of the organic coating. A first interpretation of the complex plane plot establishes that it may be described by a transfer function corresponding to an equivalent circuit built up from a series combination of the electrolyte resistance (R_s) with a constant phase element (CPE), Fig. 2, where the CPE ($Q \equiv C_m$) have an impedance dispersion relation of: $Q = 1/Y_o\ (j\omega)^{\alpha}$; if $\alpha = 0$, then $Q = 1/Y_o = R$; furthermore, if $\alpha = 1$, 0.5 or - 1 the CPE represents a capacitance (C), a Warburg diffusion coefficient (W) or an inductance (L), respectively.

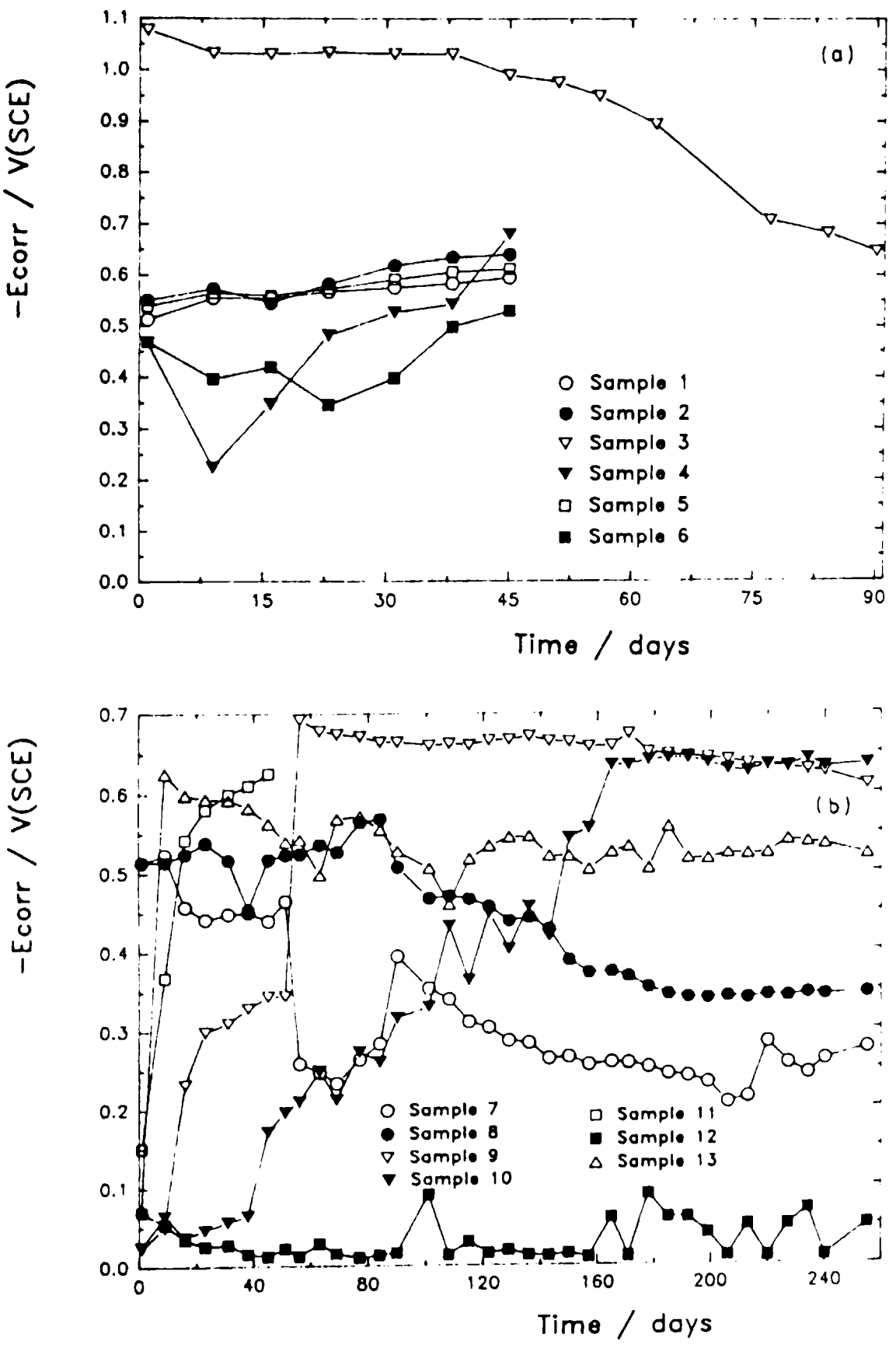

Fig. 1.- Dependence of Ecorr on exposure time for samples: a) 1-6; b) 7-13.

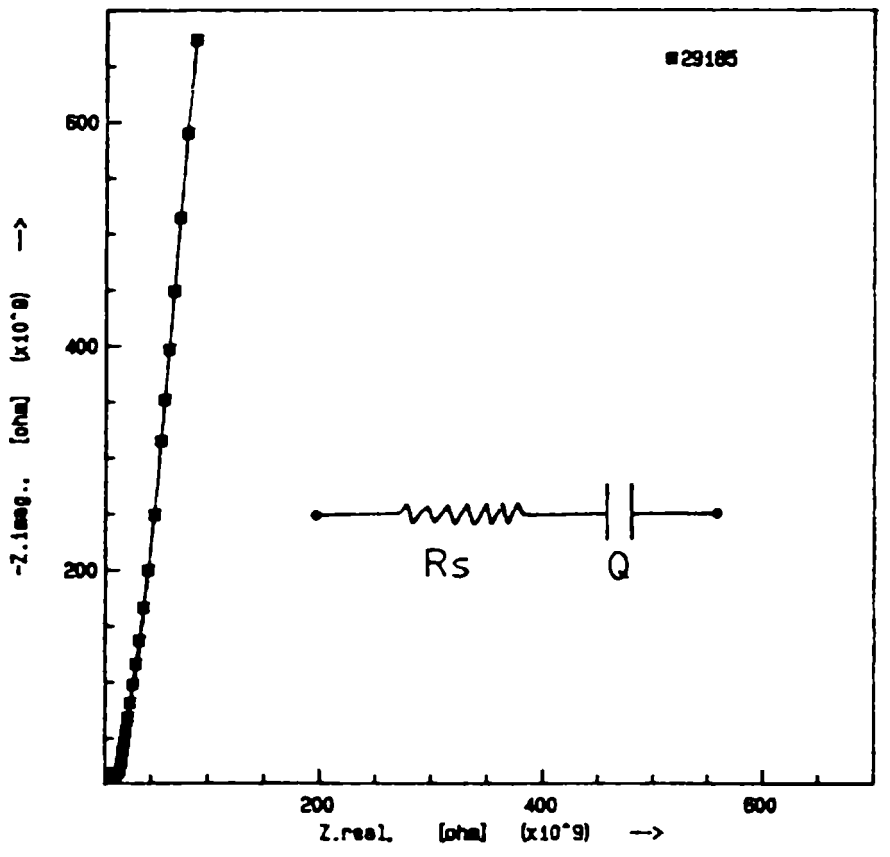

Fig. 2.- Complex plane plot for a series R(Q≡C) combination.

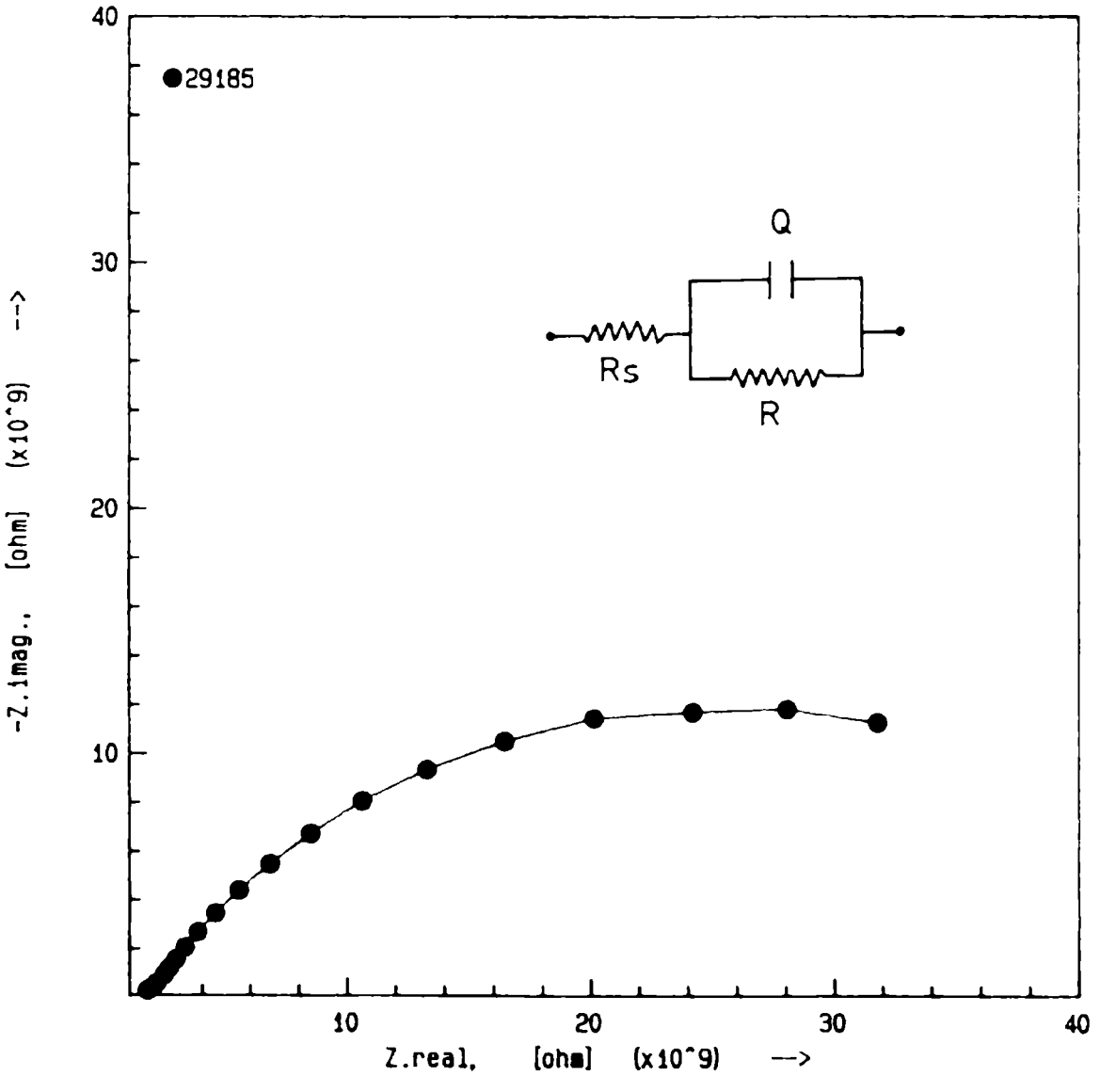

Fig. 3.- Complex plane plot for a series Rs with a parallel R(C≡Q) combination.

As the immersion time goes on, the amount of water, oxygen and ions permeated increase the coating conductivity in such a way that the resistance (R_m), associated to the dielectric capacitance ($Q \equiv C_m$), becomes measurable; in such conditions, the impedance diagram and equivalent circuit shown in Fig. 3, together with information about the membrane ionic resistance (R_m, which describes paths of lower resistance shortcircuiting the organic coating), and the dielectric capacitance (C_m, whose value is associated with the water uptake) can be obtained. Latterly, once the permeating species reach the metallic substrate, corrosion processes may initiate causing the emergence of the electrochemical double layer ($Q \equiv C_d$) and the charge transfer resistance (R_t) proper of the faradaic process, and related as $1/R_t$ with the corrosion rate. In such a case, the impedance response and the corresponding equivalent circuit modeling the coated steel/3 % NaCl solution are those exhibited in Fig. 4; in turn, this circuit would be connected with a general Warburg-type element Z_w (where $Z_w = [K (j\omega)^n]$, which is obtained at low frequencies and it is related to the relaxation of a mass transport process linked with the oxygen reduction reaction **[13]**.

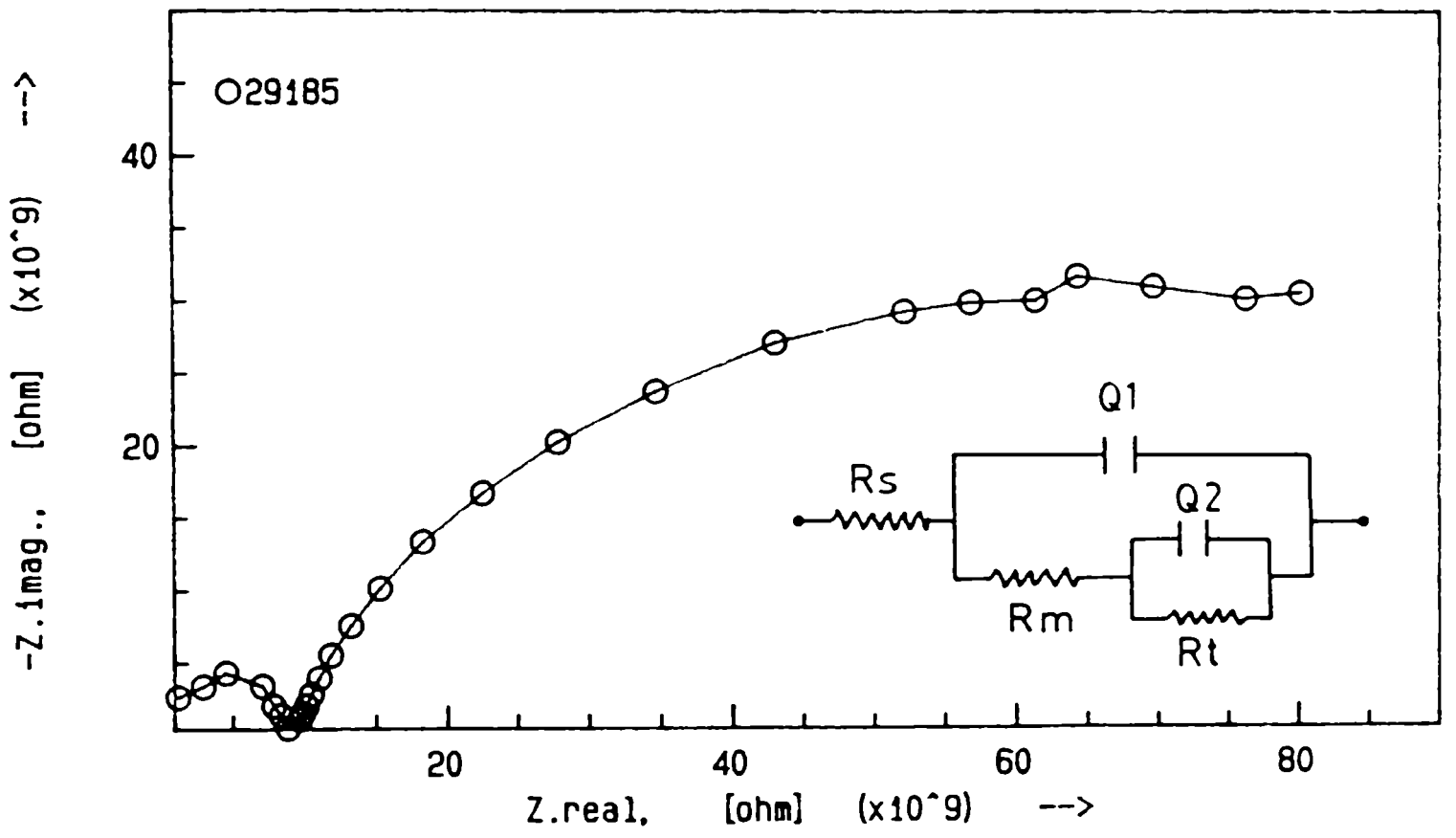

Fig. 4.- Complex plane plot for samples showing two time constants.

Summarily, the high frequency time constant would be the result of the coating capacitance ($Q_1 \equiv C_m$) and ionic resistance (R_m) interaction, while the low frequency relaxation time would be given by the charge transfer resistance (R_t), the double layer capacitance ($Q_2 \equiv C_d$) and the diffusion component W (Fig. 5). The distortion observed in the resistive-capacitive contributions indicate a deviation from the ideal behaviour in terms of a distribution of time constants due to tangential penetration of electrolyte at the metal/paint interface (usually starting at the base of coating defects), surface inhomogeneities, roughness effects and/or diffusion processes through the coating **[14, 15]**. By fitting the transfer function associated to the most probable equivalent circuit, these factors are taking into account through the CPE. Some or all these mechanisms are probably involved in the coated systems treated here, therefore, there were difficulties to provide an accurate physical description of the processes occurred. In order to select the most appropriate model of equivalent circuit, the value of the fitting process standard deviation was used as final criterion.

Fig. 6(a-b) to Fig. 10(a-b) and Table II summarize the experimental results.

TABLE II

ASTM STANDARDS D-610/64 AND D-714/87 RATING AS
A FUNCTION OF EXPOSURE TIME

Exposure time (days)	Sample 1		Sample 2		Sample 3		Sample 4		Sample 5		Sample 6		Sample 7		Sample 8		Sample 9		Sample 10		Sample 11		Sample 12		Sample 13	
	610	714	610	714	610	714	610	714	610	714	610	714	610	714	610	714	610	714	610	714	610	714	610	714	610	714
1	10	10	10	10	10	10	10	10	10	10	10	10	10	10	10	10	10	10	10	10	10	10	10	10	10	10
9	10	10	8	10	10	10	10	M,8	8	F,8	8	F,2	10	10	10	10	10	10	10	10	6	10	10	10	9	10
16	3	10	5	F,6	10	10	7	F,4	7	M,6	8	M,4	9	10	9	10	10	F,4	10	10	5	MD,6	10	10	9	10
23	3	10	4	M,6	10	10	6	M,6	6	M,6	8	M,4	9	10	9	10	10	F,2	10	10	5	MD,6	10	10	9	10
31	2	10	4	M,4	10	10	3	M,6	4	MD,6	7	M,6	9	10	9	F,6	9	F,2	10	10	4	MD,6	10	10	9	10
38	2	10	4	M,4	10	10	3	M,4	4	MD,4	5	F,2	9	10	9	F,4	9	F,2	10	10	4	MD,4	10	10	9	10
45	2	10	3	M,4	10	10	3	M,4	3	MD,4	4	D,2	9	F,4	9	F,4	9	F,2	10	10	3	MD,4	10	10	9	F,4
51	--	--	--	--	10	D,8	--	--	--	--	--	--	9	F,4	9	F,4	8	F,2	10	10	--	--	10	10	9	F,4
56	--	--	--	--	10	D,8	--	--	--	--	--	--	9	F,4	9	F,4	7	F,2	10	F,6	--	--	9	10	9	F,4
63	--	--	--	--	10	D,8	--	--	--	--	--	--	9	F,4	8	F,4	7	F,4	10	F,6	--	--	9	10	9	F,4
69	--	--	--	--	10	D,8	--	--	--	--	--	--	9	F,4	8	F,4	5	F,6	10	F,6	--	--	9	10	9	F,4
77	--	--	--	--	10	D,8	--	--	--	--	--	--	9	F,4	7	F,4	5	F,6	9	F,6	--	--	9	10	9	F,4
84	--	--	--	--	10	D,8	--	--	--	--	--	--	9	F,4	7	F,4	5	F,6	8	F,6	--	--	9	10	9	F,4
90	--	--	--	--	10	D,8	--	--	--	--	--	--	9	F,4	7	F,4	5	F,6	8	F,4	--	--	9	10	9	F,4
101	--	--	--	--	9	D,8	--	--	--	--	--	--	9	F,4	6	F,4	5	F,6	7	F,4	--	--	9	10	9	F,4
108	--	--	--	--	9	D,8	--	--	--	--	--	--	9	F,4	6	F,4	5	F,6	7	F,4	--	--	9	10	9	F,4
115	--	--	--	--	9	D,8	--	--	--	--	--	--	9	F,4	6	F,4	5	F,6	7	F,4	--	--	9	10	9	F,4
122	--	--	--	--	9	D,8	--	--	--	--	--	--	9	F,4	6	F,4	5	F,6	7	F,4	--	--	9	10	9	F,4
129	--	--	--	--	9	D,8	--	--	--	--	--	--	9	F,4	6	F,4	5	F,6	6	F,4	--	--	9	10	9	F,4
136	--	--	--	--	9	D,8	--	--	--	--	--	--	9	F,4	6	F,4	4	F,6	6	F,4	--	--	9	10	9	F,4
143	--	--	--	--	8	D,8	--	--	--	--	--	--	9	F,4	6	F,4	4	F,6	6	F,4	--	--	9	10	9	F,4
150	--	--	--	--	8	D,8	--	--	--	--	--	--	9	F,4	6	F,4	4	F,6	5	M,4	--	--	9	10	9	F,4
157	--	--	--	--	8	D,8	--	--	--	--	--	--	9	F,4	5	F,4	4	F,6	5	M,4	--	--	9	10	9	F,4
165	--	--	--	--	8	D,8	--	--	--	--	--	--	9	F,4	5	F,4	4	F,6	5	M,4	--	--	9	10	9	F,4
171	--	--	--	--	8	D,8	--	--	--	--	--	--	9	F,4	5	F,4	3	F,6	4	M,4	--	--	9	10	9	F,4
178	--	--	--	--	8	D,8	--	--	--	--	--	--	9	F,4	5	F,4	3	F,6	4	M,4	--	--	9	10	9	F,4
185	--	--	--	--	7	D,8	--	--	--	--	--	--	9	F,4	5	F,2	2	F,6	4	M,4	--	--	9	10	9	F,4
192	--	--	--	--	7	D,8	--	--	--	--	--	--	9	F,4	5	F,2	2	F,6	4	M,4	--	--	9	10	9	F,4
199	--	--	--	--	7	D,8	--	--	--	--	--	--	9	F,4	5	F,2	2	F,6	4	M,4	--	--	9	10	9	F,4
206	--	--	--	--	7	D,8	--	--	--	--	--	--	9	F,4	5	F,2	2	F,6	4	M,4	--	--	8	10	9	F,4
213	--	--	--	--	6	D,8	--	--	--	--	--	--	9	F,4	5	F,2	2	F,6	4	M,4	--	--	8	10	9	F,4
220	--	--	--	--	6	D,8	--	--	--	--	--	--	9	F,4	5	F,2	2	F,6	4	M,4	--	--	8	10	9	F,4
227	--	--	--	--	6	D,8	--	--	--	--	--	--	9	F,4	5	F,2	2	F,6	4	MD,2	--	--	8	10	9	F,4
234	--	--	--	--	6	D,8	--	--	--	--	--	--	9	F,4	5	F,2	2	M,6	4	MD,2	--	--	8	10	9	F,4
240	--	--	--	--	6	D,8	--	--	--	--	--	--	9	F,4	5	F,2	1	M,6	4	MD,2	--	--	8	10	9	F,4
255	--	--	--	--	6	D,8	--	--	--	--	--	--	9	F,4	5	F,2	1	M,6	3	MD,2	--	--	8	10	9	F,4

610: ASTM Standard D-610/68

714: ASTM Standard D-714/87 (F: Few; M: Medium; MD: Medium Dense)

Reproducible information derived from impedance data obtained for the two cells on each coated steel sheet suggests that both ionic resistance (R_m) (Fig. 6, a-b), and dielectric capacitance ($Q_1 \equiv C_m$) (Fig. 8, a-b), dependence with the exposure time point out that a quick and constant deterioration took place giving a total loss of such properties, particularly for anticorrosive and topcoat paints (samples 1 to 6) and the complete scheme (sample 11). By this reason, except sample 3 (ZRP) whose galvanic action was still active, all these samples were withdrawn from the experimental testing after 45 days immersion. As can be seen from Fig. 6 (a-b), the ionic resistance decreased with increasing exposure time. Since this resistance is inversely related to the average cross-section of the conductive pathways which allow contact between the metal and the electrolyte, these results suggest that penetration of the paint by the electrolyte solution increased with exposure. The very low values obtained for these samples coincided with the appearance of large rust spots on the specimens (Fig. 7, samples 1, 2, 4 and 6) and confirms their poor anticorrosive properties under the experimental conditions.

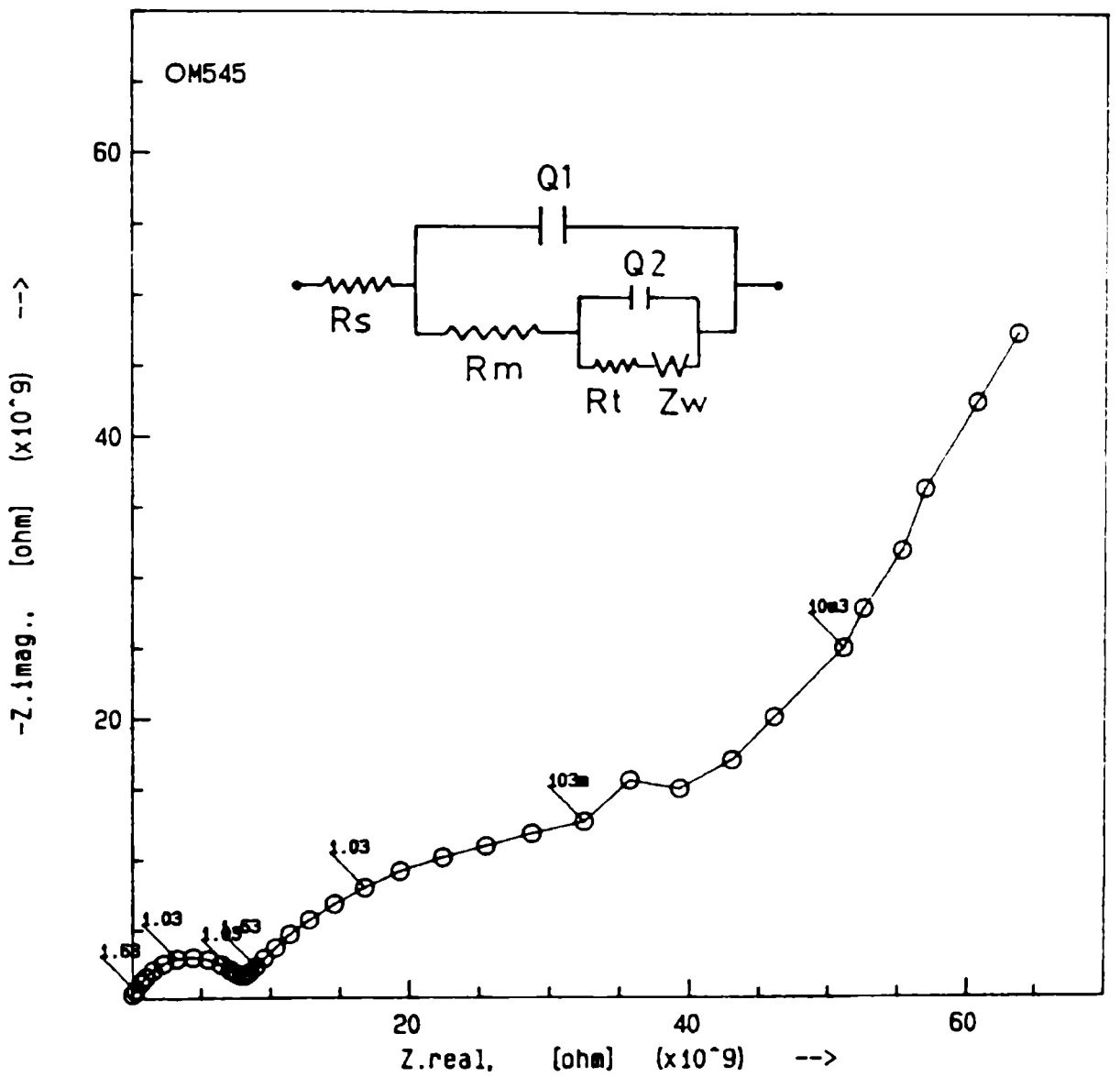

Fig. 5.- Generalized equivalent circuit.

Elapsed this period of great fluctuations, the remainder samples (7 to 13) exhibited a well differentiated behaviour up to concluding the test. So, for samples 9, 10 and 11 the slow but continuous decrease of the ionic resistance (R_m) values indicates the lost of the barrier effect afforded by the organic coating. On the other hand, the R_m of samples 7, 8, 12 and 13 showed certain stabilization in the range 10^9 - 10^{13} Ωcm^2 for almost 200 days immersion. The high anticorrosive protection in these samples was due to the great influence of the mechanism described by the barrier and insulating effect model (i.e., the paint capacity for delaying the diffusion of aggressive species up to the steel/paint interface),

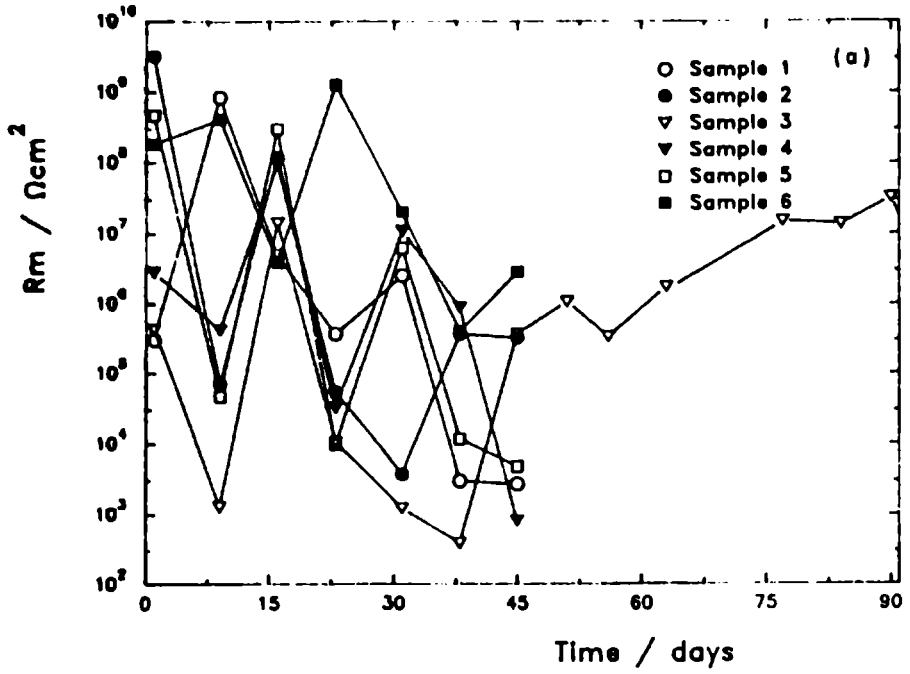

Fig. 6.- Dependence of Rm on exposure time for samples: a) 1-6; b) 7-13.

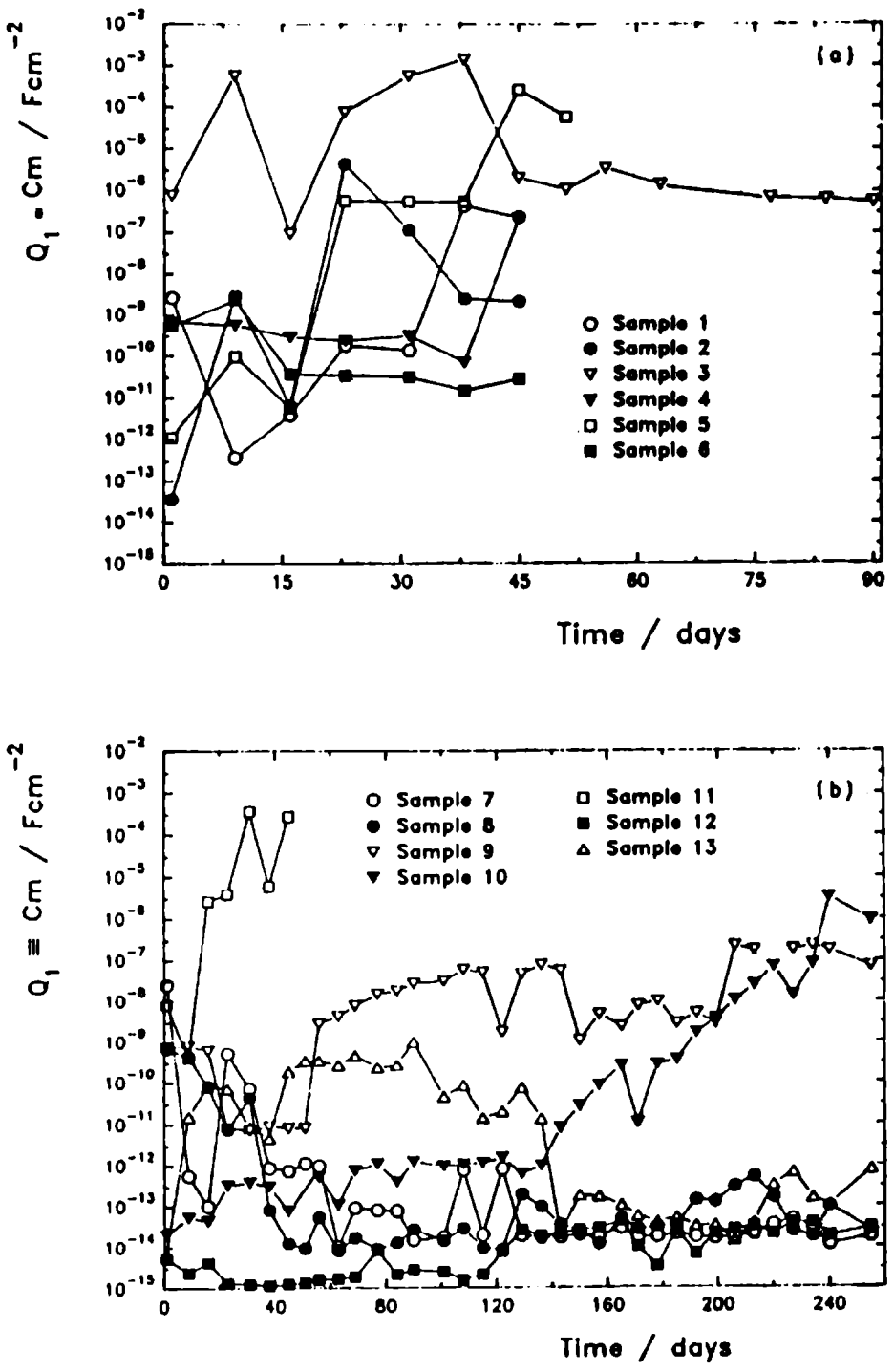

Fig. 7.- Dependence of Q1 ≡ Cm on exposure time for samples: a) 1-6; b) 7-13.

A B

C D

Fig. 8.- Photographs of samples 1, 2, 4 and 6 after 45 days immersion.

added to an effective (under these conditions) anticorrosive action of the pigments incorporated to the primers. In agreement with this mechanism, it was assumed that the steel surface was effectively kept isolated from the 3 % NaCl solution throughout the exposure time.

Referring to the dielectric capacitance ($Q_1 \equiv C_m$) dependence with the immersion time (Fig. 8, a-b), the results document that, in general, there was an ondulating performance with an initial increase in capacitance followed by some fluctuations and finally, depending on the degree of coating deterioration, it may happen that C_m either increases continuously to attain the "normal" value of an electrochemical double layer ($\cong$ 3 to 20.10^6 Fcm^{-2}) or greater (samples 1 to 5, 7, 9, 10 and 11) or else that Cm remains oscillating within a range of 1 to 3 orders of magnitude (10^{-12} - 10^{-15} Fcm^{-2}, characteristics of insulating organic coatings), for samples 7, 12 and 13.

Fig. 9 (a-b) shows the changes of the charge transfer resistance (R_t) with the immersion time. At this stage of the discussion is important to note that R_t values could only be obtained when the impedance response fitted the equivalent circuits described in either Fig. 4 or Fig. 5. It is observed a highly oscillating behaviour during the first 40-50 days immersion; changes of R_t values between 10^5 - 10^{11} Ωcm^2 denoted the progress of active (corroding) metal surface beneath the paint film when R_t decreased (due to an increase of both the pore density and the steel/electrolyte contact area), and an insulating effect of the accumulated corrosion products when R_t increased. Again, the values of this parameter and, as a consequence, the anticorrosive protective properties (lower corrosion rates), for epoxy coated steel (samples 7, 8, 12 and 13) was higher than those corresponding to the samples 1 to 5, 9 and 10, even though the differences tended to diminish as the test proceeded.

Correspondingly, as it is shown in Fig. 10 (a-b), the double layer capacitance (C_d) followed an ondulating evolution as the time elapsed. The C_d values can provide information about the extent of the underfilm corroding area as a consequence of the progressive degradation of the coating itself **[16]**.

Blistering of organic coatings applied on iron and steel is a very common phenomenon under service conditions. The lack of a quantitative explanation upon this subject is certainly due to the complexity of the phenomenon which involves physicochemical processes such as permeation of aggressive species for the system stability, loss of adhesion, coating deformation and substrate corrosion. According to Kreese **[17]**, the osmosis plays an important role in blistering due to the fact that an unidirectional transport allows the accumulation of water between the coating and the substrate. Adhesion tests performed as ASTM Standard D-4545/81 showed a poor adherence (5-12 kcm^{-2}) between the paints 1 to 6, 9, 10 and 11 and the steel, but a very high one (24-40 kcm^{-2}) for samples 7, 8, 12 and 13.

These results gave an excellent correlation with the visual assessment of corrosion and blistering, Table II, within the same cells used for impedance measurements, Fig. 6 (a-b) to Fig. 10 (a-b), as well as with the corrosion potential values, Fig. 1 (a-b). Thus, in spite of the high polarity of the epoxy resin favors the water flux into the polymer matrix, as the electrochemical parameters of samples 7, 8, 12 and 13 showed a low deterioration level and the percentage of area submitted to corrosion (ASTM Standard D-610/68) and blistering (ASTM Standard D-714/87) rating did not drop below a rust degree 8 and few (1 to 3) blisters nº 4 respectively after 255 days immersion. On the contrary, the built up with polar resins but exhibiting poor adhesion forces, samples 1 to 6, 9 and 10 displayed more corrosion (up to rust degree 2) and blistering (medium dense nº 4) after only 45 exposure days.

In brief, the E_{corr}, R_m, C_m, R_t and C_d dependence on exposure time indicated

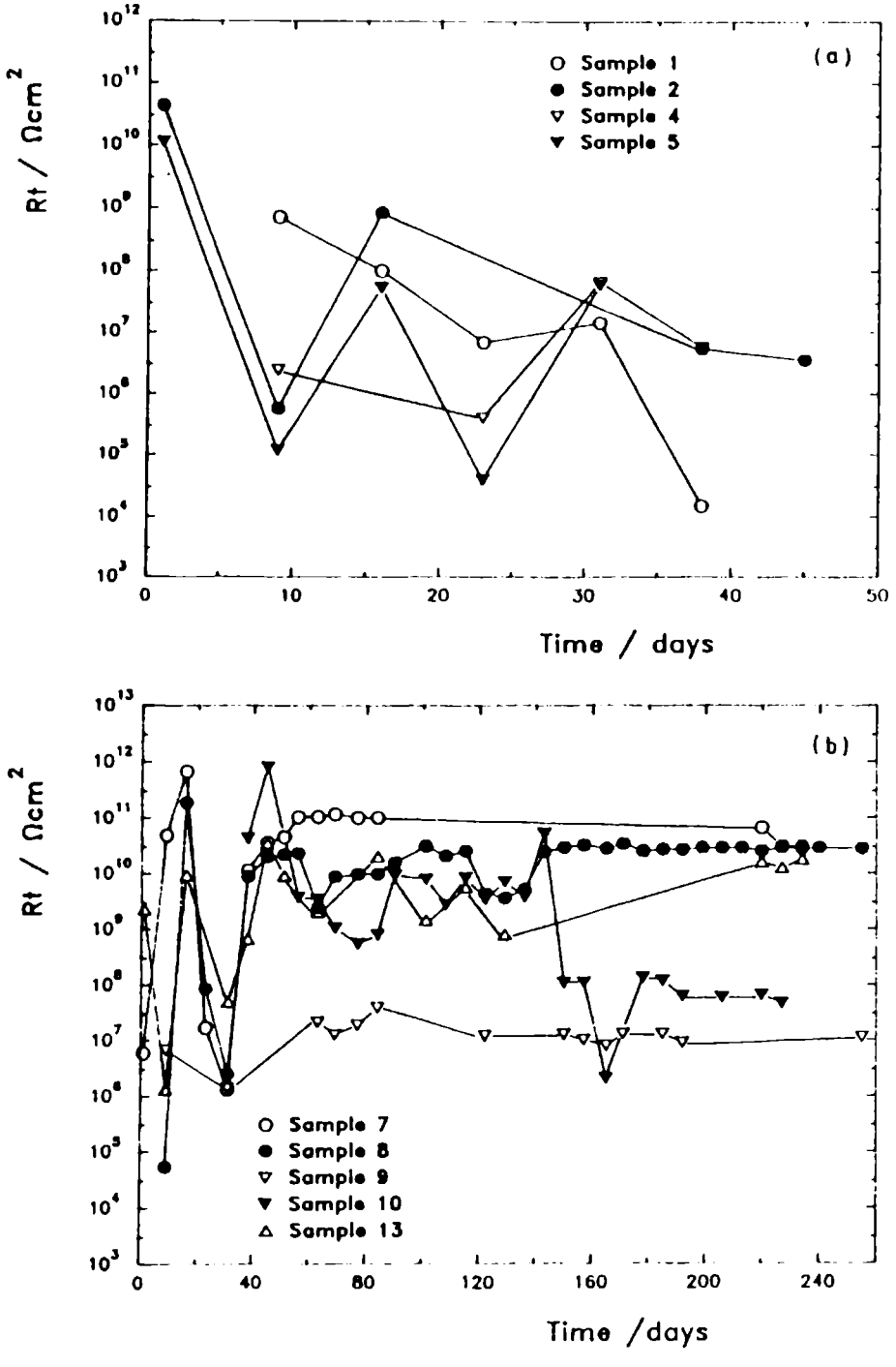

Fig. 9.- Dependence of Rt on exposure time for samples: a) 1-6; b) 7-13.

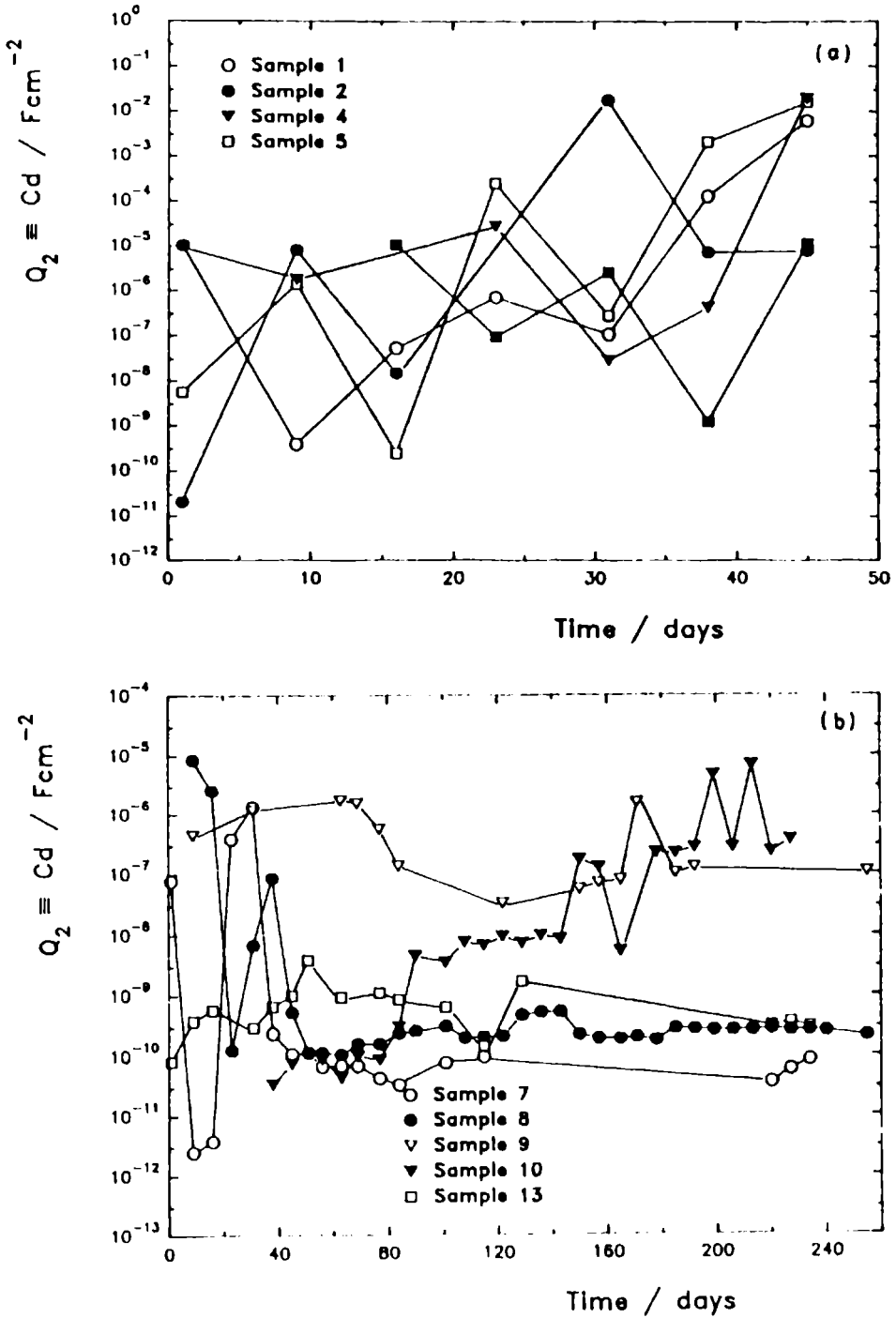

Fig. 10.- Dependence of Q2≡Cd on exposure time for samples: a) 1-6; b) 7-13.

that the gradual deterioration of the steel/paint system kept a good correlation with the characteristics observed during the periodic visual inspection. However, it must be recognized that the equivalent circuit parameters were derived with reference to the geometric area of the samples which may be different at any one time to the effective electrochemically active area. A work is in progress to eliminate this uncertainty.

CONCLUSIONS

The electrochemical analysis procedure used provided the most probable equivalent circuit. The connection and value of the different components of these circuits are such that they may be related with physical phenomena in the coated steel/electrolyte solution. Thus, the equivalent circuit models show that the high frequency response of the system can be ascribed to electrical properties of the organic coating. The effect of corrosion processes occurring at the steel/paint film interface and/or the ion mass transport through the coating, appear in the impedance diagrams at lower frequencies.

Although in some cases the effects of different processes overlap, the impedance measurements afforded valuable information about the protective properties of the paints as well as on the steel corrosion rates.

Detailed information on the rate of different degradation phenomena was obtained by correlating the fluctuations of both the equivalent circuit components and the corrosion potential values with those of the standardized visual assessment which was carried out simultaneously. It should be noted that the ratings obtained for all the paints via electrochemical measurements correlate well with that observed using visual assessment, therefore, the paints studied in the present work may be ranked in the following order of increasing anticorrosive properties:

$$1 \cong 2 \cong 4 \cong 5 \cong 6 \cong 11 < 9 < 3 < 10 < 8 < 13 \cong 7 \cong 12$$

ACKNOWLEDGEMENTS

The authors would like to thank the Comisión de Investigaciones Científicas de la Provincia de Buenos Aires (CIC), the Consejo Nacional de Investigaciones Científicas y Técnicas (CONICET) of Argentina, the Instituto Nacional de Tecnología (INT) and the Conselho Nacional de Pesquisas (CNPq) of Brasil for their financial support of this research work.

REFERENCES

[1] Scantlebury, J.D., Ho, K.N., Eden, D.A.- **Electrochemical Corrosion Testing**, Mansfeld, F. and Bertocci, U. (Ed), ASTM, STP 727, Philadelphia, PA, 187 (1981).

[2] Sekine, I.- **Corrosion Control by Organic Coatings**, Leidheiser, H. (ed)., NACE, Houston, TX, 130 (1981).

[3] Piens, M., Hubretch, J., Vereecken, J.- **Proc. 8th Int. Cong. on Metallic Corrosion**, Mainz, 1021 (1981).

[4] Padget, J.C., Moreland, P.J.- **J. Coat. Technol.**, **55**(698), 39 (1983).

[5] Hubrecht, J., Vereecken, J.- **Proc. 9th Int. Cong. on Metallic Corrosion**, Toronto, Vol. 3, 85 (1984).

[6] Hubrecht, J.C., Vereecken, J., Piens M.- **J. Electrochem. Soc., 131**, 2010 (1984).

[7] Mansfeld, F., Kendig, M.W.- **Laboratory Corrosion Tests and Standards**, Haynes, G.S. and Baboian, R. (Ed.), ASTM, STP866, Philadelphia, PA, 122 (1985).

[8] Moreland, P.J., Padget, J.C.- **Polymeric Materials for Corrosion Control**, Dickie, R.A. and Floyd, F.L. (Ed.), ACS Symp. 322, Washington, DC, American Chemical Soc., 18 (1986).

[9] Vijayan, C.P., Noel, D., Hecker, J.J.- **Polymeric Materials for Corrosion Control**, Dickie, R.A. and Floyd, F.L. (Ed.), ACS Symp.322, Washington, DC, American Chemical Soc., 58 (1986).

[10] Azim, S.S., Guruviah, S.- **Proc. 10th Int. Cong. on Metallic Corrosion**, Madras, 1393 (1987).

[11] Leidheiser, H.- **Corrosion Control by Coatings**, Leidheiser, H. (Ed.), NY, Science Press, 143 (1979).

[12] Boukamp, B.A., Report CT88/265/128, CT89/214/128, University of Twente, Netherland, may 1989.

[13] Armas, R.A., Real, S.G., Gervasi, C., Di Sarli, A.R., Vilche, J.R.- **Corrosion** (NACE), **48**(5), 379 (1992).

[14] Szauer, T., Brandt, A.- **J. Oil Col. Chem. Assoc., 67**, 13 (1984).

[15] Frydrych, D.J., Farrington, G.C., Townsend, H.E.- **Corrosion Protection by Organic Coatings**, Kendig, M.W., Leidheiser, H. (Ed.), The Electrochem. Soc. Inc., Pennington, NJ, vol.87-2, 240 (1987).

[16] Callow, L.M., Scantlebury, J.D.- **J. Oil Col Chem. Assoc., 64**, 119 (1981).

[17] Kreese, P.- **Farbe und Lack, 72**, 1179 (1966).

Note.- Submitted for publication in Corrosion Science.

MACROFOULING COMMUNITY AT MAR DEL PLATA HARBOR (1991-92): RECRUITMENT AND STRUCTURE

LA COMUNIDAD DE "MACROFOULING" EN EL PUERTO DE MAR DEL PLATA (1991-92): RECLUTAMIENTO Y ESTRUCTURA

Silvia Pezzani[1] , Miriam Pérez[2] and Mirta Stupak[2]

SUMMARY

The fouling community was examined from May 1991 to April 1992 at Mar del Plata harbor. The aim of this work was to establish the recruitment trends of macrosessile foulers, to make a comparison with previous papers and to examine the seasonal developmental sequence of the community; for that, unglazed ceramic panels were employed. Data corresponding to the abundance percentages of the species/panel/months, were analyzed throughout the clustering method using the Bray-Curtis Similarity Index (NTSYS program). Multivariate cluster analysis revealed two underlying trends of recruitment species assemblages. One of these, from late Autumn to Spring and the other one, from Summer to early Autumn. Ciona intestinalis had an important functional role in the community, as an adult might enhance the arrivals of some species as secondary space recruiters, but also was a good interference competitor for primary space occupiers. In Summer, the larvae of Ciona showed to be a poor competitor for seasonal primary space occupiers and the structure of the community was affected. This community developed a similar pathway of other fouling communities with solitary ascidian species.

Keywords: *macrofouling community, recruitment, structure, ascidian, barnacles.*

INTRODUCTION

In Mar del Plata harbor some studies about descriptive aspects on fouling community were carried out (Bastida, 1971; Bastida and Adabbo, 1977; Bastida *et al.*, 1980; Stupak *et al.*, 1980). They were interrupted and there have existed a gap of about fourteen years. At the beginning of this decade, some changes in the fouling composition were directly observed in the field.

The changes in epibenthic community structure through the time may involve several mechanisms. These changes result from the balance between physical and biological interactions. The resident species assemblages may depend of the outcome of the settlement, survival, and life cycles of the earlier and later species (Sutherland and Karlson, 1973, Levin and Paine, 1974; Menge and Sutherland, 1976; Karlson, 1978; Menge, 1978; Sousa, 1980; Ayling, 1981; Sutherland, 1981; Chalmer, 1982; Field, 1982; Greene and Schoener, 1982, 1984; Otsuka and Dauer, 1982).

[1] Departamento Biología, Fac. Cs. Exactas y Naturales, U.N. de Mar del Plata

[2] CIDEPINT

The local current adjacent to the substratum, the conditions in water column and the physical characteristics of the substratum make more attractive or prevent the attachment of the planktonic propagules (Williams, 1964; Dayton, 1971; Foster, 1975; Russ, 1980; Connell, 1985). In addition, earlier successional species may enhance or inhibit the arrival of later species by providing suitable or unsuitable environmental conditions. These species may render secondary substratum for other ones which overgrowth them, trap sediments which may enhance the arrival of build sediment tubes invertebrates or provide refuge from predators (Sutherland, 1974; Breitburg, 1985; Young, 1986). However, the primary space occupied by early colonists, the predation on planktonic larvae or on settlers and the filtered out of propagules may reduce or exclude potential larval settlement or survival of some species in the community (Dayton, 1971; Standing, 1976; Jackson, 1977; Sutherland, 1978; Dean and Hurd, 1980; Dean 1981).

Bare space opened by some disturbances, such as predation or slough off, may be invaded by other species (Smedes and Hurd, 1981). However, colonization of the open space may be affected or not by its size or shape as well as by biological aspects of surrounding species (Paine and Levin, 1981; Dayton *et al.*,1984; Young and Gotelli, 1988).

The aim of the present study is to find the answer to the following questions: 1) which are the recruitment trends of macrosessile foulers?, 2) what changes did occur in the community after a gap of about 14 years?, and 3) how do the recruitment of the species contribute to the established community?.

MATERIALS AND METHODS

Mar del Plata harbor, is situated in Buenos Aires province (38^0 02'S - 57^0 32'W); is an important harbor with a naval complex, fishery industries and nautical recreation. The study site was located inner the harbor at Club de Motonáutica (Fig.1).

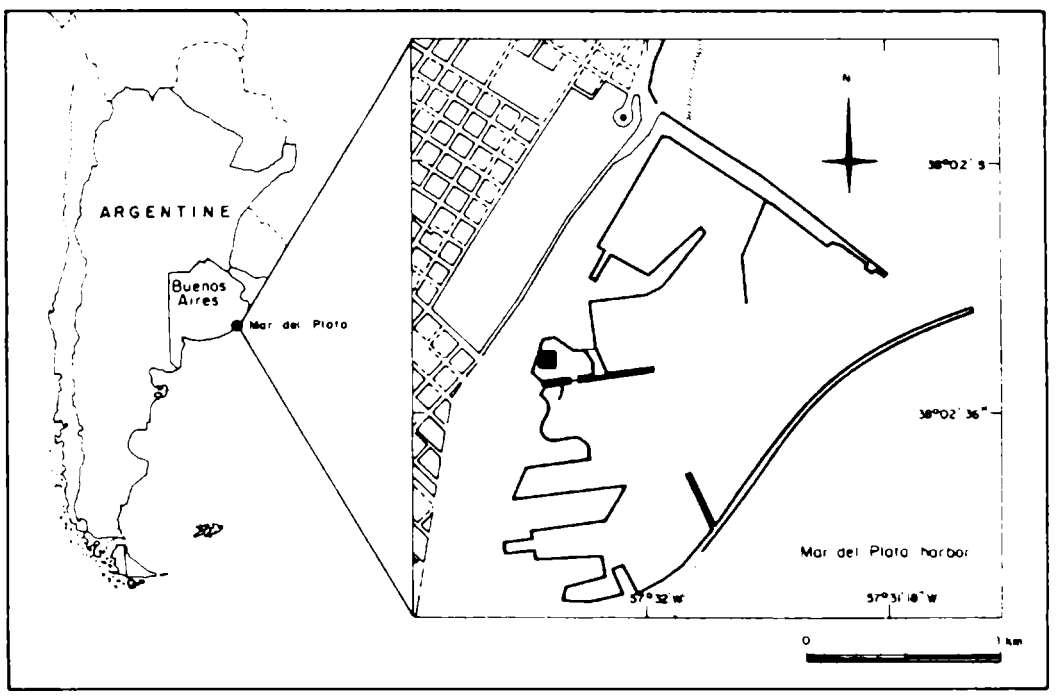

Fig. 1.- Site of study and location of test panels series (■).

The study was carried out from May 1991 to April 1992. Fouling organisms were collected by submerging 128 cm^2 unglazed ceramic tiles, with the front smooth and the back with concavities. Thirteen test panels series, with three replicas every one, were suspended from floating docks. Every month one series was removed to estimate the recruitment of macrosessile species, and was immediately replaced by

clean ones (monthly-panels). The others twelve series were removed one every month to follow the development of established community from the beginning of the exposition (accumulative-panels). Each series comprised four panels which were hung vertically from 0.3 m to 1.5 m below the water surface, with a constant distance of 20 cm from each other. The front and the back surface of the panels, from the top to the bottom were labeled as: **A,a**; **B,b**; **C,c** and **D,d**, respectively. The fouled panels were placed in plastic cages and preserved in 4% neutral solution of formalin in sea water.

Macrofouling conspicuous species on monthly and accumulative-panels were recorded. Microorganisms, motile and occasional species were not included in this analysis. Individuals were keyed to species when possible. *Enteromorpha intestinalis*, *Tubularia crocea*, *Obelia longissima*, *Polydora ligni*, *Hydroides elegans*, *Balanus amphitrite*, *Balanus* sp., *Bugula stolonifera*, *Ciona intestinalis* and colonial ascidian were recorded on the monthly-panels. In addition of these species, *Ceramium* sp., *Balanus trigonus* and *Bowerbankia gracilis* were mainly observed on the accumulative-panels, but the colonial ascidians were not recorded.

The abundance of sessile species was estimated by recording the occurrence of them in a grid of random sets marked in 1 cm^2 quadrats over all panels. The outer 1 cm margin of the plates was excluded from examination to avoid an "edge effect" (Foster, 1975). New sets of random quadrats were used for each panel/replicate/month. Five abundance categories were used: 0%, 1–25%, 26–50%, 51–75% and 76–100%. These categories were based on abundance percentages (averaged from the replica panels) for each species/panel/month.

The abundance percentages of each species/panel/month were analyzed by a multivariate clustering method, using the Bray Curtis similarity index (NTSYS-program). Dendrograms were constructed using the unweighted pair group method, arithmetic average (UPGMA) portray the similarity between the taxa list of all monthly-panels and seasonal accumulative-panels. Monthly dendrogram was the output of the data matrix between the abundance percentage of each 10 species recorded and 96 separate individuals (representing 8 panels for each of 12 sampling dates). Seasonal accumulative dendrograms were the output of the data matrices between the abundance percentage from each 12 species recorded and 16 separate individuals (8 panels for each 2 sampling dates, one for late Autumn: May and June '91, and the other for Winter: July and September '91, August panels lost), 24 separate individuals (8 panels for each 3 sampling dates; Spring: October to December'91) and 32 separate individuals (8 panels for each 4 sampling dates, Summer-early Autumn: January to April'92).

RESULTS

Recruitment

A dendrogram with the relationships among recruitment panels and the corresponding abundance percentages of species are illustrated in Figure 2. The dendrogram shows two major groups (G1 and G2); the first one includes three subgroups, late Autumn: May-June'91 (G1G1), Winter: July-August-September'91 (G1G2) and Spring: October-November-December'91 (G1G3); and the other one with two subgroups, the Summer: January-February'92 (G2G1) and early Autumn: March-April'92 (G2G2). The level of similarity intragroup indicated that the recruitment intensity of most of the species had slight differences between the back and the front of the panels and the depths.

At the beginning of the experiences, in Autumn (G1G1), *Polydora*, *Enteromorpha* and *Ciona* were the most abundant species. Although *Balanus amphitrite* was observed at low abundance, the back of the panel showed heavier recruitment than the front.

Fig. 2 - Dendrogram corresponding to the monthly-panels. The right portion of the figure represents the seasonal average percentage abundance, G1-G1: late Autumn, G1-G2: Winter, G1-G3: Spring, G2-G1: Summer, G2-G2: early Autumn.

Tubularia, *Obelia*, *Hydroides*, *Balanus* sp., *Bugula* and colonial ascidians abundances were also low. Panel **D** December was enclosed in this subgroup because of the low observed abundance of *B.amphitrite*.

In Winter (G1G2), *Enteromorpha* was the main recruit, *Polydora* and *Ciona* appeared in a lesser density. There were not recruitment of *Tubularia*, *Hydroides*, *Balanus* sp., *Bugula* and colonial ascidians.

In Spring (G1G3) *Enteromorpha* and *Polydora* were the predominant taxa. The recruitment of the others species was poor. Both **A** and **B** January panels were enclosed in this subgroup because of there was a heavier recruitment of *Enteromorpha* on these two panels.

In Summer (G2G1), *Polydora* and *Ciona*, *Hydroides* and *B.amphitrite*, were the most representative species assemblages. On the other hand, *Enteromorpha* declined in abundance.

By the end of the study, late Summer to early Autumn (G2G2), colonies of *Obelia*, *Polydora* and *Hydroides* were important recruits. This period was also characterized by a decline in *B.amphitrite* and *Ciona* abundances. *Enteromorpha*, *Tubularia*, *Bugula* and colonial ascidians were not present in this period.

Enteromorpha, *Obelia*, *Polydora*, *Hydroides*, *B.amphitrite*, and *Ciona* were the main species recruits on primary space. These species were accompanied by *Tubularia*, *Balanus* sp., *Ciona* and *Bugula* which occurred in seasonal patterns with low abundance percentages.

Community structure

The development of the community by seasonal dendrograms and average abundance percentages of the species are illustrated in Figures 3 to 6.

In late Autumn (Fig.3), the initial structure of the fouling community were dominated by *Enteromorpha* and *Polydora*, *Obelia*, *Balanus amphitrite* and *Ciona*. On the other hand, *Ceramium* sp., *Tubularia*, *Hydroides*, *Balanus* sp., *B.trigonus* and *Bowerbankia*, were found in low abundances.

In Winter (Fig.4), *Ciona* grew rapidly and a high recruitment on primary space was observed as well as over the previously attached individuals. *Ciona* became the dominant species and provided secondary space for recruitment mainly of *Polydora*, *Obelia*, and *Bugula* which grew sharply; motile species occurred among them. Species observed on primary space such as *Enteromorpha*, *Polydora*, *Hydroides* and *Balanus* sp. were maintained alive beneath *Ciona* in a low percentage but they did not grow; other taxa died as *B.amphitrite*, *B.trigonus* and *Bowerbankia*. In September, *Ciona* began to slough off, took with it the overgrown species and opened new free spaces.

Towards Spring (Fig.5), *Ciona* increased steadily in abundance by the persistence of the old cohort and new recruitments on free space occurred. During this season *Obelia*, *Polydora*, *Bugula* and *Bowerbankia* were overgrowing *Ciona* and then increasing its abundance. In spite of *Enteromorpha*, *Hydroides* and *Balanus* sp. arrivals, large amount of bare space persisted. In October, recruited species on monthly-panels did not arrive on the free space left by *Ciona* detachment, except *Enteromorpha* and *Bowerbankia* which recruited far from *Ciona* individuals.

In Summer (Fig.6), *Ciona* decreased up to low abundance, (except in two panels where this species was dominant) although a heavy recruitment was observed on monthly-panels. From February to April the opened space left by *Ciona* was invaded

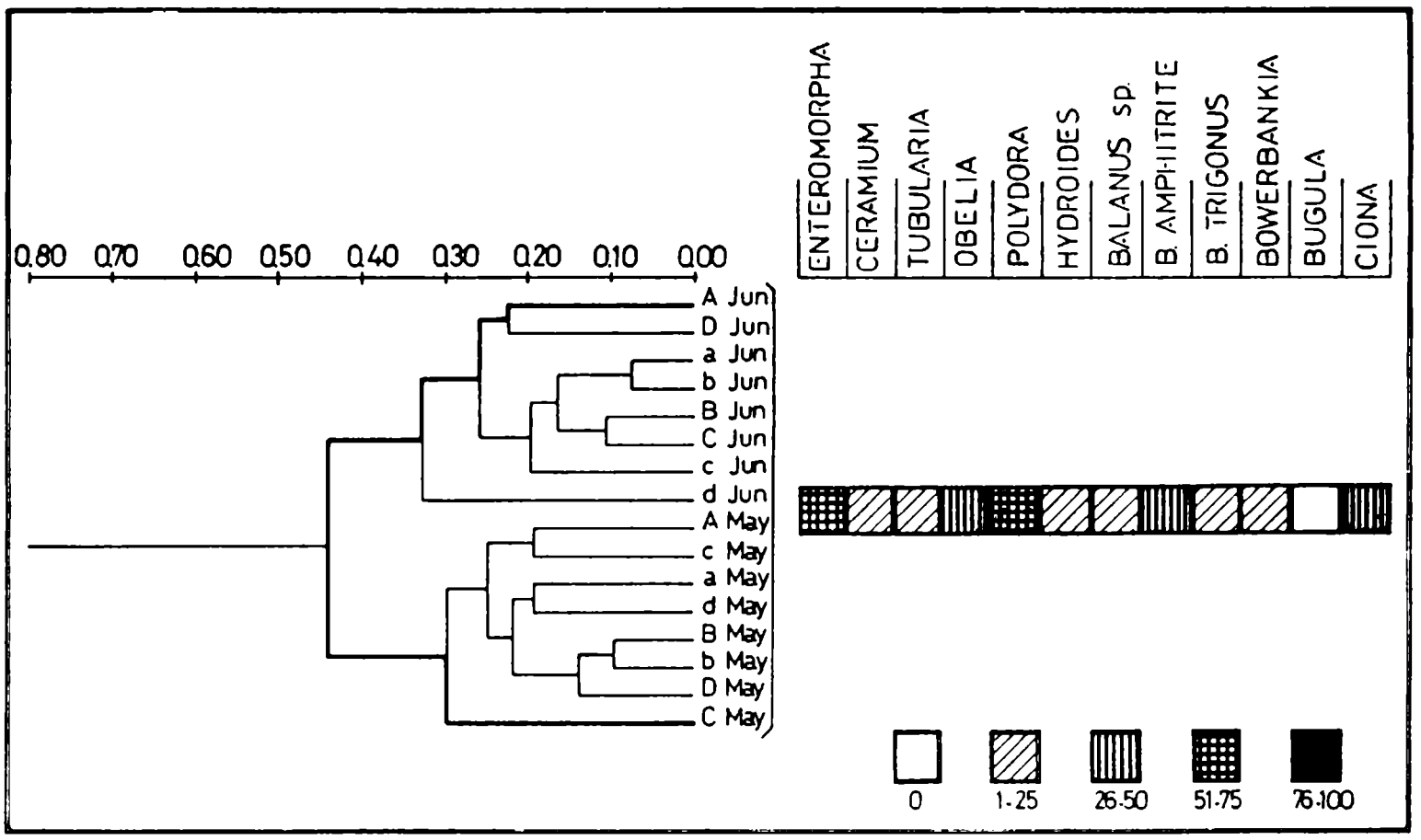

Fig. 3.- Dendrogram showing the accumulative-panels corresponding to late Autumn. The right portion of the figure represents the average percentage abundance.

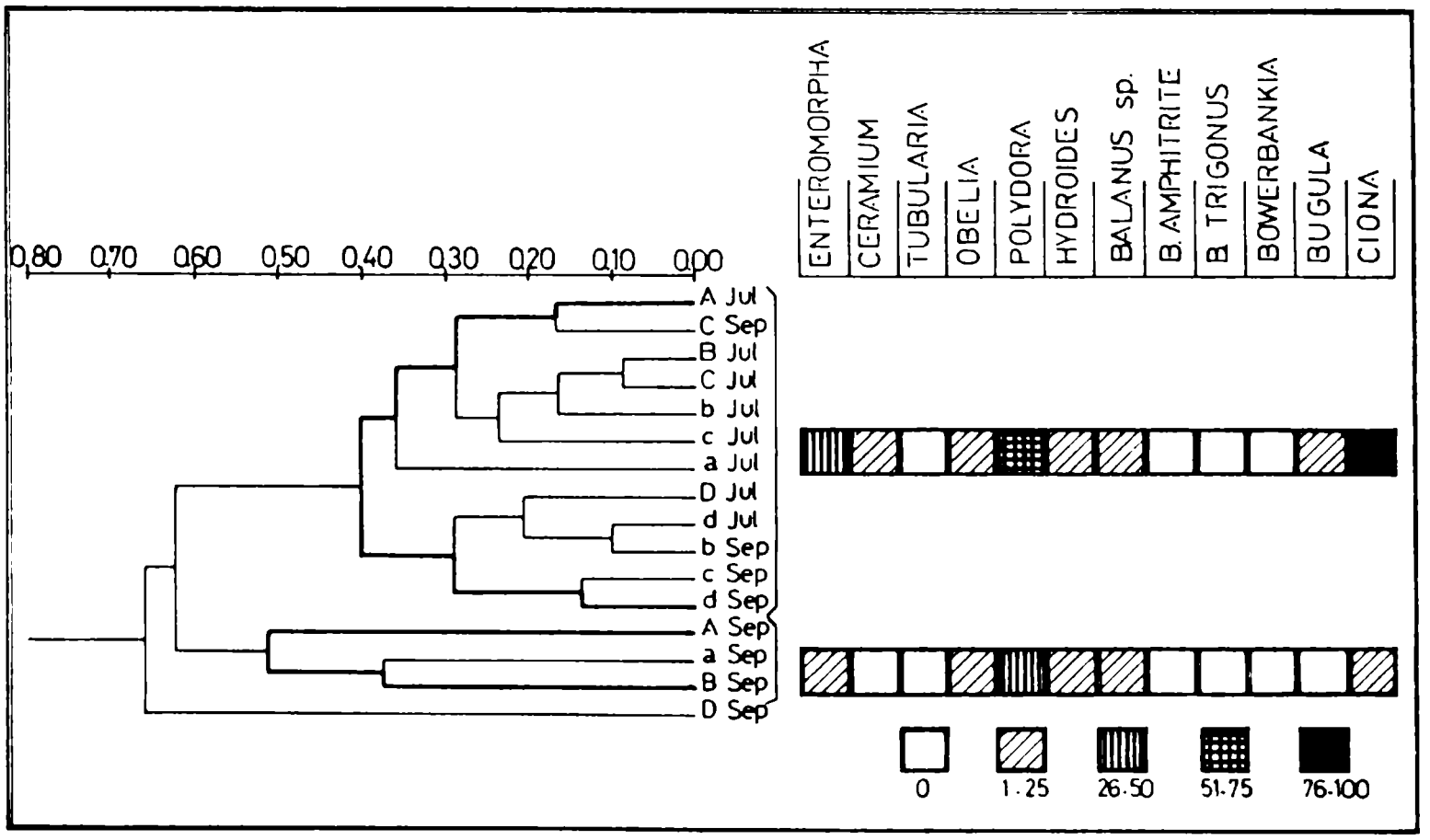

Fig. 4.- Dendrogram showing the accumulative-panels corresponding to Winter. The right portion of the figure represents the average percentage abundance.

by *Hydroides* and *B.amphitrite*. Additionally, these species became the major occupiers by their fast growth and provided secondary space for new recruits of themself, and other species such as *Obelia*, *Polydora*, *Bugula* and *Bowerbankia*. The species of *Balanus* underwent high mortality due to heavy overgrowth of some species which smothered them. *Hydroides* grew up off the substratum and its survival was higher.

DISCUSSION

Two main recruitment trends of the species assemblages on primary space were observed. One of these, from late Autumn to Spring (G1) in which *Polydora* and *Enteromorpha* had a marked recruitment; *Ciona* shown one peak of the arrival of recruits and then remained at low abundance as well as the other species. Another one, from Summer to early Autumn (G2) was characterized by *Polydora*, *Ciona*, *Balanus amphitrite*, *Hydroides* and *Obelia* arrivals.

In the present study a comparison with those carried out in 1966-69, 1969-70, 1973-74 and 1976-77 (Bastida, 1971; Bastida and Adabbo, 1977; Bastida *et al.*, 1980; Stupak *et al.*, 1980, respectively) at Mar del Plata harbor was made. In those studies, methodology differed in some aspects from the present test, it was used an experimental raft and sandblasted inert acrylic panels. Capitoli (1983) found that there are not significative differences in settlement between sandblasted acrylic and unglazed ceramic tiles. The abundance and composition of some macrosessile organisms showed certain differences between previous studies and the present one, some of these fluctuations are summarized below:

a) Changes in settlement cycles.

Enteromorpha intestinalis was the only green algae attached on our panels; it was registered in a greater abundance at different depths nearly all the year round. Due to water transparency during colder months, panels C and D showed a higher abundance percentage. In warmer months, fishery industries increase its activity and waste organic matter to the sea; consequently, transparency diminishes and only panel A receives sufficient light to allow *Enteromorpha* settlement. This suggests that this species is more limited by light entrance than water temperature, which has influence on growth rate organisms; in warmer months we observed a lesser abundance of *Enteromorpha* but of a greater size.

Tubularia crocea and *Bugula stolonifera* were found with lesser abundance than other studies.

Settlement cycle of *Balanus amphitrite* was longer; it was observed during Winter months at different depths although in low densities. It showed a marked preference to settle on the back of the panels, where the surface has concavities. It seems probable that cyprids select these pits for their attachment; this situation offers protection during the period immediately after metamorphosis (Forbes *et al.*, 1971; Crisp and Bourget, 1985).

b) Species which have not been recorded at the present period.

Among the species which have not been registered but present at different abundance in other periods, it can be mentioned: *Bryopsis plumosa*, *Chaetomorpha* spp., *Ulothrix pseudoflacca*, *Ulva lactuca*, *Ectocarpus* sp., *Polysiphonia* sp., *Mytilus platensis*, *Pachysiphonaria lessoni*, *Serpula vermicularis*, *Ficopomatus enigmaticus*, *Hydroides plateni*, *Conopeum* sp. and other species with a low abundance (Bastida, 1971; Bastida and Adabbo, 1977; Bastida *et al.*, 1980; Stupak *et al.*, 1980).

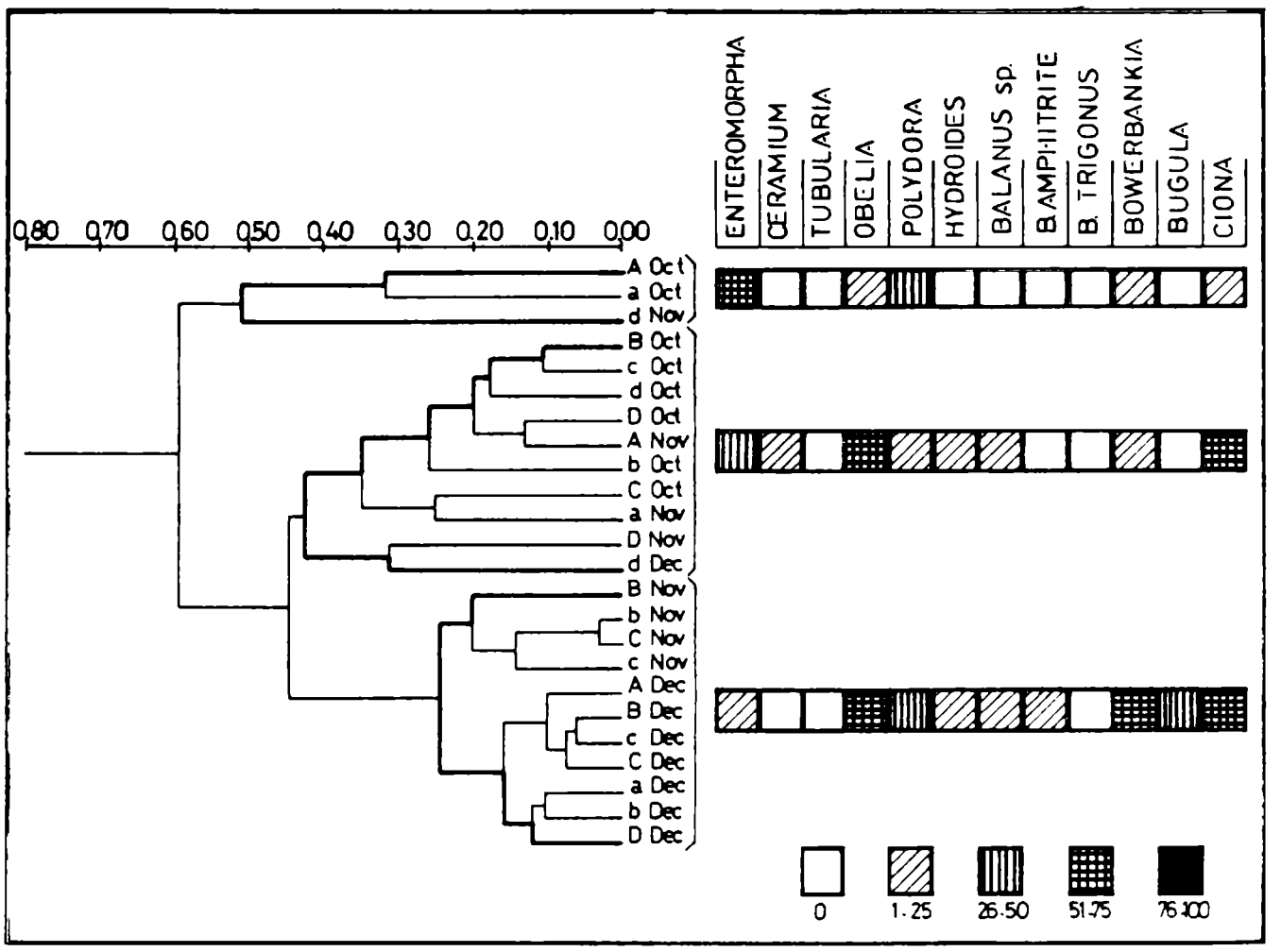

Fig. 5.- Dendrogram showing the accumulative-panels corresponding to Spring. The right portion of the figure represents the average percentage abundance.

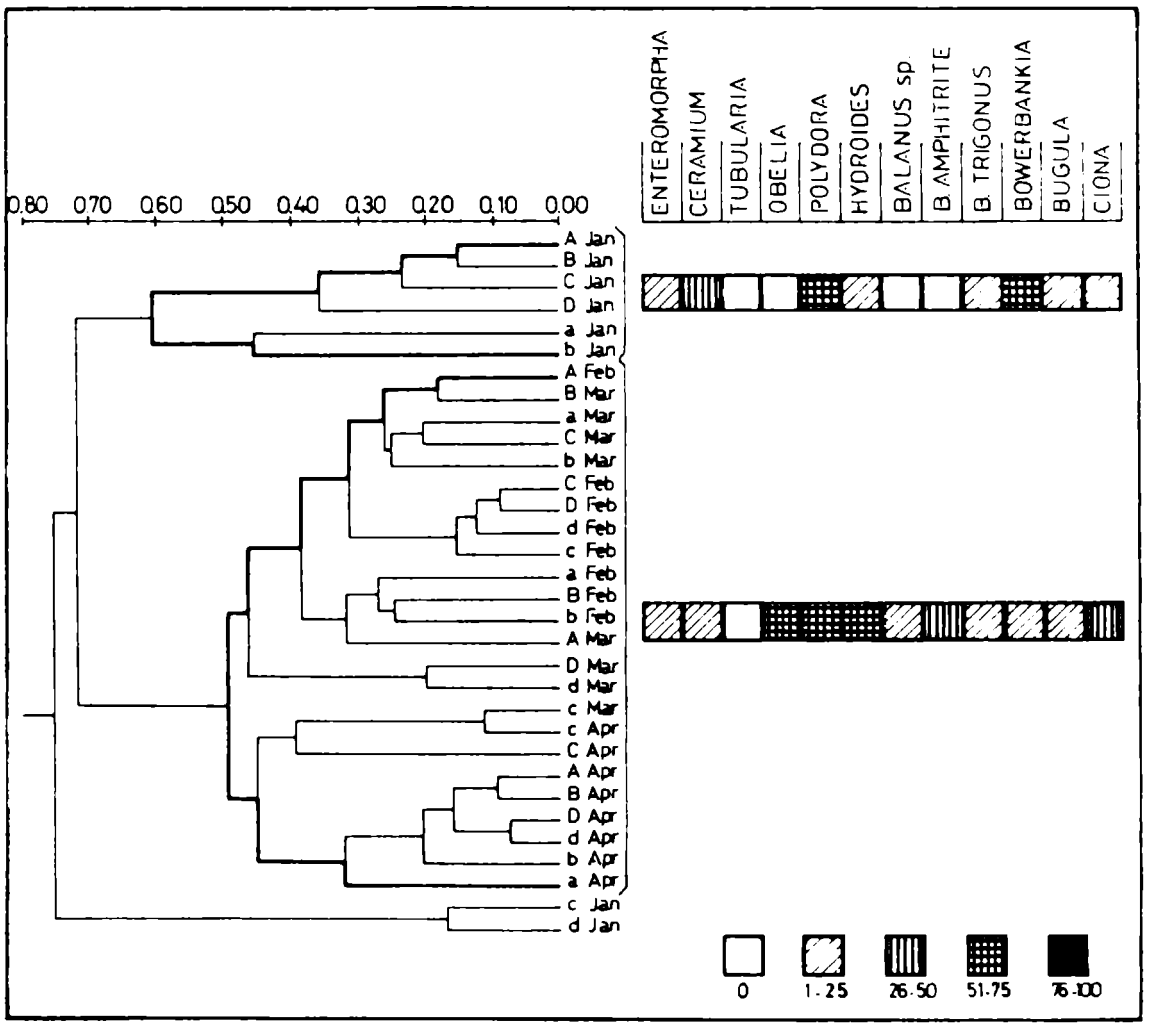

Fig. 6.- Dendrogram showing the accumulative-panels corresponding to Summer-early Autumn. The right portion of the figure represents the average percentage abundance.

c) Species registered mainly on accumulative panels.

Ceramium sp., *Balanus trigonus* and *Bowerbankia gracilis*; in other studies these taxa appeared on both monthly and accumulative-panels (Bastida, 1971; Bastida and Adabbo, 1977; Bastida *et al.*, 1980; Stupak *et al.*, 1980).

Differences found between species and certain settlement cycles in the present work and previous studies, may due to waste discharges by fishery industries and/or stochastic events. In spite of those changes, the local macrofouling community developed towards a similar community structure.

The population of *Ciona intestinalis* was one of the main components of the community. This species during its establishment and fast growth monopolizes the primary space, entraps sediments, provides vertical structure and secondary substratum which appear to enhance or to inhibit the recruitment of some species, as well as, to depress the growth of other ones.

In Winter and Spring, later cohorts of *Ciona* recruited directly onto established individuals in a higher density to the expected settlement for monthly-panels during the same period. This suggests that recruitment may be enhanced by conspecific adults. Moreover, the presence of *Ciona* mainly enhances settlement of secondary space occupiers as *Obelia* and *Bugula*. Ascidian-hydroid-bryozoan assemblage increases the recruitment of sediment-tube-worm *Polydora* and detritivore motile species upon them. Breitburg (1985) found a similar condition by trap sediment species which enhance the arrival of dwelling-sediment-tube species.

Enteromorpha was never recruited when *Ciona* monopolized the community, although the monthly-panels showed a heavy recruitment which would indicate that arrivals may potentially occur. Standing (1976) suggested that *Obelia* canopies may inhibit *Balanus* recruitment by blocked contact between larvae and substratum. Vertical structure developed by *Ciona* may constitute a similar physic barrier for *Enteromorpha* propagules. However, *B.amphitrite*, *B.trigonus* and *Bowerbankia*, attached on primary space, could not be able to expose their feeding apertures above ascidian and then died. Osman (1977) and Otsuka and Dauer (1982) pointed out that suspension-feeders species are able to survive in the community when the feeding apertures remain open to the water column. Standing (1976) reported in Bodega Harbor that when barnacles are beneath ascidian, they smother.

Ciona also inhibits the invasion of the bare space when began to slough off. The arrival of some species observed on monthly-panels did not occur in the community, only *Enteromorpha* and *Bowerbankia* attached, but far from ascidian individuals. At this time, *Ciona* reaches large size and may inhibit the arrival of species by whiplashing effect. Lewis (1964) suggested similar effects of fucoid fronds on cyprids and spat.

From Winter to Spring *Ciona* was a good interference competitor as an adult and resisted propagules recruitment on primary space. This is in agree with the ascidian *Styela* which resists invasion of other species in fouling community (Sutherland, 1974, 1978, 1981; Sutherland and Karlson, 1977). In addition, Dean (1981), suggested that tunicates and hydroids (based on structural mimic) inhibit the arrival of barnacles and tube-worms by structural effects.

Ciona had a heavy recruitment during Summer on monthly-panels but shown its inability to invade the community. This indicates that its larvae are poor competitors when *Hydroides* and *Balanus* have a heavy arrival of recruiters and a fast growth. Otsuka and Dauer (1982) suggested that adults of *Balanus* are effective competitors to the recruitment and establishment of *Molgula* ascidian by its knocking off with their opercula.

The recruitment of *Ceramium* and *Bowerbankia*, were found only onto established community. This suggests that these species have preference to arrive on established species assemblages in the community more than free space available. This is in agree with other communities where the recruitment of some species is less frequently or do not occur until the substratum is occupied by previous colonists (Haderlie, 1974; Dean, 1981; Osman, 1982; Breitburg, 1985).

Polydora recruited all the year round and was an important contributor to the community as primary and secondary space occupier. Recruitment and growth of *Polydora* was unaffected by the resident assemblage species.

In this study at Mar del Plata harbor, the fouling community was structured from Autumn to Spring by the dominant population of *Ciona*, and from Summer to early Autumn was structured by populations of different species of *Balanus* and *Hydroides*, which are overgrown by the same species assemblages. This annual structural change began when *Ciona* sloughed off and perturbed the community in late Spring. This tunicate took the overgrown species and rendered open space steadily. Then, the bare substratum was invaded by species with calcareous exoskeleton, such as barnacles and serpulids tube-worms. Likewise, in 1976-77 (Stupak *et al.*, 1980), *Ciona* was replaced by *Mytilus platensis* instead serpulids which were not registered in that period. This is in agree with other fouling communities which appear to develop similar pathways when solitary ascidians are present. Sutherland (1974, 1981), in Beaufort, observed the replace of solitary ascidian *Styela* by the bryozoan *Schizoporella*. Otsuka and Dauer (1982), in Lynnhaven Bay, found the replace of solitary ascidian *Molgula* by the bryozoan *Membranipora* and the barnacle *Balanus* sp.. Greene and Schoener (1984) in Manchester reported the replace of ascidians by the barnacle *Balanus* and the tube-worm *Serpula*; fouling communities without solitary ascidians occurrence undergo different pathways in their structure.

ACKNOWLEDGEMENTS

The authors would like to thank the Comisión de Investigaciones Científicas de la Provincia de Buenos Aires (CIC), the Consejo Nacional de Investigaciones Científicas y Técnicas (CONICET) for their support. We also would wish to thank Club de Motonáutica de Mar del Plata for the use of their marine testing site, and to Dr. Cecilia Elsner, Mrs. Viviana Segura, and Ms. Mónica García for their valuable assistences.

REFERENCES

Ayling A. M. (1981).- The role of biological disturbance in temperate subtidal encrusting communities. **Ecology**, **62** (3), 830-847.

Bastida R. O. (1971).- Las incrustaciones biológicas de las costas argentinas. La fijación anual en el puerto de Mar del Plata durante tres años consecutivos. **Corrosión y Protección**, **2** (1), 21-37.

Bastida R. and H. Adabbo (1977).- Fijación de "fouling" en el puerto de Mar del Plata. **Corrosión y Protección**, **8** (5), 1-14.

Bastida R., M. T. de Mandri, V. L. de Bastida and M. Stupak (1980).- Ecological aspects of the marine fouling at the Port of Mar del Plata, Argentina, during the period 1973/74. **Proceedings V Congreso Internacional en Corrosión Marina e Incrustaciones**, Biología Marina. Barcelona, España, 299-320.

Breitburg D. L. (1985).- Development of a subtidal epibenthic community: factors

affecting species composition and the mechanisms of succession. **Oecologia** (Berlin), **65**, 173-184.

Capitoli R. R. (1983).- Sequência temporal de colonização e desenvolvimento da comunidade incrustante na região mixohalina da Lagoa dos Patos; RS, Brasil. Tesis. Universidade do Rio Grande, 99 pp.

Connell J. H. (1985).- The consequences of variation in initial settlement vs. post-settlement mortality in rocky intertidal communities. **J. Exp. Mar. Biol. Ecol., 93**, 11-45.

Crisp D. J. and E. Bourget (1985).- Growth in barnacles. **Advances in Marine Biology, 22**, 199-244.

Chalmer P. N. (1982).- Settlement patterns of species in a marine fouling community and some mechanisms of succession. **J. Exp. Mar. Biol. Ecol., 58** (1), 73-85.

Dayton P. K. (1971).- Competition, disturbance, and community organization: the provision and subsequent utilization of space in a rocky intertidal community. **Ecol. Monogr., 41**, 351-389.

Dayton P. K., V. Currie, T. Gerrodette, B. Keller, R. Rosenthal and D. Tresca (1984).- Patch dynamics and stability of some California kelp communities. **Ecol. Monogr., 54**, 253-289.

Dean T. A. (1981).- Structural aspects of sessile invertebrates as organizing forces in an estuarine fouling community. **J. Exp. Mar. Biol. Ecol., 53** (2-3), 163-180.

Dean T. A. and L. E. Hurd (1980).- Development in an estuarine fouling community: the influence of early colonists on later arrivals. **Oecologia** (Berlin), **46**, 295-301.

Field B. (1982).- Structural analysis of fouling community development in the Damariscotta river estuary, Maine. **J. Exp. Mar. Biol. Ecol., 57** (1), 25-33.

Forbes L., M. J. B. Seward and D. J. Crisp (1971).- Orientation to light and the shading response in barnacles. **4th European Marine Biology Symposium**, 539-558.

Foster M. S. (1975).- Regulation of algal community development in a *Macrocystis pyrifera* forest. **Mar. Biol., 32**, 331-342.

Greene C. H. and A. Schoener (1982).- Succession on marine hard substrata: a fixed lottery. **Oecologia** (Berlin), **55**, 289-297.

Greene C. H. and A. Schoener (1984).- Multivariate analysis of three-dimensional data in the study of succession in marine fouling communities. **6th International Congress on Marine Corrosion and Fouling**, Marine Biology. Athens, Greece, 221-235.

Haderlie E. C. (1974).- Growth rates, depth preference and ecological succession of some sessile marine invertebrates in Monterrey Harbor. **Veliger, 17**, 1-35.

Jacksony J. B. (1977).- Competition on marine hard substrata: the adaptative significance of solitary and colonial strategies. **Am. Nat., 111**, 743-767.

Karlson R. (1978).- Predation and space utilization patterns in a marine epifaunal community. **J. Exp. Mar. Biol. Ecol., 31**, 225-239.

Levin S. A. and R. T. Paine (1974).- Disturbance, patch formation, and community structure. **Proc. Nat. Acad. Sci.** (USA), **71**, 2744-2747.

Lewis J. R. (1964).- The ecology of rocky shores. **English University Press**, London, 323 pp.

Menge B. A. (1978).- Predation intensity in a rocky intertidal community. Relation between predator foraging activity and environmental harshness. **Oecologia** (Berlin), **34**, 1-16.

Menge B. A. and J. P. Sutherland (1976).- Species diversity gradients: synthesis of the roles of predation, competition and temporal heterogeneity. **Am. Nat.**, **110**, 351-369.

Osman R. W. (1977).- The establishment and development of a marine epifaunal community. **Ecol. Monogr.**, **47**, 37-63.

Osman R. W. (1982).- Artificial substrates as ecological islands. In: Cairns J., ed. Artificial substrates. **Ann. Arbor Sci. Public.**, Massachusetts, 71-114.

Otsuka C. M. and D. M. Dauer (1982).- Fouling community dynamics in Lynnhaven Bay, Virginia. **Estuaries**, **5** (1), 10-22.

Paine R. and S. A. Levin (1981).- Intertidal landscapes: disturbance and the dynamics of pattern. **Ecol. Monogr.**, **51**, 145-178.

Russ G. R. (1980).- Effects of predation by fishes, competition and structural complexity of the substratum on the establishment of a marine epifaunal community. **J. Exp. Mar. Biol. Ecol.**, **42**, 55-69.

Smedes G. W. and L. E. Hurd (1981).- An empirical test of community stability: resistance of a fouling community to a biological, patch-forming disturbance. **Ecology**, **62** (6), 1561-1572.

Sousa W. P. (1980).- The responses of the community to disturbance: the importance of successional age and species' life histories. **Oecologia** (Berlin), **45**, 72-81.

Standing J. D. (1976).- Fouling community structure: effects of the hydroid, *Obelia dichotoma*, on larval recruitment. In: Mackie G.O., ed., Coelenterate Ecology and Behavior. Plenum Press, 155-164.

Stupak M. E., R. O. Bastida and P. J. Arias (1980).- Las incrustaciones biológicas del puerto de Mar del Plata (Argentina). Período 1976/77. **CIDEPINT-Anales**, 173-231.

Sutherland J. P. (1974).- Multiple stable points in natural communities. **Am. Nat.**, **108** (964), 859-873.

Sutherland J. P. (1978).- Functional roles of *Schizoporella* and *Styela* in the fouling community at Beaufort, North Carolina. **Ecology**, **59** (2), 257-264.

Sutherland J. P. (1981).- The fouling community at Beaufort, North Carolina: a study in stability. **Am. Nat.**, **118** (4), 499-519.

Sutherland J. P. and R. H. Karlson (1973).- Succession and seasonal progression in the fouling community at Beaufort, North Carolina. In: **3rd International Congress on Marine Corrosion and Fouling**, Maryland, USA, 906-929.

Sutherland J. P. and R. H. Karlson (1977).- Development and stability of the

fouling community at Beaufort, North Carolina. **Ecol. Monogr.**, **47**, 425-446.

Williams G. B. (1964).- The effects of extracts of *Fucus serratus* in promoting the settlement of larvae of *Spirorbis borealis* Daudin (Polychaeta). **J. Mar. Biol. Ass.**, U.K., **44**, 397-414.

Young C. M. (1986).- Defenses and refuges: alternative mechanisms of coexistence between a predatory snail and its ascidians prey. **Mar. Biol.**, **91**, 513-522.

Young C. M. and N. J. Gotelli (1988).- Larval predation by barnacles: effects on patch colonization in a shallow subtidal community. **Ecology**, **69**(3), 624-634.

Note: This paper has been submitted for publication in Oceanologica Acta.

EARLY STAGES OF BACTERIAL BIOFILM AND CATHODIC PROTECTION INTERACTIONS IN MARINE ENVIRONMENTS[1]

INTERACCIONES DE LOS PRIMEROS ESTADIOS DE LA PELICULA BACTERIANA Y LA PROTECCION CATODICA EN MEDIO MARINO

H. A. Videla[2], S. G. Gómez de Saravia[2] and M. F. L. de Mele[2]

SUMMARY

The effect of cathodic protection on the early stages of bacterial biofilm formation on stainless steel was studied at different temperatures. The influence of the applied potential on pure Vibrio alginolyticus and mixed SRB (Desulfovibrio vulgaris and Desulfovibrio desulfuricans) biofilms was assessed using saline media, in laboratory experiments under controlled conditions. Interactions between cathodic protection and bacterial settlement and growth, calcareous deposits, and current densities were successively analyzed. For aerobic bacteria, cathodic protection difficulted adhesion to the metal surface only at the early stages of biofilm formation. Higher current densities are generally required in the presence of biofilms.

Keywords: *cathodic protection, biofilm, seawater, calcareous deposits.*

INTRODUCTION

Cathodic protection (CP) is particularly attractive in marine environments or certain kinds of soils where the medium conductivity is high enough to obtain a uniform current distribution over the metal surface to be protected. It has been described **[1-3]** as an effective method of protecting stainless steel (SS) structures immersed in seawater against crevice corrosion.

CP is generally accomplished by impressing an external current to the metal, opposing the naturally occurring corrosion current. Thus, the cost of this protective method will mainly depend on the amount of the current to be applied to the metallic structure to be protected **[3,4]**.

CP alters the ionic concentration at the interface increasing hydroxyl ions concentration. The consequent pH increase diminishes the solubility of calcium and magnesium at the interface favoring the precipitation of a calcareous scale **[4-6]**.

The current required to polarize the structure depends on the electrochemical properties of the metal to be protected and the type of film formed under CP. It has been reported **[4,7,8]** that the properties of this film in natural seawater are influenced by microbial adhesion processes. Moreover, microbial adsorption depends on the electrochemical characteristics of the polarized interface **[9]**.

---

[1] Trabajo realizado dentro del marco del Proyecto 1121 (BID-CONICET II) "Pinturas Protectoras de Alta Resistencia"

[2] Sección Bioelectroquímica, INIFTA, Fac. Cs. Exactas, UNLP

As the adhesion of aerobic microorganisms frequently shifts the corrosion potential in the anodic direction **[1,4,10]** the amount of applied current required to polarize the structure to a pre-selected potential could also depend on the amount of microbial settlement. CP seems to be effective for controlling the growth of aerobic bacteria in carbon structures immersed in seawater whereas it could favour the growth of sulfate reducing bacteria (SRB) **[11]**.

The goal of this paper is to assess the interrelationships between CP on SS samples and pure aerobic and mixed anaerobic bacterial settlement and reproduction and calcareous deposits structure. The influence of seawater temperature on these interactions will also be studied under laboratory well controlled conditions.

EXPERIMENTAL

Microorganisms

Pure *Vibrio alginolyticus (V. alginolyticus)* and mixed SRB *Desulfovibrio vulgaris (D. vulgaris)* and *Desulfovibrio desulfuricans (D. desulfuricans)* were used in the experiments. *V. alginolyticus* was isolated from polluted harbor seawater and was maintained in nutrient agar with the addition of 3 % NaCl. Experiments were made using synthetic seawater supplemented with 1 g/l of yeast extract. Cell number in the culture media were initially c.a. 10^6 cells/ml.

D. vulgaris and *D. desulfuricans* were maintained in a medium containing 35 % of synthetic seawater with 1 g/l of yeast extract, 0.2 g/l sodium lactate, 0.005 g/l Na_2HPO_4, 0.05 g/l NH_4Cl, 0.001 g/l Na_2SO_3. This medium was also used as culture medium in the SRB experiments. In this case, after SRB inoculation, 10 % of the medium was removed and replaced by fresh medium every 24 h.

The initial pH of all the solutions was adjusted to 7.5 by adding 0.1 N NaOH solution.

Metal samples

Metal specimens were AISI 304L SS (50 x 20 x 1 mm). They were mechanically polished with different grits of silicon carbide paper (240, 400, 600) and later with alumina paste (1 μm grain size). After polishing, samples were cleaned and degreased with acetone, and finally rinsed with distilled water prior to their exposure to the bacterial suspension.

Exposure times

Metal specimens were exposed to SRB cultures for 7 or 15 days. Shorter immersion times (2, 4, 18, 24 and 48 h) were used in the case of *V. alginolyticus* experiments.

Cathodic protection conditions

SS samples were cathodically polarized to -0.7 V against a saturated calomel electrode (SCE) using a potentiostat and a platinum counter electrode.

SEM observations

After exposure, and in order to preserve biological material, specimens were

successively fixed with 2 % glutaraldehyde solution in synthetic seawater, washed with distilled water, dried through an acetone series to 100 %, and finally, critical point dried. To assess metal attack, samples were polished with alumina (1 μm) to remove biological and inorganic deposits from the surface. Later, samples were cleaned and degreased with acetone and finally rinsed with distilled water. SEM observations were made using a JEOL JSM-T 100 microscope.

Cell enumeration methods

1. "In situ" enumeration. It was made through a direct cell count method using epifluorescence microscopy. After exposure, the samples were removed, stained with 0.01 % acridine orange for 5 minutes, rinsed in sterile synthetic seawater to remove loose cells, and examined under ultraviolet light with an epifluorescence microscope at 400 X. Cells were counted in 12 randomly chosen 0.0464 cm^2 fields per sample.

2. "Ex situ" enumeration. For viable counts, samples were washed in sterile synthetic seawater and thereafter scraped with a scalpel. The resulting suspension was transferred into a tube containing 10 ml of sterile seawater. Enumeration of cells was made by a standard plating method for viable counts. Colonies were counted after 48 h of incubation at 28 °C.

RESULTS

V. alginolyticus sessile cell counts on 304 SS specimens after 2 and 4 h of immersion at 12 °C are shown in **fig. 1**. The number of bacteria attached to the SS surface diminished when CP was applied. Sessile cell numbers decreased from 2.4 x 10^3 cells/cm^2 to 1.2 x 10^2 for a 2 h exposure time. A longer exposure period (4 h) did not result in an increase of sessile *V. alginolyticus*.

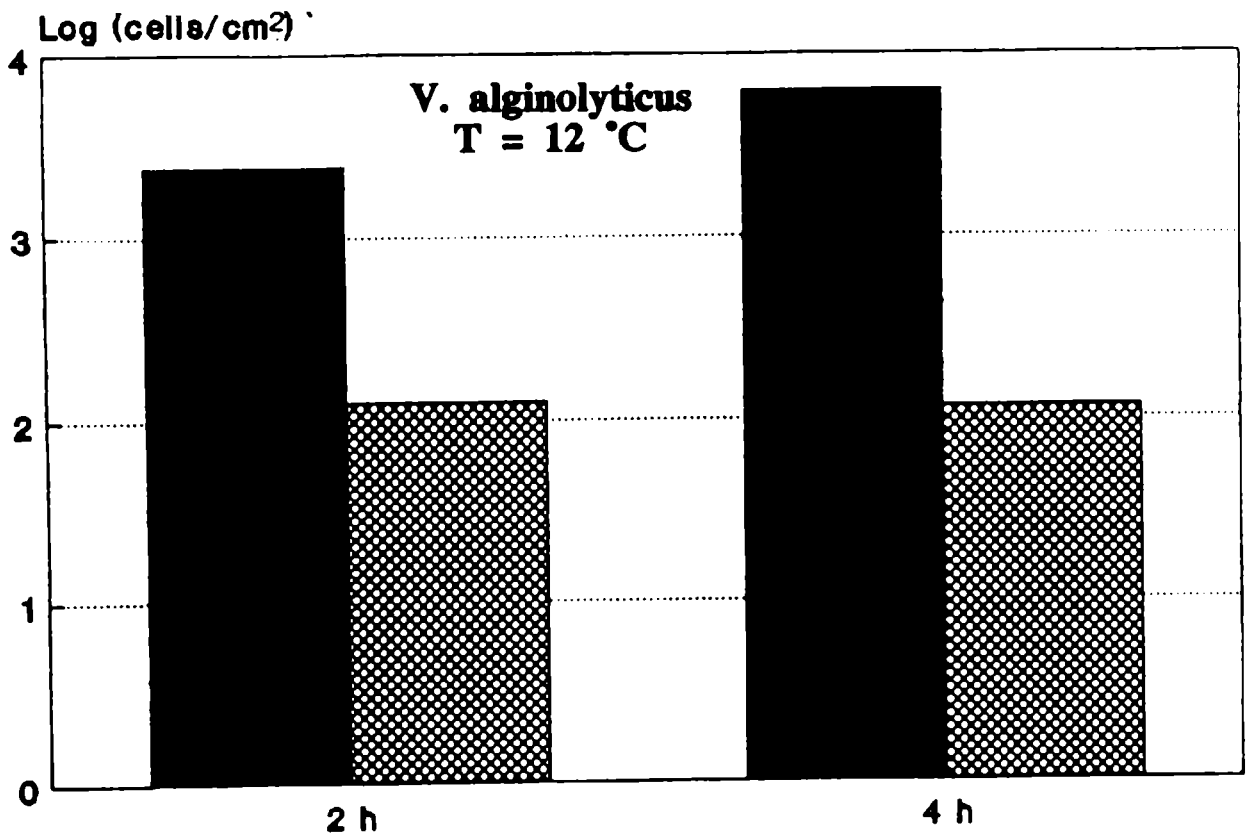

Fig. 1.- Log (cell number/cm^2) vs. exposure tiem plot. AISI 304L SS specimens were immersed in a 24 h old culture of V. alginolyticus in synthetic seawater (▩) with CP (-0.7 V); (■) without CP. Incubation temperature: 12 °C. (From Ref. 14 with permission of NACE).

Experiments made at two different temperatures (12 °C and 20 °C) for SS specimens exposed for 18 h to a *V. alginolyticus* culture, are compared in **Table 1.** A significant reduction in the cell numbers can be noticed when the temperature was increased.

TABLE I

Effect of cathodic protection on *V. alginolyticus* settlement on 304L SS immersed for 18 h in synthetic seawater at different temperatures

Protection	Cell numbers/cm^2	
	12 °C	20 °C
Unprotected	1.07×10^4	1.4×10^8
Protected	7.30×10^2	3.0×10^7

CP effect on a 2 h old *V. alginolyticus* biofilm at 12 °C is shown in **Table 2.** To analyze the balance between desorption + detachment vs. reproduction, biofilmed specimens were immersed in sterile medium, to avoid the readsorption of cells. For unprotected samples the number of bacteria slightly increased in the sterile media (desorption + detachment are slightly lower than reproduction). Conversely, an important decrease in the number of attached cells with respect to the initial value was observed when CP was applied. Thus, it can be inferred that desorption and detachment seemed to be enhanced and reproduction was reduced by CP.

TABLE II

Effect of cathodic protection on sessile *V. alginolyticus* growth on 304L SS. T = 12 °C

Protection	Cells/cm^2
2 h without CP	1.9×10^2
4 h without CP	3.4×10^2
2 h without CP + 2 h without CP in sterile media	2.1×10^2
2 h without CP + 2 h with CP in sterile media	26.3

Experiments made at 12 °C for longer exposures (**Fig. 2**) showed that the number of cells attached on the unprotected samples at this temperature increased to reach a steady value (c.a. 10^4 cells/cm^2) after 24 h, and remained nearly constant afterwards. For this temperature the number of attached cells is markedly lower than that obtained at 20 °C (see Table 1). When the samples were cathodically protected immediately after the immersion in the culture medium a lower number of attached cells with respect to that observed without protection is

again observed. Conversely, when the metal coupons remained 48 h immersed but, alternating the first 24 h unprotected and protected for the next 24 h, it could be noticed that no reduction in the number of cells was found with respect to the unprotected SS samples for 48 h. It is likely that when a steady biofilm is obtained, the effect of cathodic protection is not so relevant as in the early stages of biofilm growth.

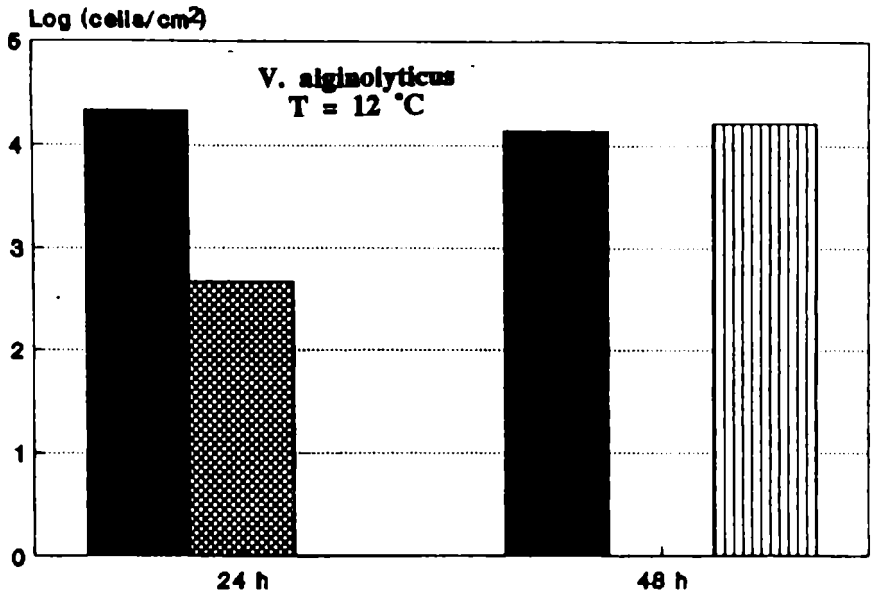

Fig. 2.- Log (cell number/cm^2) vs. exposure time plot. AISI 304L SS specimens were immersed in seawater inoculated with V. alginolyticus: (▥) with CP (-0.7 V); (■) without CP; (▥) 24 h without CP and 24 h with CP. Incubation temperature: 12 °C.

Current density vs. time curves for SS in synthetic seawater (**Fig. 3**) show the characteristic shoulder shape related to the nature of the calcareous deposits formed under these experimental conditions. It can also be noticed a different shape of the curve and a non-well defined transient time, when bacteria are present in seawater. SEM observations showed that pioneer bacteria are covered by calcareous deposits (**Figs. 4 and 5**). When cell detachment occurs, cavities reproducing bacterial shapes can be observed, revealing a discontinuity in the calcareous deposit structure (**Fig. 6**).

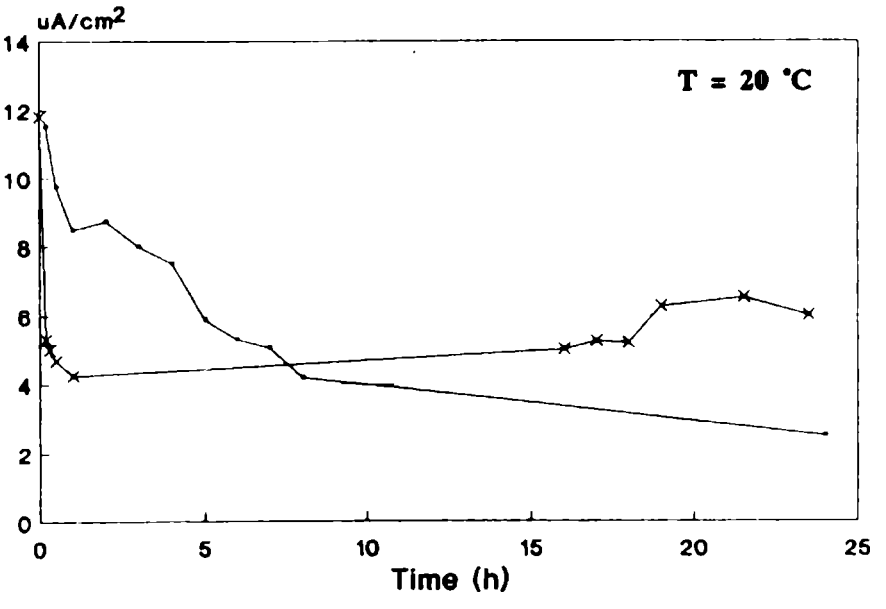

Fig. 3.- Current density vs. time plot of a cathodically protected AISI 304L SS immersed in: (■) sterile synthetic seawater and (x) synthetic seawater inoculated with V. alginolyticus. Incubation temperature: 20 °C. (From Ref. 14 with permission of NACE).

Results of Fig. 3 show that after the immersion in the inoculated seawater, current decreases sharply and then, when the biofilm is formed it began to increase reaching finally a steady state value which duplicates that of the control. Experiments made at 12 °C, i.e., when the growth of biofilm is slow, did not show this current increase in the same period.

Attachment of mixed cultures of SRB to SS specimens was analyzed at longer exposure periods than *V. alginolyticus*. After seven days of immersion a high number of cells (larger than 10^4 cells/cm^2) was found on the SS samples. No reduction in the number of sessile cells was observed when CP was applied for periods of 7 days and longer. Localized attack has been found on samples with and without cathodic protection. Small pits, which were frequently covered by bacteria were observed by SEM (**Fig. 7**). A slight current density increase was recorded after two days of immersion for the protected samples.

After 15 days exposure the number of cells markedly increased and thick biofilms were covering the metal surface (**Fig. 8**). Beneath the biofilm and on the metal surface an inorganic film, firmly adhered to the metal and small pits could be observed when the biofilm was removed (**Fig. 9**).

DISCUSSION

The attachment of bacteria to an unfouled metal surface is preceded by initial processes of transport and adsorption of organic molecules. These processes are followed by the growth of attached bacteria which results in an increase of attached cells and associated material and the detachment of portions of the biofilm. Consequently, the accumulation of cells in the metal/solution interface is the result of the balance of several processes **[12]**:

$$\frac{dX_C/tot}{dt} = \underset{\text{adsorption}}{ra_C} - \underset{\text{desorption}}{rd_C} + \underset{\text{growth-detachment}}{X_C tot(K_g - K_d)}$$

ra_C: adsorption rate for cells
rd_C: desorption rate for cells
X_C: cell concentration at the substratum
K_g: probability of cell growth
K_d: probability of cell detachment
t: time

Sorption related processes are considered to be dominant within a short period of time. For instance, in the case of *Pseudomonas aeruginosa* at 25 °C this period is about 100 minutes after the immersion of the unfouled specimens. Growth related processes begin to contribute to the accumulation in later stages. Adsorption influences the rate of the induction and growth phases but does not influence the plateau biofilm accumulation **[12]**.

Present results obtained with *V. alginolyticus* show that a relevant decrease in the cell number due to the application of CP occurs during the first hours after immersion (the extent of the period depends on temperature). Considering the model previously mentioned **[13]**, adsorption processes may be dominat in this period. Thus, CP should affect adsorption processes, reducing the number of adsorbed cells. Induction and growth periods (but not the steady phase of growth) are considered to be dependent on the number of attached cells. Thus, the effect of CP on the cell growth is appreciable for those periods (Table 2). Conversely,

CP effects are not significant in the biofilm steady state (in this case adsorption process is not relevant). Consequently, it could be inferred that CP affects adsorption processes that influence bacterial growth until steady state is reached.

Although the number of SRB attached bacteria was high after 7 days both for protected and unprotected samples, biofilms did not reach the stationary phase after this period. Consequently, adsorption processes are not reduced by CP in the case of SRB. It was not found an increase in sessile SRB cells when CP was applied as it has been previously reported **[12]**. However, shorter exposure periods must be assayed in the future.

SRB metabolites facilitate metal attack (small pits were observed in the metal surface, Fig. 9). This effect could not be eliminated with the application of CP levels used in this work.

The current density vs. time curve for SS in synthetic seawater shows the characteristic shape related to the formation of the calcareous deposits. The time necessary to reach a steady state, could be associated with the kinetics of the deposit fomation which is modified in the presence of organic material confirming previous results **[6, 7]**. The evolution of the current density as a function of time (Fig. 3) shows a similar behavior to that observed with natural biofilms, when low current densities are necessary to maintain cathodic protection **[1, 4]**. Similar depolarization effects have been extensively reported **[1, 4, 10, 13]** for several metals immersed in seawater. In all cases the increase in current density occurred when the biofilm became established **[14]**. It was suggested **[1]** that this effect could be attributed to an enhancement of the oxygen reduction by the biofilm. Edyvean et al. **[7]**, suggested that organic material slows down precipitation process.

Results reported in this paper offer evidence on the interactions between bacterial fouling, cathodic protection and calcareous deposits: i) Aerobic bacterial adsorption is reduced by the application of CP while anaerobic bacterial adsorption did not seem to be diminished; ii) current values are modified by depolarization effects due to the aerobic biofilm; iii) aerobic and anaerobic biofilms alter the calcareous deposits structure; iv) current values are decreased by calcareous film formation.

CONCLUSIONS

- CP inhibits aerobic bacterial adsorption and growth at the early stages of biofilm formation.
- After reaching a steady biofilm CP effects are not relevant.
- The reduction of bacterial adhesion can be due to an interference of CP in the adsorption processes.
- At low temperatures, when growth rate is low, the CP effect is more significant.
- For low current values, biofilms can modify calcareous deposits structure.
- In the presence of aerobic bacterial biofilms formed at 20 °C, higher current densities are needed to protect SS samples, increasing CP costs.

ACKNOWLEDGEMENTS

This research project is financially supported by the Universidad Nacional de

La Plata and the Consejo Nacional de Investigaciones Científicas y Técnicas (CONICET). The authors wish to acknowledge Merck Química Argentina for the supply of analytical reagents and culture media used in this work. Dr. Robert G. J. Edyvean (Department of Chemical Engineering, the University of Leeds, UK) is also gratefully acknowledged for his valuable discussions.

REFERENCES

[1] R. Johnsen, E. Bardal.- Effect of a microbiological slime layer on stainless steel in natural seawater, **CORROSION/86**, paper no. 227 (Houston, TX: National Association of Corrosion Engineers, 1986).

[2] T. S. Lee, A. H. Tuthill.- **Materials Performance**, **22** (1), 48 (1983).

[3] M. H. Peterson, T. R. Lennox.- **Corrosion**, **29**, 406 (1973).

[4] S. C. Dexter, S. H. Lin, **International Biodeterioration & Biodegradation**, **29**, 231 (1992).

[5] W. H. Hartt, C. H. Culberson, S. W. Smith.- **Corrosion**, **40** (11), 609 (1984).

[6] S. H. Lin, S. C. Dexter.- **Corrosion**, **44** (9), 615 (1988).

[7] R. G. J. Edyvean, A. D. Maines, C. J. Hutchinson, N. J. Silk, L. V. Evans, **International Biodeterioration & Biodegradation**, **29**, 251 (1992).

[8] B. Little, P. Wagner, D. Duquette.- **Corrosion**, **44** (5), 270 (1988).

[9] H. P. Dahr, D. W. Howell, J. O'M. Bockris.- **Journal of Electrochemical Society**, **129**, 2178 (1982).

[10] A. Mollica, E. Traverso, G. Ventura.- Electrochemical monitoring of the biofilm growth on active pasive alloy tubes of heat exchanger using seawater as cooling medium, in **Proc. 11th International Corrosion Congress**, Florence, Italy, **4**, p. 341, 1990.

[11] J. Guezennec.- **Biofouling**, **3**, 339 (1991).

[12] A. E. Escher.- Colonization of a smooth surface by *Pseudomonas aeruginosa*: Image Analysis Methods. Doctoral dissertation. Montana State University, Bozeman, MT (1987).

[13] G. Hernandez, W. H. Hartt, H. A. Videla.- Biofilms and their influence on cathodic protection: a literature survey, **Proc. 1st Pan American Corrosion and Protection Congress**, Vol. II, 391 (1992).

[14] H. A. Videla, S. Gómez de Saravia, M. F. L. de Mele, G Hernández, W. H. Hartt.- The influence of microbial biofilms on cathodic protection at different temperatures, **CORROSION/93**, paper no. 486 (Houston, TX: National Association of Corrosion Engineers, 1993).

Note: This paper has been published in Proceedings XII International Corrosion Congress, Houston, Texas, Vol. 5 B, 3687-3695 (1993).

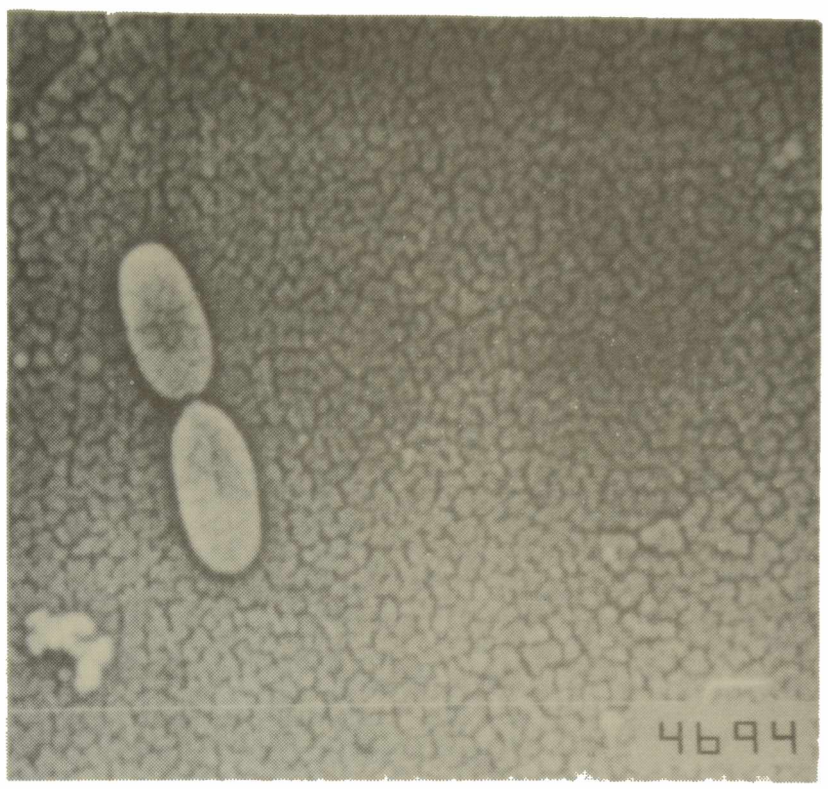

Fig. 4.- SEM microphotograph of a cathodically protected AISI 304L SS specimen after a 4 h exposure to a 24 h old culture of V. alginolyticus in synthetic seawater. Bacteria are covered by calcareous deposits. Magnification X 10,000.

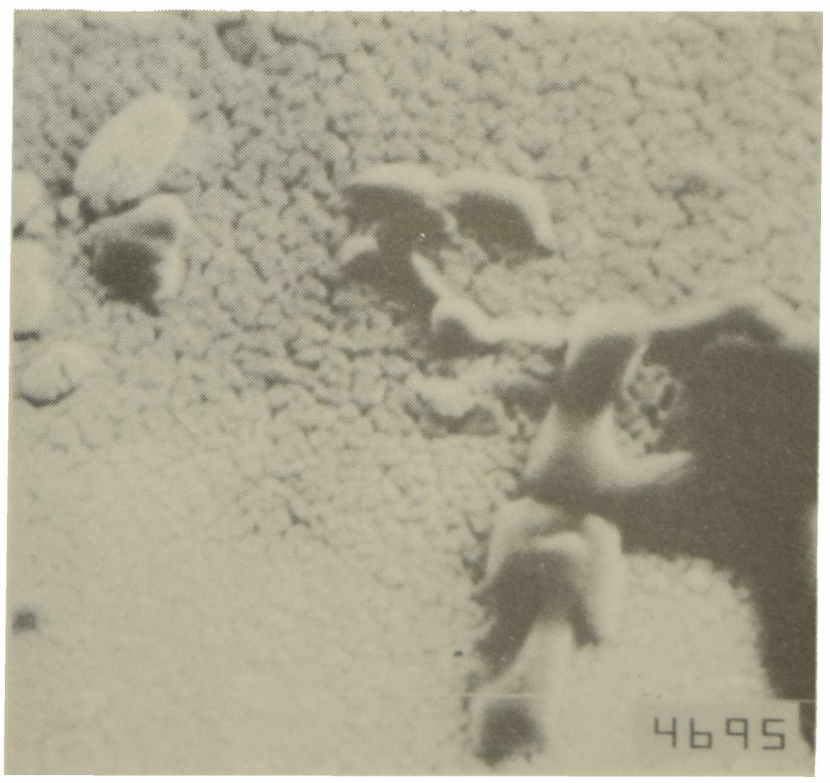

Fig. 5.- SEM microphotograph of a cathodically protected AISI 304L SS specimen after a 4 h exposure to a 24 h old culture of V. alginolyticus in synthetic seawater. Magnification X 10,000.

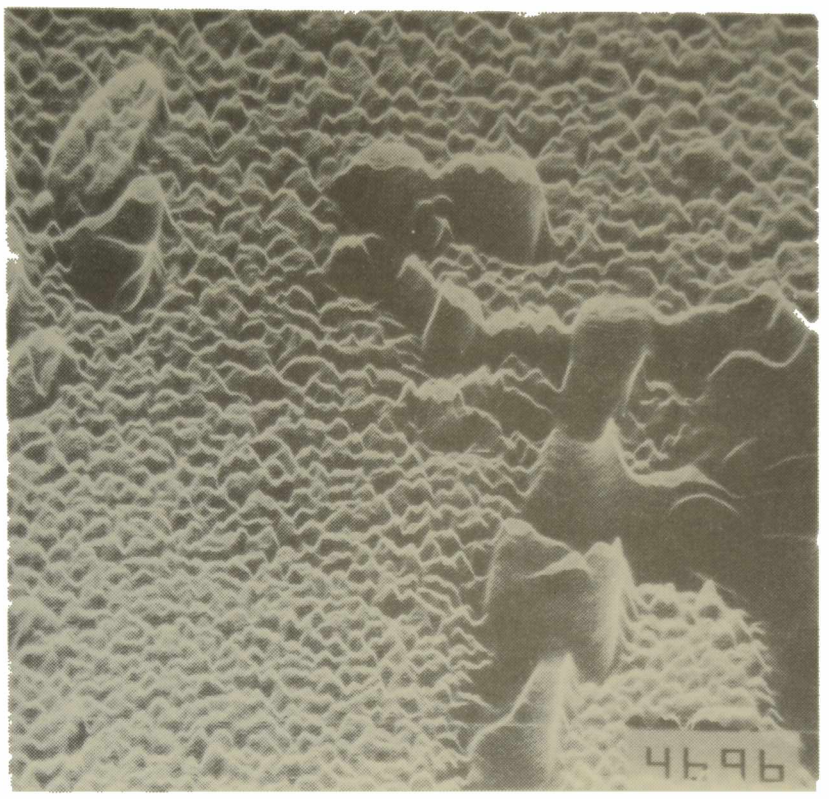

Fig. 6.- SEM microphotograph (topographical image); experimental conditions as in Fig. 5. Cavities reproducing bacterial shapes can be seen at the right side of the picture.

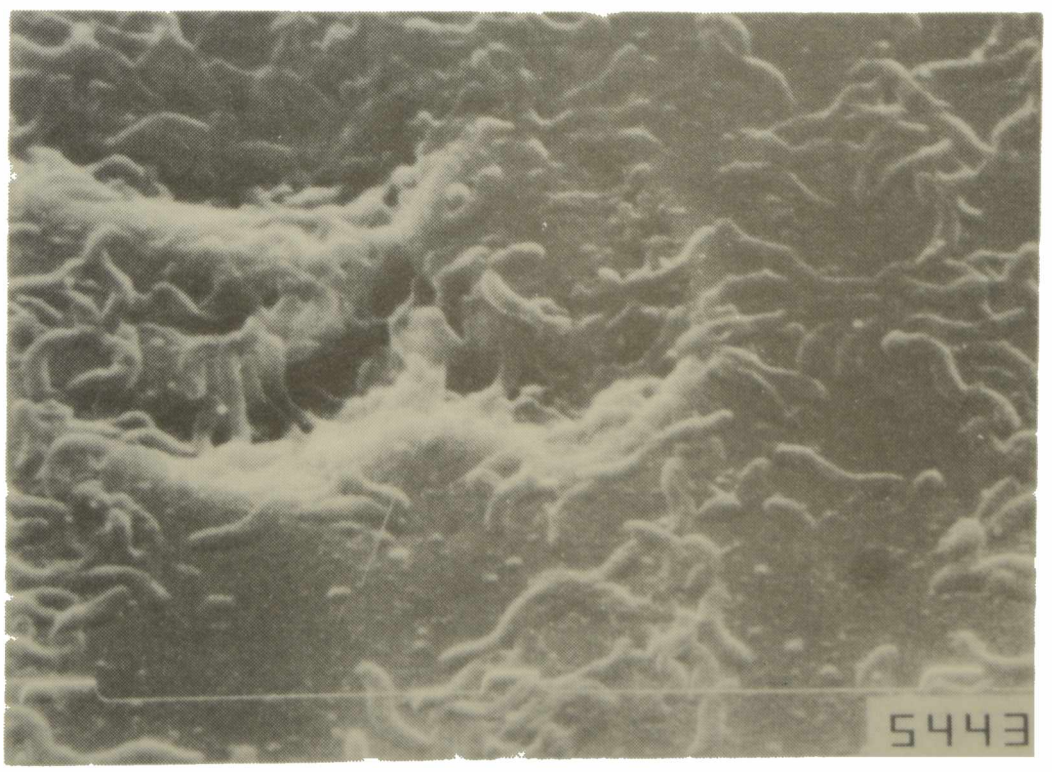

Fig. 7.- SEM microphotograph of an AISI 304L SS specimen (without CP) after a 7 days exposure to a mixed SRB culture. Localized attack beneath bacterial film can be seen. Magnification X 5,000.

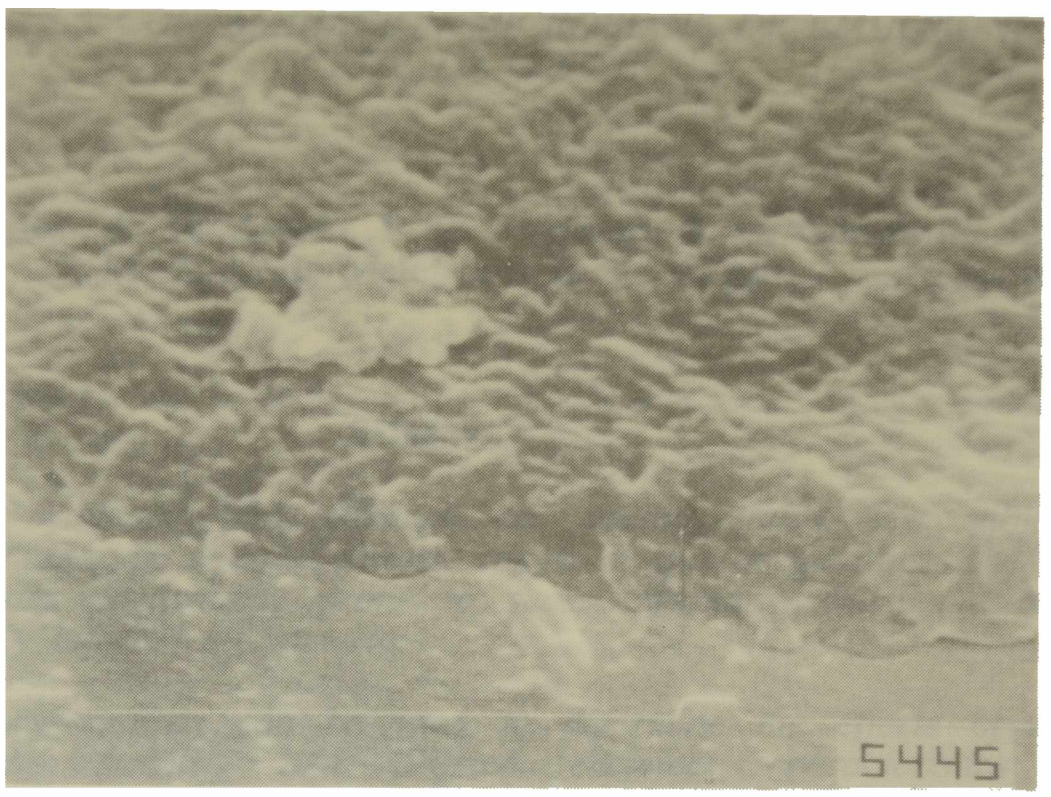

Fig. 8.- SEM microphotograph of a cathodically protected AISI 304L SS specimen after a 15 days exposure to a mixed SRB culture. The vertical arrows indicate the biofilm thickness. Magnification X 3,500.

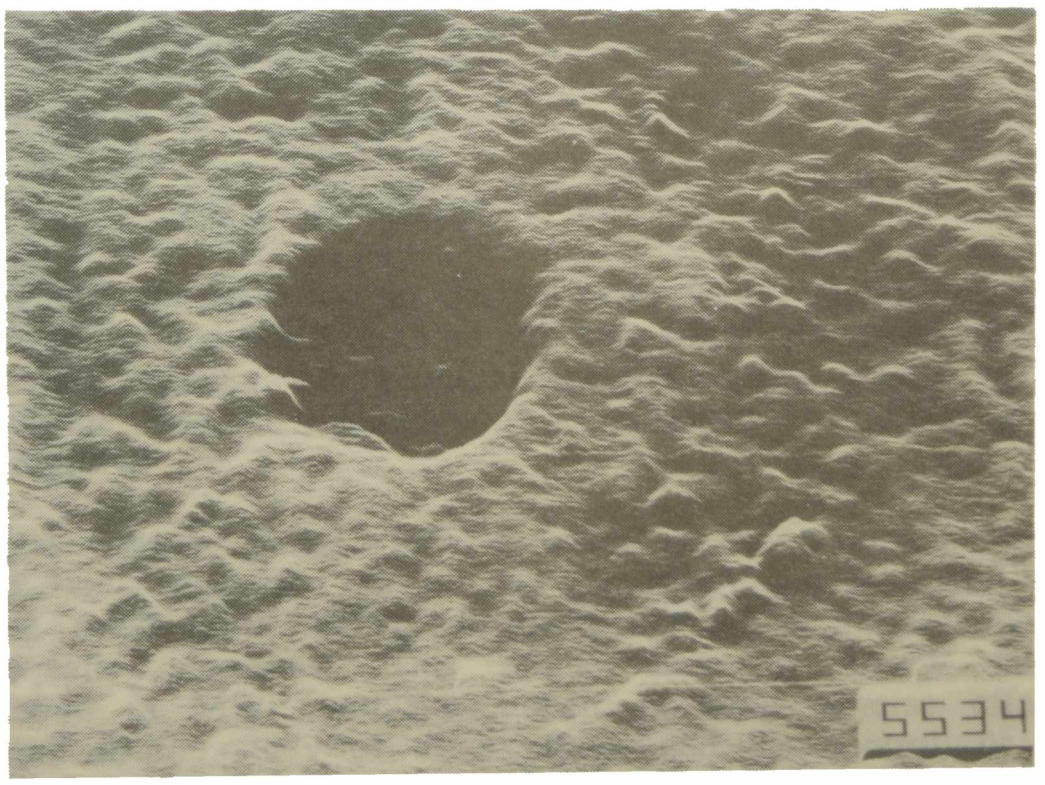

Fig. 9.- SEM microphotograph (topographical image) of an AISI 304L SS specimen (without CP) after a 15 days exposure to a mixed SRB culture. The biofilm was removed and a small pit can be seen. Magnification X 5,000.

EFFECTS OF MICROBIAL CONTAMINATION OF CUTTING OIL EMULSIONS[1]

EFECTOS DE LA CONTAMINACION MICROBIANA DE EMULSIONES DE ACEITE DE CORTE

C. C. Gaylarde[2] , P. E. Cook[3] , P. S. Guiamet[4], S. G. Gomez de Saravia[4] M. F. L. de Mele[4] and H. A. Videla[4]

SUMMARY

Synthetic, semi-synthetic and mineral oil cutting fluids are subjected to microbial contamination with a diverse range of microorganisms. The synthetic oil emulsions are particularly prone to yeast infections whilst the other two fluids are mainly infected by bacteria.

Model laboratory systems can be used to determine the effects of microbial growth on the stability and physico chemical characteristics of the emulsions, as well as to develop methods of control.

One of the important deleterious effects of microbial contamination is an increase in corrosivity against the metals employed in machining operations. Tests used in the laboratory to assess the corrosion effects on different steels are described.

A case history is given to illustrate measures which may be taken to counteract the effects of microbial contamination of cutting oil emulsions.

Keywords: *cutting oil; biodegradation; sulfate-reducing bacteria; fungi; corrosion; pitting.*

INTRODUCTION

Wherever organic materials are in contact with water, microorganisms are able to survive and grow. In hydrocarbons with no free water, microbial growth will not occur, but since one product of microbial metabolism is, itself, water, a mere trace of water in the original hydrocarbon is sufficient to initiate growth which can then proceed rapidly.

In most metal working fluids (MWF), water is the major component of the product in use (a finely dispersed oil-in-water emulsion) and microbial growth may be expected to be usual (Hill, 1977). However, not all of the microorganisms in the fluid are equally hazardous. This article aims to review the types of microorganisms found in MWF emulsions, their potential adverse effect, methods which may be used in the study of these effects and the control, or remediation, of such contamination.

---

[1] Trabajo realizado dentro del marco del Proyecto 1121 (BID-CONICET II) "Pinturas Protectoras de Alta Resistencia"

[2] Laboratorio de Solos, Fac. de Agronomía, UFRGS, Brasil

[3] Department of Health, London, United Kingdom

[4] Sección Bioelectroquímica, INIFTA, Fac. Cs. Exactas, UNLP

Types of MWF

Allsopp and Seal (1986) recognise 4 types of MWF:

- Neat oils; mineral oils of varying viscosity, or fatty oils (extreme pressure additives).

- Soluble oil emulsions; mineral oil emulsions stabilised by an emulsifying agent such as petroleum sulfonate.

- Semi-synthetic cutting fluids; a chemical "synthetic MWF" with 10 to 40 % mineral oil added.

- Synthetic cutting oils; mixtures of chemical compounds which confer lubricating and cooling properties.

The types of microbial problems associated with each type of MWF differ as a result of their chemical composition. The fluids most prone to microbial contamination are the soluble oil emulsions, which are generally diluted between 1:15 and 1:100 with water for use. The components of these fluids include oil, petroleum sulfonates, fatty acids, synthetic detergents and various additives such as antioxidants, antifoam agents, corrosion inhibitors and biocides. Many of these substances (including the biocide!) may be utilised by microorganisms as nutrient sources. The "neat" oils are least prone to microbial contamination, being low in water content, whilst synthetic and semi-synthetic MWFs are intermediate in susceptibility. When first introduced on to the market, it was thought that the synthetic fluids would be resistant to microbial attack. Although supporting the growth of bacteria less well than the soluble oils, synthetic fluids are often prone to contamination by filamentous fungi (Bennett, 1972; Rossmoore et al., 1976).

Microorganisms isolated from MWF

A wide variety of microorganisms have been isolated from contaminated cutting fluids. Some of these are listed in **Table I.**

Bacteria encountered include strict aerobes, such as *Pseudomonas*, only capable of growth in the presence of oxygen; facultative organisms, capable of growth with or without oxygen, such as members of the *Enterobacteriaceae* (e.g., *Serratia, Klebsiella, Escherichia coli*) and strict anaerobes which can only grow in the complete absence of oxygen, like *Clostridium* or sulphate-reducing bacteria (SRB) such as *Desulfovibrio.* Since MWF systems are circulating, there is generally a high level of aeration which initially favours the growth of aerobic bacteria and fungi. These organisms utilise the oxygen in the system and form biofilms on the surfaces of the pipes and reservoirs (sumps). Eventually the reduction in oxygen levels in the biofilms and in less well aerated parts of the system allows anaerobic and facultative bacteria to take over and aerobic attack is confined to the aerated fluid spraying over the workpiece.

The biofilms can harbour not only anaerobic, but also aerobic bacteria, as is demonstrated by the increase in numbers in the fluid after scrubbing biofilms from the walls of a MWF reservoir. In one study, anaerobic bacteria were found to increase 11-fold after such an exercise, whilst aerobes increased by a factor of 21 (Cook and Gaylarde, 1993).

Moulds and yeasts usually increase in numbers after the initial growth of bacteria has reduced the generally alkaline pH to around 5. In the synthetic cutting oils, however, fungi are commonly the major contaminating organisms.

TABLE I

Organisms isolated from MWF[1]

Fungi	Bacteria
Acremonium spp.	*Achromobacter* spp.
Aspergillus spp.	*Acinetobacter* spp.
Botrytis spp.	*Actinomyces* sp.
Candida lambica	*Aerobacter cloacae*
Cephalosporium spp.	*Alcaligenes* spp.
Cladosporium spp.	*Bacillus cereus*
Fusarium spp.	*Citrobacter* spp.
Geotrichum candidum	*Clostridium* spp.
Nocardia spp.	*Corynebacterium* spp.
Penicillium spp.	*Desulfovibrio* spp.
Scopulariopsis spp.	*Enterobacteriaceae*
Torulopsis candida	*Listeria monocytogenes*
Verticillium spp.	*Micrococcus* spp.
	Pseudomonas spp.
	Streptococcus spp.

[1] Sources: Hill, 1968, 1977; Foxall-VanAken et al., 1986; Allsopp and Seal, 1986; Rossmoore, 1988; Prince and Morton, 1987, 1988a; Cook and Gaylarde, 1988; Sandin et al., 1991.

Rossmoore (1986) states that fungi have never been isolated from a system without previous aerobic bacterial growth, but Prince and Morton (1988a) were able to show that fungi could grow on otherwise uncontaminated synthetic lubricants. In the factory environment, it is likely that bacteria will always be present in a MWF system and factors such as the exact make-up of the fluid, the ambient temperature and the presence of contaminating chemicals and "dirt" will determine the dominant population.

Components of MWF which may be used as nutrients by microorganisms include fatty acids (linoleic and oleic acids) and petroleum oil, used by bacterial contaminants in non-synthetic fluids (Foxall-VanAken et al., 1986), and triethanolamine and amine borate, used by fungi in synthetic fluids (Prince and Morton, 1988a). Extrinsic sources of organic matter, such as sputum and cigarette ends, will add to the general nutritional level of the fluid. The use of biocides will favour the growth of resistant microorganisms, thus altering the microbial flora.

Effects of microbial contamination

The adverse effects of microbial growth within a circulating coolant are shown in **Table II**.

The health hazards concerned with contaminated fluids have not been emphasized in the literature, but pathogens, such as *Listeria monocytogenes* (Rossmoore, 1988), have been detected in these systems and the aerosols formed as a result of the mode of use of the fluids must be a potential source of infection or possibly of allergic respiratory disease.

Chemical changes which accompany microbial growth include a decrease in levels of additives such as corrosion inhibitors, utilization of emulsifiers and

production of acids, both of the latter leading to "cracking", or breaking, of the emulsion and concommitant loss of lubricating capacity and increased risk of corrosion. Acids produced in the MWF by microbial metabolism may become dried on to the workpiece, accelerating corrosion. Other effects will be changes in viscosity, volatility and oil droplet size. The production of hydrogen sulphide by the anaerobic SRB and *Clostridium* spp. leads to the typical "Monday morning odour" when machines are switched in after a weekend of idleness. Microbial biofilms formed on the tool surfaces may increase corrosion (Ortiz et al., 1990).

TABLE II

Effects of microbial contamination of MWF

Effect	Main organisms involved
Unpleasant smell and appearance	Aerobic bacteria and fungi
H_2S production	Sulphate-reducing bacteria (SRB)
Breaking of emulsion	Bacteria and yeasts
Blocking of filters	Filamentous fungi
Surface slimes	Bacteria
Surface mats	Filamentous fungi
Corrosion of tools	Bacteria and SRB
Corrosion of workpiece	Filamentous fungi and bacteria
Health problems of personnel	Bacteria

To asses the relationship between biofilms and corrosion of steel, different electrochemical experiments complemented with scanning electron microscopic observations were made in media inoculated with two strains of bacteria isolated from cutting-oil emulsions (*Pseudomonas fluorescens* and a sulphate-reducing bacterium). The stagnant conditions used for the experiments, were similar to those usually found in sumps or holding tanks. Results showed that both bacteria were able to attach to steel surfaces, leading to the formation of biofilms (Videla et al., 1990). These biological deposits interfere in the formation of a good protective passive layer on the metal surface, facilitating the initiation of localized attack and delaying repassivation. Although stainless steel was not attacked in the experimental conditions assayed, changes in redox potential and pH caused by bacteria growth, could induce the initiation of localized corrosion for longer exposure periods. On the other side, mild steel samples were severely damaged by the synergistic action of bacterial consortia of aerobic bacteria and SRB.

Microbial aggregates dried on to the surface of the workpiece prior to annealing can result in ash deposits rich in hygroscopic minerals, which form loci for future rusting (Hill, 1977). These changes can lead to shortened tool-life, poor surface finish and rapid corrosion in machining operations and to roll pick-up, poor sheet quality and high oil costs in rolling operations (Hill, 1968).

Laboratory models

A number of workers have employed laboratory models to study the effects of microbial contamination of MWF. Such models are useful in determining the components of a fluid which make it susceptible to attack and in investigating the possibilities for control of infection.

Hill (1977) reports the use of the Coulter Counter for determining oil droplet size in contaminated fluids. The increasing droplet size indicates degradation of the emulsifying system. Prince and Morton (1988b) demonstrate the ability of fungi to degrade the emulsifier in a mineral oil emulsion using a different technique. The emulsifier level is quantified by the critical micelle concentration (CMC) method, where the degree of dilution of the fluid required to reach the CMC, detected in this case by an abrupt change in absorbance at 540 nm, indicates the emulsifier concentration in the original fluid. Breakdown of the hydrocarbon portion of the fluid can be detected by gas liquid chromatography and the capacity of microorganisms to utilise these or other components can be assessed by their ability to grow using the component as sole carbon source.

A number of systems have been developed to simulate the conditions under which a MWF will be used in practice. The emulsions are circulated over iron chips or other metal pieces, sometimes are artificially aerated, and are often run intermittently to simulate the overnight or weekend shutdown period. Such systems have been described by Pivnick and Fabian (1953), Himmelfarb and Scott (1968) and Shennan (1983). Cook and Gaylarde (1988) developed a model circulating system to monitor contamination and biofilm formation in aqueous MWF. Using this system, the effect of a triazine biocide was demonstrated to be an increase in time (from 5 to 30 days) taken for microbial numbers to reach their maximum level.

Control of contamination

The first paper describing microbial contamination of cutting oils was published in 1942 (Lee and Chandler, 1942). These authors recommended "good housekeeping" and the use of phenolic biocides to control the problem. Much work was done in this area in the 1950s by Bennett, who found phenolic and nitroparaffin biocides to be the most effective (Bennett et al., 1959; Bennet and Futch, 1960; Carlson and Bennet, 1960). These biocides are now, however, discouraged and the choices open to the factory manager are much wider and not necessarily easier. Determining the "best" biocide for a particular situation is difficult and laboratory biocide testing is always recommended. Shennan (1983) reviews the methods available for this.

Biocides used in MWF must be nontoxic, environmentally acceptable, compatible with the components of the fluid and, of course, effective. These requirements rule out many of the biocides available in today's market, such as the quaternary ammonium compounds, which are incompatible with a number of MWF constituents such as surfactants and fats, and acid and ester biocides which would destroy the alkaline status of the fluid. Formaldehyde-releasing agents, such as the triazine and imidazole derivatives, have been particularly useful in soluble oil emulsions (Rossmoore and Sondossi, 1988), as have the Omadines (Rossmoore, 1979), a group of pyridine derivatives which are particularly active against fungi. Hexamethylene biguanide is also an effective antifungal agent which is of use in controlling infection in synthetic fluids. Mixtures, generally of two biocides, are also used in the industry. These often consist of a formaldehyde-based biocide plus a fungicide, such as a mixture of formaldehyde and sodium Omadine (Sandin et al., 1991).

Although biocides may be effective for a time, they are only part of the answer to controlling infection in the workshop. Good housekeeping is paramount in reducing the initial microbial load and making the job of the biocide easier, thus prolonging its active life. The Institute of Petroleum, in the UK, publishes a Code of Practice for MWF which summarizes the various aspects of contamination control. This covers the improvement of workshop hygiene, rapid removal of swarf and use of good quality water, in addition to the use of a biocide and regular cleaning of machines. The use of biocides brings another problem in itself -the

safe disposal of the used MWF. This is a potential environmental hazard which is not within the scope of this paper.

Case History

The levels of contamination commonly found in machines using coolants and the effect of cleaning are demonstrated by the following case history, taken from Cook and Gaylarde, 1993.

A computerized numerical control (CNC) lathe using a mineral oil MWF exhibited signs of gross contamination after only 6 weeks operation, with discolouration of the fluid and separation of the oil-water phases. Frequent changes of the fluid were necessary, resulting in increased costs. Microbiological investigations showed that very high levels of bacteria, including coliforms (indicative of possible faecal contamination) were present, both in the circulating fluid and in the biofilm on the walls of the machine (**Table III**). The machine was thoroughly cleaned, using both physical cleaning (scrubbing) and a chemical systems cleaner and fresh coolant introduced. Such regular monitoring of microbial levels in a machine can be used to control potential problems and avoid unnecessary shut down. Detailed examination, as undertaken in this example, is not necessary and simple tests such as "dip slides" which indicate the general level of aerobic contamination, are generally sufficient. Using these simple tests, the educated factory manager can assess the need for biocide addition and avoid unnecessary expenditure.

TABLE III

Microbial contamination in a lathe using mineral oil lubricant

Sample	Microbial cell concentrations			
	Aerobic Bacteria	Anaerobic Bacteria	Coliform Bacteria	Fungi
Original				
Coolant	7.8×10^{10}/ml	4.3×10^{10}/ml	7.0×10^{10}/ml	2.2×10^{5}/ml
Biofilm	6.0×10^{9}/cm^2	5.3×10^{8}/cm^2	3.2×10^{10}/cm^2	1.5×10^{5}/ml
5 weeks after cleaning				
Coolant	8.3×10^{4}/ml	5.8×10^{5}/ml	1.0×10^{4}/ml	2.4×10^{2}/ml
Biofilm	6.1×10^{5}/cm^2	1.5×10^{5}/cm^2	3.6×10^{5}/cm^2	3.2×10^{3}/cm^2

REFERENCES

Allsopp, D. and Seal, K.J. (1986).- **Introduction to Biodeterioration**. Edward Arnold, London, pp. 34-35.

Bennett, E. O. (1972).- The biology of metal-working fluids. **Lubrication Engineering**, **28**, 237-249.

Bennett, E. O., Adamson, C. L. and Feisal, V. E. (1959).- Factors involved in the control of microbial deterioration. I. Variation in sensitivity of different strains of the same species. **Applied Microbiology**, **7**, 368-372.

Bennet, E. O. and Futch, H. N. (1960).- Nitroparaffin inhibitors for cutting fluids. **Lubrication Engineering, 16**, 228-230.

Carlson, V. and Bennet, E. O. (1960). The relationship between the oil-water ratio and the effectiveness of inhibitors in oil-soluble emulsions. **Lubrication Engineering, 16**, 572-574.

Cook, P. E. and Gaylarde, C. C. (1988).- Biofilm formation in aqueous metal-working fluids. **International Bioterioration, 24**, 265-270.

Cook, P. E. and Gaylarde, C. C. (1993). Microbial films in the light engineering industry. In **Microbial Biofilms: Formation and Control**. eds. S.P. Denyer, S.P. Gorman and M. Sussman, Blackwell Scientific Publ., London, pp. 267-283.

Foxall-VanAken, S., Brown, J. A., Young, W., Salmeen, I. McClure, T., Napier, S. and Olsen, R. H. (1986).- Common components of industrial metal-working fluids as sources of carbon for bacterial growth. **Applied & Environmental Microbiology, 51**, 1165-1169.

Hill, E. C. (1968).- Microbial degradation of lubricant oils and emulsions and its engineering significance. In **Biodeterioration of Materials, Microbiological & Allied Aspects**. Eds. H.A. Walters & J.J. Elphick, Elsevier, NY, pp. 381-385.

Hill, E. C. (1977).- Microbial infection of cutting fluids. **Tribiology International, 10**, 49-54.

Himmelfarb, P. and Scott, A. (1968).- Simple circulating tank test for germicides for cutting fluid emulsions. **Applied Microbiology, 16**, 1437-1438.

Lee, M. and Chandler, A. C. (1942).- A study of the nature, growth and control of bacteria in cutting compounds. **Journal of Bacteriology, 41**, 373-386.

Ortiz, C., Guiamet, P. S. and Videla, H. A. (1990).- Relationship between biofilms and corrosion of steel by microbial contaminats of cutting-oil emulsions. **International Bioterioration, 26**, 315-326.

Pivnick, H. and Fabian, F. W. (1953).- Methods for testing the germicidal value of chemical compounds for disinfecting soluble oil emulsions. **Applied Microbiology, 1**, 204-207.

Prince, E. L. and Morton, L. H. G. (1987).- Rapid assessment of emulsifier levels in industrial coolants. **International Bioterioration, 23**, 365-376.

Prince, E. L. and Morton, L. H. G. (1988a).- Fungal biodeterioration of synthetic metal-working fluids. In **Biofilms**, eds. L.H.G. Morton & A.H.L. Chamberlain, The Biodeterioration Society, Egham, pp. 107-122.

Prince, E. L. and Morton, L. H. G. (1988b).- Biofilm development and emulsifier levels in metal working fluid systems. In **Biodeterioration 7**, eds. D.R. Houghton, R.N. Smith and H.O.W. Eggins. Elsevier, Barking, pp. 26-30.

Rossmoore, H. W. (1979).- Heterocyclic compounds as industrial biocides. **Developments in Industrial Microbiology, 20**, 41-71.

Rossmoore, H. W. (1986).- Microbial degradation of water-based metal working fluids. In **Comprehensive Biotechnology**. ed. M. Moo-Young, Pergamon Press, Oxford, pp. 249-269.

Rossmoore, H. W., Holtzman, G. H. and Kondak, L. (1976).- Microbial ecology with a

cutting edge. In **Proc. 3rd International Biodeterioration Symposium**, eds. J.M. Sharplay & A.M. Kaplan, Applied Science Publ., London, pp. 221-232.

Rossmoore, H. W. and Sondossi, M. (1988).- Applications and mode of action of formaldehyde concentrate biocides. **Advances in Applied Microbiology, 33**, 223-277.

Rossmoore, H. W. (1988).- The microbiological activity of glutaraldehyde in chain conveyor lubricant formulations. In **Biodeterioration 7**, eds. D.R. Houghton, R.N. Smith & H.O.W. Eggins. Elsevier, Barking, pp. 242-247.

Sandin, M., Mttsby-Baltzer, I and Edebo, L. (1991).- Control of microbial growth in water-based metal-working fluids. **International Bioterioration, 27**, 61-74.

Shennan, J. L. (1983).- Selection and evaluation of biocides for aqueous metal-working fluids. **Tribiology International, 16**, 317-330.

Videla, H. A., Gómez de Saravia, S. G., de Mele, M. F. L. and Guiamet, P. S. (1990).- Bioelectrochemical assessment of biofilm effects on MIC of two different steels of industrial interest. **Corrosion 90**. NACE, Houston, Texas, Paper No. 123.

Nota: Este trabajo ha sido enviado para su publicación en los Anales de las III Jornadas Tribológicas de la República Argentina y Latinoamérica y III Exposición Tribológica - TRIBOS 94.

INFLUENCIA DE LA PREPARACION DE LA SUPERFICIE DE ALUMINIO SOBRE LA ADHESION DEL ESQUEMA PROTECTOR

INFLUENCE OF ALUMINIUM PRETREATMENT ON COATING ADHESION

C. A. Giúdice[1], B. del Amo[1] y M. Morcillo Linares[2]

SUMMARY

The objective of this paper was to study the preparation of the aluminium surface with the aim to achieve a suitable adhesion of the protective paint film assuming that corrosion is produced when the film shows a poor adhesion.

The panels pretreated were covered with a coat of high efficiency and exposed to aggressive conditions. Then, practical adhesion was evaluated and the results indicated that sandblasting of the aluminium surface, washing with 2 % w/w sodium carbonate and also with 10 % w/w phosphoric acid as well as the application of wash primer with 10 % aluminium powder were not effective since those panels showed the lowest adhesion values at the end of the test.

The film adhesion was improved degreasing the surface with detergent, steam exposition, wash primer application and also by immersion for 15 minutes in 5 % w/w chromic acid/29 % w/w sulfuric acid and in 5 % w/w potassium dichromate/29 % w/w sulfuric acid.

Finally, the pretreatments that showed the best behaviour were anodizing, anodizing and sealing in steam, immersion in 10 % w/w sodium hidroxide (10 minutes) and then in 2 % w/w sodium carbonate (10 minutes), immersion in 5 % w/w chromic acid/28 % w/w sulfuric acid (30 minutes), 10 % w/w potassium dichromate/35 % w/w sulfuric acid (15 minutes) and 10 % w/w potassium dichromate/2 % w/w potassium fluoride/35 % w/w sulfuric acid (15 minutes).

Keywords: *Aluminium, adhesion, pretreatment, adhesive bonds.*

INTRODUCCION

La utilización industrial del aluminio lo ha situado a la cabeza de los metales no ferrosos dado que la elevada energía libre de formación del óxido de aluminio junto con las características de refracción de la película formada permite que se comporte como un metal noble a pesar de su gran actividad química. El óxido de aluminio genera una película adhesiva y compacta [1] que, al recubrirlo, lo protege de la corrosión; la continuidad de esta película es un factor de importancia ya que zonas sin recubrir son susceptibles de corrosión.

En atmósferas industriales y marinas que contienen gases agresivos y sales, la capa protectora de óxido comienza a disolverse formando un par galvánico que origina importantes problemas de corrosión; la falla más frecuente es debida a la

[1] CIDEPINT. Miembros de la Carrera del Investigador del CONICET

[2] Centro Nacional de Investigaciones Metalúrgicas, CENIM (CSIC), España

corrosión por picaduras.

La celda galvánica puede controlarse ya sea generando una capa de óxido adherente o bien aplicando un esquema protector basado en pinturas. Para ello es necesario realizar una eficiente preparación de superficie, dado que fallas en la adhesión de la película de pintura al sustrato, en muchos casos, están determinadas por la topografía de la superficie (por ejemplo inadecuada rugosidad superficial) **[2]**, a la presencia de sales, etc.

El objetivo de este trabajo fue estudiar diferentes métodos de preparación de la superficie de aluminio con el propósito de lograr una adecuada adhesión de la capa protectora de pintura al considerar que la corrosión tiene lugar cuando la adhesión es reducida **[3, 4]**.

PARTE EXPERIMENTAL

Pretratamientos estudiados

Se emplearon placas de aluminio de 7,5 x 13,0 cm con la siguiente composición: aluminio, 99,76 %; silicio, 0,10 %; magnesio, 0,01 %; hierro, 0,13 %.

P1: Arenado (1,5 $kg.cm^{-2}$) y limpieza con solvente.
P2: Lavado con detergente.
P3: Anodizado en ácido sulfúrico al 10 %, a 20°C.
P4: Anodizado y sellado en agua a 98-100°C.
P5: Lavado con solución de carbonato de sodio 2 %.
P6: Aplicación de una capa de ácido fosfórico 10 %.
P7: Exposición al vapor de agua durante 15 minutos.
P8: Inmersión en hidróxido de sodio 10 % y luego en carbonato de sodio 2 %, durante 10 minutos en ambos casos.
P9: Aplicación de una capa de "wash primer".
P10: Aplicación de una capa de"wash primer" con 10 % de aluminio en polvo.
P11: Inmersión en ácido crómico 5 %/ácido sulfúrico 29 %, durante 15 minutos.
P12: Similar al pretratamiento P11, con 30 minutos de inmersión.
P13: Inmersión en dicromato de potasio 5 %/ácido sulfúrico 29 %, durante 15 minutos.
P14: Inmersión en dicromato de potasio 10 %/ácido sulfúrico 35 %, durante 15 minutos.
P15: Inmersión en dicromato de potasio 10 %/fluoruro de potasio 2,0 %/ácido sulfúrico 35 %, durante 15 minutos.

Preparación de las pinturas

Se formularon pinturas anticorrosiva, intermedia y de terminación de tipo vinílico. La pintura anticorrosiva se formuló con una resina de composición 83 % de cloruro de vinilo, 16 % de acetato de vinilo y 1 % de ácido maleico y con los pigmentos fosfato de cinc, dióxido de titanio, sulfato de bario y talco. La pintura intermedia se elaboró con una mezcla de una resina igual a la arriba mencionada y otra con 86 % de cloruro de vinilo/14 % de acetato de vinilo y pigmentada con dióxido de titanio, talco y sulfato de bario. La pintura de terminación estuvo constituida por una resina con 86 % de cloruro de vinilo y 14 % de acetato de vinilo y dióxido de titanio como pigmento (este fue incorporado debido a la resistencia que imparte a la luz ultravioleta) y además por talco y barita.Todas las pinturas se prepararon en un molino de bolas de 3,3 litros de capacidad total.

Esquema de pintado

Los ensayos se realizaron en un caso sobre una capa de pintura anticorrosiva vinílica, con 35 ± 5 µm de espesor de película seca y en otra serie sobre el esquema protector completo conformado por dos capas de pintura anticorrosiva, una de pintura intermedia y dos de terminación, con 150 ± 5 µm de espesor total. Los ensayos se realizaron por triplicado y se promedian los valores obtenidos.

Envejecimiento de los paneles pintados

Los paneles fueron expuestos previamente en medios de alta agresividad:

a) **Cámara de niebla salina**. Pulverización continua con solución de cloruro de sodio al 5 % y una temperatura de 35 ± 1 °C (ASTM B 117/79).

b) **Cámara de prohesión**. Atmósfera controlada con 0,40 % de sulfato de amonio y 0,05 % de cloruro de sodio. Los ciclos de funcionamiento fueron 12 en el día, formados por una hora de "spray" salino seguido por una hora de secado **[5-7]**.

c) **Agua destilada**. Inmersión en agua destilada separados los paneles uno de otro por una distancia de 1 cm.

d) **Cámara de humedad**. Los paneles se colocaron en una cámara cerrada con 100 % de humedad relativa. Temperatura 38 ± 1 °C (ASTM D 2247).

Ensayos realizados

Una de las más importantes características de las uniones de adhesión es su estabilidad frente al agua o al medio ambiente con alto contenido de humedad. La humedad reduce la adhesión y por lo tanto disminuye la protección contra la corrosión. Sin embargo cuanto mayor es la tensión residual en servicio, más alta es la capacidad protectora del esquema **[4]**.

Existen diferentes opiniones acerca del método más adecuado para medir la adhesión durante la exposición al agua **[4, 8, 9]**. Un problema que aparece en las medidas de adhesión húmeda es que éstas deben ser realizadas rápidamente después de sacados los paneles del medio, cuidando de secar muy bien la superficie. Las muestras no pueden ser sometidas a altas temperaturas ni permanecer expuestas al aire por largo tiempo antes del ensayo porque cambian las propiedades de la película de pintura, modificándose la adhesión del sistema.

Las determinaciones de adhesión húmeda para las muestras colocadas en la cámara de niebla salina, en cámara de humedad y en inmersión en agua destilada fueron realizadas luego de 24, 96, 120, 144, 168 y 268 horas, mientras que para las colocadas en la cámara de prohesión los ensayos fueron realizados luego de 11, 43, 54, 67, 79 y 104 ciclos.

Existe un gran número de ensayos para medir la adhesión de una película de pintura al sustrato. Los distintos métodos suelen proporcionar valores no coincidentes.

Para realizar las determinaciones se empleó el Elcometer modelo 106 (ASTM D-4541). El instrumento proporciona medidas directas y emplea dispositivos metálicos que se adhieren a la superficie pintada con un adhesivo epoxídico. Cuando el adhesivo ha curado se realiza un corte alrededor de dicho dispositivo para remover su exceso, se engancha el aparato y se lleva la escala a cero. Luego se procede a incrementar la tensión a velocidad constante hasta que se produce el

desprendimiento de la película. En la escala queda registrada la fuerza máxima soportada por unidad de área.

También se determinó la adhesión según lo establecido en la norma ASTM D-3359 de manera de comparar diferentes técnicas de ensayo. Para la evaluación del esquema completo se empleó el método A ya que éste está indicado para un espesor de película mayor que 125 μm, mientras que el B fue utilizado para la pintura anticorrosiva sola.

RESULTADOS Y DISCUSION

Es importante destacar que si bien los valores de adhesión no fueron iguales las muestras mostraron una tendencia coincidente en todos los medios considerados. Los resultados correspondientes a la adhesión de sólo una capa de pintura anticorrosiva, al final del envejecimiento, determinada por el método ASTM D-4541 se encuentran en la **Fig. 1**.

El arenado de la superficie (P1) junto con el tratamiento con carbonato de sodio (P5), aplicación de ácido fosfórico (P6) y "wash primer" con polvo de aluminio (P10) presentaron los valores más bajos de adhesión al finalizar el tiempo de exposición.

La observación microscópica de una superficie de aluminio sin tratar se encuentra en la **Fig. 2** mientras que una arenada se incluye en la **Fig. 3**. En esta última se puede constatar que la rugosidad de la superficie era apreciable y sin embargo los valores de adhesión registrados estuvieron entre los más bajos del conjunto, lo cual señalaría que no se puede esperar una buena adhesión sólo por anclaje mecánico.

La adhesión mejoró con los pretratamientos que consistieron en lavado con detergente (P2), exposición al vapor de agua (P7), aplicación de "wash primer vinílico" (P9) e inmersión en ácido crómico/ácido sulfúrico durante 15 minutos (P11) y en dicromato de potasio/ácido sulfúrico también durante 15 minutos (P13).

Las superficies tratadas con ácido fosfórico (P6) o con "wash primer" (P9) presentaron en ambos casos valores de adhesión altos en las primeras horas del ensayo (hasta 120 horas). La similitud de los resultados estaría relacionada con la acción del ácido fosfórico presente en ambos tratamientos debido a que en una primera etapa se remueven los óxidos existentes y luego se forma una capa de fosfato de aluminio. Es importante mencionar que cuando se empleó sólo ácido fosfórico se produjo un descenso importante de los valores a lo largo del tiempo, lo que no se observó con el"wash primer", lo cual podría ser atribuido a que éste también incluye compuestos de cromo en su composición.

Resulta oportuno indicar el hecho que si bien el arenado (P1) permite remover la misma cantidad de material que aquéllos que generan un decapado ácido, fueron mejores los resultados con los pretratamientos P11 y P13. Esto es atribuible a la distinta morfología superficial generada por la acción de los iones cromo **[10]**. Cabe mencionar que no se presentaron diferencias de comportamiento significativas con el empleo de ácido crómico o dicromato de potasio debido a la presencia del medio fuertemente ácido.

Por último, los pretratamientos que resultaron más eficientes fueron el anodizado (P3), anodizado y sellado de la superficie (P4), inmersión en hidróxido de sodio y luego en carbonato de sodio (P8), inmersión en ácido crómico/ácido sulfúrico durante 30 minutos (P12), en dicromato de potasio/ácido sulfúrico (P14) y finalmente en dicromato de potasio/fluoruro de potasio/ácido sulfúrico (P15).

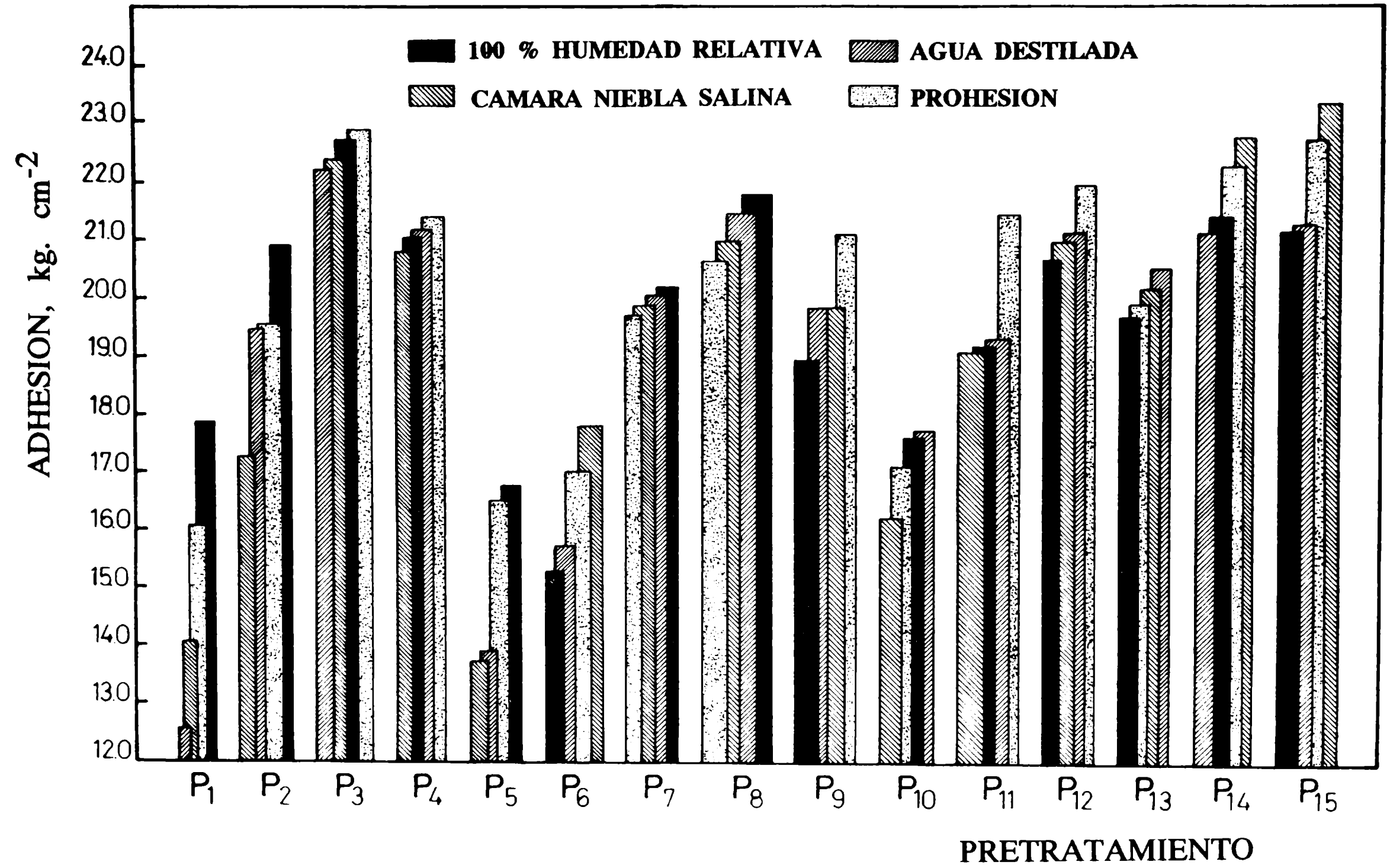

Fig. 1.- Adhesión de una capa de pintura anticorrosiva después de 268 horas en cámara de niebla salina, cámara de humedad e inmersión en agua destilada y de 104 ciclos en cámara de prohesión.

Los altos valores alcanzados con el pretratamiento P8 corrobora que la existencia de grupos oxhidrilo en la superficie de aluminio incrementa las uniones de adhesión. En todos los casos, después de las primeras horas de exposición, se observó una disminución en la adhesión lo cual correspondería a la hidratación del óxido de aluminio en la interfase saturada de agua; se produciría una sustitución de la interacción polímero-óxido (hidróxido) por polímero-agua-hidróxido. Como resultado de este proceso, se forman puentes de hidrógeno entre el metal y el polímero a través de grupos funcionales de este último. El crecimiento del hidróxido metálico colma la rugosidad superficial y pueden producirse enlaces hidrógeno entre éste y el polímero, aunque se sugiere que el óxido de aluminio hidratado decrece la estabilidad de las uniones de adhesión frente al agua **[4, 11]**.

Los pretratamientos P12 y P14 presentaron satisfactorios resultados aún cuando las condiciones operativas empleadas incluyeron una temperatura del baño de 25°C. La elección de esta temperatura se debió a que se buscó emplear condiciones de trabajo menos peligrosas que las habituales (60 a 70°C) **[10]**.

La incorporación de fluoruro de potasio (P15), **Fig. 4**, mejoró ligeramente la adhesión observada sin ese compuesto (P14), **Fig. 5**, a pesar de que el ataque superficial observado es muy importante. El ácido fluorhídrico formado ataca rápidamente el aluminio generando un depósito amorfo de aluminio, óxido de cromo y óxido de aluminio.

Los resultados obtenidos empleando el método ASTM D-3359 B indicaron que todos los pretratamientos resultan eficientes salvo los P1, P5, P6 y P10 a partir de las 268 horas en cámara de niebla salina, cámara de humedad e inmersión en agua destilada y de 104 ciclos en la cámara de prohesión.

Este ensayo no resultó suficientemente discriminatorio como para realizar una separación más eficientes de los pretratamientos.

Con respecto a la adhesión presentada por el esquema completo cabe mencionar que en casi todos los ensayos realizados con el Elcometer 106 se ha producido un desprendimiento por pérdida de cohesión entre las capas de pintura y no de tipo adhesivo entre la pintura anticorrosiva y la base de aluminio salvo en el caso de los pretratamientos P1, P5, P6 y P10 donde la adhesión presenta los valores más bajos.

En el caso del ensayo ASTM D-3359 A, sólo la muestra con el pretratamiento P6 mostró mal comportamiento, presentando un desprendimiento casi completo de la superficie cortada para todas las exposiciones realizadas a partir de las 268 horas de ensayo encámara de niebla salina, cámara de humedad e inmersión en agua destilada y de 104 ciclos en cámara de prohesión.

CONCLUSIONES

1. La adhesión de la película de pintura sobre la superficie de alumminio depende no sólo de la morfología superficial sino de las especies químicas presentes en los baños de pretratamiento.

2. Existen otros tratamientos comparables en eficiencia al anodizado pero de más fácil manipulación y de menor costo, como es la inmersión en hidróxido de sodio al 10 % o en ácido crómico o dicromato de potasio y ácido sulfúrico.

3. La adhesión de una capa de pintura sobre una superficie de aluminio puede ser mejorada si se aplica primero un "wash primer" vinílico. Este método es más económico mientras que la adhesión es sólo ligeramente inferior a la obtenida

sobre un anodizado.

AGRADECIMIENTOS

Los autores agradecen a la Comisión de Investigaciones Científicas de la Provincia de Buenos Aires (CIC), al Consejo Nacional de Investigaciones Científicas y Técnicas (CONICET) y a la Secretaría General Técnica del Ministerio de Educación y Ciencia de España por el apoyo económico prestado para la ejecución de este trabajo.

BIBLIOGRAFIA

[1] Elustondo, J.- **Corrosión y Protección, (7-8)**, 5 (1980).

[2] Bieganska, B., Snieszek, E.- **Prog.Org.Coat., 10**, 215 (1982).

[3] Funke, W., Leidheiser, H. et al.- **J.Coat.Techn., 58** (741), 79 (1986).

[4] Arslanov, V. V., Funke, W.- **Prog. Org. Coat., 15**, 355 (1988).

[5] Funke, W.- **J. Oil Col. Chem. Assoc., 68** (9), 229 (1985).

[6] Walker, P.- **J. Oil Col. Chem. Assoc., 68** (12), 319 (1985).

[7] Funke, W.- **J. Oil Col. Chem. Assoc., 69** (3), 78 (1986).

[8] Timmius, F. B.- **J. Oil Col.Chem. Assoc., 62** (4), 131 (1979).

[9] Anon.- **Paint Manufacture and Testing News, 49** (9), 20 (1979).

[10] Arslanov, V. V., Ogarev, V. A.- **Prog Org. Coat. 15**, 1 (1987).

[11] Garnish, E. W.- **J. Oil Chem. Assoc, 60** (2), 69 (1969).

Nota: Este trabajo ha sido enviado para su publicación en el Journal of the Brazilian Chemical Society.

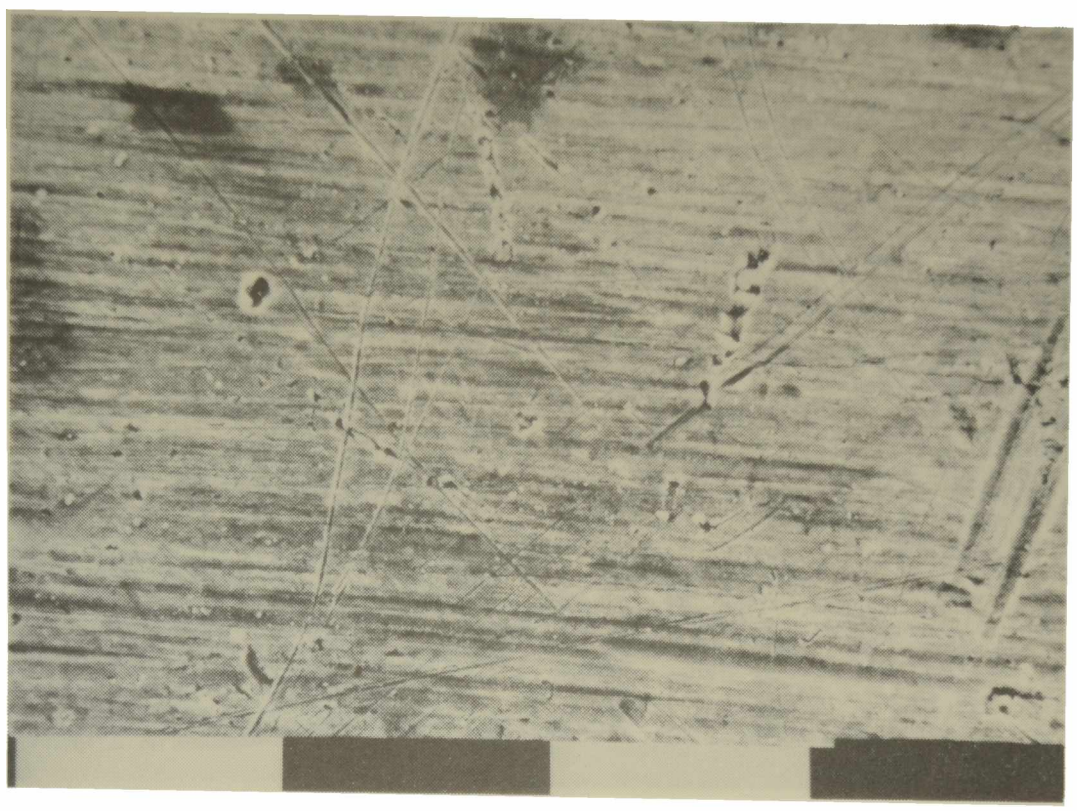

Fig. 2.- Superficie de aluminio sin pretratamiento. 1000 x.

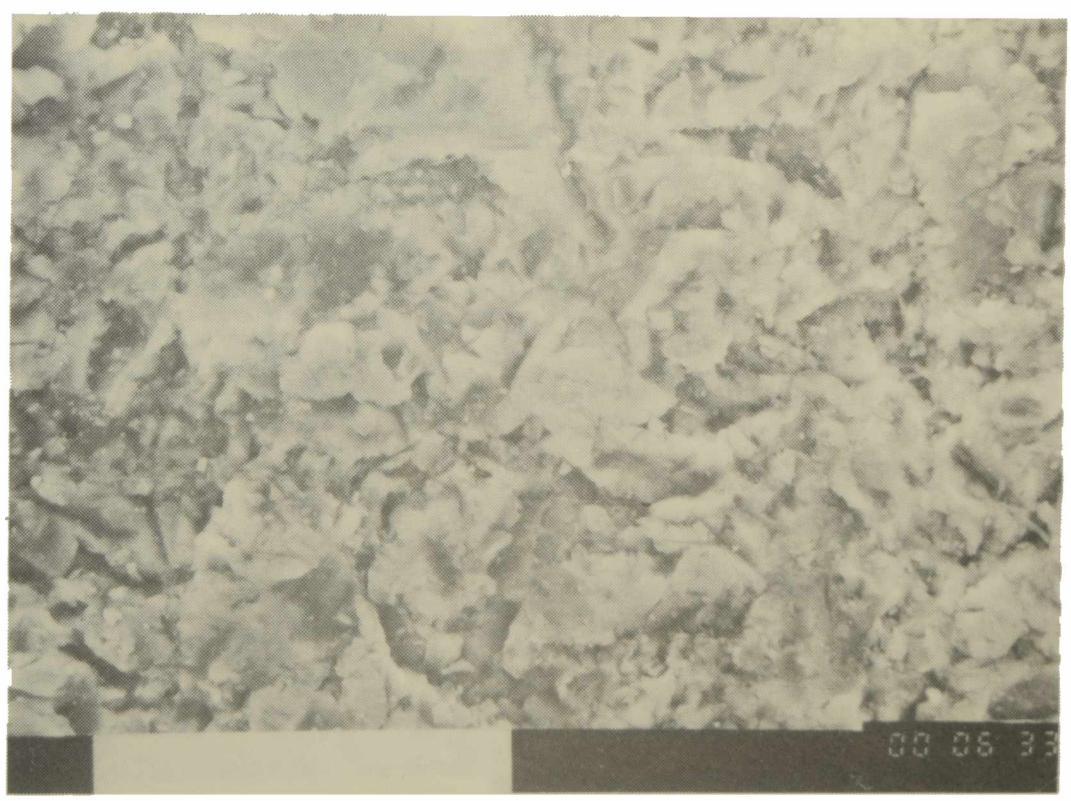

Fig. 3.- Superficie arenada (P1). 500 x.

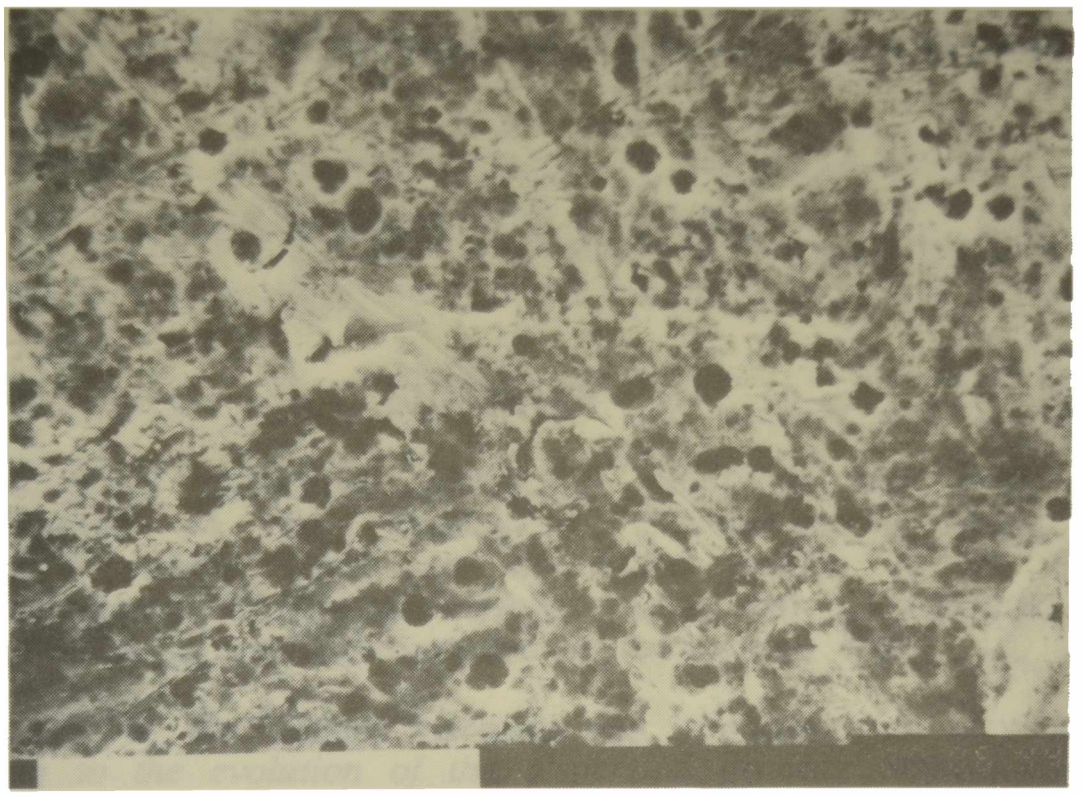

Fig. 4.- Superficie tratada con dicromato de potasio, ácido sulfúrico y fluoruro de potasio (P15). 500 x.

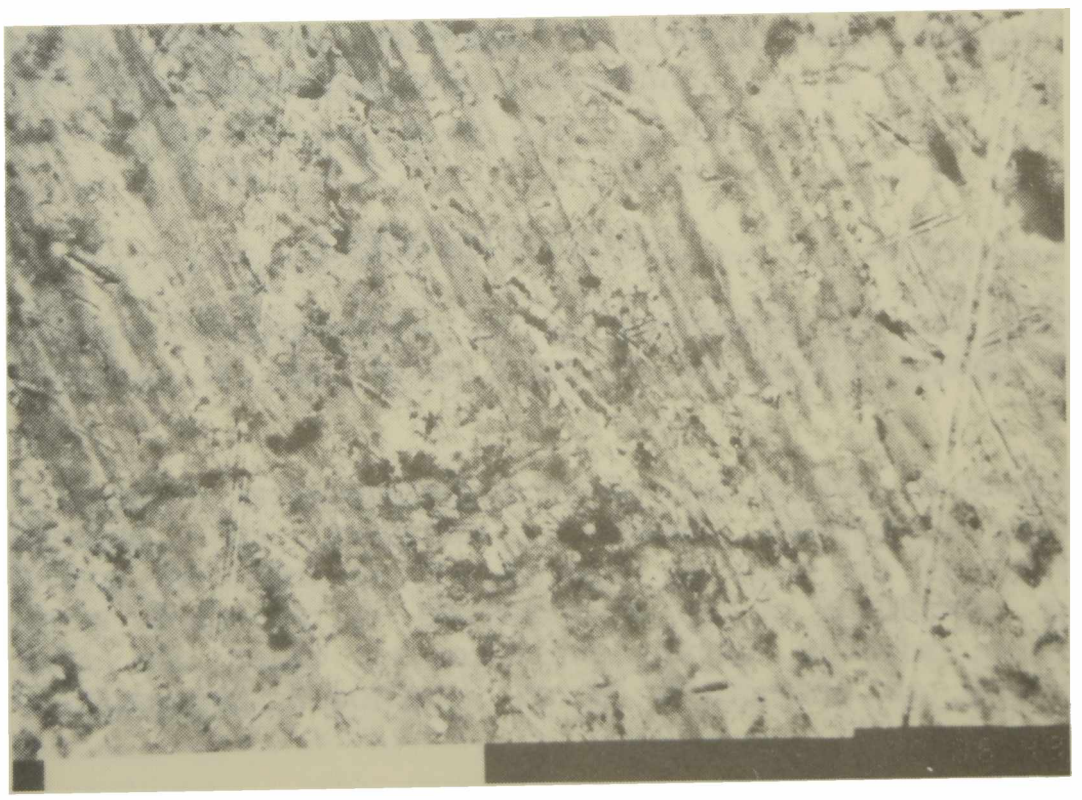

Fig. 5.- Superficie tratada con dicromato de potasio y ácido sulfúrico (P14). 500 x.

REOLOGIA DE LA DISPERSION DE LOS PIGMENTOS EN PINTURAS

RHEOLOGY OF PIGMENT DISPERSION DURING PAINT MANUFACTURE

C. A. Giúdice[1] y J. C. Benítez[2]

SUMMARY

Numerous results of laboratory experiences point out that there are two important changes in the rheological characteristics during pigment dispersion in a vehicle based on chlorinated rubber 20 cP adequately plasticized. Mentioned rheological changes were more significative at low shear rate and when pigment concentration by volume was high.

The first change in the system viscosity was registered at very low shear rate, according to the evolution of the dispersion process. Second change was in the dispersion rheology, that means in the millbase viscosity/shear rate ratio, according to dispersion continued.

Experimental results show that pigment dispersion process can be optimized selecting carefully the operative rate of the equipment employed for each one of the stages involved.

Keywords: *pigment dispersion, millbase, rheological test, pigment volume concentration, dispersion time, optimization.*

INTRODUCCION

Una de las etapas fundamentales en la preparación de una pintura es la dispersión del pigmento, la cual tiene lugar en un medio líquido denominado vehículo **[1-3]**.

Este proceso involucra la **humectación** en la cual el aire es reemplazado por el medio dispersante (las partículas asociadas permanecen prácticamente inalteradas), la **rotura mecánica** de los flóculos en otros de menor número de partículas primarias y finalmente la **estabilización de la dispersión** que permite alcanzar un producto que puede ser mantenido durante períodos prolongados sin modificaciones o alteraciones importantes en la distribución de tamaño de las partículas asociadas.

La humectación, la rotura mecánica y la estabilización de la dispersión no son necesariamente secuenciales, pero es probable que la tercera etapa se lleve a cabo fundamentalmente cuando las primeras dos están sustancialmente completadas **[4-6]**. Una adecuada dispersión usualmente significa que el pigmento está finamente dividido y defloculado en el vehículo. Muchas propiedades de la pintura líquida y

---

[1] Miembro de la Carrera del Investigador del CONICET

[2] Miembro de la Carrera del Investigador de la CIC

en estado de película seca dependen del grado de dispersión del pigmento; estudio de numerosos autores se registran en la bibliografía **[7-13]**.

El objeto de este trabajo fue determinar las características reológicas de la dispersión de un pigmento anticorrosivo en un vehículo de base solvente.

FORMULACION Y ELABORACION DE LAS PINTURAS

A los efectos de llevar a cabo el estudio, se diseñaron cinco pinturas anticorrosivas de la siguiente composición:

- **Pigmentación.** Las muestras se elaboraron con fosfito básico de cinc como pigmento anticorrosivo **[14, 15]** y con dos pigmentos inertes en forma conjunta, óxido férrico/sulfato de bario (1,1/1,0 en volumen). La relación pigmento inhibidor/pigmento inerte fue, en todos los casos, 40/60 en volumen.

- **Material formador de película.** Se empleó caucho clorado 20 cP, adecuadamente plastificado con parafina clorada 42 % (relación 67/33 en volumen).

- **Concentración de pigmento en volumen (PVC).** Se formularon muestras con valores de 30,0 hasta 50,0 % (con incrementos de 2,5 %) dada la significativa influencia que esta variable ejerce sobre diversas propiedades de la pintura **[16-21]**, entre ellas el comportamiento reológico **[5, 22]**.

- **Mezcla solvente.** Se seleccionó una mezcla de Aromasol H/aguarrás mineral, relación 3,5/1,0 en volumen. El contenido de sólidos en volumen fue el mismo en todas las muestras, 35,0 %.

La preparación de las pinturas se llevó a cabo en un molino de bolas de 3,3 litros de capacidad total **[23-26]**; las condiciones operativas del equipo fueron optimizadas en un trabajo previo **[27]**.

Como variable de elaboración se consideró el **tiempo de dispersión (td)** habiéndose empleado 2, 4, 6, 8, 10, 12, 18, 21 y 28 horas para cada una de las diferentes pinturas formuladas; en total se prepararon por duplicado 81 muestras diferentes.

MEDIDAS REOLOGICAS

Las pinturas fueron estudiadas empleando un viscosímetro Haake RV2 y un programador PG 142. La temperatura de trabajo fue de 20 ± 0,1 °C.

Las muestras fueron sometidas a distintas velocidades de corte γ, desde 0,89 s^{-1} hasta 712 s^{-1}, midiéndose el esfuerzo de cizallamiento (τ) resultante; y posteriormente se calculó el coeficiente de viscosidad η. Los valores experimentales fueron graficados de la siguiente manera: η (γ = cte) vs td para cada PVC y η (γ = cte) vs PVC para cada valor de td.

RESULTADOS Y DISCUSION

Los ensayos permitieron concluir en forma global que los cambios más significativos en las características reológicas fueron observados **a muy bajas velocidades de corte** γ (por ejemplo 0,89 y 3,56 s^{-1}) y para valores de **PVC**

razonablemente altos (superiores a 35,0 %).

Relación viscosidad/tiempo de dispersión. Los resultados correspondientes a valores constantes de γ, para cada uno de los PVC considerados, permitieron concluir que en la **etapa inicial de la dispersión** los cambios producidos resultaron difíciles de evaluar reológicamente debido a la heterogeneidad de la mezcla pigmento/vehículo. Sin embargo, los valores obtenidos indican claramente que luego de 2 horas de dispersión (**Fig. 1**), la viscosidad inicial disminuye ligeramente. La observación por microscopía óptica de películas extendidas sobre vidrio permitió observar que la **humectación** de las partículas fue parcial en este período, ya que el medio dispersante no pudo penetrar en el interior de los flóculos.

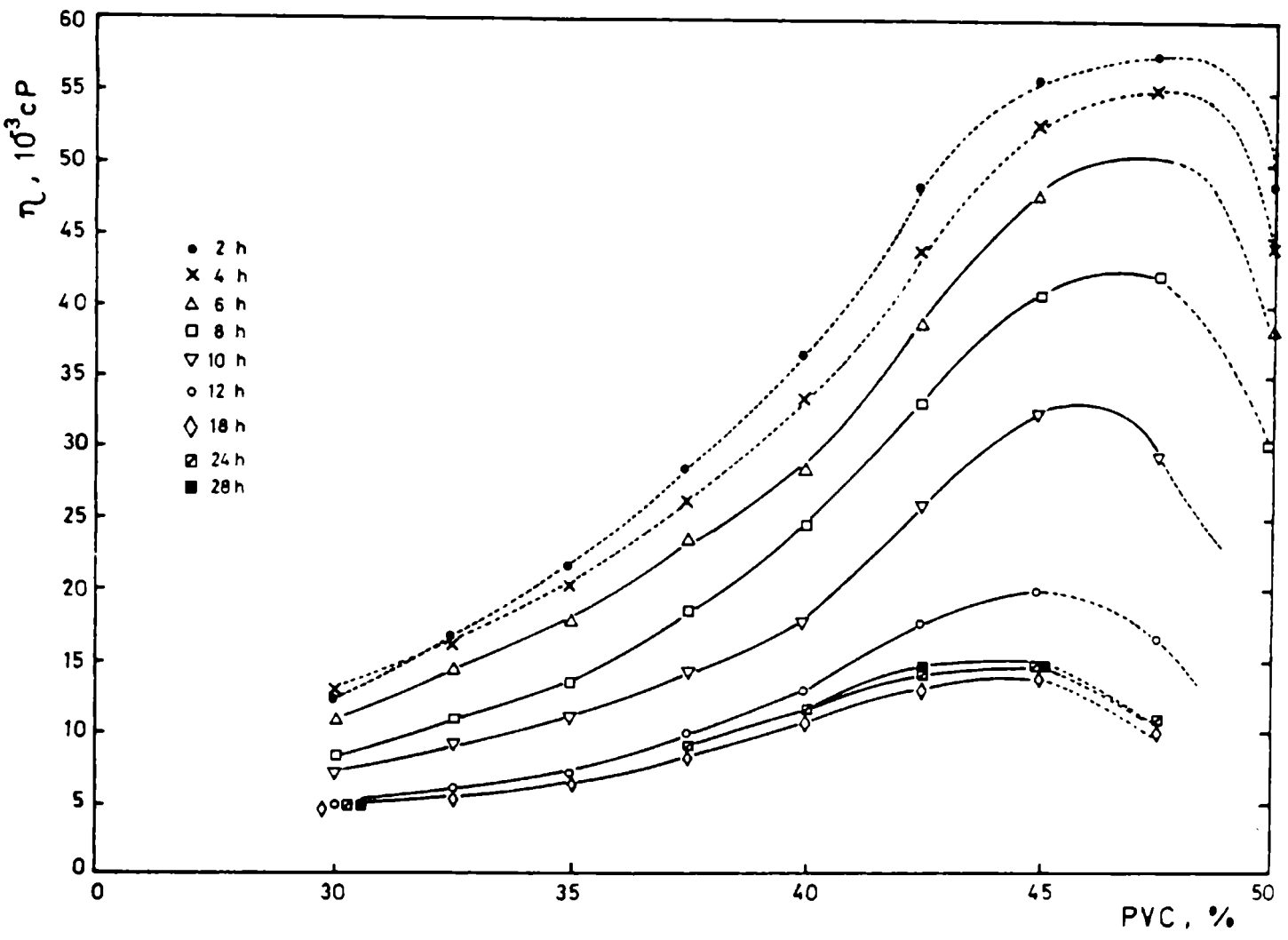

Fig. 1.- Viscosidad (γ = 0,89 s^{-1}) vs td, para cada PVC considerado.

Luego de la etapa inicial antes mencionada, **al continuar la dispersión** se produjo una disminución relativamente rápida de la viscosidad del sistema. La extensión de este período depende fundamentalmente de la composición de la mezcla base y fue más prolongada para las formulaciones de PVC más alto. En esta etapa tuvo fundamentalmente lugar la **rotura mecánica** de los flóculos, constatándose microscópicamente una sensible disminución del tamaño medio de partícula de pigmento.

La **tercera etapa del proceso** mostró que en general se produjo un ligero aumento de la viscosidad o bien ésta se mantuvo prácticamente constante. En esta última etapa no se observaron significativas variaciones en el tamaño medio de la partícula, llegándose entonces a la **estabilización de la dispersión.**

Durante todo el proceso dispersivo, se observó una menor viscosidad con más altos valores de γ, para cada PVC considerado. Además, esta última variable influyó significativamente sobre la viscosidad: un aumento del PVC, para igual tiempo de dispersión, incrementó la viscosidad del sistema. Una excepción en la

Fig. 1 estuvo constituida por la pintura formulada con el PVC 50 % que presentó valores intermedios entre los correspondientes a las muestras con PVC 40 y 45 % hasta aproximadamente 10/12 horas de dispersión, para luego disminuir más abruptamente. No fue posible evaluar experimentalmente los valores de viscosidad para tiempos de dispersión mayores.

Relación viscosidad/concentración de pigmento en volumen. Los gráficos obtenidos a γ constante, para cada tiempo de dispersión, indican que a medida que el PVC crece, la viscosidad aumenta hasta alcanzar un máximo, para luego declinar abruptamente; este descenso se debió a que no había suficiente vehículo para satisfacer la demanda del pigmento, quedando intersticios ocupados por aire. El comportamiento de la muestra con PVC 50 % observada en la Fig. 1 se corresponde con el mencionado descenso de la viscosidad.

La **Fig. 2** muestra las curvas correspondientes a la variación de la viscosidad η en función del PVC, determinadas a $\gamma = 0{,}89\ s^{-1}$. El máximo absoluto de viscosidad se obtuvo con 2 horas de dispersión y correspondió a un PVC relativamente alto (**Tabla I**). En la etapa de humectación, un mayor tiempo de dispersión condujo a máximos con ligeras disminuciones de la viscosidad y del PVC.

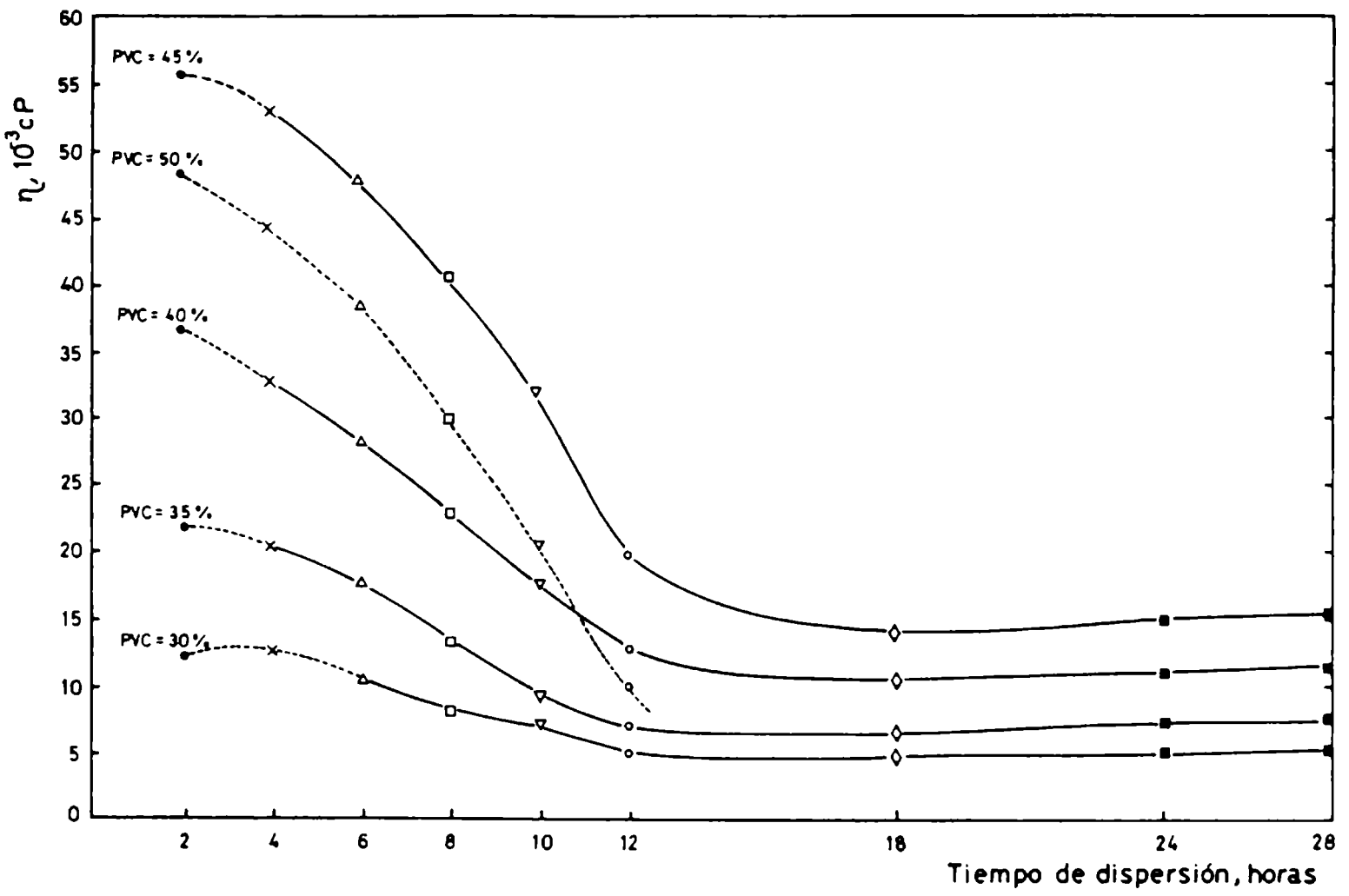

Fig. 2.- Viscosidad ($\gamma = 0{,}89\ s^{-1}$) vs PVC, para cada tiempo de dispersión considerado.

Luego de superado el período de humectación como característica fundamental de la dispersión y comenzado el de rotura mecánica del flóculo, que condujo a un menor diámetro medio de partícula asociada y por ende a una mayor área específica, se observaron máximos a valores sensiblemente decrecientes de viscosidad y PVC. Este hecho es atribuible al mayor requerimiento de vehículo para ocupar los nuevos espacios intersticiales generados por la rotura de los flóculos.

Durante el período de estabilización, tiempos de dispersión crecientes condujeron a máximos con valores ligeramente mayores de viscosidad (no hubo

cambios sensibles en el PVC) debido quizás a que el ligante del vehículo se adsorbió sobre las partículas, lo cual controló la atracción posterior y la consiguiente formación de agregados en el envase. Esta adsorción de ligante también explicaría el ligero incremento de viscosidad observado al final del proceso dispersivo (Fig. 1).

TABLA I

Tiempo de dispersión, h	PVC*, %	Viscosidad η (γ = 0,89 s^{-1}), 10^{-3} cP
2	48,6	57,6
4	48,3	55,1
6	48,1	50,2
8	47,5	42,3
10	46,7	32,5
12	45,6	20,0
18	45,1	13,7
24	45,1	14,0
28	45,1	14,2

* corresponde a los máximos de la curva η (γ = 0,89 s^{-1}) vs PVC, en función del tiempo de dispersión.

CONCLUSIONES

Los resultados de las experiencias realizadas en laboratorio indican que se observaron dos grandes cambios en las características reológicas de la dispersión del pigmento (fosfito básico de cinc y extendedores inertes) en el vehículo (caucho clorado plastificado) durante la elaboración de las diferentes muestras de pinturas anticorrosivas. Dichos cambios fueron más pronunciados a bajas velocidades de corte γ y cuando la concentración de pigmento en volumen (para igual contenido de sólidos) fue elevada.

El primer cambio se registró en la viscosidad del sistema a muy baja velocidad de corte, a medida que evolucionó el proceso dispersivo. El segundo cambio se produjo en la reología de la dispersión, es decir en la relación entre la viscosidad de la mezcla base ("mill base") y la velocidad de corte, a medida que continuaba la dispersión.

En consecuencia el proceso de dispersión de los pigmentos puede ser **optimizado seleccionando adecuadamente la velocidad operativa del equipo empleado para cada una de las etapas involucradas** (humectación, rotura mecánica de los flóculos y estabilización); durante la dispersión, una más alta velocidad de rotación del molino (mayor velocidad de corte γ) conduce a un descenso de la viscosidad del sistema y en consecuencia a una mayor eficiencia del proceso (disminución de los tiempos correspondientes a cada una de las etapas mencionadas).

AGRADECIMIENTOS

Los autores agradecen a la Comisión de Investigaciones Científicas de la Provincia de Buenos Aires (CIC) y al Consejo Nacional de Investigaciones Científicas y Técnicas (CONICET) por el apoyo económico brindado para la realización de este trabajo.

BIBLIOGRAFIA

[1] Crowl, V. T.- **J. Oil Col. Chem. Assoc., 55** (5), 388-420, 1972.

[2] Patterson, D. (Editor).- **Pigments; an introduction to their physical chemistry**, Elsevier, London, 1967.

[3] Patton, T. C.- **Paint flow and pigment dispersion**, J. Willey and Sons, New York, 1979.

[4] Brownlie, G., Faraus, G. C.- **J. Paint Technology, 38** (494), 113-122, 1966.

[5] Jefferies, H. D.- **J. Oil Col. Chem. Assoc., 45** (10), 681-700, 1962.

[6] Asbeck, W. K.- **J. Coatings Technology, 49** (635), 59-70, 1977.

[7] Fisher, E. K., Jerome, C. W.- **Ind. Eng. Chemistry, 35**, 336-343, 1943.

[8] Patton, T. C.- **J. Paint Technology, 40** (522), 301-343, 1968.

[9] Daniel, F. K, Piñeiro, R.- **J. Coatings Technology, 49** (631), 74-77, 1977.

[10] McKay, R. B.- **J. Oil Col. Chem. Assoc., 71** (1), 7-10, 1988.

[11] Cowley, A. C. D., Gallon, M. R.- **J. Oil Col. Chem. Assoc., 71** (10), 310-329, 1988.

[12] Hall, J. E., Benoit, R., Bordeleau, R., Rowland, R.- **J. Coatings Technology, 60** (756), 49-61, 1988.

[13] Hall, J. E., Bordeleau, R., Brisson, A.- **J. Coatings Technology, 61** (770), 73-81, 1989.

[14] Giúdice, C. A., del Amo, B.- **CIDEPINT-Anales**, 61-79, 1993.

[15] Claxton, A. E.- **Official Digest, 36** (470), 268, 1964.

[16] Asbeck, W. K., Van Loo, M.- **Ind. Eng. Chemistry, 41**, 1470, 1949.

[17] Bierwagen, G. P.- **J. Paint Technology, 44** (574), 46-55, 1972.

[18] Boxall, J., von Fraunhofer, J. A., Werren, S. C.- **J. Oil Col. Chem. Assoc., 55** (1), 24-34. 1972.

[19] Villoria, G., Giúdice, C. A.- **American Paint and Coatings Journal, 74** (12), 38-46, 1989.

[20] Asbeck, W. K.- **J. Coatings Technology, 49** (635), 59-70, 1977.

[21] Giúdice, C. A - **American Paint and Coatings Journal, 75** (55), 36-46, 1991.

[22] Giúdice, C. A.- **Pitture e Vernici, 67** (1), 5-13, 1991.

[23] Soto, T.- **J. Coatings Technology, 51** (657), 79-85, 1979.

[24] Carr, W.- **Progress in Organic Coatings, 4** (3), 161-188, 1976.

[25] Hornby, M. R., Murley, R. D.- **Progress in Organic Coatings, 3** (3), 261-279, 1975.

[26] Oyarzún, J.- **J. Coatings Technology, 55** (704), 27-85, 1983.

[27] del Amo, B., Giúdice, C. A., Rascio, V.- **J. Coatings Technology, 56** (719), 63-69, 1984.

PIGMENTOS IGNIFUGOS DE ACCION FISICA EN PINTURAS RETARDANTES DE LLAMA

FIREPROOF PIGMENTS OF PHYSICAL ACTION IN FLAME RETARDANT PAINTS

B. del Amo[1] y C. A. Giúdice[1]

SUMMARY

The influence of fireproof pigments such as chalk, talc, aluminium hydroxide, borax, kaolin and boric acid on efficiency of flame retardant paints was studied. All the above mentioned pigments exert a physical action.

Formulated paints had a 45 % pigment volume concentration (PVC) and were manufactured in ball mill jars of 3.3 liters capacity.

The performance of these paints applied on panels of Araucaria Angustifolia was assessed by means of exposure to a Bunsen burner flame.

Paints formulated with chalk, talc, aluminium hydroxide or borax showed a very high performance.

Keywords: *flame retardant paint; pigment volume concentration; chalk; talc; aluminium hydroxide; kaolin; boric acid; borax (pintura retardante de llama; concentración de pigmento en volumen; tiza; talco; hidróxido de aluminio; caolín; ácido bórico, bórax)*

INTRODUCCION

La verdadera magnitud del problema del incendio resulta notable cuando se manejan cifras sobre las pérdidas materiales y humanas que se producen año tras año. Las pérdidas económicas en países industrializados alcanzan el 0,25 % del Producto Bruto Interno.

A menudo se producen también importantes pérdidas indirectas de díficil evaluación tales como disminución de ingresos por la interrupción total o parcial de la actividad de una empresa, pérdida de clientes, diferencias sustanciales en el costo de sustitución de edificios y equipos, etc. Se estima que de cada cinco empresas que han tenido un incendio importante, cuatro de ellas desaparecen dentro de los tres años siguientes de ocurrido el siniestro.

Desde hace algunos años las compañías de seguro han encontrado que el camino para hacer frente a esa situación es por medio de la prevención. El empleo de pinturas retardantes de llama ocupa un lugar importante en este tema. Estas pinturas no son capaces por ellas mismas de soportar la acción de la combustión cuando están expuestas a un calor intenso o fuego. Están formuladas para

---

[1] Miembro de la Carrera del Investigador del CONICET

autoextinguirse cuando la fuente irradiante es removida.

La sola presencia de pigmentos no inflamables en una pintura ofrece un grado limitado de protección. El pigmento divide los componentes en dominios aislados por ocupación de los poros y regiones amorfas del polímero, por lo que se requiere una mayor cantidad de calor para alcanzar la temperatura de pirólisis. Este efecto es mejorado por el elevado calor específico y baja conductividad térmica de los productos utilizados. Otra opción es el efecto debido a la posible descomposición endotérmica del ignífugo con actividad física, con desprendimiento de agua, lo que disminuye sensiblemente la temperatura de reacción **[1]**.

Existen otros pigmentos que ejercen un rol importante en la inhibición o supresión del fuego, produciendo liberación de gases no combustibles que diluyen a los combustibles o la formación de vidrios a partir de sustancias de bajo punto de fusión que sellan el sustrato combustible; también puede formarse una capa resistente al fuego, que aisla el sustrato del calor o provoca la alteración de la reacción de combustión debido a la acción de un catalizador adecuado.

Ciertos pigmentos son conocidos por su capacidad para aumentar la eficiencia de las pinturas retardantes de llama mientras que otros la reducen [1]. Los más perjudiciales son los pigmentos orgánicos y, de ser posible, sólo deberían ser usados los pigmentos metálicos.

En este tipo de pinturas juega un rol importante la elección de un eficiente formador de película. Generalmente se utilizan resinas cloradas que a temperaturas elevadas liberan hidruros que reaccionan con los radicales hidroxilo presentes en la llama y también con los átomos de hidrógeno activados, generando gases incombustibles que actúan impidiendo el acceso del oxígeno del aire.

La acción de los compuestos halogenados no se limita en general sólo a su activación en la fase gaseosa sino que también aumentan el residuo carbonoso durante la pirólisis del polímero, mostrando así una acción ignífuga en fase sólida.

El objetivo del presente trabajo fue estudiar el efecto del empleo de pigmentos ignífugos de acción física (como tiza, talco, hidróxido de aluminio, caolín, bórax y ácido bórico) sobre la acción retardante del fuego.

COMPOSICION DE LAS PINTURAS

Pigmento

Se empleó dióxido de titanio variedad rutilo (26,7 % en volumen sobre pigmento) para lograr un buen poder cubritivo y además porque dadas sus características físicas requiere una elevada cantidad de calor para alcanzar la temperatura de pirólisis.

Como pigmento ignífugo se empleó el trióxido de antimonio (7,7 % en volumen sobre pigmento), dado que el oxicloruro y/o el tricloruro de antimonio formados interfieren en la reacción de propagación de la llama.

El sulfato de bario fue utilizado debido a que es un ignífugo que actúa en fase sólida (16,4; 32,8 y 49,2 % en volumen sobre pigmento); por acción del calor se descompone en ácido sulfúrico provocando la formación de un residuo carbonoso y la disminución de gases inflamables **[2]**. Además, incrementa la dureza de la película.

Los pigmentos ignífugos de acción física **[3-5]** estudiados fueron la tiza, el talco, el hidróxido de aluminio, el caolín, el bórax y el ácido bórico (**Tabla I**),

en tres niveles hasta completar la pigmentación (49,2; 32,8 y 16,4 % en volumen).

TABLA I

Características de los pigmentos ignífugos de acción física estudiados

	Indice de absorción de aceite, % en peso	Tamaño medio de partícula, μm	Densidad, $g.cm^{-3}$
Tiza natural	30	1,5	2,7
Talco	42	0,9	2,5
Hidróxido de aluminio	47	2,2	2,4
Caolín	32	3,5	2,8
Bórax	74	6,0	1,8
Acido bórico	70	18,0	1,5

Ligante

Como material formador de película se seleccionó una resina alquídica clorada **[6-8]** empleada en trabajos previos **[9,10]** debido a las excelentes propiedades ignífugas que posee.

Aditivos y disolvente

Como agentes secantes fueron utilizados el naftenato de cobalto y el naftenato de zirconio mientras que para regular la viscosidad y alcanzar un adecuado nivelado sin escurrimiento de la película se empleó el estearato de aluminio.

El aguarrás mineral se empleó como disolvente por su reducido poder contaminante **[9]**.

Concentración de pigmento en volumen

El PVC influye sobre la capacidad ignífuga de las pinturas. En el presente trabajo se seleccionó un PVC de 45 % **[10]**.

PREPARACION DE LAS MUESTRAS

Se realizó en un molino de bolas de 3,3 litros de capacidad. En una primera etapa se incorporó la resina alquídica clorada en solución y luego se dispersaron los pigmentos durante 24 horas.

Las condiciones operativas del molino fueron establecidas de manera de alcanzar una adecuada distribución de tamaño de partícula **[11]**. Finalmente se adicionaron los aditivos y se ajustó la viscosidad en el envase. Cada una de las muestras se preparó por triplicado.

ENSAYOS REALIZADOS

Evaluación de la capacidad ignífuga

Las probetas para ensayo (200x100x3 mm) se elaboraron con madera de Araucaria Angustifolia estacionada durante 6 meses. Antes de la aplicación de las muestras dichas probetas fueron cuidadosamente lijadas en el frente y en los bordes. La primera capa de pintura se aplicó diluyendo las muestras al 50 % en aguarrás mineral; luego de 24 horas de secado se aplicaron otras dos capas también con un lapso de 24 horas entre ellas. El espesor final de la película seca fue de 110 ± 10 μm.

Luego de 10 días de pintada la última capa las probetas se colocaron en estufa a 45-48°C durante 24 horas para favorecer la eliminación del solvente retenido.

Las probetas fueron expuestas a la acción intermitente de la llama de un mechero Bunsen de acuerdo con la metodología indicada en un trabajo previo **[6]**. La evaluación de los resultados se realizó en función de lo establecido en la escala indicada en la **Tabla II**.

TABLA II

Escala de calificación empleada para evaluar el comportamiento de las pinturas experimentales

10.	Durante el ensayo no hay ninguna llama excepto la del mechero. La zona carbonizada no excede los 3 cm^2.
7.	Cinco segundos después de retirar el mechero no persiste llama sobre la superficie. La zona carbonizada no excede los 6 cm^2.
5.	Cinco segundos después de retirar el mechero no persiste llama sobre la superficie pero sí puntos de ignición sobre la zona carbonizada que perduran como máximo 10 segundos. Esta última no excede los 12 cm^2.
2.	Cinco segundos después de retirar el mechero persiste la llama: el ensayo se considera no aprobado.

Nota: El ciclo de exposición al fuego/descanso se repite si la calificación es igual o superior a 5.

Como muestras testigo se seleccionaron una pintura alquídica comercial no ignífuga y otra retardante de llama formulada con el mismo ligante empleado en esta experiencia y pigmentada en volumen con 26,7 % de dióxido de titanio, 7,7 % de trióxido de antimonio y 65,6 % de sulfato de bario **[4]**.

La clasificación de las muestras se realizó de acuerdo a lo indicado en la **Tabla III**.

RESULTADOS Y DISCUSION

Los resultados obtenidos en el ensayo de exposición a la llama intermitente se indican en la **Tabla IV** y corresponden al promedio de las determinaciones realizadas.

TABLA III

Clasificación de las pinturas

Puntaje promedio en ensayo de llama intermitente	Calificación de la pintura	Clasificación de la pintura
100 o más	Aprobado	Clase A
70 a 99	Aprobado	Clase B
30 a 69	No aprobado	Clase C
29 o menos	No aprobado	Clase D

TABLA IV

Resultados del ensayo de llama intermitente

Pigmento de acción física	Contenido de pigmento*	Puntaje promedio	Calificación de la pintura	Clasificación de la pintura
Tiza	16,4	148	Aprobado	Clase A
	32,8	165	Aprobado	Clase A
	49,2	180	Aprobado	Clase A
Talco	16,4	132	Aprobado	Clase A
	32,8	145	Aprobado	Clase A
	49,2	156	Aprobado	Clase A
Hidróxido de aluminio	16,4	142	Aprobado	Clase A
	32,8	157	Aprobado	Clase A
	49,2	171	Aprobado	Clase A
Bórax	16,4	140	Aprobado	Clase A
	32,8	156	Aprobado	Clase A
	49,2	170	Aprobado	Clase A
Caolín	16,4	66	No aprobado	Clase C
	32,8	60	No aprobado	Clase C
	49,2	52	No aprobado	Clase C
Acido bórico	16,4	110	Aprobado	Clase A
	32,8	98	Aprobado	Clase B
	49,2	90	Aprobado	Clase B
Testigo ignífugo	---	130	Aprobado	Clase A
Testigo no ignífugo	---	2	No aprobado	Clase D

* Pigmento de acción física expresado en volumen % sobre pigmento

El tipo de pigmento empleado demostró tener influencia sobre la capacidad retardante de llama de las películas. Las pinturas que aprobaron el ensayo de resistencia a la llama fueron las formuladas con pigmentos de acción física tales como **tiza, talco, hidróxido de aluminio** y **bórax**, en los tres niveles considerados en este estudio. Estas pinturas fueron clasificadas como **Clase A** y en todos los casos, su comportamiento como retardante de llama fue superior a las muestras seleccionadas como **testigo ignífugo (Clase A)** y **no ignífugo (Clase D)**.

La **tiza** basa su acción retardante en el hecho que en presencia de ácidos se descompone con desprendimiento de dióxido de carbono y además presenta una elevada absorción de energía térmica. Puede ser incorporada en niveles importantes como extendedor, ya que tiene un bajo índice de absorción de aceite y bajo costo.

El **talco** debido a su alto calor específico y baja conductividad térmica, presentó también una satisfactoria eficiencia. Además, contribuyó a impartir a las pinturas formuladas adecuadas propiedades antisedimentantes, excelente pintabilidad, satisfactorio nivelado y también buena resistencia al agua, a la humedad y a la mayoría de los reactivos químicos.

Por su parte, la significativa acción retardante del **hidróxido de aluminio** es atribuible a que libera moléculas de agua frente a un aumento de la temperatura, con el consiguiente consumo de energía en la deshidratación. Lamentablemente presenta un elevado índice de absorción de aceite, lo cual limita el nivel que puede ser incorporado en la composición.

Los **boratos** y el **bórax** en particular, actúan como retardantes de fuego debido a la formación de vidrios de bajo punto de fusión que aislan la superficie del frente de fuego: favorecen la generación de cadenas carbonosas más que el desprendimiento de monóxido o dióxido de carbono. Sin embargo, en general presentan el inconveniente de poseer un muy elevado índice de absorción de aceite y de ser solubles en agua **[4, 5]**, hecho que limita su empleo.

Un análisis particular merece el comportamiento del ácido bórico como ignífugo. Este pigmento, que basa su acción en una forma similar a la mencionada para el bórax, presentó una adecuada capacidad ignífuga cuando se lo incluyó en la menor concentración de las tres consideradas en este trabajo (16,4 % en volumen sobre pigmento). Esta pintura fue clasificada como **Clase A** mientras que las formuladas con los restantes niveles, si bien aprobaron el requerimiento del ensayo, fueron clasificadas como **Clase B**.

Las pinturas formuladas con **caolín** no aprobaron el ensayo (**Clase C**), pese a que en presencia de altas temperaturas este pigmento desprende agua de hidratación en forma de vapor. Sin embargo, es importante señalar que usualmente se lo emplea en la industria de la pintura como extendedor, ya que presenta un bajo índice de absorción de aceite, es fácil de dispersar e imparte buenas características de pintabilidad y nivelado. Además, la incorporación de dióxido de titanio en la formulaciones con caolín, mejora, como es obvio, el poder cubritivo de la pintura.

AGRADECIMIENTOS

Los autores agradecen a la Comisión de Investigaciones Científicas de la Provincia de Buenos Aires (CIC) y al Consejo Nacional de Investigaciones Científicas y Técnicas el apoyo económico brindado para la realización de este trabajo.

BIBLIOGRAFIA

[1] Giúdice, C.A.- **European Coatings Journal**, (5), 248 (1992).

[2] Patton, T. C. (Ed.).- Barium Sulfate, Natural. **Pigment Handbook**, Vol. I, John Wiley & Sons, EE.UU. (1962).

[3] Bishop, D. M., Bottomley, D., Zobel, F. G. R.- **J. Oil Col. Chem. Assoc., 66** (12), 373 (1983).

[4] Wake, L. V.- **J. Oil Col. Chem. Assoc., 71** (11), 378 (1988).

[5] Smith, A.- **Paint Manufacture and Resin News, 50** (8), 24 (1980).

[6] Hancock, R. A., Leeves, N. J.- **Progress in Organic Coatings, 17** (3), 321 (1989).

[7] Patton, T. C.- **Alkyd Resin Technology**. John Wiley & Sons, New York, EE. UU. (1962).

[8] Bravo Rey, A.- **Tecnología de las resinas alquídicas**. Reverté S.A., Barcelona, España (1950).

[9] Giúdice, C. A., del Amo, B.- **European Coatings Journal**, (11), 740 (1991).

[10] Giúdice, C. A., del Amo, B.- **European Coatings Journal**, (1-2), 8 (1992).

[11] Giúdice, C. A., Benítez, J. C., Rascio, V.- **J. Oil Col. Chem. Assoc., 63** (3), 151 (1980).

PINTURAS ANTIINCRUSTANTES VINILICAS TIPO ALTO ESPESOR BASADAS EN RESINA COLOFONIA DESPROPORCIONADA

HIGH BUILD VINYL ANTIFOULING PAINTS BASED ON DISPROPORTIONATED WW ROSIN

J. C. Benítez[1] y C. A. Giúdice[2]

SUMMARY

Rosin is a natural non toxic resin which is widely used in the paint industry. It consists of nearly 85 per cent of resinic acids (abietic acid and its isomers) and the rest are complex esters of before mentioned acids with unsaponifiable materials. Its physical and chemical characteristics point out to this resin as a fundamental material in the manufacture of soluble antifouling paints for controlling marine organisms settlement on fixed and in movement structures immersed in seawater.

However, the air exposure gives binders with variable dissolution rate and uncertain protection periods. This problem was solved by employing disproportionated rosin which was obtained and characterized at laboratory.

Painted panels with high build antifouling paints based on binders of different disproportionated rosin/vinyl resin ratios were exposed to air: a series for 24 hours and a similar one for 30 days. Then, they were submerged in seawater. Some paints showed promissory results for three years immersion.

Keywords: *antifouling paint; soluble matrix; disproportionated WW rosin; co-binder; dissolution rate; bioactivity.*

INTRODUCCION

La resina colofonia es un producto natural, no tóxico, de amplia aplicación en la industria de la pinturas. Está compuesta fundamentalmente por ácidos resínicos (ácido abiético y sus isómeros en aproximadamente un 85 % ; el resto son ésteres complejos de estos ácidos junto con algunas sustancias insaponificables **[1, 2]**. Los ácidos resínicos contienen un grupo fenantreno con dobles ligaduras y distintos grupos en diferentes posiciones; isomerizan de una forma a otra y por lo tanto resulta difícil determinar la exacta proporción de cada uno de ellos. La fórmula empírica es $C_{20}H_{30}O_2$, con un peso molecular de 302.

Sus características físicas y químicas así como su bajo precio, la convierten en una resina fundamental para la elaboración de pinturas antiincrustantes tipo matriz soluble. Un correcto funcionamiento y una adecuada bioactividad de estas pinturas evita la fijación de organismos colonizantes en todas las estructuras fijas o móviles en contacto con agua de mar, permite mantener la continuidad del esquema protector y en consecuencia, la eficacia del mismo.

---

[1] Miembro de la Carrera del Investigador de la CIC

[2] Miembro de la Carrera del Investigador del CONICET

En una pintura antiincrustante tipo matriz soluble, el tóxico y la matriz se disuelven simultáneamente, la velocidad de liberación del tóxico, que es función entre otras variables, de la naturaleza química del ligante, define la capacidad biocida de la pintura. La resina colofonia (resin WW) presenta algunos inconvenientes en servicio, como por ejemplo la oxidación que ocurre cuando es expuesta al aire y también durante la inmersión en agua, influyendo así sobre la variable fundamental que es la velocidad de disolución de la película. Por tal motivo en el presente trabajo se formularon y elaboraron en laboratorio algunas pinturas antiincrustantes basadas en resina colofonia desproporcionada y se evaluó su comportamiento biocida en balsa experimental utilizando placas pintadas con diferentes períodos de exposición al aire previo a su inmersión, con el objeto de establecer la influencia de esta variable.

PREPARACION Y CARACTERIZACION DE LA RESINA COLOFONIA DESPROPORCIONADA

La elaboración en escala de laboratorio y la caracterización de la resina colofonia desproporcionada se llevaron a cabo en forma similar a la mencionada en un trabajo previo [3] La resina obtenida experimentalmente presenta con respecto a la resina colofonia original una reducción del numero ácido, del punto de fusión y del punto de ablandamiento, y está constituida fundamentalmente por una mezcla de ácido dehidroabiético, ácido dihidroabiético y ácido tetrahidroabiético, lo cual conduce a una mayor resistencia a la oxidación en su exposición al aire.

FORMULACION Y ELABORACION DE LAS PINTURAS ANTIINCRUSTANTES

En lo referente a los ligantes, se consideraron tres composiciones con contenido decreciente de coligante (relacion resina colofonia/coligante 1/1, 2/1 y 3/1 en volumen) Se elaboraron dos series, la primera de ellas, con la resina colofonia original y la otra con la resina colofonia desproporcionada, preparada esta ultima en laboratorio

El coligante empleado fue un copolímero no modificado de mediano peso molecular, de composicion cloruro de vinilo 86 % - acetato de vinilo 14 % , soluble en una mezcla de solventes acetato de cellosolve/xileno/MIBK 60/30/10 y plastificado con parafina clorada al 42 % (relación coligante/plastificante, 77/23 en volumen).

Los seis ligantes formulados (2 resinas x 3 relaciones resina colofonia/coligante) se elaboraron en un equipo de alta velocidad de agitación.

Como tóxico fundamental se empleó óxido cuproso rojo [4] y como tóxico de refuerzo óxido de cinc, en la proporción de 10 por ciento en peso con respecto al óxido cuproso. La diagramación experimental contempló un único nivel de pigmentación y una relación tóxico/ligante 0,58 en volumen. Como extendedor se incorporó carbonato de calcio natural (tiza), ya que proporcionó resultados satisfactorios en ensayos previos [5].

La elaboración de las pinturas se realizó en un molino de bolas con jarras de porcelana de 3,3 litros de capacidad total; las condiciones operativas del molino han sido definidas con anterioridad [6]. Primeramente se efectuó la dispersión del óxido de cinc y de la tiza durante 21 horas, incorporando posteriormente el óxido cuproso hasta completar un lapso de 24 horas. Finalmente, se adicionó a cada una de las muestras el aditivo reológico (gel al 5 % en peso de ácido silícico amorfo), realizando la operación a temperatura ambiente en un equipo de alta velocidad de agitación.

ENSAYO EN BALSA EXPERIMENTAL

La capacidad biocida de las pinturas se determinó por inmersión en el medio natural, empleando una balsa experimental. Si bien se trata de un ensayo estático, numerosas experiencias demuestran que reproduce satisfactoriamente las condiciones de la carena de una embarcación anclada en puerto **[7]** donde la acción del "biofouling" es más intensa. La balsa estuvo fondeada en aguas de la Base Naval Puerto Belgrano (latitud 38° 54' S, longitud 62° 06' W), zona de clima templado en la que el ritmo de crecimiento de las diferentes especies animales y vegetales se acentúa en primavera y verano (período de aproximadamente cinco meses de duración) **[8, 9]**.

Para la experiencia se utilizaron placas de acero doble decapado nuevas, de 20 x 30 cm, las que fueron arenadas, desengrasadas y protegidas mediante la aplicación de un "wash primer" vinílico y tres capas de una pintura anticorrosiva de alta resistencia. El espesor del esquema anticorrosivo fue aproximadamente de 120 μm. Sobre dicho fondo se aplicaron las diferentes pinturas antiincrustantes experimentales hasta alcanzar espesores de 220-250 μm de película seca. La aplicación se realizó empleando un equipo de pulverización sin aire comprimido ("airless spray") dejando transcurrir 24 horas entre capas.

Posteriormente los paneles fueron expuestos al aire para su envejecimiento: una serie durante 24 horas y otra similar durante 30 días; luego, los mencionados paneles fueron dispuestos en los bastidores de la balsa experimental y sumergidos en el mar.

RESULTADOS Y DISCUSION

Ensayo de inmersión

El ensayo en balsa fue diagramado de modo de poder realizar observaciones periódicas de los paneles pintados y registrar así la fijación de incrustaciones biológicas luego de 13, 19, 25, 30 y 36 meses de inmersión. Como referencia se emplearon paneles de acrílico sumergidos a la misma profundidad que los pintados **(Fig. 1)**.

La evaluación de la fijación de las incrustaciones biológicas, que permite juzgar el grado de bioactividad o eficiencia de cada pintura, se efectuó empleando la escala mencionada en trabajos previos **[10-12]**. En ella el valor 0 corresponde al panel sin fijación y 5 a aquél totalmente incrustado. Se fijó como límite máximo aceptable el valor 1 (poco), que corresponde a un 80 % de eficiencia de la pintura antiincrustante. El "fouling" de la zona de ensayo al cabo de 36 meses se puede observar en la figura citada más arriba.

Los ensayos en balsa experimental, cuyos resultados se presentan en las **tablas I** y **II** permitieron realizar las siguientes consideraciones.

Resina colofonia original/coligante, relación 1/1. La reducida bioactividad de las pinturas expuestas al aire durante 24 horas antes de la inmersión es atribuible a la baja velocidad de disolución del ligante (el alto espesor de película remanente al final del ensayo así lo indicó); se registró una abundante fijación de organismos del "fouling" marino luego de 36 meses de ensayo debido al insuficiente "leaching rate" del tóxico por bloqueo superficial de la película.

Sin embargo, la misma pintura expuesta durante 30 días al aire antes de la iniciación de la experiencia en balsa presentó un satisfactorio comportamiento

TABLA I

Bioactividad de las pinturas expuestas durante 24 horas al aire antes de la inmersión

Tipo de resina	Colofonia original			Colofonia desproporcionada		
Resina/coligante, en volumen	**1/1**	**2/1**	**3/1**	**1/1**	**2/1**	**3/1**
13 meses de inmersión	0	0	0	0-1	0	0
19 meses de inmersión	0-1	0	0-1	1	0	0-1
25 meses de inmersión	1-2	0	1**	2	0	1**
30 meses de inmersión	3	0	3	3-4	0	4
36 meses de inmersión	5	0*	5	5	0-1*	5

* Primeros indicios de agotamiento (bajo espesor remanente)

** Película agotada (muy bajo espesor remanente)

TABLA II

Bioactividad de las pinturas expuestas durante 30 días al aire antes de la inmersión

Tipo de resina	Colofonia original			Colofonia desproporcionada		
Resina/coligante, en volumen	**1/1**	**2/1**	**3/1**	**1/1**	**2/1**	**3/1**
13 meses de inmersión	0	0	0-1	0	0	0
19 meses de inmersión	0	0-1	1**	1	0	0
25 meses de inmersión	0	1*	3	2	0	1**
30 meses de inmersión	0-1	2-3	5	3-4	0	3
36 meses de inmersión	1*	5	5	5	0-1*	4-5

* Primeros indicios de agotamiento (bajo espesor remanente)

** Película agotada (muy bajo espesor remanente)

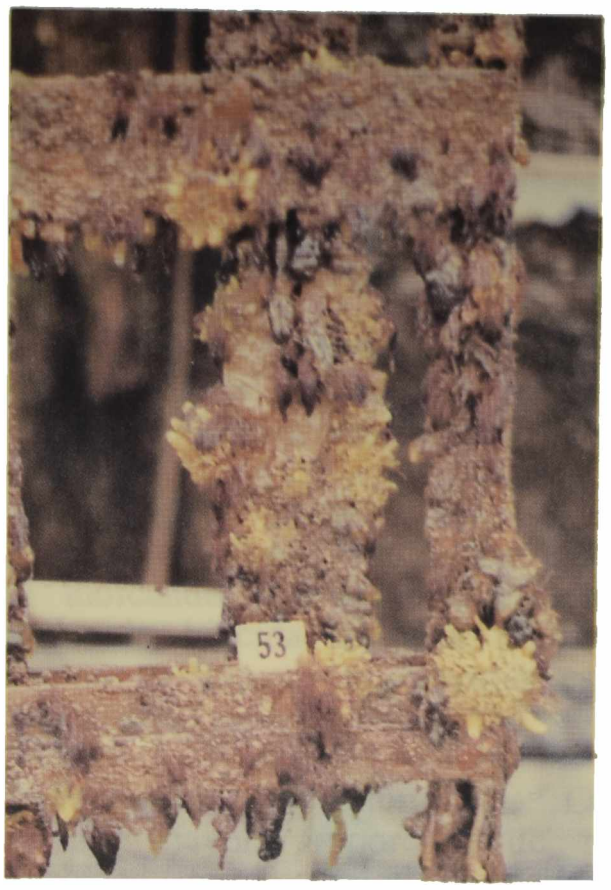

Fig. 1.- Panel testigo de acrílico (sin protección antiincrustante), 36 meses de inmersión.

Fig. 2.- Pintura basada en resina colofonia original (relación 2/1), 24 horas de exposición al aire antes de la inmersión, 36 meses de ensayo.

Fig. 3.- Pintura basada en resina colofonia desproporcionada (relación 2/1), 30 días de exposición al aire antes de la inmersión, 36 meses de ensayo.

antiincrustante debido a la adecuada disminución del espesor de la película (luego de 36 meses se observaron los primeros indicios de agotamiento); la oxidación del material soluble por acción del aire incrementó su velocidad de disolución y en consecuencia la lixiviación del tóxico.

Cabe mencionar que esta pintura no resulta confiable; su eficiencia depende del tiempo de exposición al aire.

Resina colofonia original/coligante, relación 2/1. Las pinturas formuladas con este ligante y expuestas al aire sólo durante 24 horas antes de la inmersión mostraron una excelente bioactividad: 100 % de eficiencia (fijación 0) **(Fig. 2)**.

Sin embargo, la misma pintura pero en contacto con la atmósfera durante 30 días antes de la inmersión presentó un ligero agotamiento de la película a los 25 meses de ensayo, lo cual está indicando una elevada velocidad de disolución; esto último fundamenta la nula eficiencia biocida de esta pintura (fijación 5) para un período de 36 meses. En este caso se requerirían mayores espesores de película que los aplicados para prolongar la vida útil.

Resina colofonia original/coligante, relación 3/1. Las pinturas formuladas con este ligante, por incluir una mayor proporción de material soluble en su composición exhibieron una velocidad de disolucion de película más elevada que la de la pintura formulada con la relación 2/1. Las muestras expuestas al aire durante 24 horas y 30 días antes de la inmersión presentaron un rápido agotamiento, más significativo aún en este último caso.

Resina colofonia desproporcionada/coligante, relación 1/1. En ambos casos, es decir con 24 horas y 30 días de exposición al aire antes de la inmersión, las pinturas formuladas con este ligante presentaron una insuficiente velocidad de disolución y en consecuencia, para el nivel de tóxico de la composición, un pobre "leaching rate" del óxido cuproso. Esto último explica el reducido poder biocida de las muestras, no registrándose diferencias de comportamiento en función de las diferentes condiciones de exposición al aire previo a la inmersión.

Resina colofonia desproporcionada/coligante, relación 2/1. Este ligante condujo a pinturas de mayor capacidad biocida, ya que registraron una eficiencia del 90 % (fijación 0-1) luego de 36 meses de inmersión (**Fig. 3**).

La relación 2/1, para el contenido de óxido cuproso empleado, proporcionó una pintura con adecuado "leaching rate", que controló la fijación de organismos de "fouling". Su velocidad de disolución prácticamente invariable en función del tiempo de exposición al aire previo a la inmersión, permitió formular productos altamente confiables.

Resina colofonia desproporcionada/coligante, relación 3/1. Este material con un alto contenido de resina soluble en su composición, mostró signos de agotamiento por su alta velocidad de disolución, luego de dos años de ensayo. Mayores espesores de película seca incrementarían la vida útil pero probablemente estaría lixiviando un elevado (e innecesario) nivel de tóxico por unidad de área y de tiempo; ello surge de analizar los resultados relativos de esta muestra y la formulada con la relación 2/1, ambas con resina desproporcionada en su composición. No hubo influencia del tiempo de exposición al aire previo al inicio de la experiencia.

AGRADECIMIENTOS

Los autores agradecen a la Comisión de Investigaciones Científicas de la Provincia de Buenos Aires (CIC), al Consejo Nacional de Investigaciones Científi-

cas y Técnicas (CONICET), al Departamento de Talleres Generales y Laboratorio de la Base Naval Puerto Belgrano por el apoyo prestado para la realización de las experiencias y al Lic. R. Perez Duprat e Ing. Qca. S. Zicarelli por su colaboración en la caracterización de las resinas.

BIBLIOGRAFIA

[1] Goldschmidt, E.- **Industria y Química**, (246), 25 (1978).

[2] Champetier, G., Rabaté, H.- **Chimie des peintures, vernis et pigments**, Dunod Ed., París, Vol I, 610 (1956).

[3] Giúdice, C. A., Benítez, J. C.- **Anales 4° Congreso Iberoamericano de Corrosión y Protección**, Mar del Plata, Vol. II, 653-668 (1992).

[4] Giúdice, C. A., Benítez, J. C., del Amo, B., Rascio, V.- **J. of Chem. Tech. and Biotech., 38** (4), 265 (1987).

[5] Giúdice, C. A., Benítez, J. C., Rascio, V.- **Rev. Iberoamericana de Corrosión y Protección, 15** (2), 21 (1984).

[6] Giúdice, C. A., Benítez, J. C., Rascio, V., Presta, M.- **J. Oil Col. Chem. Assoc., 63** (4), 153 (1980).

[7] Giúdice, C. A., Benítez, J. C., Rascio, V.- **J. Oil Col. Chem. Assoc., 67** (11) 283 (1984).

[8] Bastida, R. et al.- **Corrosión y Protección, 8** (8-9), 11 (1977).

[9] Bastida, R., Lichtschein, V.- **Corrosión y Protección, 10** (3-4),7 (1979).

[10] Fletcher, R. L.- **Bulletin du Liaison du COIPM** N° **8**, 5 (1980).

[11] Bastida, R.- **Proc. 3rd Int. Congress on Marine Corrosion and Fouling**, Gaithersburg, Maryland, 847 (1972).

[12] del Amo, B., Giúdice, C. A., Sindoni, O.- **Progress in Organic Coatings**, 17, 287 (1989).

APPLICATION OF POWDER COATINGS. A BIBLIOGRAPHIC REVIEW TO OBTAIN A CALCULATION SYSTEM FOR THE DESIGN OF A CONVENTIONAL FLUIDIZED BED

APLICACION DE LAS PINTURAS EN POLVO. REVISION BIBLIOGRAFICA PARA DESARROLLAR UN SISTEMA DE CALCULO PARA EL DISEÑO DE UN LECHO FLUIDIZADO CONVENCIONAL

J.J. Caprari[1] , A.J. Damia, M.P. Damia and O. Slutzky

SUMMARY

The protection of metallic substrata against aggressive agents by means of products working by "barrier effect", may be made by solvent based paints of high solids contents, by solventless paints or by powder coatings. In the last case, film formation may be made by curing or sintering the powder, which was deposited by means of a fluidized bed.

As well as the fluidization of particulate solids and pneumatic transport theory is useful for powder coatings, particular considerations are necessary due to the characteristic of the material to be used, which determines their own requeriments for the fluidized bed operation.

Starting from the formulation and elaboration of powder coatings and from an adequate selection of particle size distribution, quantity and weight of each component (that is, each one of the granulometries of the final mixture), particle properties such as softening point, glass transition temperature, etc., were determined.

Joining this data with the air characteristics at working temperature (density, viscosity, etc.), it may be made the calculation of apparent density and "viscosity" of static bed, so obtaining the main part of the design theoretical initial values.

This aspect is studied using those data for solving calculus equations of the minimum working conditions such as pressure drop, air proportion in the bed, gas velocity, bed height and porosity, apparent volume, static bed height, maximum bed density, etc.

Based on a bibliographic review, a work is developed in order to obtain a calculation system to stablish the design and correct performance of a conventional fluidized bed for powder coatings application. Epoxy based thermosetting paints were employed for this experiences.

Keywords: *fluidization; fluidized bed; apparent density and volume; minimum porosity; maximum bed density; pressure drop; Stokes law; Newton law.*

---

[1] Miembro de la Carrera del Investigador del CONICET

INTRODUCTION

Metallic substrata protection against aggressive agents by means of products working by "barrier effect" may be made by using solvent based paints of high solids contents, solventless paints or by powder coatings. In the last case, paint application may be made by curing or sintering the powder deposited in a fluidized bed. This operation is defined as the coating of a hot metallic surface, with thermoplastic or thermosetting finely powdered materials, suspended in a rapid ascending gas current.

The basic fluidization principles, implies the knowledge of particle size distribution, gas flow properties at working temperature, "viscosity" and apparent density of the static bed, particle last free falling velocity and the lesser bed porosity, to obtain the minimum operation conditions.

The development of a fluidized bed for powder coatings application, is a function of the properties of the used materials, which determines the particular working requirements of the bed. During the fluidization operation and when an adequate surface velocity is reached, is developed a compact phase of similar characteristics of a liquid. The behavior of the fluidized solid mass, is a function of the fluid nature and the particle size.

When the fluid is a liquid, the fluidization begins when a soft oscillatory movement of the solid particles is obtained. Gradually, this movement increases until a complete fluidization is reached, with the particles moving in random directions through the liquid. Strong transient currents are formed with many particles travelling in thesame direction loosing accidentally their individual movement. This mode of action is called particulate fluidization **[1]**.

When the fluid is a gas, the bed behavior is independent of his nature, and the solid particle size begins to have more influence.

Under conditions of good fluidization in a bed containing particles of the proper size and density, some gas portion travels through the bed carrying individuals particles since others travels through in "bubbles" or "pockets" which may contain solids or not. At the bed surface this bubbles breaks, "splashing" individual particles in the surrounding space. In the bed itself the particles move in different aggregates, which are lifted by the bubbles or which move aside to let the bubbles to pass. A fluidization action of this kind is known as aggregative fluidization **[2]**.

If the solid particles are very small, with diameters less than 10 micrometers, the interparticle attraction may be very strong, enough to give a special kind of aggregative fluidization known as cohesive fluidization **[2]**. Particles of such type, when aerated, tend to "ball up" into spheres which may be several millimeters in diameter. Such a problem, may introduce an error in the calculations or design. Slugging is characteristic of a large, heavy particles fluidized in tall, narrow vessels. The bubbles of gas tend to join and grow as they rise through the fluidized bed **[3]**.

The rate of growth depends on the size and density of the particles: it is quick when the particles are large and heavy, slow when they are small and light. If a vessel, small in diameter, contains a deep bed of solids, the bubbles may grow until they fill the entire cross section of the vessel. Successive bubbles then travel up the vessel separated by slugs of solid particles. Operation is erratic and unstable. Slugging may be avoided by the proper choice of particle size and by using beds with adequate height-section ratio.

This bibliographic review and the experimental corroboration tests is a

contribution to develop a single calculus system for the correct design and operation of a conventional fluidized bed for powder coating application. Epoxy based thermosetting paints were employed for this experiences.

CONVENTIONAL FLUIDIZED BEDS. THEORETICAL DESIGN ASPECTS.

There are many factors to be studied in the design of a conventional fluidized bed, specially the physical variables which affect the system, if it is considered that the basic charge is a granular solid with a definite particle size distribution. They affect the final appearance of the film and the work conditions of the bed, wherefore it is necessary an adequate control of these parameter, to make a correct selection of the mathematical expression to be used.

The quantitative correlation of the powder behavior with the typical parameters, has been particularly troublesome because the difficulty to establish sufficiently meaningful the described parameters such as size, size distribution, shape and surface characteristics of the particles.

The most general characterization of a powder is in terms of its mean diameter, whatever the method the absolute size measurements was made (sieving, sedimentation, microscopy, etc.), it is a general practice to relate the measurements to equivalent spherical particle diameters, for which hydrodynamic correlations are applied, by means of a suitable shape factor.

The single property of mean particle diameter with appropriate shape factors, though not entirely satisfactory, has sufficed thus for engineering purposes. In this case, the obtained experimental values shows that the use of the ponderal mean diameter is valid **[2]**.

The ponderal mean diameter or ponderal diameter (D_{pm}) is the ratio between weight fraction of every one component (f_{wi}) and the individual particle diameter (D_{pi}), according to :

$$D_{pm} = \sum_{i=1}^{i=n} f_{wi}.D_{pi} \qquad (1)$$

From the granulometric analysis may be obtained the components quantity (n), defined as the ratio between the different particle diameters groups (D_{pi}), which make the granulometric distribution of the paint, the weight of each component i (W_i) of the mixture and the total weight (W_t) of the fluidized paint.

For the calculation sequence participates too the particle density (ρ_s) determined as the solid density by the picnometer method (ASTM D-153), the support fluid density (ρ_f) and its respective viscosity (μ_f) of clean and dry air, taken from manuals, since the used experimental equipment has filters, desiccator and regulation temperature system.

APPARENT DENSITY AND VOLUME CALCULATION

The objective of the apparent density and volume determination is to establish the initial state values (as the static bed height) to arrive at the necessary theoretical predictions in order to be used in the equipment design and operation **[4]**.

The theoretical determination of the apparent density may be made, by the use of the mixed size particle packing volume fraction for uniform spheres (ϕ_{ii} = 0.639), experimentally obtained by Do Ik Lee for a dense bed with random particles.

If D_1, D_2, D_3,...,D_n are, in increasing order, the n particle diameters, each of them having a volume fraction (x_j), the following expression may be obtained:

$$1.0 = \sum_{j=1}^{j=n} x_j \tag{2}$$

and

$$(\phi_p)_i = \sum_{j=1}^{j=n} \phi_{ij} . x_j \tag{3}$$

where $(\phi_p)_i$ is the packing fraction of the component i in respect to j.

For spheres, the ideal packing fraction of binary mixtures is defined as the maximun packed fraction (ϕ_{max}) for a determined diameter ratio (D_i/D_j), (straight lines Dsm ϕ_{ji} y Dlm ϕ_{ij} in **Fig. 1**).

Using Fig. 1 the respective binary coefficients ϕ_{ij} and ϕ_{ji} in the inflection point of the line (M for ϕ_{max}) may be obtained, so:

$$\phi_{ij} = 0.639 + [\phi_{max}.(D_i/D_j) - 0.639]/0.265 \tag{4}$$

$$\phi_{ji} = 0.639 + [\phi_{max} . (D_i/D_j) - 0.639]/0.735 \tag{5}$$

Where $D_i/D_j \geq 1$ or $i \geq j$. The values for the solution of expressions (4) and (5) are taken from the paper of Do Ik Lee. Then the packing factor of n mixture components is obtained, which may be represented for the minimum value of $(\phi_p)_i$ from the expression (3) and designed as k_e.

With k_e values, the apparent density (ρ_A) may be calculated, which is proportional to the solid density, i.e. to the paint density (ρ_s) used for the bed operation.

$$\rho_A = k_e \cdot \rho_s \tag{6}$$

The apparent volume (V_A) is the ratio between the paint volume (V_s) and the packing factor (k_e):

$$V_s = \frac{W_t}{\rho_s} \tag{7}$$

$$V_A = k_e \cdot V_s \tag{8}$$

Using V_A value the static bed height (H_{fb}) may be calculated as the ratio between the apparent volume (V_A) and the equipment free section (S_e):

$$H_{fb} = \frac{V_A}{S_e} \tag{9}$$

MINIMUM POROSITY AND MAXIMUM BED DENSITY CALCULATION

In a study made on viscosity and density measures in a conventional fluidized bed **[5]**, specific equations has been found. This equations are modifications of the proposed by Matheson **[6]** and applied to paints.

With them, the maximum bed density (ρ_{mb}) can be determined, which is just the point where the bed is in conditions to be fluidized.

$$\rho_{mb} = (\log D_{pm} - 1) \cdot \rho_s / 3.17 \tag{10}$$

The minimum bed porosity defines and quantifies the minimum gas-solid ratio in the "emulsion" produced when the true bed fluidization is reached.

$$E_{mb} = 1 - (\log D_{pm} - 1) / 3.17 \tag{11}$$

The values of the maximum bed density and minimum bed porosity are related with the minimum bed height (L_m) and it may be calculated as the fixed bed height (H_{fb}) and fixed bed porosity (E_{fb}) ratio. They may be correlated with the minimum fluidized bed porosity by the folowing equation:

$$L_m = H_{fb} \cdot [(1 - E_{fb}) / (1 - E_{mb})] \tag{12}$$

PRESSURE DROP CALCULATION

When true fluidization just begins, pressure drop through the bed is nearly the gravity force action over the solids. The real pressure drop may be a little greater than that, because there are many other effects, such as size, shape and particle distribution, electrostatic and friction effects between particles may appear, due to the nature of the powder materials.

As a first approximation, the pressure drop at the beginning of the fluidization may be found by equaling floating force of the support fluid over the solids, to the force of gravity minus the friction force due of the displaced intersticial fluid.

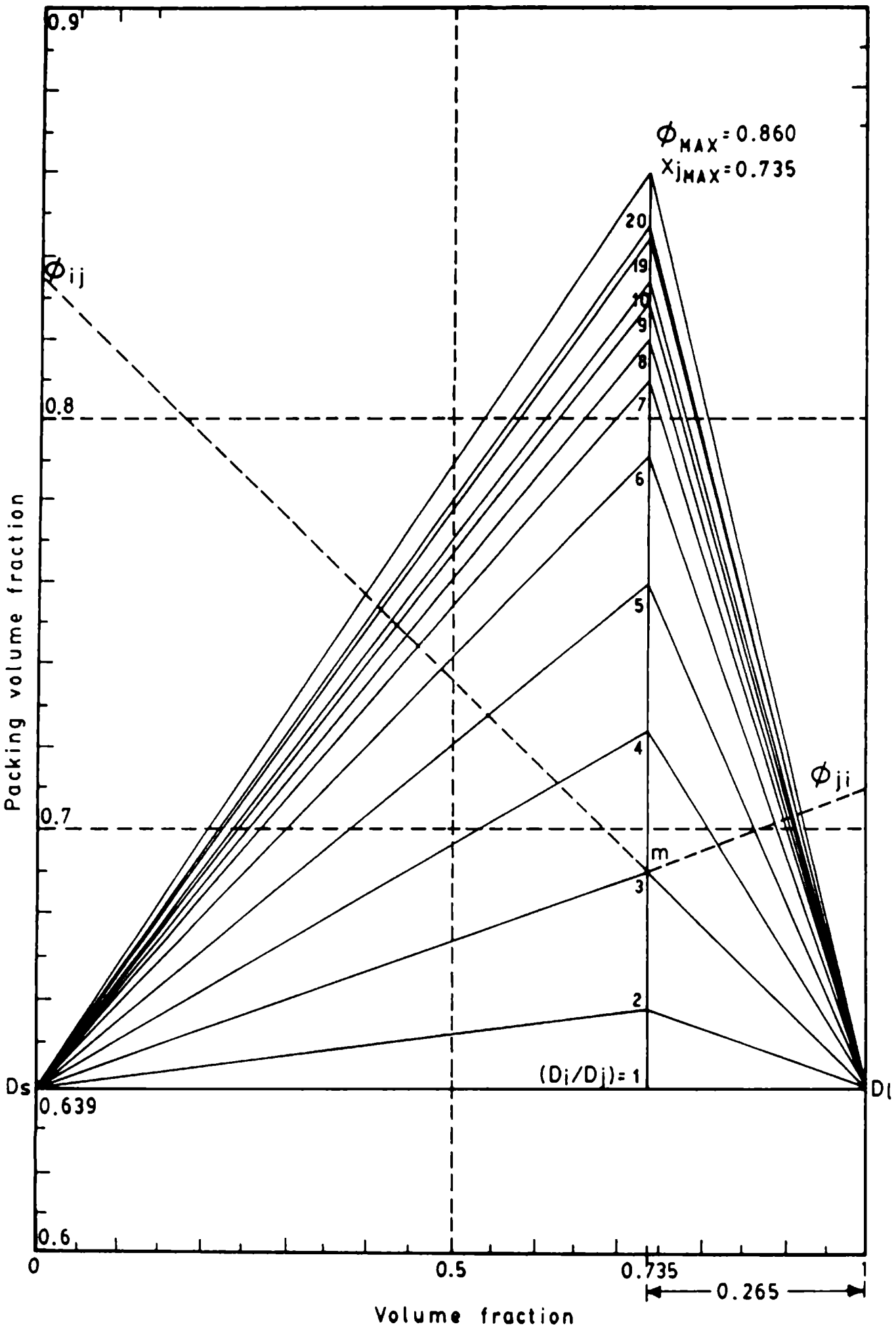

Fig. 1.- Do Ik Lee graph for volume fraction of binary mixtures.

When the fluid viscosity increases over the fluidization starting value, the pressure drop (Δp) verifies a slight increase. As at the same time the bed expands, the pressure drop per height unit of expanded bed diminishes. This parameter may be estimated using the Carman-Kozeny equation **[7]**:

$$\Delta p = L_m (1 - E_{mb}) (\rho_s - \rho_f) \qquad (13)$$

which relates the pressure drop (Δp) with the minimum fluidization height (L_m), the minimum bed porosity (E_{mb}), the particle density (ρ_s) and the fluid density (ρ_f).

FLUIDIZATION VELOCITY

When a gas is circulating through the voids of a bed of solid particles, the resistance to the flow is the resultant of the friction between particles. The flow may be laminar or turbulent, without rough transition between both types owing to the low flow velocity involved in the system.

The studies made to relate the pressure drop (Δp) of a circulating fluid through the voids of a bed **[8]**, were applied principally in petroleum refining processes, using in the bed several materials such as glass, sand, lead grit, crushed granite **[9]**, iron **[10]**, etc. There are not references about beds constituted of synthetic materials, polymers or pigments of powder coatings formulations.

For this reason it is not possible the use of direct equations for the calculation of the fluidization velocity, because generally all include, in one or another way, parameters or coefficients that are not possible to measure by the existing methods.

To obtain the fluidization velocity value without the friction factor may be applied another empirical expression of the Carman-Kozeny equation **[11]** used for laminar flow:

$$- \frac{\Delta p \; g_c \; D_{pm}^2 \; E_{mb}^3}{L_m \; V_o \; \mu_f \; (1 - E_{mb})^2} = 150 \qquad (14)$$

Then, the fluidization velocity (V_o):

$$V_o = \frac{\Delta p \; g_c \; D_{pm}^2 \; E_{mb}^3}{150 \; L_m \; \mu_f \; (1 - E_{mb})^2} \qquad (15)$$

When the circulating fluid surpass the bed surface, the superficial velocity diminishes, due to the very high increase of the free surface, causing the falling down of the particles.

Only when fluidization conditions are maintained in a discontinuous way and particles velocity are increasing, the lower size particles may get free and be taked out from the system.

FREE FALLING TERMINAL VELOCITY CALCULATION

The movement of particles through a fluid require a density difference between the particles and the fluid. The efficiency of the process is a function of the existing difference between both. If the particles density and fluid density are the same, the flotation force produced by the inmersion of the solid in the fluid will make void any external force (as large as it will be) and the particle remain fixed in the mass of the fluid.

Three forces acts on a particle, moving it through a fluid: the external force (gravitational or centrifugal) in this case gravitational; the buoyant force, which acts parallel with the external force but in an opposite direction; and the drag or friction force, which appears whenever there is a relative motion between the particle and the fluid.

The direction of movement of the particle relative to the fluid, generally is not parallel with the direction of the external and buoyant forces, then the drag force makes an angle with the other two. In this situation, which is called bidimensional motion, the drag must be resolved into components, which complicates the treatment of particle mechanics **[12]**.

The working conditions who implies less Reynolds' numbers and small particle diameters allow the use of monodimensional motion equations. Then, the total force on the particle is:

$$F_t = F_e - F_f - F_r \tag{16}$$

which is a balance between the external force (F_e), the buoyant force (F_f) and the drag force (F_r).

By the Newton's movement law, used in the case of a remaining constant mass:

$$F_t = \frac{1}{g_c} m_p a_p \tag{17}$$

which implies as the total force (F_t) is proportional to the particle mass (m_p) multiplied by the acceleration (a_p) and being the gravitational force (g_c), the convertion factor of the mentioned law.

The following equation which allow to know the external force, assume that the acceleration (a_e) is produced over the particle by that force:

$$F_e = \frac{1}{g_c} m_p a_e \tag{18}$$

Applying the Archimedes' principle, the buoyant force (F_f) is,

$$F_f = \frac{1}{g_c} \frac{m_p \rho_f a_c}{\rho_s} \tag{19}$$

where ρ_f is the support fluid density value and ρ_s is the particle density.

According to Mc Cabe and Smith [11], the drag force can be expressed as a dimensionless drag factor f. If the movement is caused by the gravitational field, like in this case:

$$a_e \frac{(\rho_s - \rho_f)}{\rho_s} = \frac{f\ u^2\ \rho_f\ A_p}{2\ m_p} \tag{20}$$

where u is the particle velocity, A_p is its area and a_e is the acceleration.

To solve the preceding equation it is necessary to know the drag factor value (f) as a function of Reynolds' number.

For this purpose, the drag curve shown in **Fig. 2** is applied, however, only under restricted conditions . The particle must be a solid sphere, it must be free to move without being influenced by other particles or by the wall or bottom of the vessel, it must move at a constant velocity, not be too small, and the fluid through which it moves must be still.

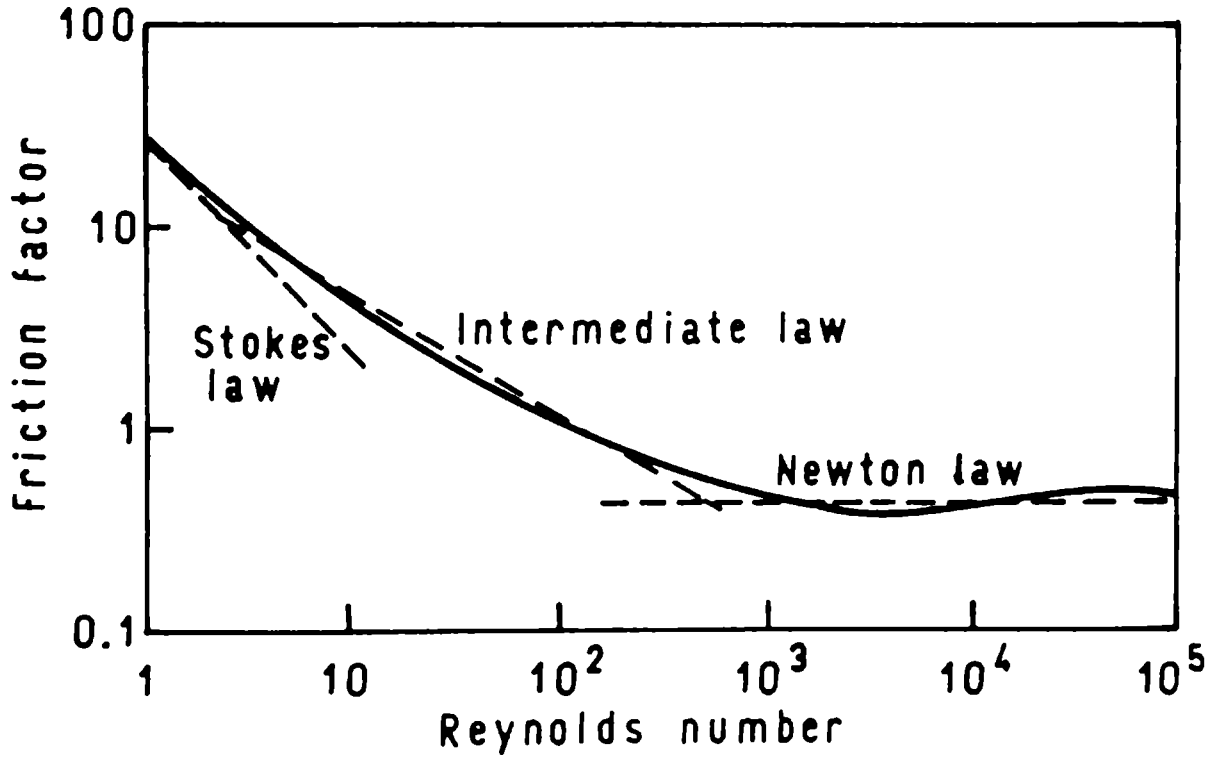

Fig. 2- Friction factor as a function of Reynolds' number.

In this conditions, it is possible to obtain by calculation the terminal free falling velocity (U_t), particle shape variations can be accounted, obtaining

different curves for each shape **[12]**. Certain correlations that can be used for particles of known geometry are available, but in the following treatment will be assumed to be spherical, since the same principles may be applied to any other shape.

If the motion of the particles is obstructed by other particles, which will happen when the particles are one near each other, even though may not actually colliding, the process is called hindered settling.

When the particle is at sufficient distance from the boundaries of the container and from other particles, so that its fall is not affected by them, the process is called free settling.

The drag coefficient in hindered settling is greater than in free settling. The relation between the drag coefficient and the Reynolds' number (indicated in Fig. 2), is a continuous curve, and can be substituted by three straight lines without exactitude detriment (dotted lines).

Everyone of this lines may determine different values of drag coefficient (f) and drag force (F_r), which can be applied at determined ranges of Reynolds' number.

So, according with this:

$$\text{If} \quad N_{Rep} < 2 \quad ; \quad f = \frac{24}{N_{Rep}} \tag{21}$$

$$F_D = \frac{3\ \pi\ \mu_f\ U_t D_{pm}}{g_c} \tag{22}$$

This defines **Stokes' law range**.

$$\text{If} \quad 2 < N_{Rep} < 500 \quad ; \quad f = \frac{18.5}{(N_{Rep})^{0.6}} \tag{23}$$

$$F_D = 2.31\ \frac{(U_t\ D_{pm})^{1.4}\ \mu_f^{0.6}\ \rho_f^{0.4}}{g_c} \tag{24}$$

The equation 24 defines the **intermediate law range**.

$$\text{If} \quad 500 < N_{Rep} < 200000 \quad ; \quad f = 0.44 \tag{25}$$

$$F_D = \frac{0.055\ \pi\ (U_t\ D_{pm})^2\ \rho_f}{g_c} \tag{26}$$

being this the **Newton's law range** definition.

The equations 20, 21, 22, 23, 24, 25 y 26 may be expressed as a generalization, by the following one:

$$f = \frac{b_1}{N_{Rep}^n} \tag{27}$$

$$F_D = \frac{\mu_f^n\ b_1\ \pi\ (U_t\ D_{pm})^{2-n}\ \rho_f^{1-n}}{8\ g_c} \tag{28}$$

It is necessary the use of b_1 and n as the constants for all the exposed laws. Their numerical values may be expressed as shown in the following table:

Range	Constants	
	b_1	n
Stokes law	24.00	1.00
Intermediate law	18.50	0.60
Newton law	0.44	0.00

The final equation obtained for particles free falling is:

$$Ut = \left[\frac{4\ a_e\ D_{pm}^{1+n}\ (\rho_s - \rho_f)}{3\ b_1\ \mu_f^n\ \rho_f^{1-n}}\right]^{1/(2-n)} \tag{29}$$

The acceleration produced by an exterior force (a_e), is produced in the gravitatory settling by the gravity attraction (g) and for intervals into Stokes' law:

$$Ut = \frac{g\ D_{pm}^2\ (\rho_s - \rho_f)}{18\ \mu_f} \tag{30}$$

For the knowledge of the ultimate velocity of a particle of certain value, it is necessary to eliminate the velocity value of the equation, and replace it for its value in equation (30):

$$N_{Rep} = \frac{D_{pm}\ U_t\ \rho_f}{\mu_f} \tag{31}$$

$$N_{Rep} = \frac{D_{pm}^3\ a_e\ \rho_f(\rho_s - \rho_f)}{18\ \mu_f^2} \tag{32}$$

The Reynolds' number values obtained in a bed for powder coating application, indicates that it is necessary to employ the Stokes' law. So, for $N_{Rep} < 2$ can be defined a new parameter, the "settling criterion" (K) and its equation is:

$$K = D_{pm} \left[\frac{a_e\ \rho_b\ (\rho_s - \rho_b)}{\mu_f^2}\right]^{1/3} \tag{33}$$

where ρ_b is the bed density.

If we obtain D_{pm} from equation (33):

$$D_{pm} = \frac{K}{\left[\frac{a_e\ \rho_b\ (\rho_s - \rho_b)}{\mu_f^2}\right]^{1/3}} \tag{34}$$

Then we can made the substitution in the equation (32) obtaining for N_{Rep}:

$$N_{Rep} = \frac{K^3}{18} \tag{35}$$

If D_{pm} is known, the K value can be calculated from the equation (33). Otherwise:

$$K = (18\ N_{Rep})^{1/3} \tag{36}$$

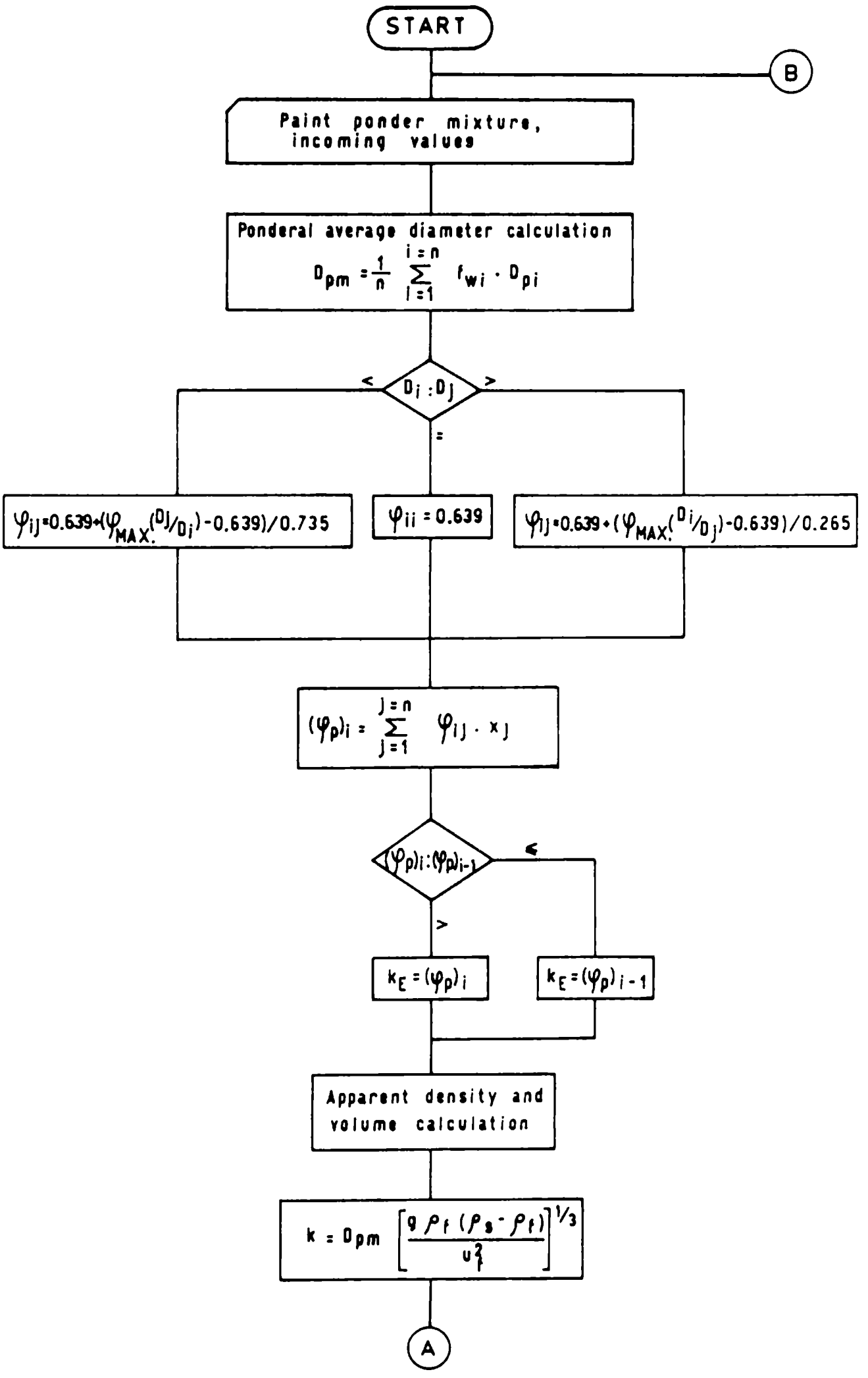

Fig. 3.- Flow chart of the employed calculation system (start).

To know which is the adequate law to be taken in mind, it is necessary to use the maximum N_{Rep} values taken from fig. 2. So, the criterion equation allows to determine:

N_{Rep} values	K values	Law to be used
$N_{Rep} \leq 2.00$	$K \leq 3.3$	Stokes'
$2.00 < N_{Rep} \leq 500.00$	$3.3 < K \leq 43.6$	Intermediate
$500.00 < N_{Rep} \leq 200000.00$	$43.6 < K \leq 2360$	Newton's

In this way, all the necessary equations for the calculation development are get under way.

CALCULATION LAYOUT

In previous paragraph, it were put on the theoretical basis of the employed calculation system, in such a way to allow the understanding of the applied methodology.

For the electronic processing the system was divided in six steps: one of data input, four of calculations and one for results to be tabulated. The flow diagrams are shown in **Figs. 3** and **4.**

In the first step, the paint variables incoming the system are particle size, different particle diameters (according the granulometric distribution) and the weight of the corresponding fractions; and for the support fluid, density and viscosity. Input data are registered and printed **(Table I)**.

With three different paints (samples 1, 2, and 3) and using sieves according to ASTM E-11 specification, with a vibratory equipment, the granulometric distribution of the samples was determined.

Density and apparent volume values were obtained, using the packing fraction, calculating the final free falling velocity of the particles (according Stokes', intermediate or Newton's laws) **(Table II)**.

Subsequently, and fixing the geometric configuration and the respective size of the bed were determined the running specifications **(Table III)**.

Being all the shown values of Tables II and III, the theoretically calculated for the four samples, to determine the correction coefficients to be used for changes in materials which produces variations in the process performance, it is necessary to made an experimental comprobation.

DESIGN OF THE EQUIPMENT FOR EXPERIMENTAL EVALUATION

Even if the determination of the performance of the four samples is outside of this paper, based on the theoretical calculations was designed the equipment which is being used in the experimental confirmation of the proposed calculation model **(Fig. 5)**.

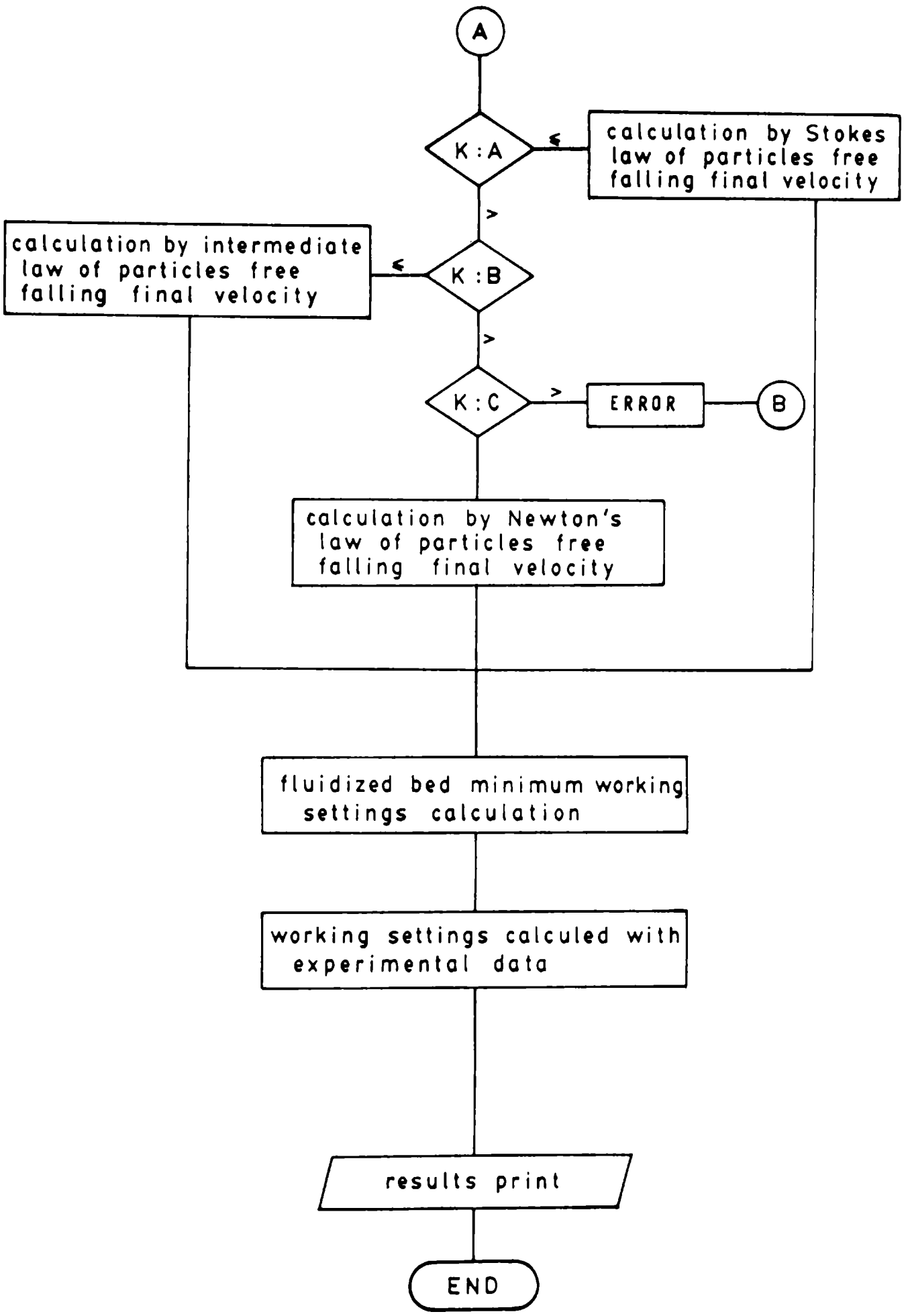

Fig. 4.- Flow chart of the employed calculation system (continuation).

TABLE I

Mixture characteristics

Parameters	Sample N^{er}		
	1	2	3
Particle density ($k\ m^{-3}$)	1663	1663	1663
Number of components	6	6	6
Weight of component N^{er} 1 ($k\ 10^{-2}$)	10.248	0.418	0.418
Diameter of particle N^{er} 1 ($m\ 10^{-4}$)	0.37	0.37	0.37
Weight of component N^{er} 2 ($k\ 10^{-2}$)	3.822	1.344	1.354
Diameter of particle N^{er} 2 ($m\ 10^{-4}$)	0.44	0.44	0.44
Weight of component N^{er} 3 ($k\ 10^{-2}$)	2.542	1.616	2.542
Diameter of particle N^{er} 3 ($m\ 10^{-4}$)	0.53	0.53	0.53
Weight of component N^{er} 4 ($k\ 10^{-2}$)	1.616	2.542	10.248
Diameter of particle N^{er} 4 ($m\ 10^{-4}$)	0.74	0.74	0.74
Weight of component N^{er} 5 ($k\ 10^{-2}$)	1.344	3.822	3.822
Diameter of particle N^{er} 5 ($m\ 10^{-4}$)	1.05	1.05	1.05
Weight of component N^{er} 6 ($k\ 10^{-2}$)	0.418	10.248	1.616
Diameter of particle N^{er} 6 ($m\ 10^{-4}$)	1.49	1.49	1.49
Mixture weight ($k\ 10^{-2}$)	19.99	19.99	20.00
Particle average diameter ($m\ 10^{-4}$)	0.5028	1.1389	0.8051
Fluid density ($k\ m^{-3}$)	1.1	1.1	1.1
Fluid viscosity ($k\ m^{-1}\ sec^{-1}\ 10^{-4}$)	0.18	0.18	0.18

TABLE II

Values for the calculation of the fluidized bed operation in minimum conditions

Calculated conditions	Samples		
	1	2	3
Apparent density, k m^{-3}	1081.37	1101.89	1084.48
Apparent volume, m^3 10^{-4}	1.8485	1.8141	1.8441
Terminal velocity, m sec^{-1}	0.1271*	0.5104@	0.3260*
Packing fraction	0.6502	0.6625	0.6521
Reynolds' number	0.3907	3.5522	1.6042

* calculated by Stokes' law; @, calculated by the intermediate law.

TABLE III

Minimum settings for running a fluidized bed

Bed characteristics	Samples		
	1	2	3
Bed shape	Cylindrical	Cylindrical	Cylindrical
Recipient diameter, m	0.0685	0.0685	0.0685
Minimum height of fluidization, m	0.1306	0.0867	0.1011
Bed minimum porosity	0.7503	0.6238	0.6775
Pressure minimum drop, k m^{-2}	54.2056	54.2065	54.2335
Fluidization minimum velocity, m sec^{-1}	0.0258	0.0505	0.0377
Fixed bed height, m	0.0501	0.0492	0.0501
Air flow, l min^{-1}	5.7077	11.1778	8.3433

The apparatus is constituted with a precision flow valve (1) and a manometer (2) as the feed section of the support fluid (air) to a heating chamber (3) which is the responsible to maintain the air flow at a constant temperature.

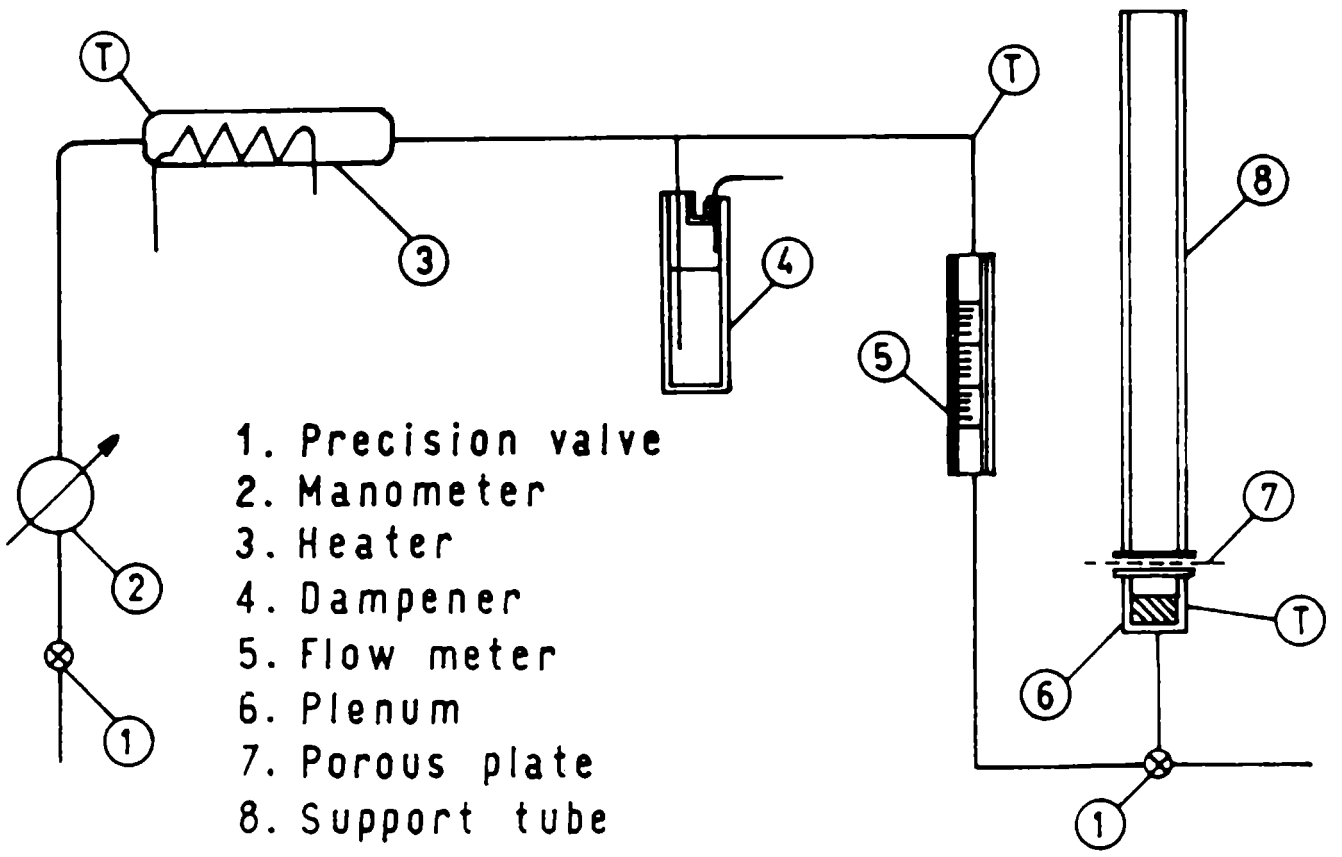

Fig. 5.- Experimental equipment used to confirm the calculated values.

The thermostatized air enter to a dampening chamber (4) to regulate the system pressure and volume, avoiding overpressure problems, and finally passing through a rotameter (5) which indicates the used air volume (l min^{-1}).

Preceding the fluidization bed, a two way precision quick relief valve was installed to eliminate overpressure if it is produced.

The fluidized bed is arranged in three parts: a pressure equalizing plenum chamber, a glass porous plate (60 mm diameter, 5 mm thick) and the upper part of the tube, where fluidization takes place (which is the remainder part of whole tube of the apparatus, which has 425 mm height), graduated with divisions of 3 mm each one in a total de 310 mm. This height of the cylinder was chosen to avoid the finest particles of powder (below 35 μm) escape from the system.

The objective of this paper was the study of the fluidization as a pure physical operation, since as well there are a beginning of chemical reaction, this is only over the interface of the heated surface and the paint, and it is not appreciable during the powder coating application by means a conventional fluidized bed; it has more influence on the paint-substratum adhesion than over the application operation.

The fluidized bed method, is being slowly replaced by application via electrostatic guns, in which system, the fluidized bed is a part of the equipment (paint reservoir, dust recuperation, etc.), being the calculations to be used for them, basically the same.

ACKNOWLEDGEMENTS

The authors thank the Comisión de Investigaciones Científicas de la Provincia

de Buenos Aires (CIC) and the Consejo Nacional de Investigaciones Científicas y Técnicas (CONICET) for financial support of this research work.

SYMBOLS AND UNITS

D_{pm}: ponderal average diameter, m

f_{wi}: weight fraction of component i

D_{pi}: individual particle diameter (D_1, D_2,..., D_i), m

n : number of components

W_i: weight of each components, k

W_t: total mixture weight, k

ρ_s: particle density, k m^{-3}

ρ_f: support fluid density, k m^{-3}

μ_f: support fluid viscosity, k m^{-1} sec^{-1}

ϕ_{ii}: random compact volume packing fraction of uniform spheres (ϕ_{ii}=0.639)

x_j: volume fraction of each component

$(\phi_p)_i$: packing fraction of the component i in respect to all the j components

ϕ_{ij}; ϕ_{ji} : packing fraction of all the ij or ji binary component mixtures

ϕ_{max}: maximum packing fraction of the binary mixtures

0.265 : volume fraction of component i in j corresponding to ϕ_{max}

0.735 : volume fraction of component j in i corresponding to ϕ_{max}

k_e: packing factor of the mixture of n components ($(\phi_p)_i$ minimum value)

ρ_A: apparent density, k m^{-3}

V_A: apparent volume, m^3

V_s: paint volume, m^3

H_{fb}: static bed height, m

S_e: equipment free section, m^2

ρ_{mb}: maximum density of fluidized bed, k m^{-3}

L_m: minimum height of fluidization, m

E_{mb}: minimum porosity of fluidized bed

E_{fb}: fixed bed porosity

Δp: bed pressure drop, k m^{-2}

g_c: Newton's law conversion factor

V_0: fluidization velocity, m sec^{-1}

F_e: external force

F_f: buoyant force

F_r: drag force

m_p: particle mass, k

a_p: particle acceleration, m sec^{-2}

a_e: particle acceleration produced by external force, m sec^{-2}

u: particle velocity, m sec^{-1}

A_p: particle area, m^2

F_D: drag force for fluidized bed

f: drag coefficient

U_t: particle free falling velocity, m sec^{-1}

K: "settling criterion"

g: gravitatory acceleration, m sec^{-2}

ρ_b: bed density, k m^{-3}

N_{Rep}: particle Reynolds' number

REFERENCES

[1] Wilhelm, R. H., Moosonkwauk.- **Chemical Engineering Progress**, **44** (3), 201, 1948.

[2] Zenz, F. A., Othmer, D. F.- Fluidization and fluid-particle systems. New York, Reinhold Publishing Corp., 1960.

[3] Harris, S. T.- **The technology of powder coatings**. London, Portcullis Press, 1976.

[4] Do Ik Lee.- **Journal of Paint Technology**, **42** (550), 1970.

[5] Damia, A. J., Caprari, J. J.- **Journal of Chem. Tech. and Biotech.**, **44** (4), 261, 1989.

[6] Matheson, G. et al.- **Ind. & Eng. Chem.**, **41** (6), 1099, 1949.

[7] Carman, P. C.- **Trans. Inst. Chem. Eng. London**, 15, Part. 1, 150-66, 1937.

[8] Sabri Ergun.- **Chemical Engineering Progress**, **48** (2), 89, 1952.

[9] Lewis, W. K. et al.- **Ind. Eng. Chem.**, **41** (6), 1104, 1949.

[10] Leva, M. et al.- **Chemical Engineering Progress**, **44** (9), 707, 1949.

[11] Mc Cabe, W., Smith, J.- **Operaciones básicas de ingeniería química**. Buenos Aires, Reverté, 1977.

[12] Brown, G. G. et al.- **Unit operations**. New York, Wiley, 1950.

COMPARISON BETWEEN ELECTROCHEMICAL IMPEDANCE AND SALT SPRAY TESTS IN EVALUATING THE BARRIER EFFECT OF EPOXY PAINTS

COMPARACION ENTRE ENSAYOS DE IMPEDANCIA ELECTROQUIMICA Y CAMARA DE NIEBLA SALINA PARA EVALUAR EL EFECTO BARRERA DE PINTURAS EPOXIDICAS

C.I. Elsner[1] and A.R. Di Sarli[2]

SUMMARY

The aim of this work is to establish the reliability of an electrochemical test based on the electrochemical impedance measurements of metallic substrate/organic coating/aqueous electrolyte as a function of the immersion time. Thus, naval steel/epoxy bituminous or epoxy-enamel coats/3 % NaCl solution systems were chosen in order to try out the test. The electrochemical results and those obtained from visual assessment using the ASTM standard D-610 were compared. The total agreement between the electrochemical and visual tests results allows to confirm that the described technique is highly encouraging, as it has proven that a fairly straightforward test (like electrochemical impedance) can, under certain circumstances, indicate whether an anticorrosive paint coating is able to protect satisfactorily, as well as to detect differences between the anticorrosive properties of commercially available products.

KEYWORDS: *Corrosion, impedance measurements, salt spray test, epoxy paints.*

INTRODUCTION

Though there exist a great variety of commercial equipment for carrying out electrochemical tests based on "in-situ" impedance measurements in the systems metal/organic coating/electrolyte, their higher development was made in laboratories where the possibility to have available a greater quantity of more sofisticated instruments led to a better implementation of simplest, quickest and more reproducible methods to determine the protection degree afforded by the organic coatings on the metallic substrate.

The tests must allow: a) the evaluation of anticorrosive, intermediate and topcoat paint properties; b) the quality control of painted instruments, structures or parts and c) the prediction of their service behaviour.

Transitory or stationary DC techniques were commonly used because they allow the assessment of some kinetic parameters used in the corrosion rate calculus for activation controlled processes; however, they have important limitations which, in many cases, may nullify their employment **[1-4]**. With painted metals, such

---

[1] Miembro de la Carrera del Investigador del CONICET

[2] Miembro de la Carrera del Investigador de la CIC

limitations are related with both the high ohmic resistance (in the order of several MΩ) due to the barrier effect of some organic coatings, and the diffusion controlled corrosion processes. Likewise, the DC flux produces other interfacial processes, that may mask the accurate determination of the most adequate electrochemical parameter (charge transfer resistance) used in the corrosion rate calculus **[5]**. In such a case, the practical conditions are far from the theoretical ones used for the statement of the Stern-Geary equation **[6]**, therefore, the calculated corrosion rate may not be correct **[7]**.

Nevertheless, at the present time the industry applies a method based on high DC voltage (50-100 V) to detect defects, air bubbles, etc. This method is only effective to identify very low resistance values (0-1000 Ω) but intact organic coatings have a resistance range in the order of 10^4 - 10^{12} Ωcm^2.

The AC measurements do not present these objections because they bring into play only those processes whose time constant is less than the alternancy period of the electric field. Therefore, the use of small electrical signals in a large frequency range may provide the necessary information to deduce both the qualitative and the quantitative contribution of each element to the equivalent circuit reproducing the analyzed electrochemical interface. During the last decade, considerable success has been achieved by the use of wide frequency scan electrochemical impedance analysis. Many examples in the literature illustrate the utility of this method with regard to various types of coatings and oxide films on iron and steel **[8-17]**. However, relatively few reports have been published describing results obtained from protective organic coatings.

The aim of this work is to compare the experimental results related to the protective performance of two epoxy paints (epoxibituminous and epoxy-enamel) applied in different thicknesses on naval steel plates and exposed either to a 3 % NaCl solution (electrochemical test) or to a standardized aggressive environment (salt spray test, ASTM Standard D-117).

EXPERIMENTAL DETAILS

SAE 1020 naval steel plates (15x8x0.2 cm) were employed as metallic substrate. The surface was sandblasted to SA $2^{1/2}$ (SIS standard 05 59 00/67). Plates were degreased with toluene and coated with the paints whose formulations are shown in **Table I**. The organic coatings were applied by means of a Bird applicator. During the drying period (7 days) the coated plates were placed in a desiccator at a constant temperature (20 ± 2 °C). The dry film thickness was measured by Foucault currents using a bare sanded plate and known thickness standards as reference.

On each coated plate two cylindrical acrylic tubes were placed. An epoxy adhesive was used in order to get good adhesion to the metallic substrate. The geometrical area of each cell was 14 cm^2. A large area graphite cylinder was used as counter-electrode while a saturated calomel electrode (SCE) was employed as reference. The electrolytic solution was 3% NaCl and all the measurements were carried out at room temperature (20 ± 2 °C).

Similar samples to those used in a) but with their edges and back side isolated by a 600 μm film of an epoxy bituminous paint were exposed, in duplicate, for 500 hours in a salt spray cabinet. Its operating characteristics were in accordance to ASTM Standard D-117.

At different immersion times, the electrochemical impedance measurements in the frequency range 10^{-3} Hz ≤ f ≤ 5.10^4 Hz were performed in the potentiostatic mode at the corrosion potential using the Frequency Response Analyzer (Solartron

FRA 1255) and the Electrochemical Interface (EI 1186). The amplitude of the applied AC voltage was 10 mV peak to peak. All data were processed with an AT Olivetti PCS 286 and a set of programs developed at the CIDEPINT. The visual evaluation of the samples submitted to those different tests was done using the scale 1-10 of the ASTM Standard D-610.

TABLE I

Chemical composition of tested paints (g/100 g)

Paint	Components	
Epoxibituminous	Epoxy resin (70 % solids)	44.00
	Bituminous material	20.50
	Talc	20.50
	Polyamide	9.00
	Hardner	2.50
	Isopropyl alcohol	3.50
Epoxy-enamel	Epoxy resin (70 % solids)	35.20
	Titanium dioxide (TiO_2)	17.50
	Moistening	0.30
	Polyamide	14.50
	Hardner	0.50
	Xylene	25.00
	MIK	3.50
	Butyl alcohol	3.50

RESULTS AND DISCUSSION

Fig.1-a shows the corrosion potential (E_{corr}) vs immersion time (t) curves for epoxy bituminous and epoxy-enamel coated naval steel, samples A and B and samples C, D and E, respectively, with low thicknesses (20-50 μm). For sample E the corrosion potential remains constant along the 60 days immersion. While those corresponding to samples A, B, C and D tend rapidly to more active values at short immersion times; this displacement was continuous for sample D and oscillatory for samples A, B and C.

Impedance spectra contain valuable information about the electrical coating parameters and kinetics of the corrosion processes taking place on the metallic substrate. Due to the dynamic character of rust formation the impedance spectra of coated steel/3 % NaCl solution systems change throughout the exposure time. A fairly good description of the experimental impedance diagrams was obtained in terms of a transfer function analysis using non-linear fit routines like those developed by Boukamp [18]; the complex nature of the processes at a coated steel interface makes necessary to derive models that account for the impedance data measured at such interfaces.

Figs.1-b and **1-c** show, respectively, the ionic resistance (R_m) and the dielectric capacitance (C_m) of the membrane vs t. The fluctuations of R_m and C_m with t are according with those of E_{corr}. The stability of E_{corr} for sample E (**Fig.1-a**) is similar to that of R_m and C_m. Otherwise, the fast changes of E_{corr} for samples A, B, C and D to more active values are accompanied by R_m and C_m ones indicating that at this time, the protective capacity of the paint begins to

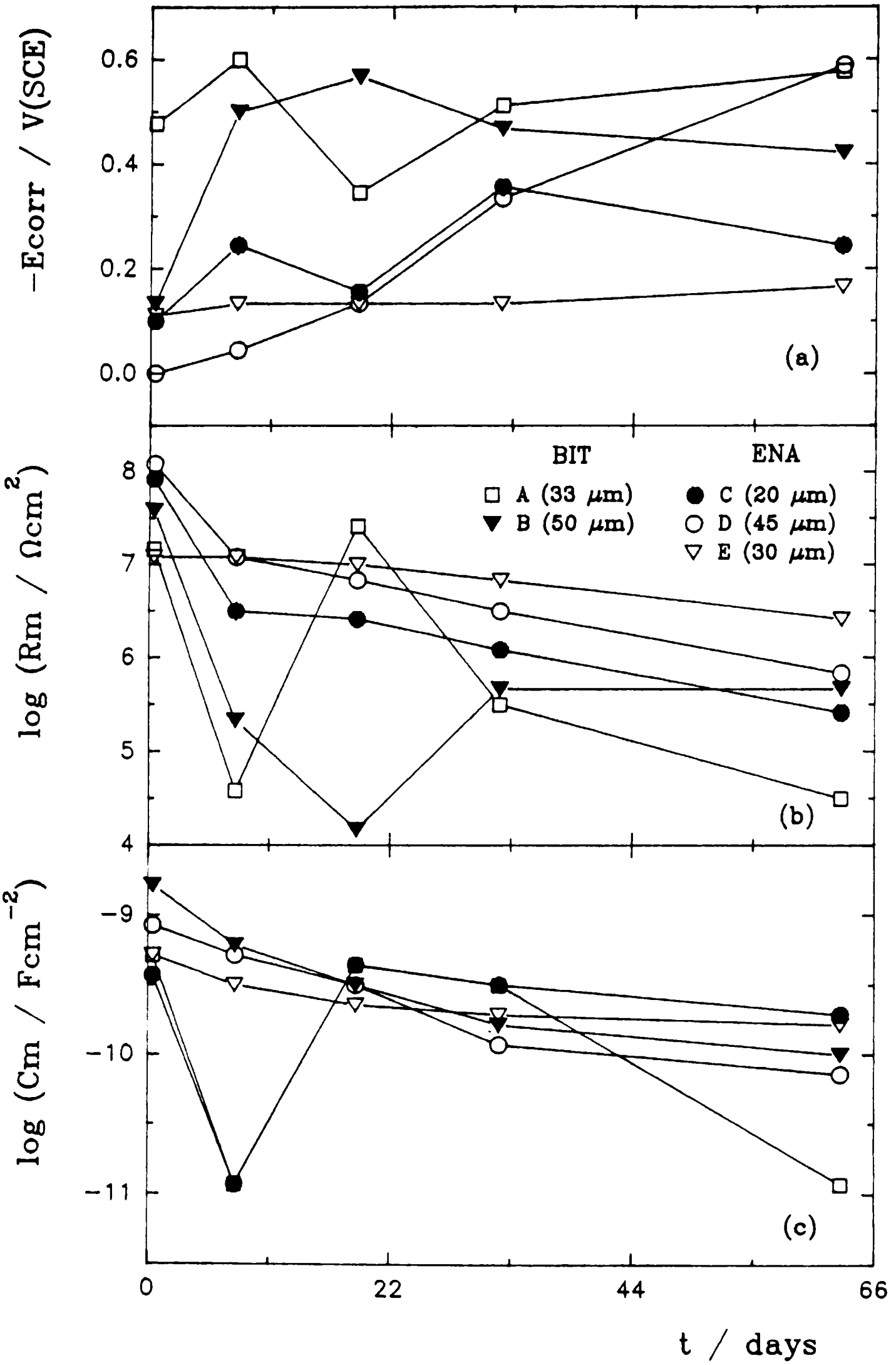

Fig. 1.- a) Corrosion Potential (Ecorr), b) Ionic Resistance (Rm) and c) Dielectric Capacitance (Cm) vs Immersion Time (t) for epoxybituminous paints (BIT), samples A and B and epoxy-enamel (ENA), samples C, D and E.

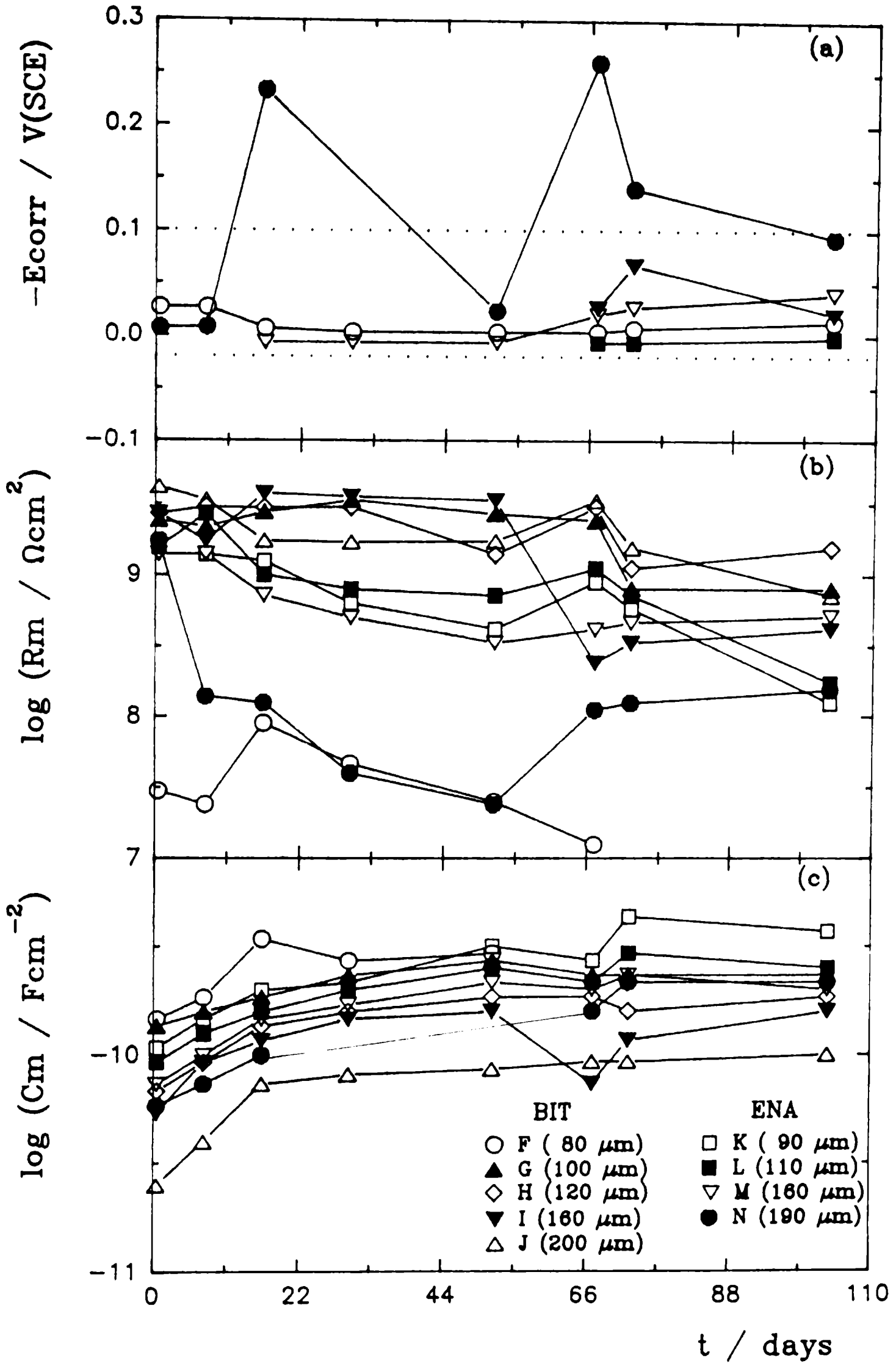

Fig. 2.- a) Corrosion Potential (Ecorr), b) Ionic Resistance (Rm) and c) Dielectric Capacitance (Cm) vs Immersion Time (t) for epoxybituminous paints (BIT), samples F. G, H, I and J and epoxy-enamel (ENA), samples K, L, M and N.

decrease while the elusion of Fe as Fe^{++} increases rapidly. Sometimes, samples A and C did not respond to the general equivalent circuit **[12]** used for fitting the experimental data, due to the fast deterioration of their thin coatings. Therefore, the R_m and C_m changes were not those predicted by the theory thus resulting different, if not impossible, to determine their physical meaning. Nucleation, growth, and accumulation of the corrosion products in the coating defects lead to an increase in the barrier effect accompanied with changes of E_{corr} and R_m to values indicating a greater protection (more positive E_{corr} and higher R_m) and, in general, a quasi-stability of C_m. New changes of these parameters, in the opposite sense, suggest that the corrosion-protection cycle in other less resistant areas of the organic film is starting. This process feedbacks itself up to the total degradation of the organic coating.

Figs.2-a-b-c show the experimental values of E_{corr}, R_m and C_m for samples with thicker coatings. The E_{corr} vs t curves (**Fig.2-a**) illustrate that, except for sample N, the potential remains steady until 65 days immersion. At long exposure times, samples F, I, L and M have a low tendency to reach more active values but always below -0.1V/(SCE). The evolution of R_m denotes that: 1) sample N is the most unstable; 2) the ionic resistance of sample F starts to decrease from the 19th day immersion and 3) for samples G, H, I, J, K, L and M, R_m does not change for 100 days. The initial R_m decrease and C_m increase (**Fig.2-c**) are attributed to the water absorption accompanied by the elusion of the soluble components of the paint **[19]**. From the behaviour of samples F, G, H, I, J, K, L, M and N after 100 days immersion: $-E_{corr} > 0.1$V/(SCE); $R_m > 10^7\ \Omega cm^2$ and $C_m < 10^{-9}\ Fcm^{-2}$, it can be inferred that epoxy paints thicker than 80 μm show an excellent protective behaviour and absence of damage. These results are in good agreement with those obtained from water permeability measurements **[20]**. Thus, by comparing the transport properties of the epoxy bituminous paint (diffusion coefficient $D = 7.58\ 10^{-9}\ cm^2s^{-1}$; solubility $S = 9.68\ 10^{-3}$ and permeability $P = 7.33\ 10^{-11}\ cm^2s^{-1}$) and the epoxy-enamel coating ($D = 4.60\ 10^{-8}\ cm^2s^{-1}$, $S = 7.90\ 10^{-3}$ and $P = 3.64\ 10^{-10}\ cm^2s^{-1}$) result that the epoxy bituminous paint is less permeable due to not only its greater chemical inactivity but also its solids content.

Fig.3 is the summary of the experimental results obtained from the salt spray tests and electrochemical impedance measurements. It can be observed a good agreement between the visual assessment of the corrosion degree (ASTM Standard D 610) and the ionic resistance R_m measured at the end of the test. The corrosion scale averages between 1 and 10 and the $\log(R_m)$ between 3 (for the reference bar steel sample) and 10. The thicker organic films are correlated with higher R_m values and greater protection degree. Therefore, it can be expected that if the coatings are applied in an adequate thickness for each specific service condition a successful anticorrosive protection will be obtained for longer periods.

CONCLUSIONS

The current experimental results point to demonstrate that a non-destructive laboratory technique will indicate if under determined environmental conditions the anticorrosive protection afforded by a paint or a painting scheme is satisfactory ($R_m > 10^7\ \Omega cm^2$, $C_m < 10^{-9}\ Fcm^{-2}$ and 8-10 in the scale of visual assessment). The test also seems to be useful for predicting the behaviour of organic coatings exposed to aqueous environments which could be profitable in quality control. Nevertheless, it is assumed that the study must be extended to other paints, substrates and environments, all of which is now in progress.

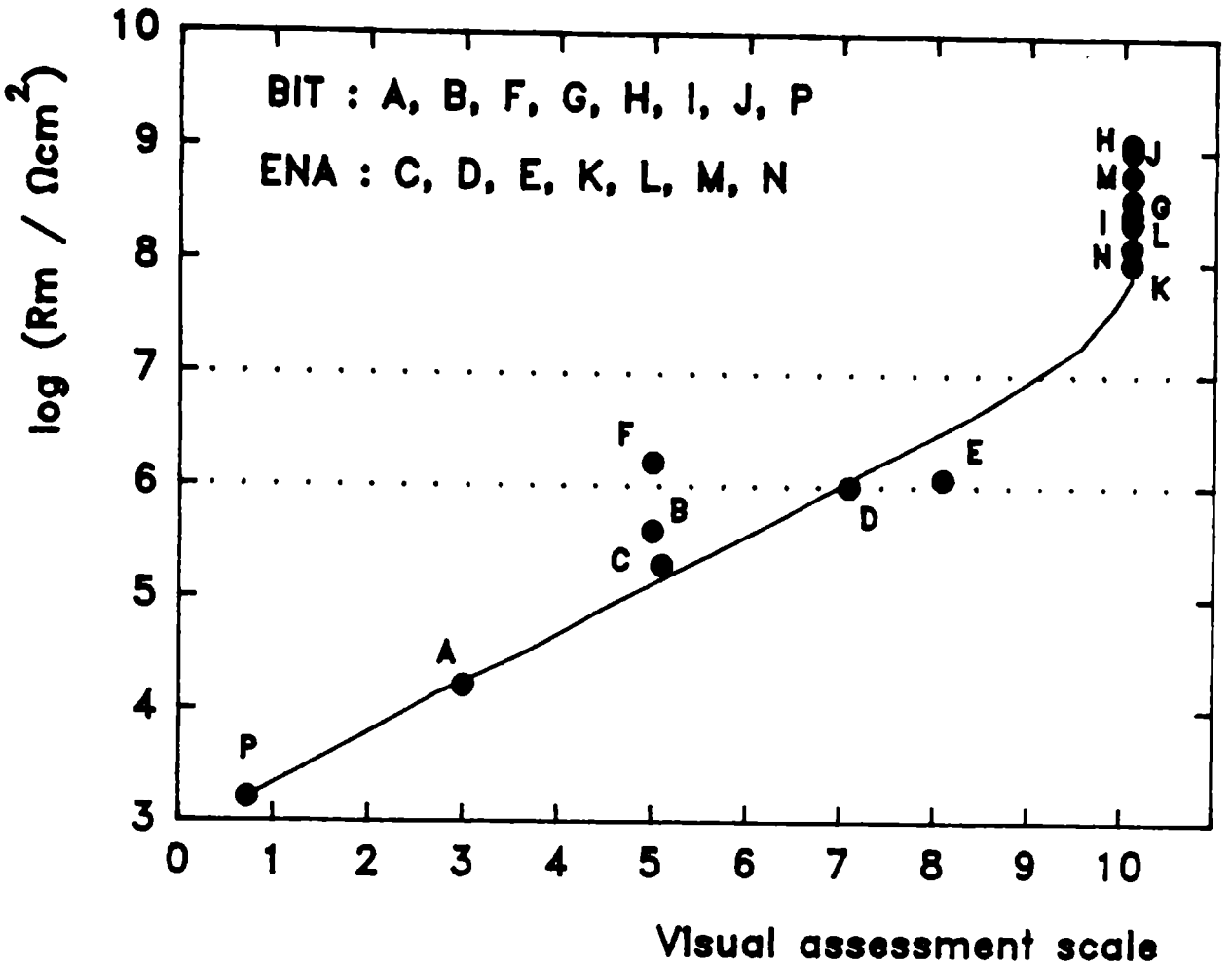

Fig. 3.- Correlation between log Rm and the results obtained by visual inspection (visual assessment scale), for every sample.

ACKNOWLEDGEMENTS

The authors would like to thank the Comisión de Investigaciones Científicas de la Provincia de Buenos Aires (CIC) and the Consejo Nacional de Investigaciones Científicas y Técnicas (CONICET) for their financial support to this research work.

REFERENCES

[1] Kargin V. A., Kariakina M. I., Berestneva Z.- **Dokl. Akad. Nauk SSSR, 120**, 1065 (1958).

[2] Alzenfel'd T. S. B., Builina L. P., Skobeleva I. A., Krasil'schikov A. I.- **Zashch. Matall, 4**, 195 (1968).

[3] Clay H. F.- **J. Oil Col. Chem. Assoc., 48**, 356 (1965).

[4] Bureau M.- **Corrosion, 16**, 235 (1968).

[5] Piens M., Verbist R.- **Corrosion Control by Organic Coatings**, NACE Meeting, Lehigh University, Bethlehem, Pennsylvania, August (1980).

[6] Stern M., Geary A. L.- **J. Electrochem. Soc., 104**, 56 (1957).

[7] Bois D. B., Northan B. J., McDonald W. P.- **Mat. Prot., 8**, 30 (1969).

[8] Scantlebury J. D., Ho K. N., Eden D. A.- **Electrochemical Corrosion Testing**, Mansfeld, F. and Bertocci, U. (Ed), ASTM, STP 727, Philadelphia, PA, 187 (1981).

[9] Sekine I.- **Corrosion Control by Organic Coatings**, Leidheiser, H. (ed)., NACE, Houston, TX, 130 (1981).

[10] Piens M., Hubretch J., Vereecken J.- **Proc. 8th Int. Cong. on Metallic Corrosion**, Mainz, 1021 (1981).

[11] Padget J. C., Moreland P. J.- **J. Coat. Technol., 55** (698), 39 (1983).

[12] Hubrecht J., Vereecken J.- **Proc. 9th Int. Cong. on Metallic Corrosion**, Toronto, vol. 3, 85 (1984).

[13] Hubrecht J. C., Vereecken J., Piens M.- **J. Electrochem. Soc., 131**, 2010 (1984).

[14] Mansfeld F., Kendig M. W.- **Laboratory Corrosion Tests and Standards**, Haynes, G.S. and Baboian, R. (Ed.), ASTM, STP866, Philadelphia, PA, 122 (1985).

[15] Moreland P. J., Padget J. C.- **Polymeric Materials for Corrosion Control**, Dickie, R.A. and Floyd, F.L. (Ed.), ACS Symp. 322, Washington, DC, American Chemical Soc., 18 (1986).

[16] Vijayan C. P., Noel D., Hecker J. J.- **Polymeric Materials for Corrosion Control**, Dickie, R.A. and Floyd, F.L. (Ed.), ACS Symp.322, Washington, DC, American Chemical Soc., 58 (1986).

[17] Azim S. S., Guruviah S.- **Proc. 10th Int. Cong. on Metallic Corrosion**, Madras, 1393 (1987).

[18] Boukamp B. A.- **Report CT88/265/128, CT89/214/128**, University of Twente, Netherland, may 1989.

[19] Ohyabu Y., Kawai H., Ikeda S.- **Shikizai Kyokaishi, 37**, 90 (1964).

[20] Schwiderke E., Di Sarli A. R.- **Prog. Org. Coatings, 14**, 297 (1986).

NOTE: This work has been accepted for publication in the Journal of the Brazilian Chemical Society.

EVALUATION OF ZINC-RICH-PAINT COATING PERFORMANCE BY ELECTROCHEMICAL IMPEDANCE SPECTROSCOPY

EVALUACION DEL COMPORTAMIENTO DE PINTURAS RICAS EN ZINC POR ESPECTROSCOPIA DE IMPEDANCIA ELECTROQUIMICA

E.C. Bucharsky[1], S.G. Real[1], J.R. Vilche[1]

A.R. Di Sarli[2] and C.A. Gervasi[2]

SUMMARY

The influence of pigment volume concentration (PVC) and alkyd vehicle content employed in the formulation of zinc rich paint (ZRP) coatings has been investigated to evaluate the corrosion protection of steel substrates in sea water. Both dc and ac electrochemical techniques have been used to gain a deeper insight concerning the effect of coating composition on corrosion resistance of alkyd ZRP as a function of immersion time in artificial sea water. Standard accelerated tests were carried out with the painted steel surfaces in order to assess their degree of rusting and blistering.

Keywords: *Zinc rich alkyd paints, electrochemical impedance, cathodic protection.*

INTRODUCTION

The ability of coatings to protect metallic structures against corrosion generally depends on coating characteristics as well as on properties of the metal/coating interface. For iron-type metallic sustrates exposed to either industrial or marine atmospheres zinc rich coatings are commonly used for corrosion protection **[1,2]**. Thus, zinc rich primers (ZRP) with organic or inorganic binders are extensively employed for corrosion protection of steel structures when they are in contact with aggressive media such as sea water. Both pigment volume concentration and binder content can affect markedly the performance of a ZRP. Commonly, two fundamental protection mechanisms operating in the ZRP can be recognized, namely the galvanic protection stage and the barrier effect stage **[3,4]**.

The aim of the present paper is to investigate the corrosion protection behaviour of zinc rich alkyd paints for different PVC and vehicle levels, by using electrochemical impedance spectroscopy and open circuit corrosion potential measurements at different exposure times in artificial sea water. The ASTM standard test procedures were carried out to assess rusting and degree of blistering suffered by the coated steel surfaces as well as to evaluate typical physicochemical properties.

---

[1] Instituto de Investigaciones Fisicoquímicas Teóricas y Aplicadas (INIFTA), Fac. Cs. Exactas, UNLP

[2] CIDEPINT, Miembros de la Carrera del Investigador de la CIC

EXPERIMENTAL

SAE 1020 (UNS G10200) steel plates 20x8x0.2 cm were used as metallic substrate. Metal surfaces were sandblasted to AS 2 1/2 degree (SIS Standard 05 59 00/1967), degreased with toluene and coated with paints whose PVC were varied in the 76-88 % range. For the sake of comparison, in samples with relatively low Zn content (76-77 %) chlorinated rubber was added to the coating composition. The ZRP thickness (about 60 μm) was measured with an electromagnetic gauge employing bare sanded plates and standards of known thickness as reference. The experimental setup and the electronic equipments used for the *dc* and *ac* electrochemical measurements have been described elsewhere **[3-5]**. Potentials were measured and referred to in the text against a saturated calomel electrode (SCE). Electrochemical impedance spectroscopy (EIS) measurements in the frequency range 1 mHz ≤ f ≤ 65 kHz were performed in the potenciostatic mode at the corrosion potential after different exposure times in artificial sea water prepared according to the ASTM Standard D-1141/90. For impedance measuraments, an activated Pt probe was coupled to the SCE through a 10 μF capacitor to reduce phase shift errors at high frequencies.

The following standard accelerated tests were carried out on painted steel samples: (i) salt spray cabinet for 500 h (ASTM B 117/85); (ii) immersion in top water (500 h), in white spirit (24 h), in 1 % HCl (24 h), and in 1 % NaCl (24 h), according to BS 3900 G5/76; (iii) ageing in weatherometer (300 h); and (iv) pull-off adhesion (ASTM D-4541/85).

RESULTS AND DISCUSSION

The dependence of the corrosion potential E_{corr} on immersion time in artificial sea water illustrates about the galvanic protection supplied to the steel substrate by alkyd ZRP coatings loaded with different PVC. The observed gradual shift of E_{corr} towards more positive values suggests a progressive deterioration of the coating. Initially, E_{corr} is about -1.10 V a value which lies in the range of the corrosion potential of pure zinc electrodes in sea water **[6]**, whereas after prolonged exposure time in the electrolyte it reaches the typical value corresponding to the corrosion potential of steel in sea water (-0.65 V). The more negative E_{corr} measured in the case of samples containing chlorinated rubber indicates a greater availability of the protective Zn pigment even for PVC values lower than those used in the other samples.

For the naval steel/ZRP/artificial sea water system, both Bode and Nyquist plots at different immersion times showed that the Zn content and the binder concentrations employed in the paint formulation strongly affect the corrosion behaviour of ZRP coatings tested in this work. Impedance spectra were analyzed by using non-linear fit routines according to the following total transfer function:

$$Z_T(j\omega) = R_S + Z \qquad (1)$$

where Z denotes the frequency response of the corrosion system which can be expressed by:

$$Z^{-1} = CPE^{-1} + \frac{R_C + R_{DO}(jS)^{-1/2} + R_A}{[R_C + R_{DO}(jS)^{-1/2}]R_A} \qquad (2)$$

In eq. (2), the constant phase element CPE involves the capacitance C and a parameter α that was close to 0.5 which is a typical value of active porous electrodes. The resistance R_C can be associated with the series combination of the electrolyte resistance inside the pores and the charge transfer resistance of the oxygen reduction reaction (ORR). Therefore, a finite diffusion impedance was considered in order to account for the transport process involved in the cathodic partial reaction through the coating, being $S = l^2\omega/D$ where l and D denote the diffusion length and the diffusion coefficient, respectively, and R_{DO} the diffusion resistance when $\omega \rightarrow 0$. On the other hand, R_A is related to the charge transfer resistance of the zinc dissolution process ocurring in paralell with the ORR.

Figs. 1 and **2** show the good agreement between experimental results and calculated data. Accordingly, it is possible to evaluate the relative impedance contributions of the anodic and cathodic processes. Thus, the dependences of R_A, R_C, and C on the immersion time are depicted in **Figs. 3-5**, respectively.

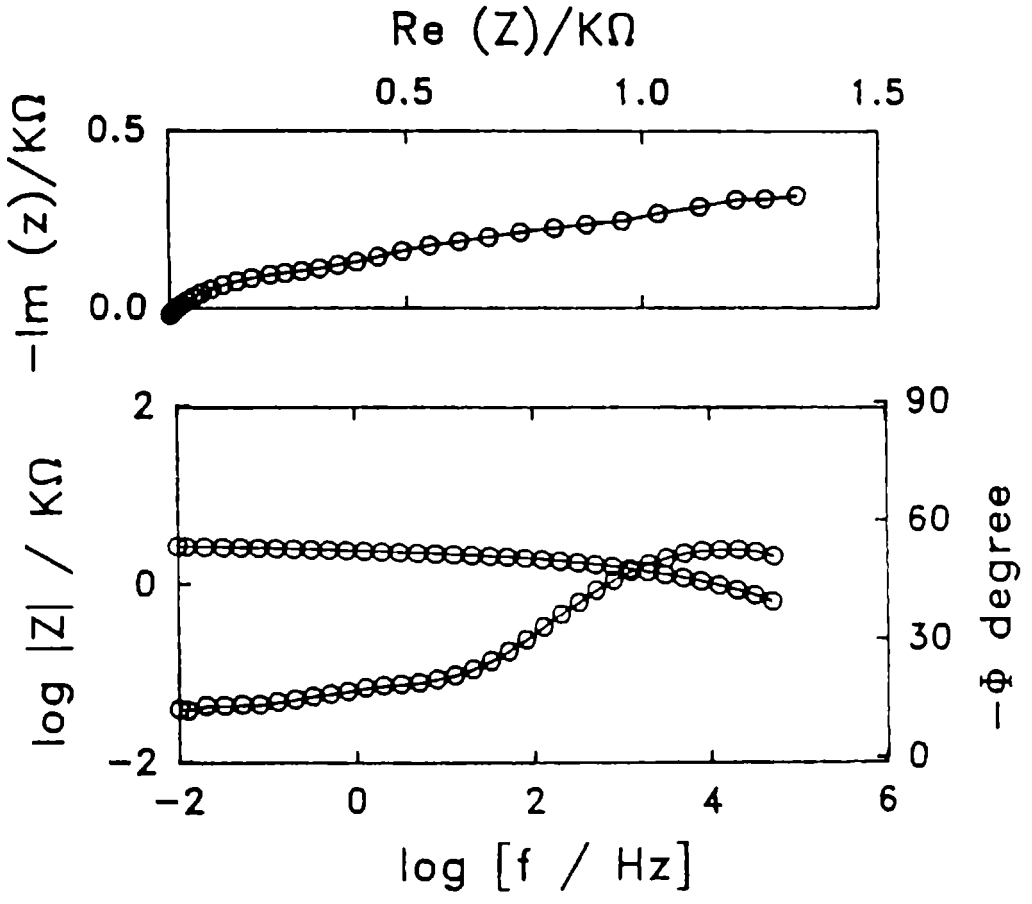

Fig. 1.- Experimental (o) and simulated (-) Nyquist and Bode plots obtained for a sample containing PVC = 86 % after 15 days immersion time in artificial sea water.

Measurements carried out with samples whose compositions include 87-88 % of pigment concentration were interrupted after about 25 days immersion since blistering of the coatings were visually detected. This fact can be attributed to a loss of the coating adhesion properties caused by insufficient binder content. Accordingly, the higher the binder content the lower PVC levels and consequently the longer the useful lifetime.

The changes of the capacitance values, the increase of the resistances R_A and R_C, and the appearence of a diffusional process with increasing immersion time can be explained by the accumulation of zinc corrosion products within the pores of the coating. This decreases the effective pore radius in the ZRP, diminishes the area of the Zn/solution interface, and provokes a progressive loss of electrical connection between the Zn particles.

The cathodic protection effect was practically similar for samples with PVC

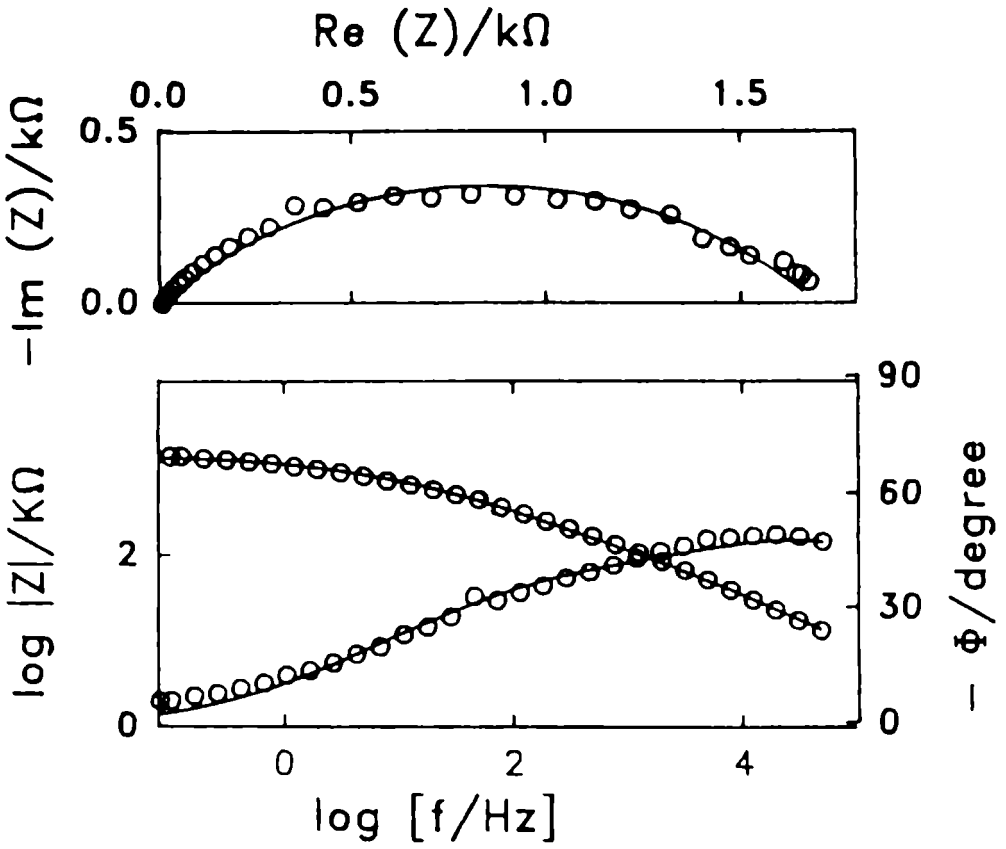

Fig. 2.- Experimental (o) and simulated (-) Nyquist and Bode plots obtained for a sample containing PVC = 77 % and chlorinated rubber, after 34 days immersion time in artificial sea water.

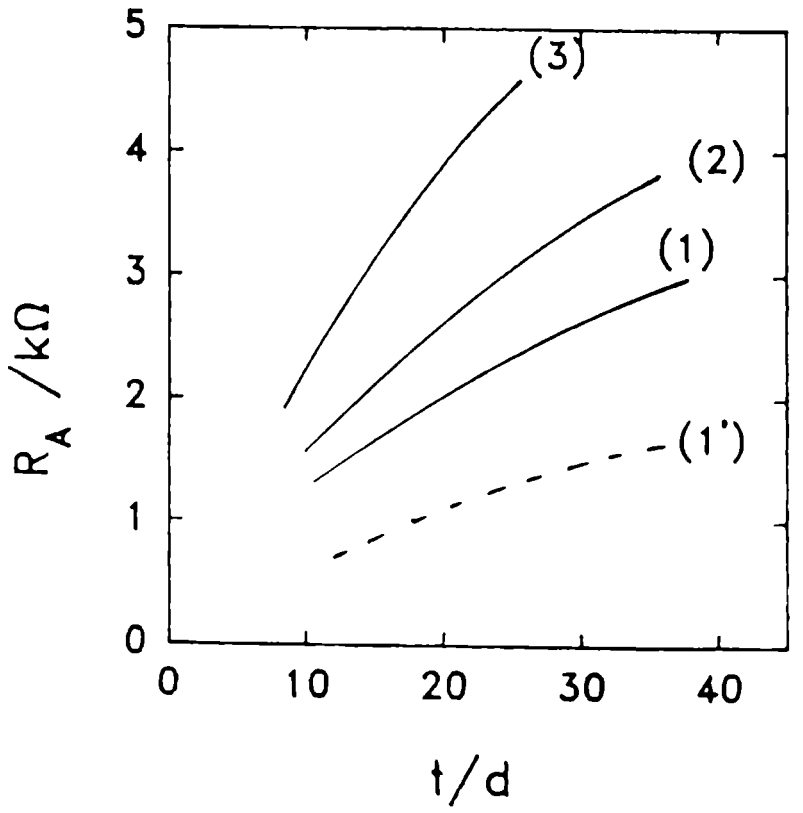

Fig. 3.- Dependence of R_A on immersion time for samples whose Zn contents are: 77 % (curves 1 and 1', without and with chlorinated rubber, respectively), 85 % (curve 2), and 88 % (curve 3).

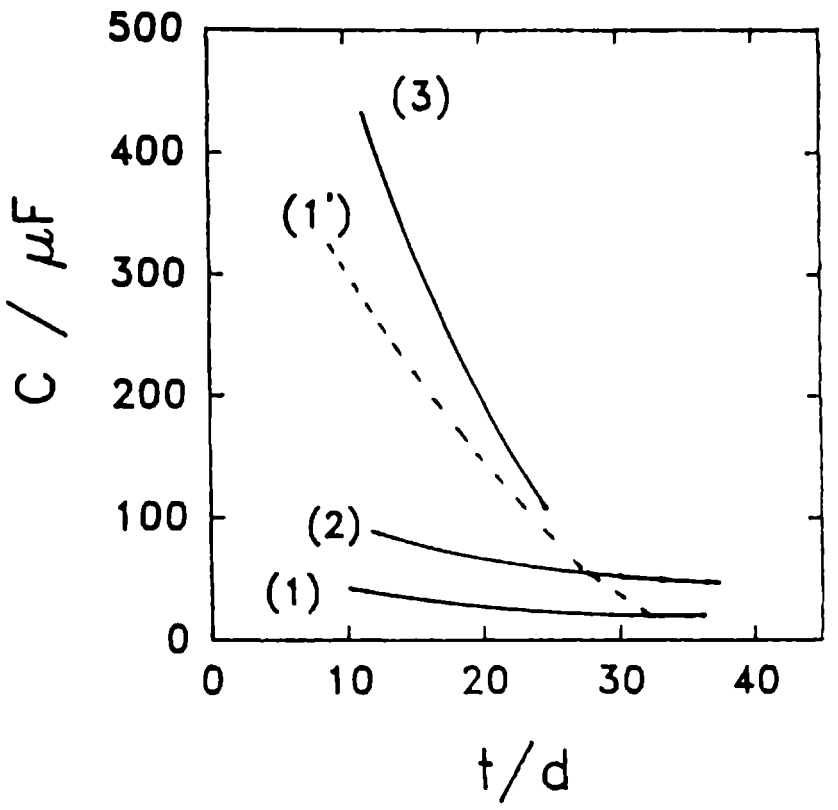

Fig. 4.- Dependence of C on exposure time for samples indicated in Fig. 3.

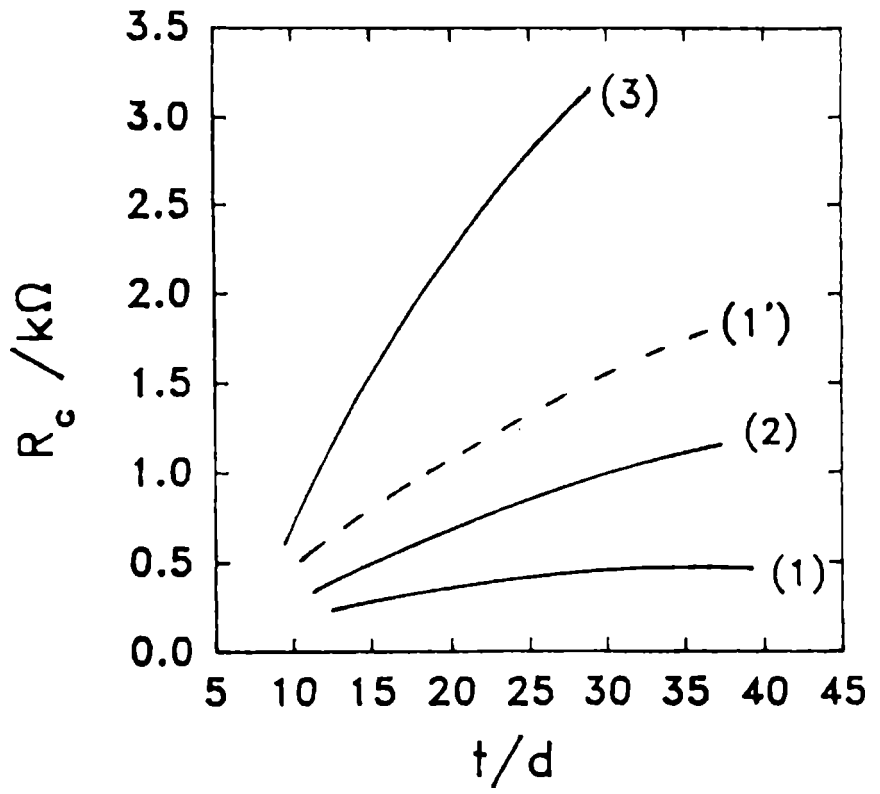

Fig. 5.- Dependence of Rc on exposure time for samples indicated in Fig. 3.

values in the range 76-85 %, although a relatively faster deterioration was found for samples whose content of zinc was about 76-77 %. These results exhibited a satisfactory agreement with conclusions derived from standard accelerated physicochemical tests.

Before immersion in the electrolyte, tests carried out on painted steel panels revealed a good adhesion (28-30 Kg cm^{-2}) between the zinc rich alkyd paints and the metallic substrate. However, after exposure to the electrolyte the interfacial bonding forces were remarkably weakened (up 80 % in some cases) presumably due to the high electrochemical activity of the Zn pigment particles contributing to the polymeric matrix deterioration, as well as to the accumulation of water at the metal/coating interface causing wet adhesion.

Taking into account that the highly reactive anticorrosive ZRP coatings are not directly exposed to the aggressive medium but they are usually covered with an almost non-permeable topcoat paint, which modifies (generally delaying) the kinetic of the interfacial processes, zinc-rich alkyd paints can be used to protect naval steels. Standard physicochemical tests and visual assessment indicate also that this type of primers afforded a satisfactory corrosion protection performance.

CONCLUSIONS

EIS has provide to be a useful tool to assess the protective behaviour of ZRP organic coatings. The whole set of impedance spectra have been interpreted using a non-linear fit routine according to transfer function analysis employing a suitable physical model. Results clearly demonstrate that the galvanic protection stage requires a good electrical contact among the zinc particles. In samples with a Zn content higher than 80 % the cathodic protection effect was still in action after about 45 days of immersion in sea water.

ACKNOWLEDGMENTS

This research project was financially supported by Consejo de Investigaciones Científicas y Técnicas (CONICET), Comisión de Investigaciones Científicas de la Provincia de Buenos Aires (CIC), and Fundación Antorchas. Part of the equipment used in this work was provided by the DAAD and the Alexander von Humboldt-Stiftung.

REFERENCES

[1] Brodd R. J., Leger V. E.- **Encyclopedia of Electrochemistry of the Elemements**, A. J. Bard (ed.), Vol. 5, Marcel Dekker, N.Y., p. 35 (1976).

[2] Munger C. G.- **Corrosion Prevention by Protective Coatings**, NACE, Houston (1984).

[3] Armas R. A., Gervasi C. A., Di Sarli A. R., Real S. G., Vilche J. R.- **Corrosion, 48**, 379 (1992).

[4] Real S. G., Elías A. C., Gervasi C. A., Di Sarli A. R., Vilche J. R.- **Electrochim. Acta, 38**, 2029 (1993).

[5] Castro E. B., Real S. G., Milocco R. H., Vilche J. R.- **Electrochim. Acta, 36**, 117 (1991).

[6] Pourbaix M.- **Atlas d'Equilibres Electrochimiques**, Ganthier- Villars, Paris, p. 312 (1963).

NOTE: This paper was sent for publication in the Journal of the Brazilian Chemical Society.

POLIMERIZACION EN EMULSION SEMICONTINUA DEL SISTEMA METACRILATO DE METILO, ACRILATO DE ETILO Y ACIDO METACRILICO.CARACTERIZACION, PROPIEDADES DEL LATEX Y SU EMPLEO EN LA FORMULACION DE PINTURAS EMULSIONADAS

SEMICONTINUOUS EMULSION POLYMERIZATION OF METHYL METHACRYLATE ETHYL ACRYLATE AND METACRYLIC ACID SYSTEM. CHARACTERIZATION, PROPERTIES OF LATEX AND THEIR USAGE IN EMULSION PAINTS FORMULATION

J. I. Amalvy[1]

SUMMARY

By semicontinuous emulsion polymerization method in "semi-starved" conditions, a terpolimeric latex of methyl methacrylate, ethyl acrylate functionalized with metacrylic acid was synthesized. Conversion and reactor temperature vs. time were followed during reaction. Characterization of latex system was performed by particle size measurements, infrared spectroscopy, viscometric molecular weight, potentiometric titrations, viscosity, etc. The latex was incorporated in a typical latex paint formulation and the test of washability was performed.

Keywords: *acrylic latex, latex paint, semicontinuous emulsion polimerization, acrylates.*

INTRODUCCION

El campo de las pinturas basadas en agua está creciendo rápidamente debido a regulaciones sobre el uso de solventes orgánicos y de emisión de esos solventes tanto durante la elaboración como durante la aplicación del producto. El nivel de emisión de una pintura se mide a través del índice VOC (Volatile Organic Compounds), que en el caso del producto ideal debería ser cero. Los sistemas basados en agua como solvente, son una alternativa viable ya que los aditivos modificadores de las propiedades se agregan en pequeñas proporciones, y se obtienen productos de bajo índice VOC. Valores típicos de estas pinturas son del orden de 5 a 15 %.

Las emulsiones acrílicas en general y las denominadas variedades "carboxiladas" en particular, son ampliamente usadas en formulaciones de pinturas tanto para decoración como para protección de paredes y la importancia e interés de éstas aumenta continuamente.

Si bien hay mucha información de las empresas elaboradoras de látices acrílicos, estireno-acrílicos, etc., la composición de los látices comerciales es

---

[1] Miembro de la Carrera del Investigador de la CIC

compleja y muy variada y en general no es conocida en forma precisa. Por otra parte los procesos de elaboración (sus variables, composición, secuencia de agregados, etc. pueden ser muy diversos y complejos) están protegidos por patentes. Además no todos los componentes que intervienen en la polimerización son conocidos y están disponibles comercialmente. Todo ésto conduce a que sistemas con la misma composición global presenten propiedades distintas, ya sea por que la vía de síntesis fue diferente o por que se usaron diferentes estrategias para la incorporación de monómeros. Un caso concreto de estas diferencias se observa cuando se utiliza un proceso de síntesis tipo "batch" y uno semicontinuo. Aún en este último caso la velocidad de agregado de monómeros influye marcadamente en las propiedades del látex. Entre los procesos mas utilizados, se conoce el denominado "starved" donde la concentración de los monómeros está por debajo del valor de saturación en agua y la velocidad de agregado es tal que se cumple con esa premisa. En la práctica, se alimenta al reactor con una mezcla de monómeros en la relación deseada a una velocidad que es menor que la velocidad de polimerización. De esta manera la polimerización se vuelve controlada por la velocidad de adición y el copolímero formado tiene aproximadamente la misma composición que la alimentación. Sin embargo la velocidad de polimerización es pequeña y los tiempos de síntesis son grandes. Otro proceso mas reciente conocido como "semi-starved", consiste en agregar los monómeros a la misma velocidad con que se consumen, requiere menos tiempo y además produce copolímeros de composición mas homogénea [1,2]. Por ende las formulaciones de pinturas derivadas de esos látices presentan también propiedades diferentes.

Los látices de polímeros derivados totalmente de monómeros acrílicos en particular (látices acrílicos), utilizados para elaborar pinturas y recubrimientos, no son aptos en todas las aplicaciones debido a que sus propiedades, por ejemplo, de resistencia al agua y factores atmosféricos o de brillo no cumplen con las exigencias del caso. Para mejorar estos aspectos en que los látices acrílicos no son aptos, se pueden agregar aditivos plastificantes, absorbedores de luz UV, etc.. Sin embargo estos aditivos aportan componentes volátiles al producto, perdiéndose en parte la ventaja de ser un sistema en base acuosa. La otra alternativa, es trabajar sobre las características del sistema y utilizar por ejemplo, látices compuestos por partículas pequeñas para lograr un empaque más denso y una mejor penetración en el sustrato. También es posible aumentar la resistencia a la abrasión sintetizando sistemas con altos valores de temperatura de transición vítrea (T_g). Estas propiedades se pueden modificar alterando los componentes y/o las condiciones de síntesis (surfactantes, iniciador, temperatura, modalidades de agregado de monómeros, etc.), sin recurrir al agregado de aditivos.

En virtud de que la formulación de una pintura ha sido un arte empírico durante mucho tiempo, es que por ejemplo, no se conocen los factores que controlan la cantidad mínima de metacrilato de metilo que puede ser usado como comonómero en un co- o terpolímero acrílico sin disminuir la durabilidad al exterior. Tampoco se conocen como los mecanismos de la interacción polímero-pigmento en la pintura afectan, por ejemplo, la fotodegradación de la misma. Asimismo, se sabe que el surfactante es necesario para la estabilidad del látex y que su presencia favorece la formación de película, pero no se conoce exactamente en que proporción debe ser usado en cada sistema. Otro aspecto interesante es conocer cómo los diferentes métodos de síntesis influyen en las propiedades y cómo las desviaciones de la composición del látex influyen en sus propiedades y por ende en la pintura o recubrimiento. De lo expuesto surge la necesidad de contar con información detallada sobre los componentes de la pintura y en particular del polímero, y poder así correlacionar estas propiedades con los resultados obtenidos en servicio.

El presente trabajo forma parte de un proyecto tendiente a:
a) desarrollar e implementar la infraestructura necesaria para la síntesis de

látices, tanto a escala de laboratorio como de planta piloto;
b) caracterizar en forma completa los látices obtenidos y,
c) evaluar el comportamiento de pinturas elaboradas en base a esos sistemas.

Esta información permitirá realizar las correlaciones necesarias con las propiedades y características de los látices. Una de estas correlaciones tiene en cuenta el tipo de síntesis utilizada. En particular se intenta obtener pinturas de alta resistencia a factores externos (agua, oxígeno, microorganismos, luz, etc.), donde la composición y propiedades del polímero juegan indudablemente un papel preponderante.

PARTE EXPERIMENTAL

La síntesis se llevó a cabo mediante una polimerización en emulsión semicontinua (o semibatch), bajo condiciones "semi-starved", siguiendo el método propuesto por Arzamendi y col. [1].

Se utilizaron los siguientes monómeros derivados de los ácidos acrílico y metacrílico, de calidad p.a., sin eliminar inhibidores de polimerización:
- metacrilato de metilo (MMA) con 25 ppm de hidroquinona,
- acrilato de etilo (EA) con 100 ppm del éter monometílico de la hidroquinona y
- acido metacrílico (MMA) con 250 ppm del éter monometílico de la hidroquinona.

Se utilizó lauril sulfato de sodio (SLS) como agente tensioactivo, bicarbonato de sodio como "buffer" y peroxidisulfato de potasio como iniciador, todos de calidad p.a..

Durante toda las experiencias se utilizó agua doblemente destilada de una solución de $KMnO_4$ - NaOH.

La polimerización fue realizada en un reactor de vidrio separable de forma cónica, de doble pared para termostatizar y con robinete para la toma de muestras. El volumen del reactor es de aproximadamente 470 ml de capacidad (**Fig. 1**). La tapa del reactor tiene cinco bocas que permiten la entrada de un gas purga, la adición de reactivos y la introducción de un sensor de temperatura (en éste trabajo se utilizó una termocupla de inmersión tipo K envainada en acero inoxidable 316), un condensador de vapores y un agitador (**Fig. 1**). La agitación se realizó desde la parte superior con un varilla de acero y una paleta de Teflon. La velocidad de agitación se reguló entre 200 y 250 rpm.

Los componentes de la polimerización en emulsión se dan en la **tabla I** y las cantidades fueron calculadas para lograr la relación de monómeros deseada y teniendo en cuenta la ecuación de copolimerización:

$$\frac{dM_1}{dM_2} = \left[\frac{M_1.(r_1M_1 + M_2)}{M_2.(r_2M_2 + M_1)}\right]$$

donde (dM_1/dM_2) es la relación de monómeros en el polímero al comienzo de la reacción, M_1 y M_2 son las concentraciones adecuadas de los monómeros 1 y 2, y r_1 y r_2 son las relaciones de reactividad de cada monómero.

Para el presente caso, M_1 corresponde a metacrilato de metilo con $r_1 = 2{,}03$ y M_2 a acrilato de etilo con $r_2 = 0{,}24$ [3]. El ácido metacrílico al ser incorporado en la última etapa del proceso y en una concentración tan baja, no es tenido en cuenta para el caso.

TABLA I
Componentes usados en la síntesis del látex

componentes (g)	carga inicial	alimentación
acrilato de etilo (EA)	100,00	-
metacrilato de metilo (MMA)	46,36	81,54
$K_2S_2O_8$ (KPS)	0,58	-
lauril sulfato de sodio (SLS)	0,73	0,43
$NaHCO_3$ (SBC)	0,19	-
Agua bidestilada (DDW)	176,36	86,10
ácido metacrílico (MAA)	-	4,56

Las emulsiones y el ácido metacrílico fueron desoxigenados haciendo pasar N_2 libre de oxígeno. El oxígeno residual del nitrógeno fue removido por burbujeo del gas en una solución alcalina de pirogalol. Luego de la remoción de oxígeno de los reactivos, se mantuvo durante toda la polimerización, un pequeño caudal del gas.

El iniciador fue disuelto en 30 ml de agua y el procedimiento para la polimerización en emulsión fue el siguiente: la cantidad inicial de SLS y el "buffer" SBC, fueron adicionados a la cantidad de agua inicial en el reactor. Se agregó todo el acrilato de etilo (monómero menos reactivo) con agitación y se burbujeó N_2 durante 30 minutos, mientras se calentaba a 60 °C. Entonces se agregó la solución concentrada del iniciador y luego de un período de inducción de 6 minutos, comenzó la polimerización, evidenciada por un opalescimiento de la emulsión y se permitió que reaccionara durante 30 minutos de tal manera que se formaron partículas-semillas, luego se comenzó el agregado de la emulsión de alimentación a una velocidad de aproximadamente 3 g/min. El tubo de burbujeo de N_2 se elevó por encima del nivel del líquido para prevenir la coagulación del polímero. La emulsión de alimentación, fue preparada utilizando un emulsificador a 1500 rpm, puesta en el embudo de adición y desaireada por 30 minutos. El tiempo total de adición de la emulsión fue de 308 minutos. La velocidad de agregado de la emulsión de alimentación, se controló periódicamente, tratando de ajustarla a la reportada por Arzamendi y col. [1], ya que esta velocidad de agregado genera copolímeros de composición constante durante toda la reacción, obteniéndose por lo tanto un producto homogéneo.

Debido a la dependencia de la descomposición del ión persulfato con el pH, éste último parámetro se controló periódicamente. El valor inicial fue de 8 y se mantuvo constante durante la reacción, hasta la adición del ácido metacrílico (agregado a 234 minutos de reacción) momento en que descendió hasta 5-6, siendo el valor final de pH del látex 5.

Con el fin de completar la polimerización, se mantuvo el sistema a 60 °C durante una hora luego de la adición total de los monómeros.

Durante la polimerización se extrajeron muestras suficientemente pequeñas como para mantener constante la composición de la emulsión. Las muestras de látex fueron enfriadas con hielo para detener la polimerización. La conversión fue determinada gravimétricamente evaporando la muestra a 20 mm de Hg y 50 °C.

La temperatura de la reacción fue monitoreada continuamente, enviando la señal de la termocupla a un registrador X - t. La termocupla fue calibrada utilizando agua-hielo y agua en ebullición.

El pH del látex fue ajustado con solución de NH_3 al 10 % a un valor entre 8 y 9. El látex fue equilibrado a ese pH antes de incorporarlo en una formulación de la pintura.

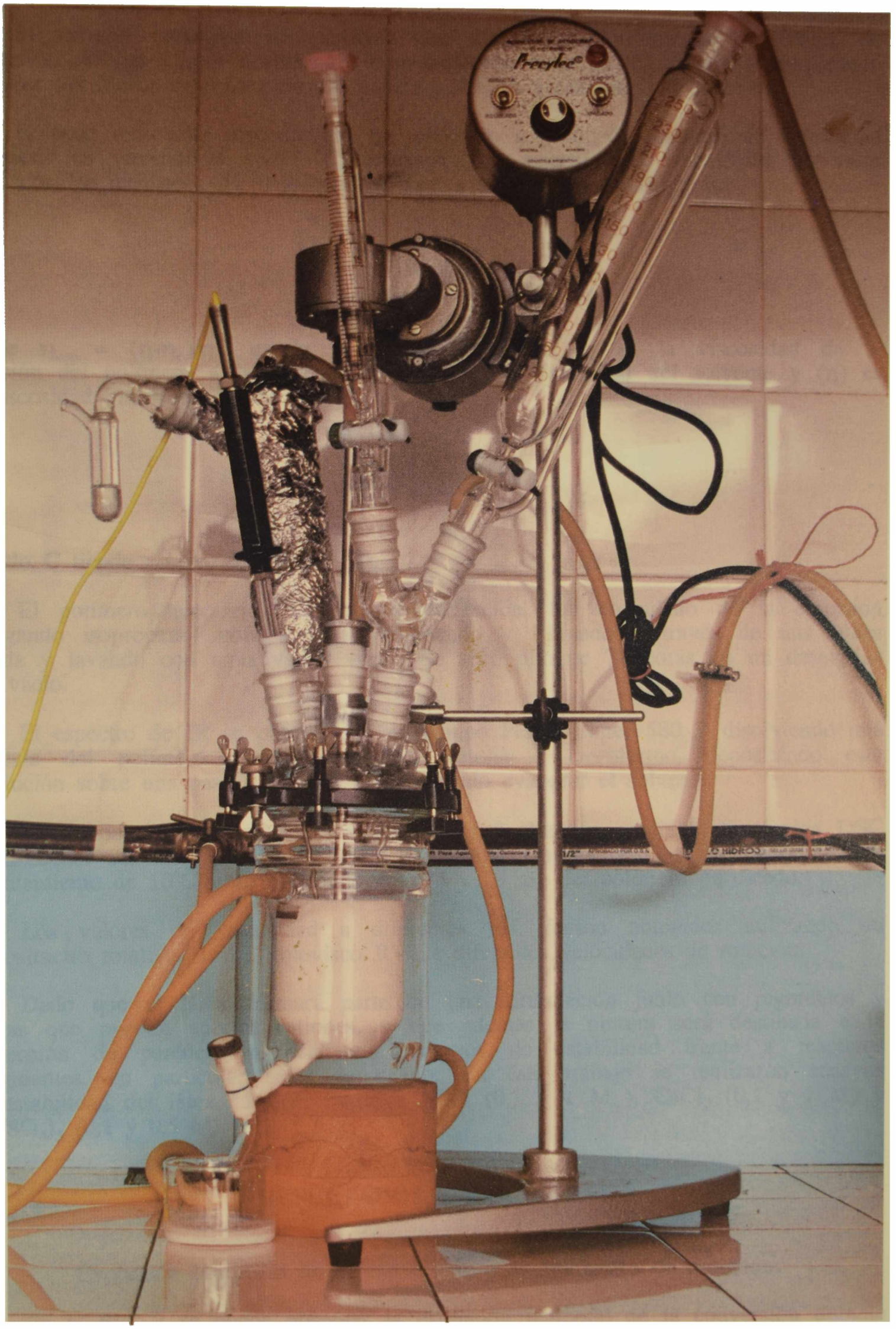

Fig. 1.- Reactor utilizado en la síntesis del látex.

El tamaño promedio de partícula fue determinado utilizando la técnica de dispersión de luz ("light scattering") con radiación láser de 632,8 nm y empleando un valor del índice de refracción del polímero de 1,5 a esa longitud de onda.

El peso molecular viscométrico fue obtenido a partir de medidas de viscosidad intrínseca en cloroformo a 30 °C, utilizando un viscosímetro Ubbelöhde. El valor de viscosidad intrínseca fue calculado en base a la ecuación de Huggins:

$$\left[\frac{\eta_{esp.}}{C}\right] = (\eta) + K.(\eta)^2.C$$

donde $\eta_{esp.} = (\eta-\eta_o)/\eta_o$, es la viscosidad específica, η es la viscosidad de la solución del polímero a la concentración C, η_o la viscosidad del solvente y (η) es la viscosidad intrínseca. De la relación

$$\left[\frac{\eta_{esp.}}{C}\right] \text{ vs. } C,$$

cuando C tiende a cero, se obtiene (η).

El polímero necesario para la caracterización, fue coagulado de la emulsión agregando isopropanol gota a gota y agitando y filtrando a través de una placa fritada y lavando con agua varias veces. Se secó durante 72 horas en un desecador con vacío.

El espectro de IR se obtuvo con un equipo Perkin-Elmer 580 B disolviendo una película del polímero o el polvo, en acetona o cloroformo, depositándo ésta disolución sobre una pastilla de CsI y permitiendo evaporar el solvente.

La temperatura de transición vítrea (T_g) fue obtenida mediante la técnica DSC ("differential scanning calorimetry") en un equipo DuPont 910, a una velocidad de calentamiento de 10°C/min., utilizando entre 5 y 10 mg del polímero purificado.

Los valores de viscosidad a diferentes pH, fueron obtenidos utilizando un viscosímetro rotativo Haake Rotovisco RV2 a diferentes velocidades de rotación.

Dado que el látex formará parte de una formulación junto con pigmentos y cargas que pueden aportar cationes, y que además la pintura será destinada a la protección de paredes, se realizaron ensayos de estabilidad frente a reactivos coagulantes, en particular sales de calcio. En éste trabajo se realizaron ensayos de estabilidad del látex "ácido", frente a NaCl (0,1 y 1 M), $CaCl_2$ (0,1 y 1 M) y $Al_2(SO_4)_3$ (0,1 y 0,5 M).

RESULTADOS Y DISCUSION

Evolución temporal de la conversión y temperatura de reacción.

En la **Fig. 2** se puede observar la evolución temporal de la conversión durante la polimerización en emulsión. La conversión fue definida como:

$$\% \text{ conversión} = \frac{\text{cantidad de polímero en el reactor}}{\text{cantidad total de monómeros en el reactor}}$$

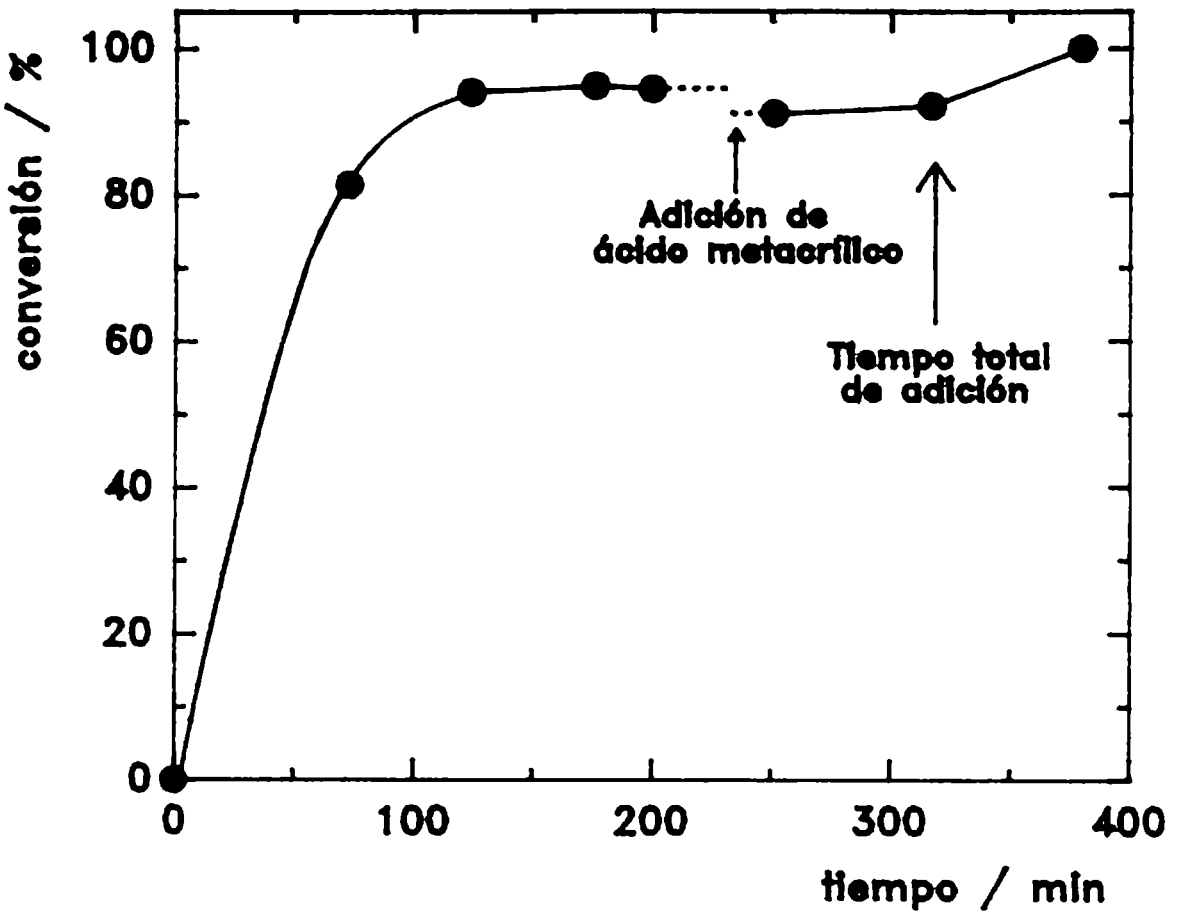

Fig. 2.- Evolución temporal de la conversión.

Los cálculos fueron corregidos teniendo en cuenta las muestras extraídas durante el proceso. La curva obtenida hasta la adición de ácido metacrílico, es similar a la obtenida por otros investigadores **[1]**.

Puede observarse que a los 60 minutos de la adición total de monómeros, se llega a la conversión total.

En la **Fig. 3** se puede ver la evolución temporal de la temperatura de reacción. Se puede observar que luego del agregado del iniciador, hay un período de inducción de aproximadamente 6 minutos. Tomando como cero este momento, el máximo de temperatura (70 °C) ocurre aproximadamente a los 14 minutos. Luego la temperatura baja al valor de termostatización. Es interesante apuntar que la forma de esta última parte de la curva, sigue la forma de la concentración de radicales libres formados en función del tiempo tal como ha sido determinada por Cutting y col. mediante espectroscopía de resonancia de spin electrónico **[4]**.

Es sabido que las reacciones por radicales libres son extremadamente rápidas y altamente exotérmicas. La efectividad del proceso de polimerización en emulsión utilizado puede evaluarse calculando cuál sería el aumento de la temperatura sin la termostatización externa, realizando el balance térmico considerando el reactor como aislante perfecto y despreciando las pequeñas cantidades de surfactante e iniciador. Teniendo en cuenta las cantidades iniciales en la tabla I, el calor de polimerización de los monómeros es de 104.700 Joule y la capacidad calorífica del medio (agua + monómeros) es de 1021 J/°C, siendo por lo tanto el incremento de temperatura esperado de aproximadamente 102 °C, sustancialmente mayor que el observado de 10 °C. Luego del proceso inicial de polimerización, la temperatura se mantiene prácticamente constante a 60 °C, por lo que la velocidad de agregado de la emulsión de MMA es tal que permite una efectiva disipación del calor de polimerización.

Parámetros característicos del látex y estabilidad química

En la **tabla II** se pueden ver los parámetros característicos del látex en sus dos formas.

TABLA II

Parámetros característicos del látex

	sólidos	D partícula	pH	densidad
látex "ácido"	47,7 %	144 nm	5	1,08 $g.cm^{-3}$
látex "básico"	44,2 %	158 nm	8-9	---

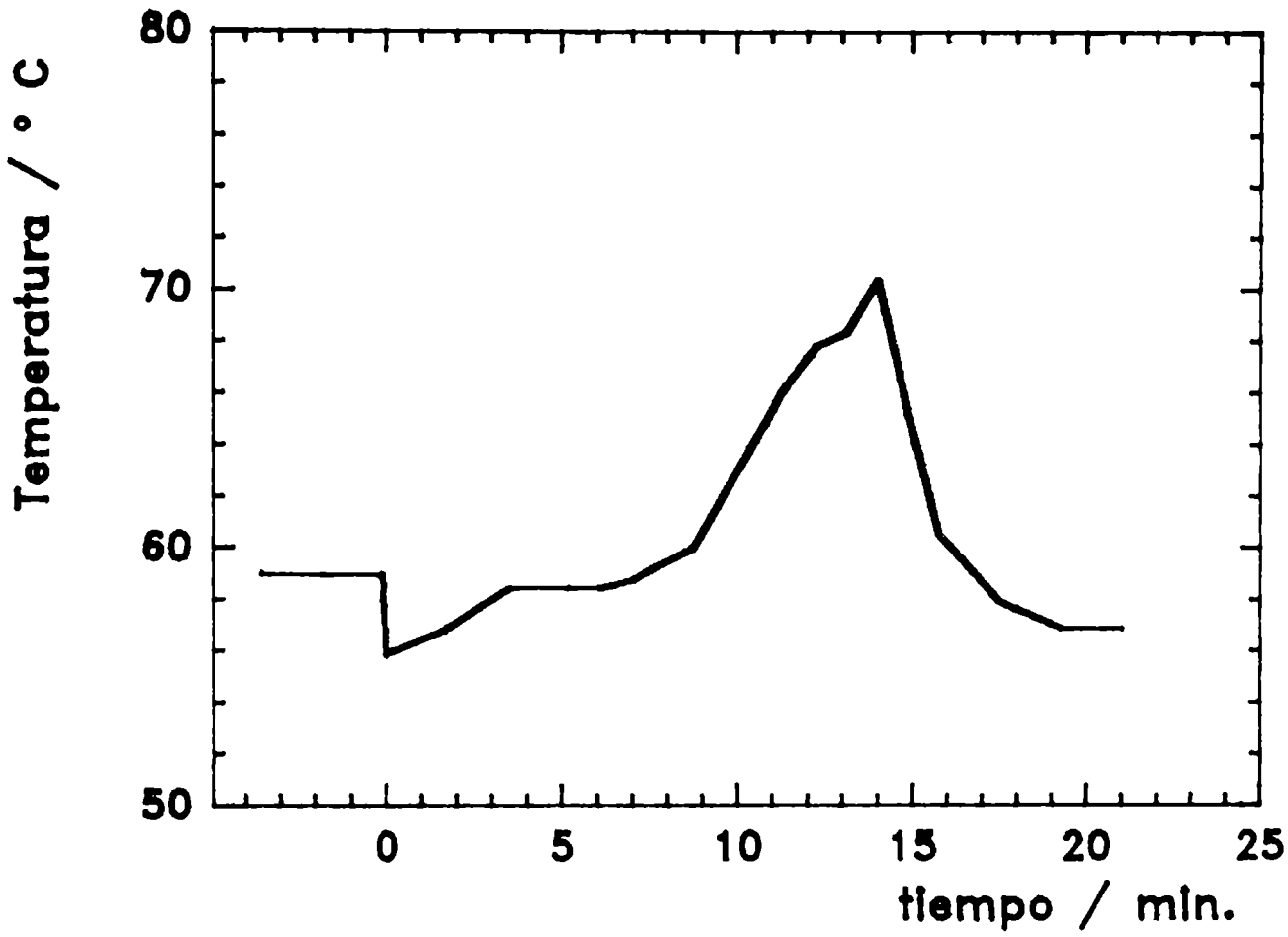

Fig. 3.- Evolución temporal de la temperatura en el reactor, termostatizado a 60 °C.

La **tabla III**, presenta los resultados del test de estabilidad química frente al agregado de sales de cationes mono, di y trivalentes en diferentes concentraciones.

TABLA III

Resultados del test de estabilidad química

Sal	NaCl		$CaCl_2$		$Al_2(SO_4)_3$	
Conc.	0,1 M	1 M	0,1 M	1 M	0,1 M	0,5 M
Observ.	N.C.	N.C.	C.T.	C.T.	C.P.	C.P.

N.C.: No coagula, C.P.: coagula parcialmente, C.T.: coagula totalmente

Viscosidad intrínseca y peso molecular viscométrico

De los resultados de tiempo de escurrimiento con el viscosímetro Ubbelöhde y

en base a la ecuación de Huggins se obtuvo, mediante un ajuste por cuadrados mínimos, la siguiente expresión:

$$\left(\frac{\eta_{esp.}}{C}\right) = 2{,}08 + 4{,}18.C \quad (r = 0{,}9997)$$

Por lo tanto se puede calcular la viscosidad intrínseca, $(\eta) = 2{,}08$ y la constante de Huggins, $K = 0{,}9695$. Lamentablemente, no se conocen las constantes de la ecuación que vincula la viscosidad intrínseca y el peso molecular (ecuación de Mark-Houwink-Sakurada):

$$(\eta) = K'.M^{a}$$

para el sistema en estudio. Sí se conocen, relaciones para polimetacrilato de metilo (PMMA) y poliacrilato de etilo (PEA). También se conocen valores de (η) del sistema MMA/EA, con diferentes relaciones MMA/EA **[3,5]**. De esa información y con el valor de la viscosidad intrínseca experimental, se puede estimar que el peso molecular viscométrico se encuentra comprendido entre 10^5 y 10^6.

Espectro de infrarrojo

En la **Fig. 4**, se puede ver el espectro de infrarrojo en el rango 4000-200 cm^{-1}, del polímero obtenido por evaporación del látex. En la **tabla IV** se dan los números de ondas, asignaciones tentativas e intensidades.

El espectro obtenido es muy similar a espectros reportados en la literatura, tanto para terpolímeros de composición conocida, como de productos "acrílicos" comerciales **[6]**.

Algunos aspectos de interés son la presencia del grupo carbonilo del ácido metacrílico que aparece como hombro debido a su baja concentración y la estructura fina comprendida entre 815 y 750 cm^{-1} asociada al modo rocking del grupo $(-CH_2-)_n$ con n = 1, 2, 3, etc. **[7]**.

Por último, las bandas observadas a 598 y 532 cm^{-1} no corresponden al terpolímero ya que no aparecen en el espectro del polímero obtenido por coagulación con isopropanol y lavado con agua.

Temperaturas de transición vítrea y mínima de formación de película

El valor de la temperatura de transición vítrea (T_g) obtenida del análisis de la curva "DSC" es de aproximadamente 48 °C. Esta temperatura se compara bien con el valor de 47°C, reportado para el sistema MMA/EA/AA(56/43/1) **[8]**.

Si bien no fue posible determinar la temperatura mínima de formación de película (MFT), ésta puede ser estimada en base a datos reportados previamente para el sistema MMA/EA **[9]**. Utilizando la información disponible en esa referencia y ajustando por cuadrados mínimos, se obtuvo la relación:

$$MFT\ (°C) = 2{,}145.[\%\ MMA] - 84{,}0 \quad (r = 0{,}9989)$$

En este caso el porcentaje de MMA es de 55-56 % y la MFT estimada según la ecuación es de 34-36 °C.

En general, la presencia de agua y surfactante disminuyen la MFT y en nuestro caso es de esperar un valor cercano a 30 °C, si se lo compara con el látex (MMA/EA/AA-56/43/1) [8].

TABLA IV

Números de ondas, asignaciones e intensidades observadas en el espectro de IR correspondientes al terpolímero MMA/EA/MAA.

Número de ondas (cm^{-1})	Asignación	Intensidad
3442	$2\nu_{C=O}$	débil
2985	ν_{aCH}	fuerte
2952	ν_{sCH}	fuerte
2880	ν_{CH}	mediana
2847	ν_{CH}	mediana
1735	$\nu_{C=O}$ (éster)	muy fuerte
1690	$\nu_{C=O}$ (ácido)	hombro
1477	$\delta(CH_2)+\delta_a(\alpha\text{-}CH_3)$	hombro
1450	$\delta(CH_2)+\delta_a(CH_3\text{-}O)$	fuerte
1439	$\delta_s(CH_3\text{-}O)$	hombro
1384	$\delta(\alpha\text{-}CH_3)$	fuerte
1365	$\delta(\alpha\text{-}CH_3)$	hombro
1300	$\delta(CH_2)$	hombro
1266	$\delta_s(\alpha\text{-}CH_3)$	hombro
1243	$\nu_{C\text{-}O\text{-}C}$	muy fuerte
1178		muy fuerte
1160	$\nu_{C\text{-}O\text{-}C}$	muy fuerte
1100		fuerte
1026		mediana
990	$\gamma_r(CH_3\text{-}O)$	hombro
969	$\gamma_r(\alpha\text{-}CH_3)$	débil
914		débil
852		débil
815	$\gamma_r(CH_2)$	débil
780	$\gamma_r(CH_2)$	hombro
750	$\gamma_r(CH_2)$	débil
482		muy débil
360		débil

Propiedades reológicas

El sistema estudiado al contener grupos carboxílicos superficiales, presenta propiedades reológicas particulares y muy interesantes **[10]**.

Existen varios motivos que justifican el agregado de ácidos acrílicos que aportan grupos carboxílicos a la partículas de látex. Las más importantes desde el punto de vista de la pintura, son el aumento de la eficiencia ligante y el aumento de la concentración crítica de pigmento en volumen (CPVC) **[11]**. Además, el que una pintura tenga buena nivelación, sea de fácil aplicación y qué espesor de capa puede lograrse con una mano aplicada a pincel, depende de las propiedades reológicas del látex, aún en las formulaciones donde la cantidad del mismo es baja. Por otra parte, este agregado le confiere mayor estabilidad coloidal al látex, mejorando la resistencia a la coagulación frente a los ciclos frío-calor y, la estabilidad mecánica del sistema **[8, 12]**.

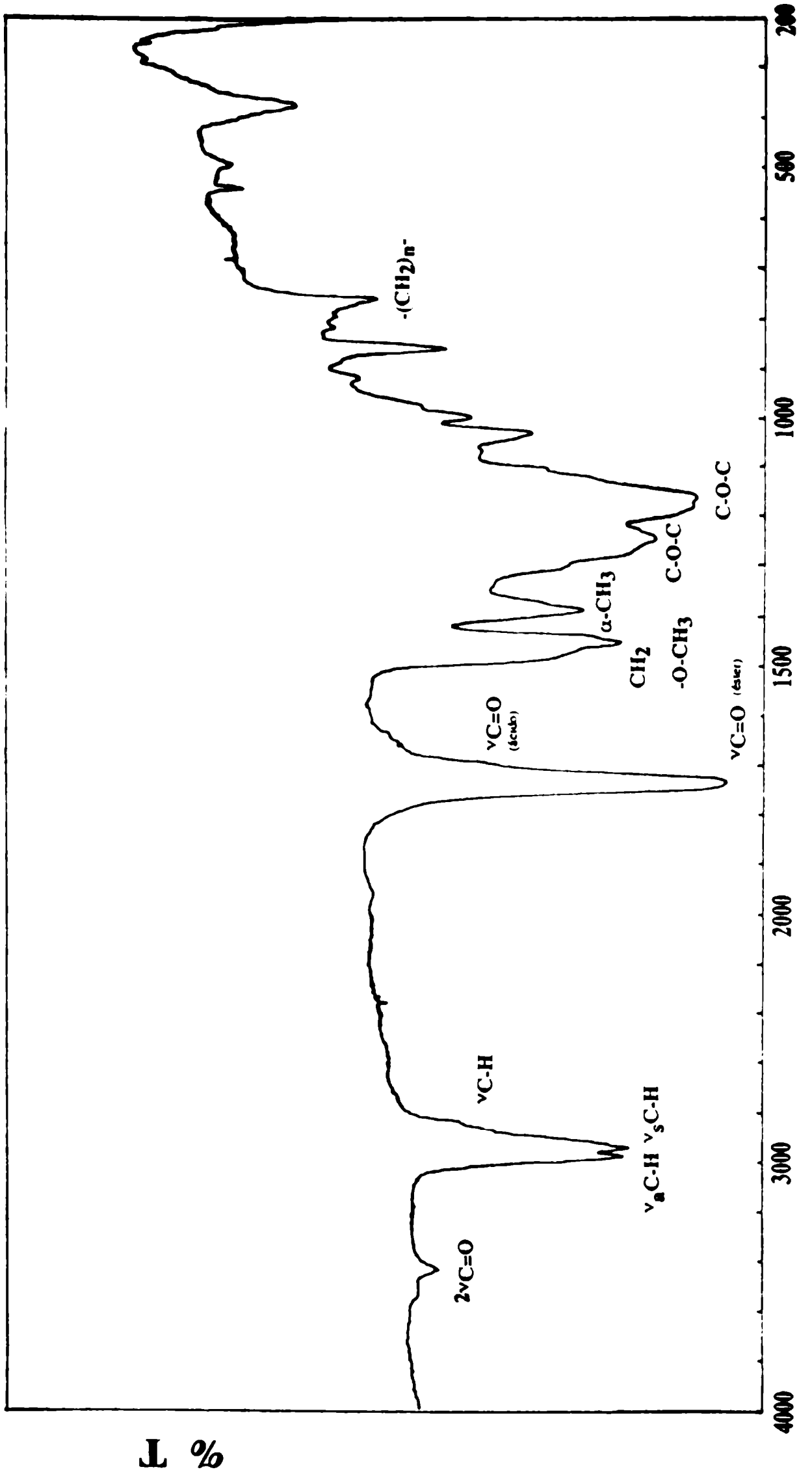

Fig. 4.- Espectro de infrarrojo del terpolímero MMA/EA/MAA.

En la **Fig. 5**, se observa la variación de la viscosidad en función del pH del látex, para diferentes valores del esfuerzo de corte. Si bien las medidas no son totalmente exactas por las dificultades experimentales que estos sistemas presentan, se puede observar el pronunciado aumento que se obtiene al llegar a un pH cercano a 8. Este comportamiento es característico de látices conteniendo pequeñas cantidades de grupos carboxílicos (en éste caso aportado por el 2 % de ácido metacrílico y en una pequeña extensión por hidrólisis del enlace éster), y se puede explicar en base a la contribución de tres efectos. Un efecto electroviscoso primario asociado a un aumento en la viscosidad intrínseca provocado por una distorsión de la doble capa eléctrica, un efecto secundario asociado a la interacción culómbica entre las dobles capas de diferentes partículas, y, por último, un efecto terciario asociado a la distorsión de la partícula en sí misma como resultado de las fuerzas electrostáticas debido a la presencia de cargas sobre las partículas.

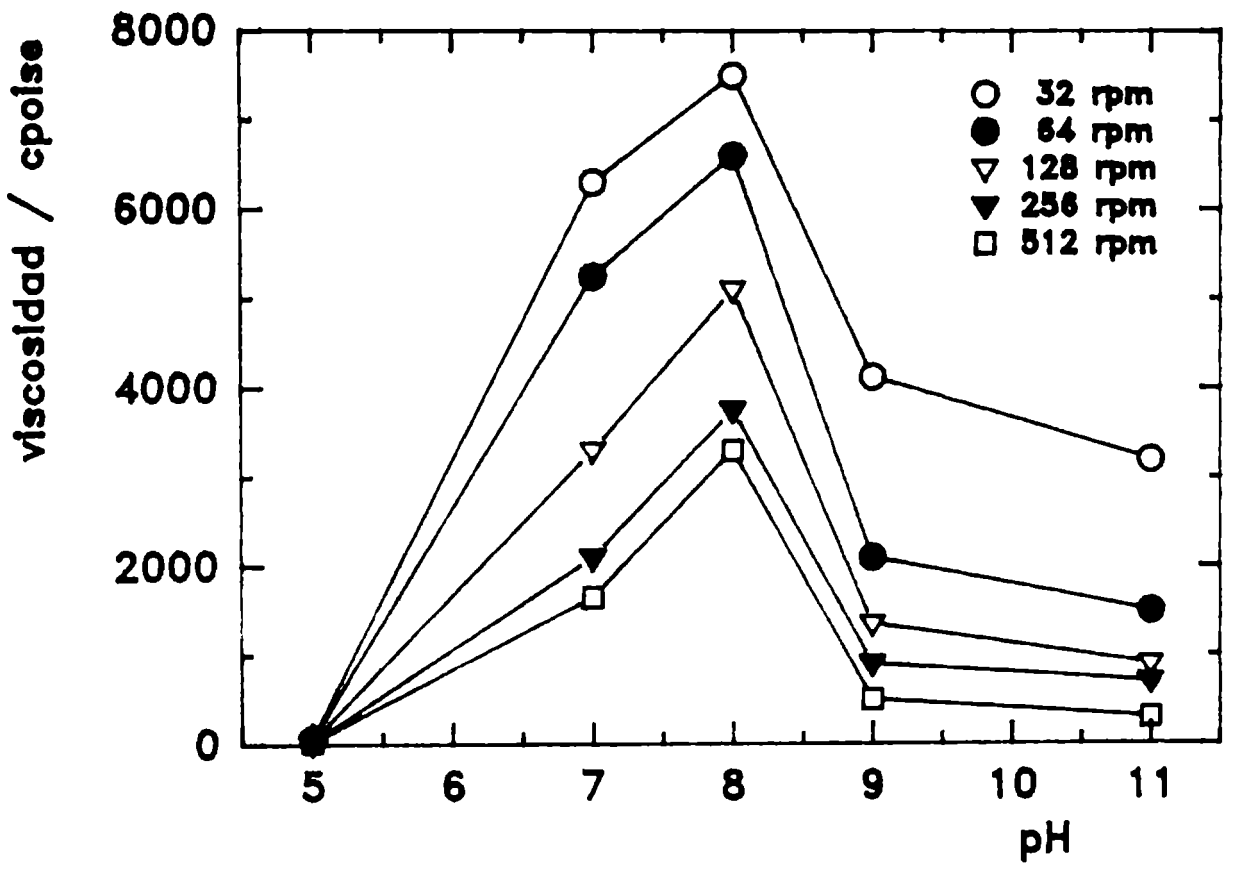

Fig. 5.- Variación de la viscosidad con el pH a diferentes esfuerzos de corte.

El látex a pH 5 presenta un comportamiento relativamente cercano a un fluído Newtoniano, mientras que las muestras a valores mayores de pH, presentan un marcado comportamiento no-Newtoniano. En particular se observa una disminución de la viscosidad con un aumento del esfuerzo de corte característico de sistemas pseudoplásticos (Fig. 6) y típico de estos látices [10].

Sin embargo, no hay demasiada información experimental y estudios detallados sobre las propiedades reológicas en función del pH para sistemas como el presente.

Otros análisis

Los análisis tendientes a caracterizar el sistema desde el punto de vista de su distribución de carga y grupos ácidos superficiales, se encuentran en su faz preliminar, pero en base a estos resultados, se puede establecer la presencia de dos tipos de grupos ácidos superficiales, que pueden atribuirse a:

a) grupos sulfonato ($-SO_3H^-$) y sulfato ($-OSO_3H$), fuertes provenientes del iniciador ($K_2S_2O_8$) y,

b) grupos -C(O)OH débiles, aportados mayormente por el ácido metacrílico y en parte por hidrólisis del enlace éster **[10,13]**.

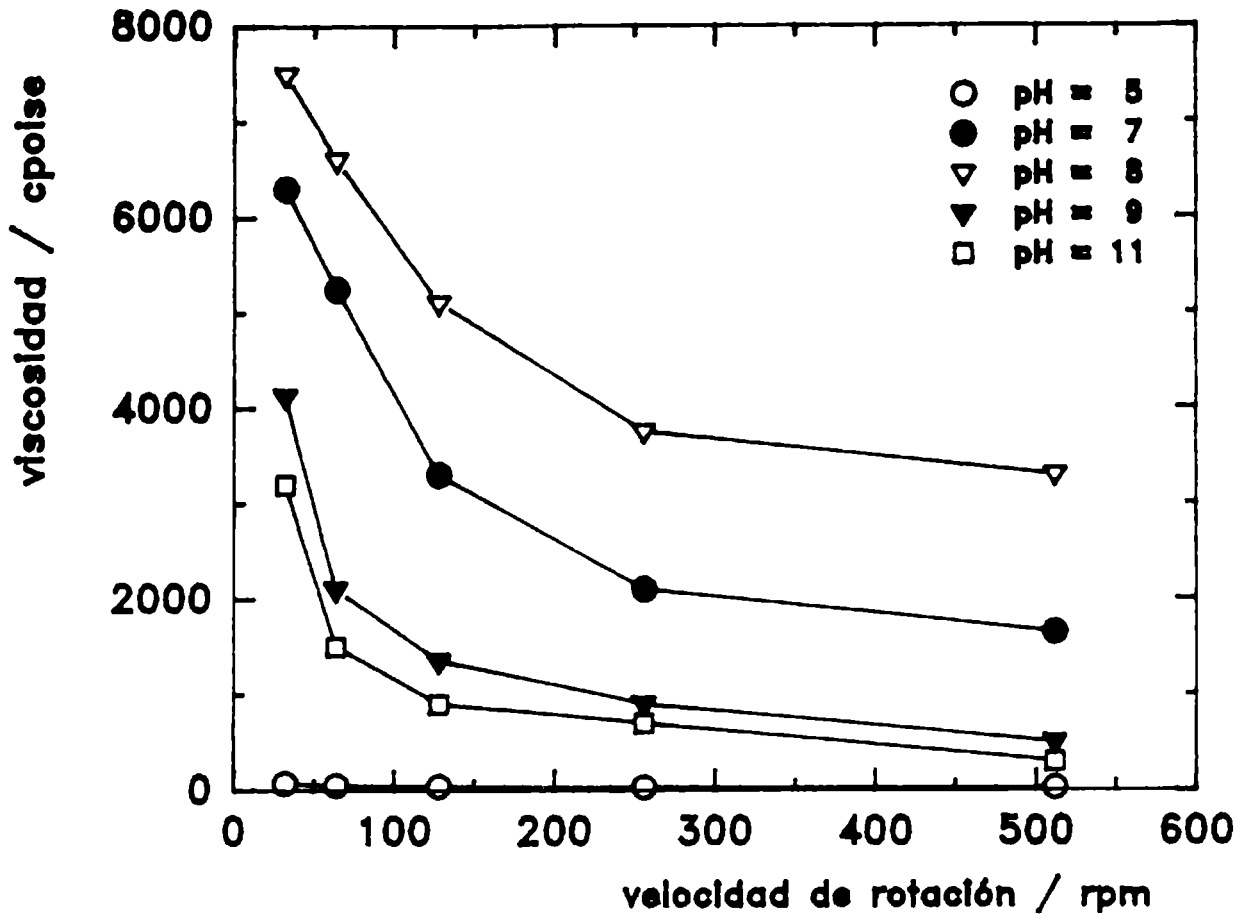

Fig. 6.- Variación de la viscosidad con el esfuerzo de corte a diferentes valores de pH.

Incorporación del látex en una formulación de pintura

Por último, se complementó éste estudio incorporando el látex en una formulación de pintura destinada a la protección de paredes exteriores. De los diversos ensayos determinantes del comportamiento de una pintura en servicio, se tuvo muy en cuenta el de lavabilidad, debido a que éste es en la práctica excluyente. En la **tabla V**, se presenta una formulación orientativa utilizada, para el ensayo de lavabilidad.

TABLA V

Formulación de pintura utilizada

Componente	% en peso
agua	35,0
dispersante	1,0
antiespumante	1,0
$CaCO_3$ ppdo.	15,0
$CaCO_3$ natural	7,6
TiO_2	15,0
látex	20,0
espesante	1,0
coalescente	2,4
amoníaco	2,0

El ensayo de lavabilidad se realizó en base a la norma IRAM 1109 - Método B XV, extendiendo una película de aproximadamente 150 μm. La película cumple con las exigencias de la Norma IRAM 1077 (Pinturas al agua tipo emulsión blancas y de colores claros), requisito "Resistencia a la abrasión húmeda - Emulsiones al látex".

CONCLUSIONES

El método de síntesis mediante polimerización semicontinua, en condiciones "semi-starved", permite obtener un látex con un alto contenido de sólidos, con una conversión total de monómeros y con un adecuado control de la temperatura de reacción. El producto obtenido presenta propiedades físicoquímicas características de estos sistemas, y el ensayo preliminar del comportamiento en servicio de una pintura formulada en base al mismo, es satisfactorio.

CONSIDERACIONES FINALES

Se continúa trabajando en otros ensayos para lograr una evaluación completa del comportamiento en servicio de la pintura. Además, se ensayarán otras combinaciones del sistema MMA/EA/MAA, como así también de otros sistemas que contengan otros monómeros (estireno, 2-etilhexil-acrilato, etc.). La información obtenida permitirá establecer correlaciones entre las propiedades fisicoquímicas de los látices y el comportamiento en servicio de formulaciones basadas en ellos.

AGRADECIMIENTOS

A la Comisión de Investigaciones Científicas de la Pcia. de Bs. As. (CIC) y a CONICET por el apoyo económico brindado para la realización de éste trabajo. A la Dra. D. B. del Amo por la realización de las medidas de viscosidad, al Técnico O. Pardini por la colaboración en la realización de algunas técnicas analíticas y al Ing. R. A. Armas por la colaboración en la elaboración de la pintura y en la realización del ensayo de lavabilidad.

BIBLIOGRAFIA

[1] Arzamendi G., Leiza J. R., Asua J. M.- **J. Polym. Sci.**, Part. A. **29**, 1549 (1991).

[2] Arzamendi G., Asua J. M.- **J. Appl. Polym. Sc., 38** (11) 2019 (1989).

[3] Capek I., Barton J., Tuan L. Q., Svoboda V., Novotny V.- **Makromol. Chem., 188**, 1723 (1987).

[4] Cutting G. R., Tabner B. J.- **Macromolecules 26**, 951 (1993).

[5] Anzur I., Osredkar U., Ukmar I., Vizovisek I.- **Makromol. Chem. Suppl. 10/11**, 311 (1985).

[6] **An Infrared Spectroscopy Atlas for the Coating Industry**, Federation of Societies for Coating Technology, 1980.

[7] **Spectroscopy of Polymers**, J.L. Koenig, A.C.S. Prof. Ref. Book 1992, página 40.

[8] Sperry P. R.- Rohm and Hass Company, comunicación privada.

[9] Okubo M.- **Makromol. Chem. Macromol. Symp., 35/36**, 307 (1990).

[10] Quadrat O., Snuparek J., Jr.- **Progress in Organic Coatings, 18**, 207 (1990).

[11] Vijayendran B. R.- **Makromol. Chem. Suppl., 10/11**, 271 (1985).

[12] Karunasena A., Glass J. E.- **Prog. Org. Coat., 17**, 301 (1989).

[13] Graillat C., Pichot C., Guyot A.- **Coll. Surf. 56**, 189 (1991).

ÉVALUATION ÉLECTROCHIMIQUE DE LA PERMÉABILITÉ À L'OXYGÈNE DES PELLICULES DE PEINTURES ANTICORROSIVES

ELECTROCHEMICAL EVALUATION OF THE OXYGEN PERMEABILITY FOR ANTICORROSIVE COATING FILMS

C.I. Elsner[1] , R.A. Armas[2] et A.R. Di Sarli[3]

RÉSUMÉ

On a étudié l'influence du type et de l'épaisseur de trois peintures anticorrosives utilisées comme "primers" (liants à base de caoutchouc chloré, résine vinylique et résine alkyde) sur le transport de l'oxygène à travers le film. Le coefficient de perméabilité à l'oxygène a été évalué à partir de l'évolution du courant de réduction de l'oxygène en fonction du temps d'immersion. Les éprouvettes en acier recouvert ont été exposées à une solution de NaCl à 3 % dont le contenue en oxygène dissous a été varié par barbotage de l'oxygène, air ou azote. En plus, on a fait un contrôle visuel avant, pendant et après le temps d'immersion pour suivre l'évolution du recouvrement.

Les résultats obtenus ont permis concluir que: a) la polarisation de l'acier recouvert et la mesure du courant de réduction de l'oxygène fournisent profitable information quantitative des propriétés de transport de chaque système métal recouvert/électrolyte étudié, b) on a vérifié que le courant mesuré touche particulièrement la réduction de l'oxygène sur la surface de l'acier recouvert et que sa valeur limite est caractéristique du système étudié. Cette valeur est fixée par le transport de l'oxygène à travers le film, et c) la méthode utilisée est simple et nous a permis d'ordonner les peintures essayées en fonction de leur efficience de protection selon: caoutchouc chloré > résine vinylique > résine alkyde.

Mots Clés: *transfert de matière, perméabilité, oxygène, peintures anti-corrosives.*

INTRODUCTION

Le recouvrement des métaux avec peinture est une des méthodes la plus courante de protection contre la corrosion. Malgré cela, fréquemment on ne connaît pas le mécanisme pour lequel le film protège chaque métal dans un milieu donné. En général, les recouvrements organiques protègent le substrat métallique de la corrosion par deux mécanismes: a) en jouant le rôle de barrière au transport de l'oxygène, de l'eau et des ions et/ou b) en jouant le rôle de réservoir des inhibiteurs de la corrosion. Cependant comme aucun recouvrement est totalement

---

[1] Miembro de la Carrera del Investigador del CONICET

[2] Profesional de Apoyo del CONICET y Planta Permanente CIC

[3] Miembro de la Carrera del Investigador de la CIC

imperméable, des ions, de l'eau et de l'oxygène diffusent, dans une proportion qui depend du type de recouvrement employé, vers la surface métallique rendant possible la corrosion.

Pour un temps d'immersion donné, en mantenant les autres propriétés constantes, au four et à mesure que la solubilité de l'eau augmente la quantité qui peut être absorbée par la peinture, augmente aussi jusqu'au moment où le gradient de pression osmotique entre la solution située dedans et dehors le film soit zéro **[1]**. Néanmois, un état d'équilibre différent, propre des conditions expérimentales ou de service pourrait être atteindre si la pression mécanique excercée sur la solution intérieure (résultant de la résistance au gonflement et à la déformation du film organique) égale la pression osmotique. Cette condition est fonction des propriétés mécaniques et d'adhesion du système employé. En plus, elle pourrait expliquer l'influence de la nature de la couverture sur son comportement global **[2]**. Expériences realisées avec différentes solutions salines ont demontrée que l'augmentation de poids et de volume d'un film polimérique exposé au milieu salin est seulement due à l'absorption de l'eau pur **[3]**.

Généralement, la corrosion d'un acier recouvert par une couche de peinture commence aux points faibles ou dans des surfaces mécaniquement dommagées du recouvrement tandis que le reste de la surface joue le rôle de cathode. Une consequence de cela peut être la délamination cathodique des parties intactes du revêtement. Ce processus conduit à une perte d'adhésion métal/peinture due aux élevées valeurs du pH interfacial provoquées par la réaction de réduction de l'oxygène. Celle-ci est une façon courante de fail en surfaces peintes exposées aux solutions salines type eau de mer.

En plus de l'eau, l'oxygène est indispensable pour la corrosion. Malgré la information expérimentale peu abondante rapportée sur la perméabilité à l'oxygène, on peut démontrer que dans quelques recouvrements étudiés la valeur de ce paramètre est par dessous du seuil ou dedans l'intervalle dans lequel la fourniture de l'oxygène est suffisante pour permettre la corrosion; dans très peu de cas la vitesse de perméation de l'oxygène était plus élevée. La vitesse de la réaction de réduction de l'oxygène dépend de la fourniture de l'eau, de l'oxygène, des ions, des électrons et de la capacité cathodique de la surface métallique.

Les études des processus diffusives à travers des films libres ont démontré que le transport de l'eau ne limite pas la réaction de corrosion, mais qu'il peut le faire le transport de l'oxygène **[4,5]**. Il faut prendre en considération que ces conclusions ont été fondées sur des données obtenues avec films libres, mais ils peuvent être non representatives dans le cas des films attachés au substrat métallique. Dans ce cas les réactions qui ont lieu sur la surface métallique affectent les caractéristiques du revêtement, par exemple, en rendant possible la migration des ions. Avec très peu des exceptions on ne connaît pas la vitesse de réaction de l'oxygène sur des surfaces d'acier peint **[6]**.

L'épaisseur du recouvrement est un autre facteur important. Essais realisés avec films vinyliques et en caoutchouc chlorée, appliqués avec des épaisseurs variables, mais soumis aux mêmes conditions du séchage, ont demontré que le coefficient de perméabilité n'est pas constant. Pour cela, les données de perméabilité obtenues pour les différents films essayés peuvent être seulement confrontées si les essais ont été realisés dans les mêmes conditions et avec des films ayant la même histoire préalable **[4]**.

Il y a des nombreux méthodes électriques pour étudier les propriétés protectrices des recouvrements organiques **[7,8]**. Parmi les essais accélérés de laboratoire qui ont démontré leur utilité pour prédire la vie utile des

recouvrements de différente qualité, on trouve: a) la mesure de la conductivité ionique du film avec courant continu **[9-11]** et b) la mesure de l'impedance avec courant alternatif **[12-15]**.

L'objectif du présent travail a été de quantifier le coefficient de perméabilité (P) à l'oxygène moléculaire de différents systèmes acier naval/film organique/solution de NaCl à 3 %. Dans la technique électrochimique employée le système a été soumis à une polarisation potentiostatique. Le calcul de P a été fait a partir de la mesure de l'évolution du courant de réduction de l'oxygène en fonction du temps d'immersion et de la concentration de l'oxygène dissous.

PARTIE EXPÉRIMENTALE

Des plaques d'acier SAE 1020 (20x8x0,2 cm) ont été utilisées comme substrat métallique. La surface a été nettoyée au jet de sable conformément au Standard Suédois SIS 05 5900/67 ASa 2 1/2. Le profil de rugosité superficielle de l'acier nue a été obtenu avec une équipe Hommel Tester P-3 n-z avec enregistrer. A partir de l'enregistrement (**Fig. 1**) les valeurs des rugosités maximale (Rm), moyenne (Rz) et moyenne arithmétique (Ra) ont été calculées [16]; la valeur de Rz obtenue pour les éprouvettes essayées a été de 25 µm. Après le sablage, les éprovettes ont été degraissées avec du toluène et revêtues avec des peintures commercielles indiquées dans le **Tableau I.**

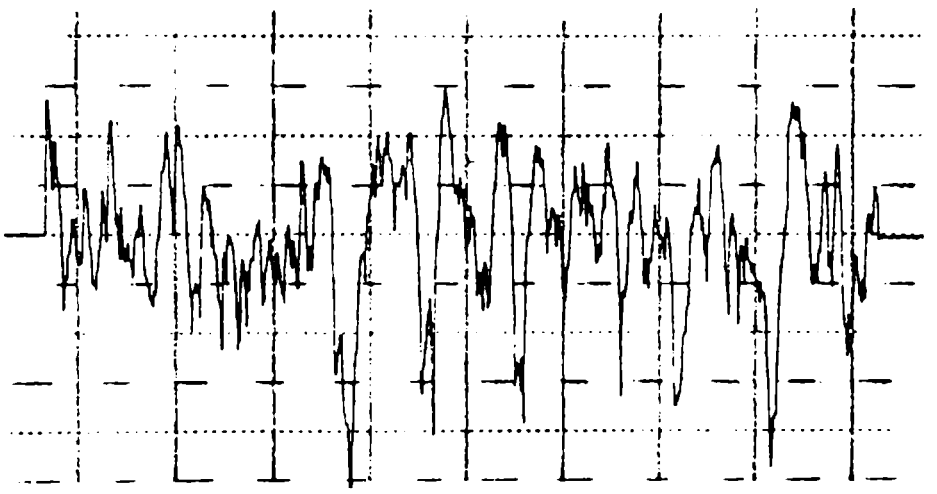

Fig. 1- Profil de rugosité du substrat métallique [16]

Afin d'éviter la contamination par la poussière atmosphèrique, les plaques d'essai ont été gardées dans des dessiccateurs à la température de laboratoire (20°± 2°C). Les épaisseurs des films secs ont été mésurées avec une jauge électromagnetique (Elcometer 300), utilisant comme référence une plaquette sablée et des standards d'épaisseurs connue

TABLEAU I

Composition des formulations essayées

Échantillon	Revêtement Anticorrosive	Solides en poids	Teneur en pigment
1	Alkyde rouge	43,3%	27,0%
2	Vinylique rosé	54,2%	26,0%
3	Caoutchouc chloré rouge	60,8%	34,5%

(Les % sont en rapport du poids total de la peinture)

Dans chaque plaque deux cellules électrochimiques ont été montées, en fixant dans chaque cas un tube cylindrique transparent à l'aide d'un adhésif époxidique, dans le but d'assurer une bonne adhérence au substrat revêtu. La surface géométrique de l'électrode de travail était de 15,9 cm^2. Comme contre-électrode on a utilisé un grand cylindre en graphite et un électrode au calomel saturé (ECS) a été utilisé comme référence. L'électrolyte était une solution de NaCl à 3 % saturée par un gaz de concentration en oxygène connue. Dans chaque cas la concentration d'oxygène dissous a été établie conformement au Standard ASTM D 888-66. Tous les essais ont été effectués à la température de laboratoire (20°± 2°C).

La technique que nous avons employée consiste à utiliser un substrat métallique comme cathode à fin de réduire électrochimiquement la totalité de l'oxygène diffusé à travers le film de peinture.

Si la réduction à la cathode est rapide et totale, la concentration de l'oxygène sur la cathode reste toujours nulle: la diffusion de l'oxygène à travers la membrane, qui dépend de la différence des concentrations des deux côtés de la membrane, tend vers une valeur limite après une période de transition. Le courant de réduction de l'oxygène sur la cathode tend donc vers une limite I_∞ pour laquelle la disparition de l'oxygène par voi électrochimique est exactement compensée par l'apport d'oxygène par diffusion.

La mesure du courant I lorsque l'état stationnaire est atteint, c'est-à-dire lorsque I = f(t) = constante, permet le calcul de la vitesse de diffusion de l'oxygène à travers le revêtement.

RÉSULTATS ET DISCUSSION

Les éprouvettes en acier revêtues ont été polarisées potentiostatiquement à -0,75V(ECS). Au pH de la solution employée, et pour le potentiel appliqué, la réaction de réduction de l'oxygène est celle qui predomine. Cet effet a été vérifié puisque le courant de réduction qui traverse la cathode pour une concentration d'oxygène donnée, est proportionel à cette concentration (**Fig.2**).

Les liants des peintures anticorrosives utilisées ont été: résine alkyde (echantillon 1), résine vinylique (echantillon 2) et caoutchouc chloré (echantillon 3). Dans tous les cas l'acier recouvert a joué de cathode, la réaction cathodique était la réduction d'oxygène et le courant mésuré etait la valeur limite caractéristique du système essayé. Par cette raison, pour chaque type de peinture essayée, dans des films d'épaisseur uniforme, nous avons vérifié que le flux d'oxygène qui traverse le film est inversement proportionnel à l'épaisseur du revêtement. Cela est tout a fait d'accord avec un control par transfert de matière à travers le film.

Comme il a été établi auparavant **[4,5]**, l'apport d'eau est suffisant mais celui de l'oxygène peut limiter le courant.

La **Fig.3** montre l'allure des courbes expérimentales. L'examen de ces courbes montre une période de transition avant que la diffusion de l'oxygène à travers le film n'attaigne un équilibre de régime pendant lequel la vitesse de diffusion de l'oxygène à travers le film de peinture est égale à sa vitesse de réduction sur la cathode. En relevant les valeurs du courant à l'état stationnaire (I_∞) pour un même film, en fonction de la concentration d'oxygène dans le sein de la solution (c_s) nous avons vérifié que le flux d'oxygène qui traverse le film, dans l'état stationnaire, est proportionnel à la concentration c_s, pendant que la concentration de l'oxygène sur le substrat métallique est nulle.

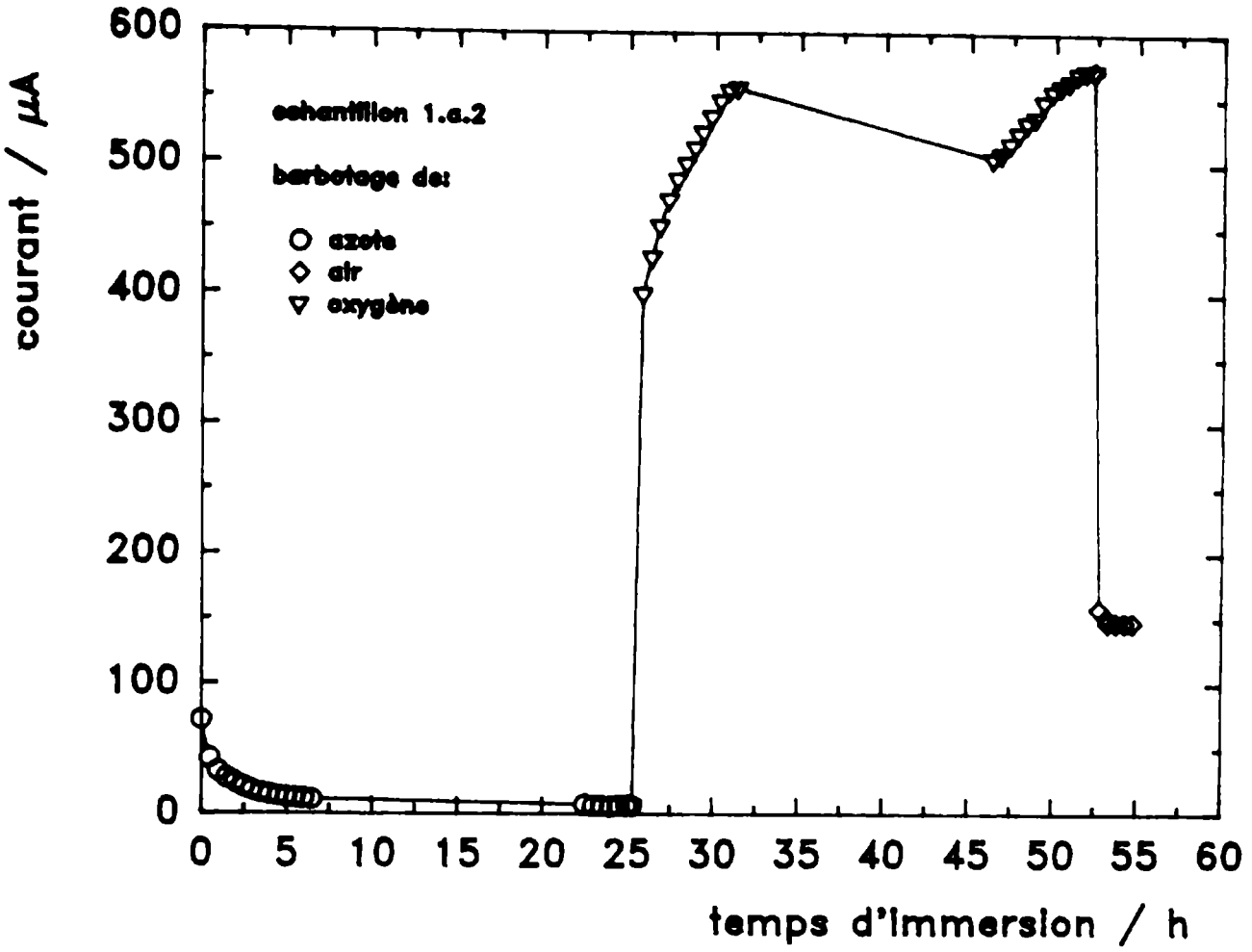

Fig. 2.- Transitoire de courant en fonction de la concentration d'oxygène dissous.

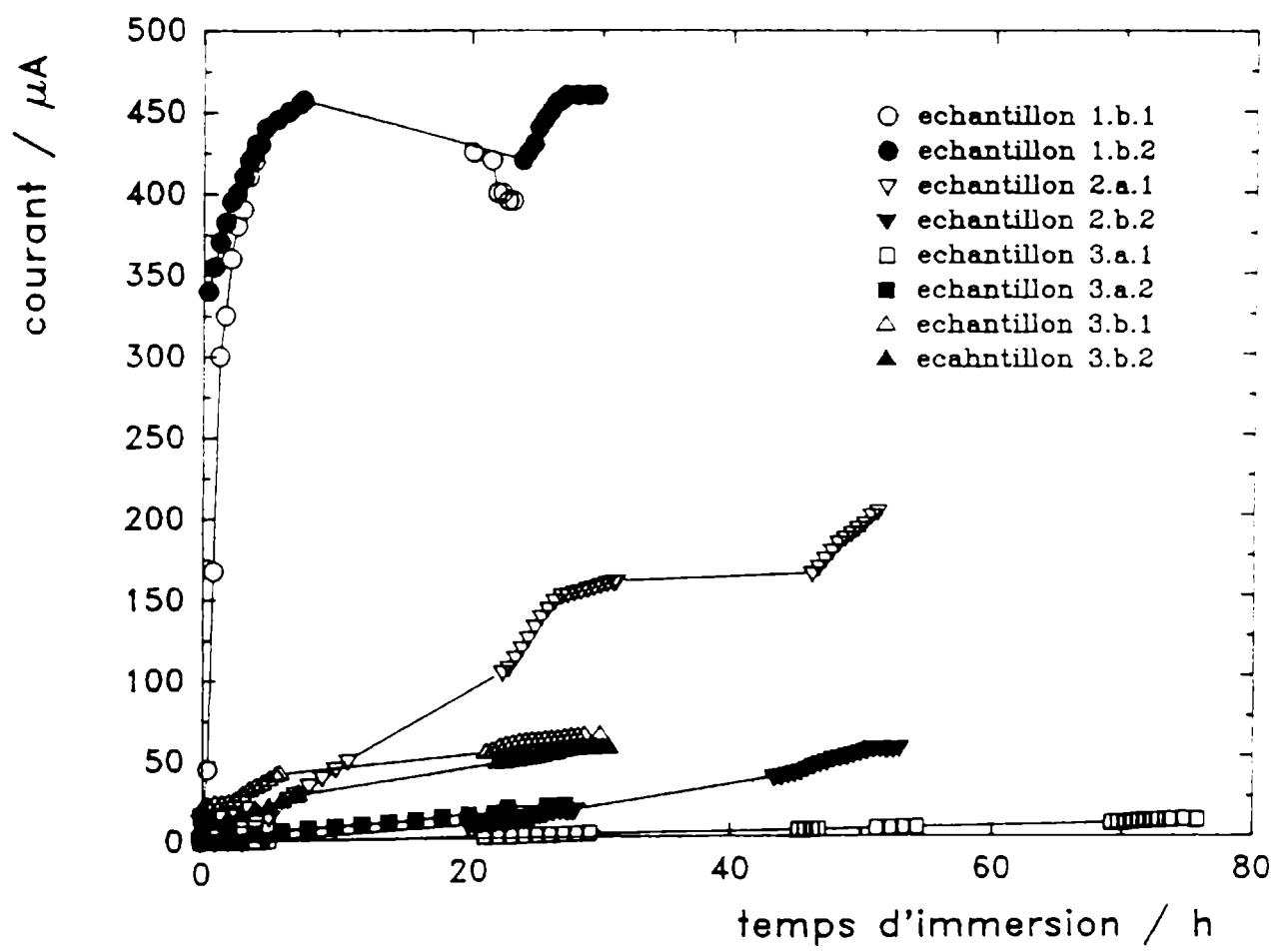

Fig. 3.- Transitoire de courant pour les échantillons essayés dans une solution de NaCl à 3 % barbotée avec de l'oxygène pur.

La première loi de Fick s'applique donc et la perméabitité de ces films peut être exprimée par un coefficient de perméabilité (P) **[17]**. Nous définissons ce coefficient de perméabilité comme le produit du coefficient de diffusion (D) de l'oxygène dans le film et du coefficient de partage (k) de l'oxygène entre le film et le fluide en contact avec lui **[18]**; il s'écrira donc:

$$P = k\ D \tag{1}$$

et sera exprimé en cm^2s^{-1}. Etant donné que la valeur de I_∞ correspond toujours à une concentration zéro sur le substrat métallique, le gradient de concentration dans le film est pratiquement égal a kc/dx soit, si dx = d est l'épaisseur du film

$$\frac{d[O_2]}{dx} = -\frac{k\ c_s}{d} \tag{2}$$

La première loi de Fick s'écrira donc:

$$\vec{N} = -\ D_{O_2}\ \frac{d[O_2]}{dx} = \frac{P\ c_s}{d} \tag{3}$$

où $\vec{N}$ est le flux d'oxygène qui traverse le film.

Attendue que la réduction de l'oxygène se produit à la cathode suivant la réaction

$$O_2 + 2\ H_2O + 4\ e^- \longrightarrow 4\ OH^- \tag{4}$$

lorsque l'équilibre de régime est réalisé, $\vec{N}$ d'après l'équation (3) peut être exprimé par:

$$\vec{N} = \frac{j\infty}{z\ F} = \frac{I\infty}{4\ F\ A} \tag{5}$$

où 4F répresent le nombre de Faradays nécessaires pour la réduction d'une mole d'oxygène à l'électrode revêtue et A la surface de réaction en cm^2. En remplaçant dans l'équation (3)

$$I\infty = \frac{4\ F\ P\ A\ c_s}{d} \tag{6}$$

Donc, le coefficient de perméabilité à l'oxygène peut être déterminé à partir des valeurs mésurées de I_∞, du moment que aucune autre réaction n'épuise l'oxygène dissous en solution.

Dans le **Tableau II** ont été presentées aussi bien les valeurs du coefficient de perméabilité de différentes peintures que les épaisseurs des revêtements employés.

À la fin des essais, les éprouvettes peintes avec l'anticorrosive alkyde ont présentée une attaque géneralisée. Les photos 1 et 2 montrent l'existence de différents produits de corrosion à l'interface acier revêtue/électrolyte. Celles peintes avec l'anticorrosive vinylique ont présentée le cloquage du revêtement. Ce processus était partiellement irréversible pendant le temps du sèchage (photos 3

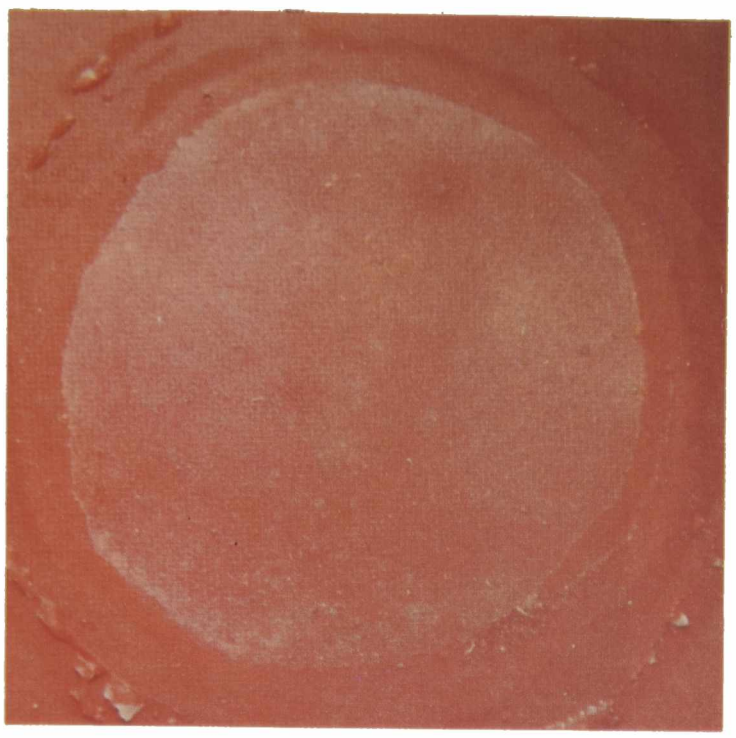

Photo 1: Echantillon 1.a.2

Photo 2: Echantillon 1.b.1

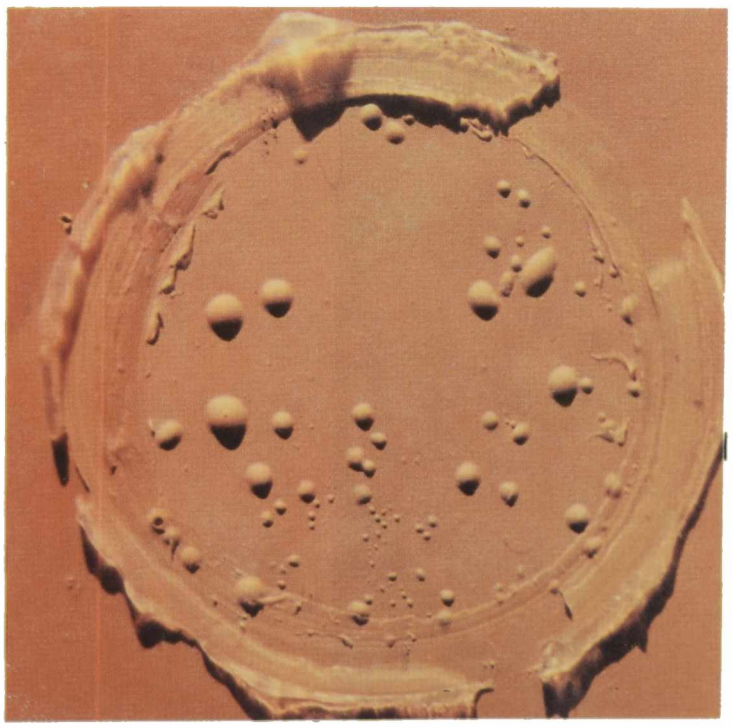

Photo 3: Echantillon 2.a.1

Photo 4: Echantillon 2.b.2

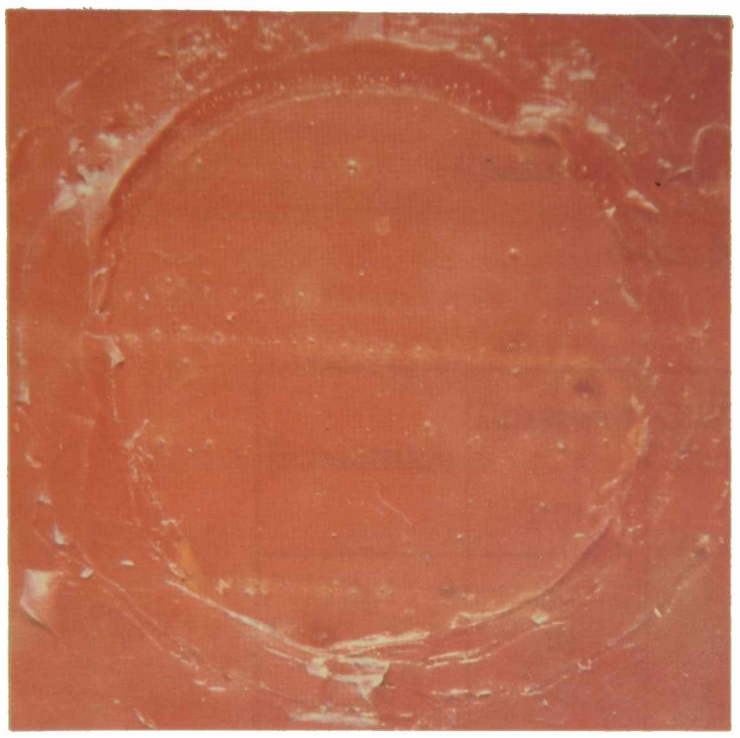

Photo 5: Echantillon .3.b.2

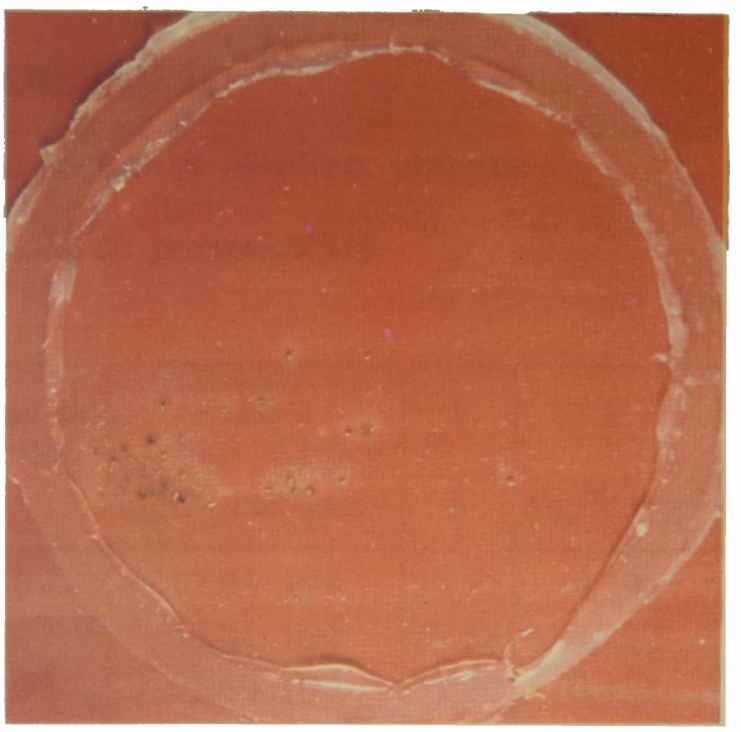

Photo 6: Echantillon 3.b.1

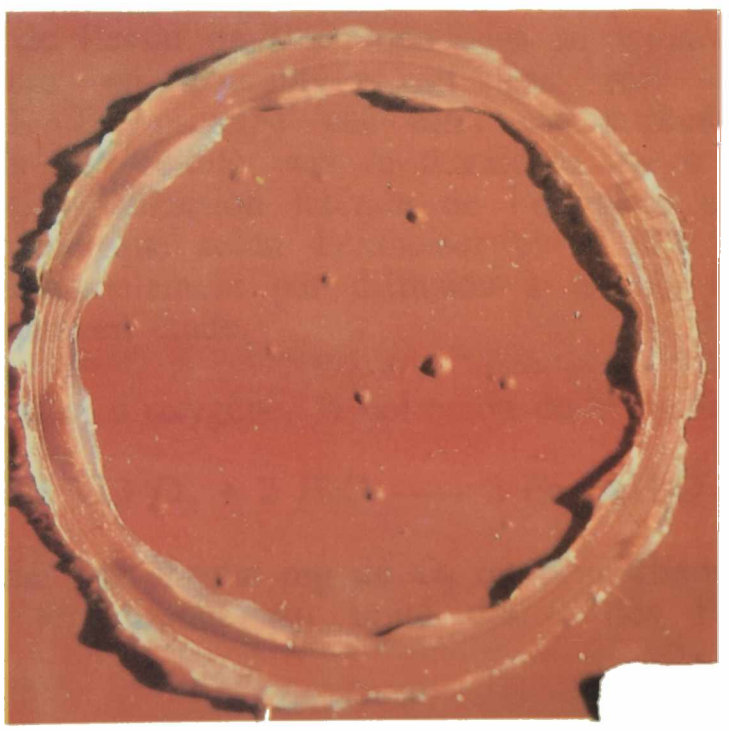

Photo 7: Echantillon 3.a.2

et 4). Les éprouvettes revêtues avec l'anticorrosive à base de caoutchouc chloré ont presentée corrosion qui n'est pas uniforme (photos 5, 6 et 7). Dans ce dernier cas, la piqûre ("pitting") presentée par le substrat métallique est atribuée à l'existence des imperfections ponctuelles caractéristiques des films avec peu d'épaisseur. Dans ces points, la densité de courant est beaucoup plus élevée.

TABLEAU II

Épaisseurs des films sèches et résultats obtenus

dans les essais de perméabilité

Échantillon	Épaisseur μm	Coefficient de Perméabilité cm^2s^{-1}	$\vec{N}$ $mgO_2\ cm^{-2}jour^{-1}$	t h	F $mgFe\ cm^{-2}$
1.b.1	30	$1,85\ 10^{-7}$	$17,63\ 10^{-2}$	23,21	0,396
1.a.2	40	$3,61\ 10^{-7}$	$56,81\ 10^{-3}$	29,58	0,162
2.a.1	60	$1,92\ 10^{-7}$	$91,50\ 10^{-3}$	51,20	0,453
2.b.2	116	$9,23\ 10^{-8}$	$22,75\ 10^{-3}$	52,90	0,116
3.b.2	29	$2,32\ 10^{-8}$	$22,87\ 10^{-3}$	30,70	0,068
3.b.1	32	$2,95\ 10^{-8}$	$26,35\ 10^{-3}$	30,00	0,087
3.a.2	57	$1,72\ 10^{-8}$	$8,62\ 10^{-3}$	27,40	0,023

Dans quelques cas, la diffusion latérale des ions peut augmenter la vitesse de réaction de l'oxygène. Bien que dans le présent travail cette augmentation ne soit pas évidente, les éprouvettes 1 et 3 ne montrent pas le même comportement que les autres. Au début de l'essai on a vu que dans la deuxième cellule mise dans une éprouvette, la réponse en courant n'était pas zéro ($I \neq 0$), **Fig.2**. échantillon 1.b.2, 3.a.2 et 3.b.1. En principe cet effet est atribué à la diffusion latérale de l'électrolyte depuis une cellule vers la deuxième qui a été montée sur la même éprouvette. De même, la diffusion latérale de l'oxygène est aussi possible mais il n'est pas probable parce que selon Leidheiser et al **[7]**, l'oxygène arrive au front de délamination fondamentalement par diffusion à travers le revêtement. Toutes ces questions sont maintenant en étude.

En présence d'eau et d'oxygène, la corrosion du fer a lieu selon:

$$4\ Fe + 3\ O_2 + 2\ H_2O \longrightarrow 2\ Fe_2O_3.H_2O \qquad (7)$$

Par stoechiométrie, par chaque mg de O_2 on peut dissoudre 2,32 mg de Fe; pour cela la quantité de fer dissous par unité d'aire, dès l'instant d'immersion peut être établie par:

$$F\ (mg\ Fe\ cm^{-2}) = \frac{\vec{N}\ (mgO_2\ cm^{-2}jour^{-1})\ t\ (h)\ 2,32\ (mgFe/mgO_2)}{24\ (h\ jour^{-1})} \qquad (8)$$

Les résultats obtenus pour les différents systèmes substrat métallique/peinture anticorrosive/électrolyte, ont était présentés dans le **Tableau II**. Le niveau de protection plus important a été donné par la peinture

anticorrosive à base de caoutchouc chloré, celle qui présente aussi le plus bas coefficient de perméabilité à l'oxygène.

Au même temps d'immersion, t = 30 h, il est posible remarquer que pour arriver au même niveau de protection (dissolution de ≅ 6,8 10^{-4} mgFe cm^{-2}) avec les éprouvettes 3.b.2 et 2.b.2, il faut appliquer un film de l'anticorrosive vinylique d'un épaisseur quatre fois superieur à celui de l'anticorrosive à base de caoutchouc chloré. Par surcroît, on a vérifié que pour un temps d'immersion donné, la puissance protectrice de chacun des anticorrosives essayés augmente d'autant plus que l'épaisseur du film appliqué. En rapport aux données presentées dans le **Tableau II**, on a ordonné les revêtements essayés en fonction de leur efficacité protectrice selon:

caoutchouc chloré > résine vinylique > résine alkyde

CONSIDÉRATIONS FINALES

1) La polarisation des éprouvettes en acier recouvert par peinture et la mesure du flux de courant fournisent information utile et importante en rapport des propriétés de transport de l'oxygène dans les systèmes métal peint/électrolyte essayés.

2) On a constaté que le courant mésuré correspond à la réduction de l'oxygène sur le substrat métallique et que sa valeur limite était caractéristique du revêtement essayé. Cette valeur est réglée par le flux d'oxygène à travers le film.

3) On a constaté, en general, que le taux de protection est directement proportionnel à l'épaisseur du film. Par surcroît, on a pu évaluer que l'efficacité protectrice de différentes peintures anticorrosives suivre l'ordre: caoutchouc chloré > résine vinylique > résine alkyde.

4) Dans le but de comprendre et d'approfondir la connaissance d'un sujet très peu étudié comme celui des procès de transport à travers des films de peinture, on est en train de mettre en marche des recherches qui tendent à déterminer l'influence des facteurs tels comme: composition de l'électrolyte, épaisseur et composition chimique de différents schèmes de peinture, etc..

5) La méthode employée est simple et apporte en plus information quantitative relative au comportement des revêtements en service.

REMERCIEMENTS

Les auteurs veulent exprimer leurs remerciements à la Comisión de Investigaciones Científicas de la Provincia de Buenos Aires (CIC) et au Consejo Nacional de Investigaciones Científicas y Técnicas (CONICET) pour le support financier accordé pour ce travail de recherche.

BIBLIOGRAPHIE

[1] Lowry, H. H., Kohman, C. T.- **J. Phys. Chem.**, **31**, 23 (1927).

[2] Guruviah, S.- **J. Oil Col. Chem. Assoc.**, **53**, 669 (1970).

[3] Kittelberger, W. W., Elm, A. C.- **Ind. Eng. Chem., 38**, 7 (1946).

[4] Haagen, H., Funke, W.- **J. Oil Col. Chem. Assoc., 58**, 359 (1975).

[5] Corti, H., Fernández Prini, R., Gomez D.- **Prog. Org. Coatings, 10**, 5 (1982).

[6] Husa, E.M., Bardal, E.- **The Use of Electrochemical Techniques to Evaluate the Performance of Epoxy Paints**, UK National Corrosion Conference, London (1982).

[7] Leidheiser, H. Jr.- **Prog. Org. Coatings, 7**, 79 (1979).

[8] Sato, Y.- **Prog. Org. Coatings, 9**, 85 (1981).

[9] Kinsella, E. M., Mayne, J. E. O.- **Brit. Polym. J., 1**, 173 (1969).

[10] Bacon, R. C., Smith, J. J., Rugg, F. M.- **Ind. Eng. Chem., 40**, 161 (1948).

[11] Mayne, J. E. O., Mills, D. J.- **J. Oil Col. Chem. Assoc., 58**, 155 (1975).

[12] Leidheiser, H. Jr., Kendig, M. W.- **Corrosion, 32**, 69 (1976).

[13] Touhsaent, R. E., Leidheiser, H. Jr.- **Corrosion, 28**, 435 (1972).

[14] Brasher, D. M., Kingsbury, A. H.- **J. Appl. Chem., 4**, 62 (1954).

[15] Holtzman, K. A.- **J. Paint Technol., 43**(554), 47 (1971).

[16] Slutzky, O., Caprari, J. J., Pessi, P. L., Meda, J. F.- **CIDEPINT-Anales**, 1 (1987).

[17] Treagear, R. T.- **J.Invest. Dermato, 4**, 16 (1966).

[18] Crank, J., Park, G. S.- **Diffusion in Polymers**. Academic Press. London (1966)

Note: Ce travail a été adressé pour son publication dans **Double Liaison**. *Physique et Chimie des peintures et adhesifs*

STUDY OF THE HETEROGENEOUS REACTION BETWEEN STEEL AND ZINC PHOSPHATE

ESTUDIO DE LA REACCION HETEROGENEA ENTRE ACERO Y FOSFATO DE CINC

R. Romagnoli[1] and V. F. Vetere[2]

SUMMARY

Despite of their unhealthy and environmental pollutant characteristics, primers containing anticorrosive pigments based on lead or hexavalent chromium are commonly used in practice. Thus, other formulations pigmented with less dangerous compounds such as zinc phosphate, ferrite or barrier type particles of lamellar structure are also employed.

The protective effect due to the zinc phosphate includes the phosphatizing of the metal substrate as well as the development of complex compounds in reacting with the paint binder. Such a behaviour improves the coating/metal adhesion. However, very different experimental results were obtained in using this pigment.

The object of this research was to study the anticorrosive mechanism of zinc phosphate through electrochemical tests (corrosion potential vs time curves, polarization curves and corrosion rate measurements) performed in pigment suspensions. SEM analysis of steel surfaces bare or covered with zinc phosphate pigmented anticorrosive paint, exposed to zinc phosphate suspensions was also carried out.

All the results showed that the zinc phosphate does not passivate the metal substrate, but it reacts with iron creating a protective oxide layer, which grows with a somewhat crystalline structure.

Keywords: *zinc phosphate, electrochemical tests, surface analysis, cathodic inhibitor, protective oxide layer.*

INTRODUCTION

Formulation and usage of organic coatings to protect metals against corrosion are of great importance. The most commonly employed anticorrosive pigments contain lead or hexavalent chromium compounds, which are particularly hazardous and contribute to the environmental pollution.

Due to the toxicity of conventional pigments and to legal regulations imposed on their employment, present world trends are mainly focused on their substitution by different phosphates **[1-3]**. Thus, the pigments manufacturers have accomplished extensive research and development programms about non toxic and corrosion

---

[1] Miembro de la Carrera del Investigador del CONICET

[2] Profesional de Apoyo del CONICET y Planta Permanente CIC

inhibitive compounds. The replacement of zinc chromate by zinc phosphate (ZP), ferrites and/or barrier pigments with lamellar structure in environmentally compatible anticorrosive priming compositions is often recommended.

According to Meyer **[1, 2]**, the protective properties of ZP implies both the phosphatizing of the metal substrate, and its reaction with the paint binder giving complex substances. These substances can react with the corrosion products yielding a layer strongly adhered to the substrate.

The phosphatizing of the metal substrate rests on the fact that humidity penetrating through the pores of the coating causes a slight solubilization of phosphate ions; in turn, these ions affect the anodic corrosion reaction through the formation of a protective layer **[3-8]**, which grows until reaching a thickness enough to provide apparent passivity **[5]**. The low solubility of ZP and its extremely coarse crystalline structure could affect the protective layer homogeneity **[3, 9-11]**, whose composition has not been adequately defined yet, although either γ-Fe_2O_3 **[6-8]** or zinc and iron phosphates are possibly formed **[12, 5]**. Several authors **[13, 14]** have suggested that the protection mechanism involved the polarization of cathodic areas due to precipitation of sparingly soluble basic salts, which adhered to the surface.

Zinc phosphate is widely applied as anticorrosive pigment and can be used with all types of binders **[1, 3, 15, 16]**. However, very different experimental results were obtained when it was used **[16-20]**. ZP performs well in industrial atmospheres because it activates in acid media **[21]**. Accelerated tests gave bad results, but outdoor long exposure tests were encouraging **[16-18, 21, 22]**. For moderate outdoor exposure tests, modern specifications **[23]** recommend about 20 % by volume as the maximum content of ZP (standard micronization degree type) in the dry film. When the shape and the particle size distributions are optimized, the ZP content can be lowered to 10 % and the painted panel is able to withstand more severe exposures.

The anticorrosive performance of the ZP pigment may be improved by means of a correct surface preparation **[24]**, modifying the particle shape **[25]**, employing adhesion promoting substances **[26]**, wetting and dispersing agents **[27]** or in mixtures containing chromates/organic chromates **[28]**, borates **[17, 29]**, molybdates **[30]** and zinc nitrophtalate **[17]**.

Some researchers **[10, 11, 28, 31]** claimed that the protective characteristics of zinc chromate are not achieved by ZP. In order to avoid such difficulty, the ZP is being replaced by new phosphate based pigments **[10, 11, 32]**. The most important changes are concerned with one of the following cases:

a) adequate particle size distribution
b) addition of aluminium, molybdenum, manganese, etc.
c) addition of basic groups.
e) an organic pretreatment.

Accelerated tests have shown that the protection obtained with ZP is much lesser than with other phosphates. Modified zinc phosphates are corrosion inhibitors as effective as a mixture of ZP plus chromates **[3, 10, 22, 24, 33]**. Besides modified zinc phosphates, other phosphates were proposed to replace current toxic anticorrosive pigments **[5, 12, 34-48]**. For instance, with a phosphated polyepoxide paint **[49]**, the steel surface conversion and the organic film barrier effect were satisfactorily combined in a single corrosion resistance coating. Phosphated polymers and related treatments were successfully employed in both zinc and zinc alloy coatings **[50]**.

The aim of this work was to study the ZP anticorrosive mechanism. The first

stage involved electrochemical tests such as the measurement of the steel corrosion potential as a function of time, the study of its voltammetric response and the corrosion rate determination in ZP suspensions, to evaluate its anticorrosive properties. These tests were done according to procedures described elsewhere **[51-53]**.

The second stage included the study of the protective layer formed on the steel plates during their exposure to pigment suspensions. Finally, the reactions ocurring when a painted specimen was allowed to corrode in a normally aerated aqueous solution, were also analyzed.

EXPERIMENTAL

All the experiments were carried out by triplicate and employed zinc phosphate prepared in the laboratory, following a procedure described in the literature **[54]**. X-ray diffraction results indicated that, as previously reported **[55]**, the product obtained was $Zn_3(PO_4)_2.4\ H_2O$ particles having a lamellar structure. Their morphology was determined by scanning electron microscopy (SEM), and the particle size distribution by means of a Sedigraph-5000 D MICROMERITICS analyzer. This last characteristics was compared with that of the zinc tetroxychromate pigment **(Fig 1)**.

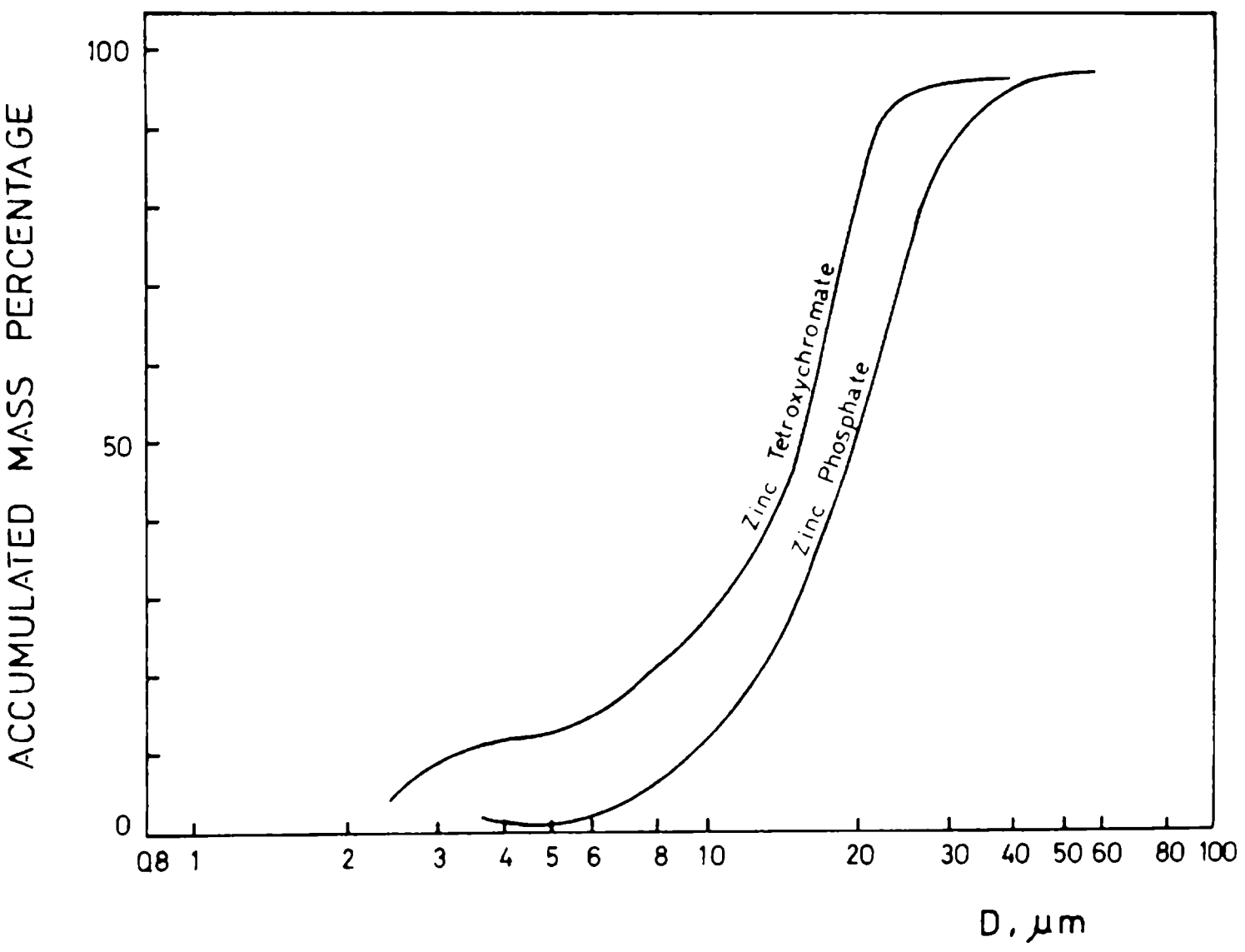

Fig. 1.- Percentage of accumulated mass vs. logarithm of the equivalent spherical particle diameter (D) for zinc phosphate and zinc tetroxychromate.

Electrochemical tests in pigment suspensions

The corrosion potential of steel samples, either in a 0.5 M sodium

perchlorate solution (blank) or in ZP suspensions in the same electrolyte solution, were measured with an ORION model 701A voltmeter as a function of the immersion time. Steel (AISI 1010) samples, 1.5 cm in diameter, and a Ag/AgCl were used as working and reference electrodes, respectively. The pigment suspension was stirred at 1800 rpm with a synchronous rotator in order to avoid the pigment settlement. The results are plotted in **Fig. 2.**

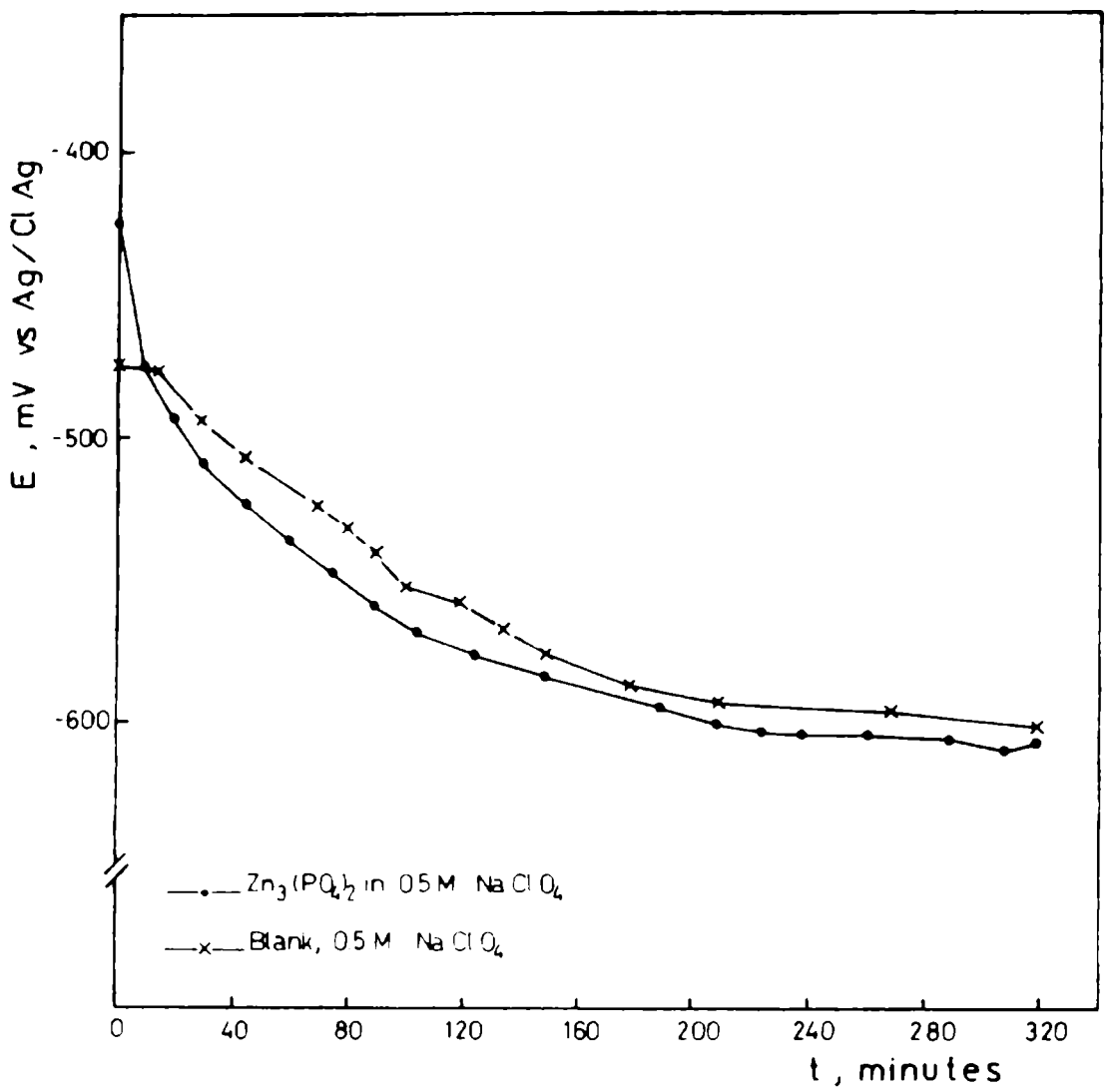

Fig. 2.- Iron electrode potential (E) as a function of time (t).

Polarization curves for steel in both, a 0.5 M sodium perchlorate solutions and ZP suspensions were obtained. The working electrode was a steel disc (AISI 1010), 0.5 cm in diameter. Both a Ag/AgCl and a platinum disc (0.5 cm in diameter) were used as reference and counterelectrode, respectively. The electrochemical cell was similar to that described elsewhere **[56]. Figs. 3 to 6** illustrates the anodic and cathodic voltammograms obtained at different exposure times (0, 2 and 4 hours); every polarization curve was started close to the corrosion potential with a scan rate of 2 mVs^{-1}.

Reaction products accumulated on the working electrode during anodic sweeps were identified dissolving them with a cathodic current density of 0.6 $mAcm^{-2}$. This was achieved employing graphite anodes and steel plates (AISI 1010) of 2.5x2.5x0.1 cm previously polarized at -100 mV/(Ag/AgCl), in a 10% H_2SO_4 solution. The Zn^{2+}, PO_4^{3-} and Fe^{3+} ions were determined by both analytical **[57]** and atomic absorption methods **(Table I)**.

Previous to each test, the steel electrodes were mechanically polished with a 120 emery paper and degreased with alkaline substances such as calcium hydroxide.

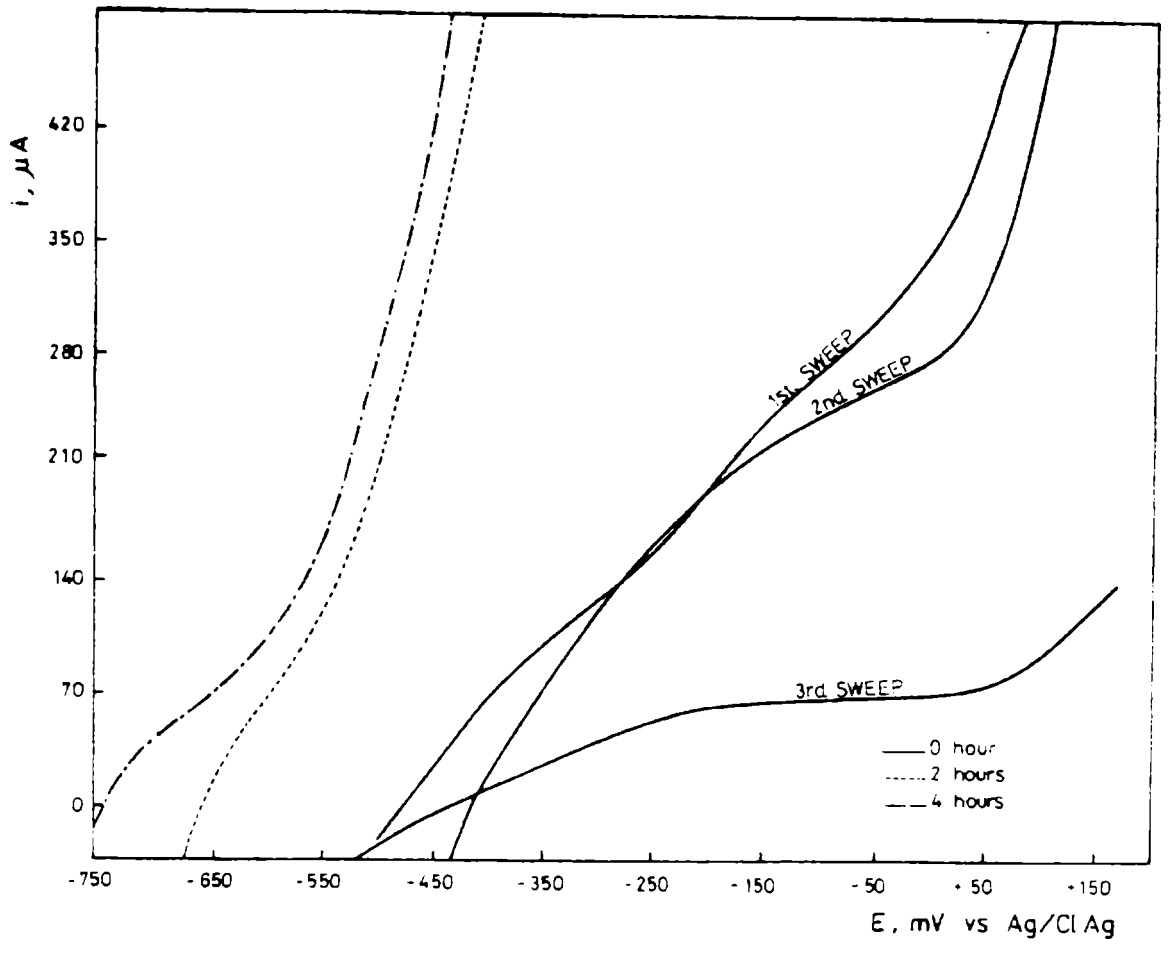

Fig. 3.- Anodic polarization curve for iron exposed to a ZP suspension. Scan rate: 2 mVs^{-1}.

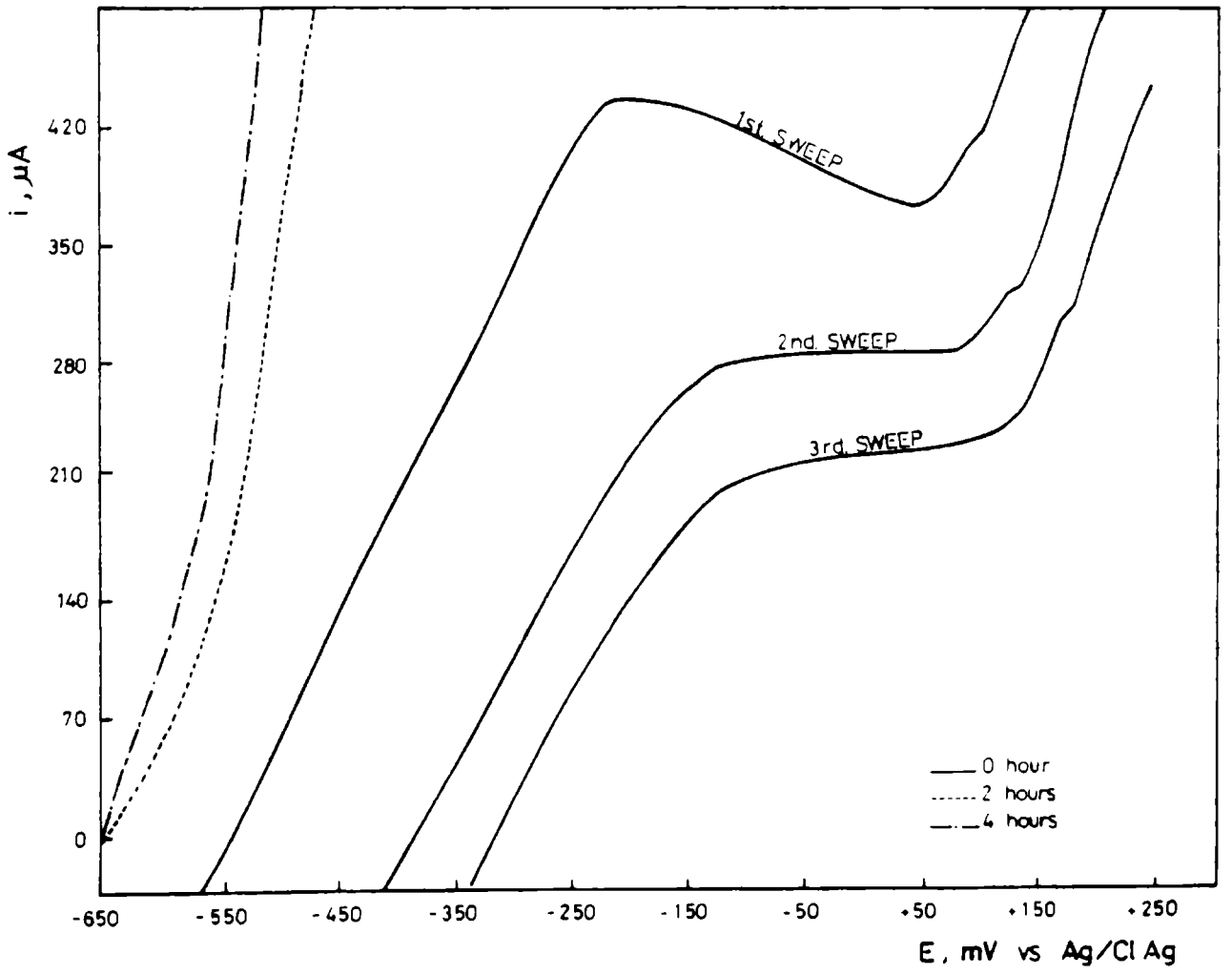

Fig. 4.- Anodic polarization curve for iron exposed to a 0.5 M sodium perchlorate solution. Scan rate: 2 mVs^{-1}.

The steel corrosion rate was determined through the polarization resistance method **[58-61]** in solutions containing ZP. The results were confirmed by calorimetrical analysis of dissolved iron **[62]**.

Composition of the protective layer

In order to analyze the composition of the protective layer close to the substrate, the steel plates were rotated for no more than 96 hours in the pigment suspensions. The exposed area was 23 cm^2. At the end of the tests, all plates were wiped off to remove the poor adherent corrosion products. The adherent ones were dissolved in a stirred 10 % H_2SO_4 solution protecting cathodically the base metal as it was indicated in the above paragraph. Zinc, iron and phosphate content were determined in the acid extract; zinc was determined by atomic absorption and iron and phosphate by colorimetric procedures **[63, 64]**.

Figs. 7 and **8** show the state of the treated steel surface studied by SEM. Steel (AISI 1010) panels exposed to a more soluble anticorrosive pigment, calcium acid phosphate, were also observed **(Fig. 9)**. **Fig. 10** presents a surface defect where a galvanic action has taken place. The amount of zinc and phosphorous deposited on the steel surface was determined by EDAX.

Corrosion studies on painted specimens

An anticorrosive paint containing 60 % of ZP by weight, 10 % plasticized chlorinated rubber as binder and 30 % toluene, was prepared without inert pigments to avoid interferences. A sandblasted steel substrate (AISI 1010) was painted by brushing until reaching 30 μm of dry film thickness. Due to the paint composition a porous coating was obtained. The coated panel was immersed for 24 hours in a 0.5 M sodium perchlorate solution. Then, the binder was removed with trichloroethylene and non adherent products wipped off. The surface was studied by SEM **(Figs.11 and 12)** and the products composition determined by EDAX.

RESULTS AND DISCUSSION

The size distribution of ZP particles is similar to that of zinc tetroxychromate, **Fig. 1.** Although the ZP particles are coarser than zinc tetroxychromate ones, their differences are not very important as several researchers suggested **[3, 10, 11]**. It is thought by the authors that the ZP failure as an effective anticorrosive pigment must be mainly attributed to other factors.

Electrochemical tests employing pigment suspensions

Corrosion potential (E) vs. time (t) curves, **Fig. 2**, clearly show that steel behaves similarly either in sodium perchlorate solution or in ZP suspension in the same electrolyte. It was not observed a rise towards more positive values as it could be expected for an inhibitive pigment **[65]**.

Although potential measurements did not reveal passivity, the growing of a blueish film on the metal surface was detected. In the laboratory atmosphere, this film prevented steel from rusting for 1 month; however, small oxide spots appeared on the metal surface after this period. The variation coefficient for these measurements was lesser than 2.0 %.

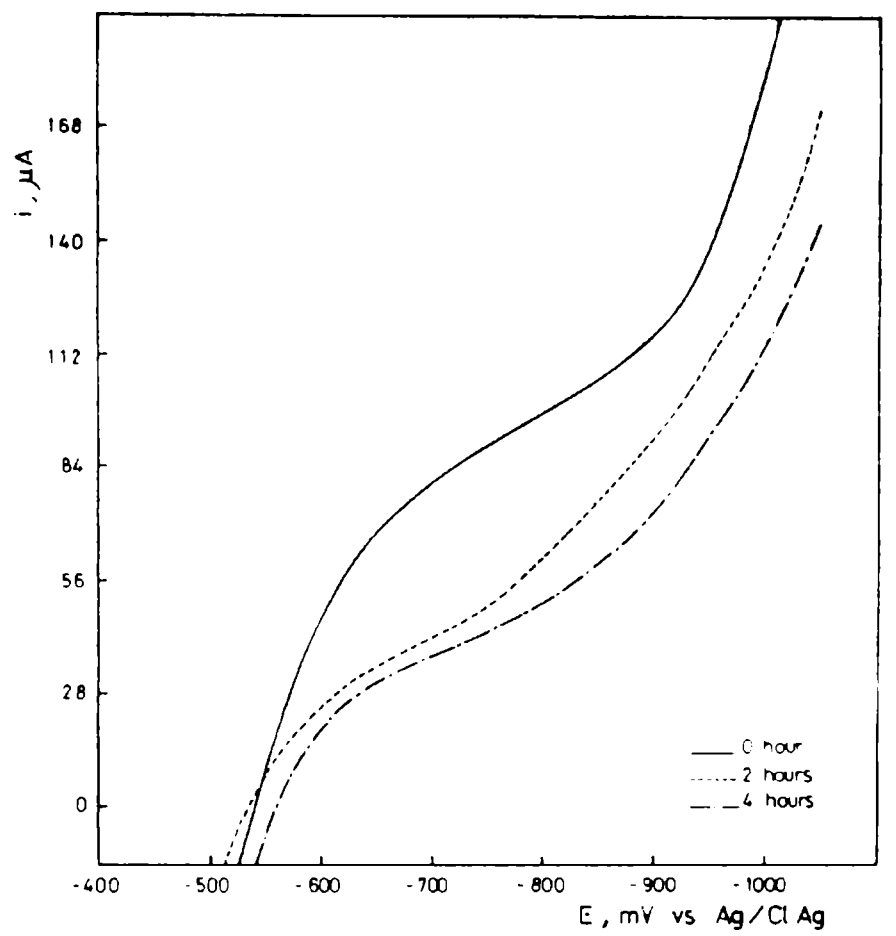

Fig. 5.- Cathodic polarization curve for iron exposed to a ZP suspension. Scan rate: 2 mVs^{-1}.

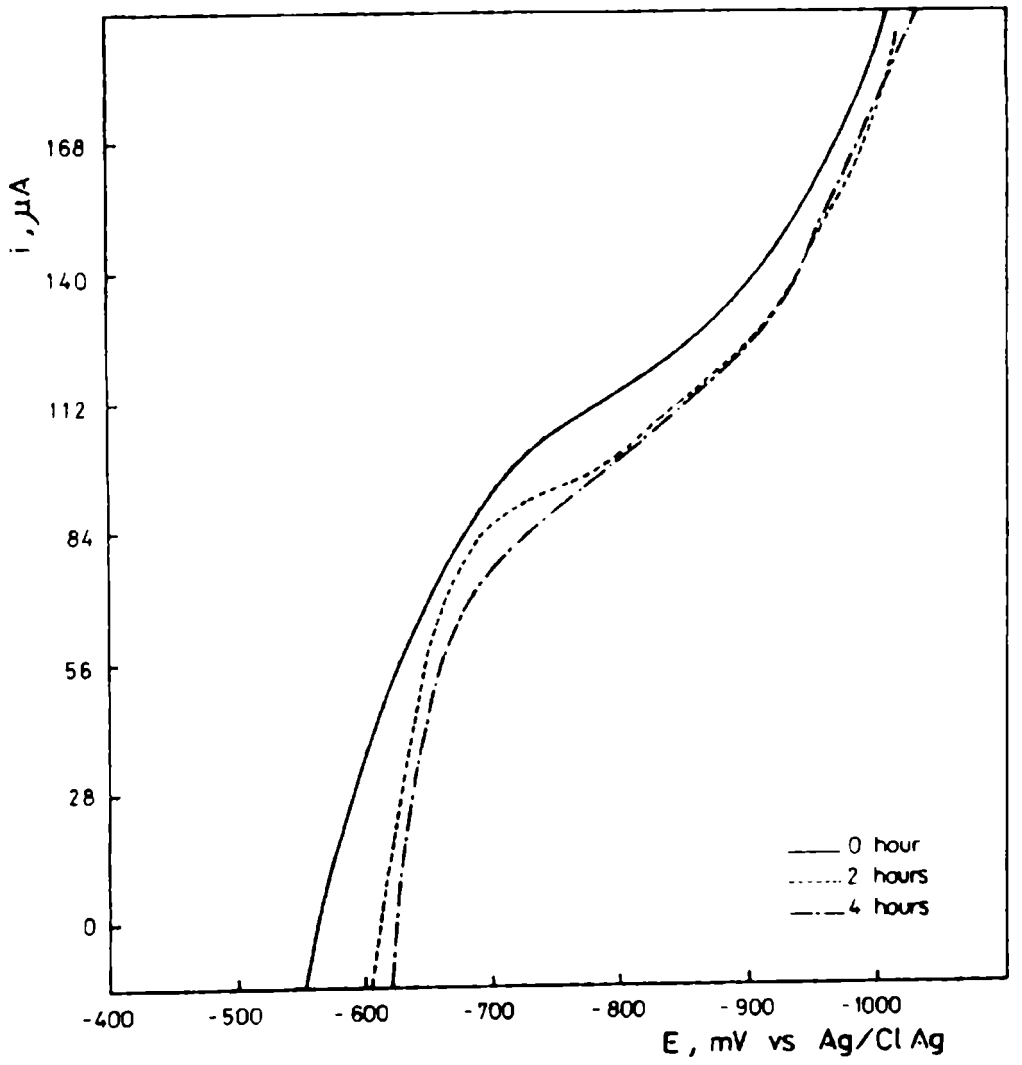

Fig. 6.- Cathodic polarization curve for iron exposed to a 0.5 M sodium perchlorate solution. Scan rate: 2 mVs^{-1}.

TABLE I

Composition of the anodic film formed on a steel substrate/zinc phosphate suspension system

Applied potential (mV)/(Ag/AgCl)	Exposure time (s)	Iron	Zinc ($mgcm^{-2}$)	Phosphate
-100	650	1.58	0.01	0.17

TABLE II

Composition of the corrosion film formed in a steel substrate/zinc phosphate suspension system

Exposure time (h)	Iron	Zinc ($mgcm^{-2}$)	Phosphate
48	0.058	0.075	0.010
72	0.056	0.094	0.017
96	0.056	0.101	0.021

The **anodic polarization curves** for a steel electrode in ZP suspension, **Fig. 3**, exhibited lower currents than the voltammogram in the sodium perchlorate solution **(Fig. 4)**, although passivity was not observed. As in both cases the current decreased with the successive sweeps, it may be assumed that a film with certain protective properties was being formed. However, after four hours exposure, the anodic curve for the ZP suspension appeared at more negative potentials due to the surface activation. Besides, the film did not protect the surface and the non-adherent ferric phosphate passed into the solution. The more important products staying on the steel electrode surface were iron oxides, but phosphate and zinc have also been found **(Table 1)**.

The analysis of cathodic polarization curves for steel electrodes in ZP suspensions showed that the corrosion products plus the solids formed by cathodic reactions, caused a decrease of the oxygen reduction current after an exposure of four hours **(Fig. 5)**. This effect was not very important when using the sodium perchlorate solution **(Fig. 6)**. Therefore, it must be concluded that ZP is also a cathodic inhibitor.

After addition of ZP to the sodium perchlorate solution, the steel corrosion rate diminished from 1.50 to 0.70 $mgFe.cm^{-2}day^{-1}$, indicating that a certain protection was achieved. In ZP suspensions, the corrosion rate was still high (28 $\mu A.cm^{-2}$ and its value decreased as the oxygen limiting current did.

Corrosion studies employing pigment suspensions. Composition of the protective layer

SEM revealed that steel surfaces treated with ZP showed the presence of a light appearing material located on certain zones, having the rest a uniform aspect **(Fig. 7)**. Apart from the light appearing material, the surface composition obtained by EDAX was almost 100 % Fe and small amounts of zinc. This white film (averageing 14.0 % Zn and 0.40 % P) was mainly distributed around the metal surface defects **(Fig. 8)**. The appearence of zinc oxide agrees with results obtained by atomic absorption **(Table II)**. It could be responsible for the polarization of cathodic areas and, therefore, for the corrosion rate decrease ocurring when ZP is used.

A cross-section of the test panel displayed a thin, non-continuous (not more than 2 μm thickness), compact and adherent film of iron oxides accompanied by little amounts of zinc oxide that appear surrounding the surface heterogeneities **(Fig. 9)**. The film became thicker when a more soluble anticorrosive pigment such as calcium acid phosphate **[56]**, was employed **(Fig. 10)**.

From these results it may be concluded that the protective layer on the steel substrate would not be ferric phosphate **[5]** but an iron oxyhydroxides one, which is in agreement with results obtained by electrochemical impedance spectroscopy **[8]**.

The nature of the adherent oxide film formed on the steel surface was determined by Mössbauer spectroscopy. The isomer shift relative to iron, due to the film produced on the corroded steel plates exposed to ZP suspensions, corresponds to that of α-Fe_2O_3 and is equal to 0.39 ± 0.02 mms^{-1} **[67]**. On the other hand, chemical analysis of this film showed that it contained relatively high and non-stoichiometric amounts of zinc and iron but a lower one of phosphate **(Table II)**, although this last increased with the exposure time. This could be due to ferric phosphate trapped in the pores of the oxide layer. Such results agree with those obtained by EDAX.

Corrosion studies on painted specimens

SEM analysis of the painted surface, performed once the binder and loose products were removed, showed that the surface was covered with an iron oxide film of a rather compact structure, and sometimes plates, whose average composition was 50 % Fe, 48 % Zn and 2.0 % P **(Figs. 11 and 12)**. Plates were detected when the steel was covered with a paint film containing ZP.

From this study it is concluded that the protection of a steel substrate is also due to the formation of an oxide layer which grows with a rather crystalline structure although seemed to be not as expansive as the iron oxides. In absence of ZP, the iron oxides grew with a globular morphology given an uncompacted expansive layer **(Fig. 13)**. These results agree with those obtained by Pryor **[7]** with soluble phosphates.

According to the previous discussion, the following reactions are proposed in order to explain the heterogeneous interaction between steel and ZP:

Anodic reaction: $Fe^0 \Leftrightarrow Fe^{2+} + 2\ e^-$

↓ Atmospheric oxidation

$2\ Fe^{3+} + Zn_3(PO_4)_2 \Leftrightarrow 3\ Zn^{2+} + 2\ FePO_4$ (non-adherent solid passes into solution)

↙

α-Fe_2O_3 (adherent film on the anode)

↓

$Zn(OH)_2$ (adherent film on the cathode)

↑

Cathodic reaction: $O_2 + 2\ H_2O + 4\ e^- \Leftrightarrow 4\ OH^-$

CONCLUSIONS

1. The **steel substrate is not passivated by ZP but a protective oxide layer** with a low phosphate content is built. Ferric phosphate formed by the corrosion process is not adherent, although some ferric phosphate could be trapped in pores of the film.

2. The **thickness** of the compact oxide layer depended on the phosphate solubility.

3. As **ZP did not passivate the steel substrate**, its corrosion rate remained high.

4. As the phosphate anion is consumed during the corrosion reactions, **the useful life of the anticorrosive film would depend on both the oxygen flux through it and its phosphate content.**

5. Zinc oxide formed on cathodic areas **diminishes the oxygen reduction current.**

6. The foregoing arguments explain by which **ZP is recommended only for moderate exposures [23].**

7. As a general rule, **results obtained in accelerated tests were pretty bad [16, 18, 21, 22, 55, 66].** Taking into account the small ZP solubility, the effects of aggressive agents on the metal substrate largely exceeds the anticorrosive action of both, the phosphate anion and the thick, non-adherent iron oxides layer.

8. ZP performs well in industrial environments since in this case the phosphates solubility increases as the pH decreases.

ACKNOWLEDGEMENTS

The authors are grateful to the Comisión de Investigaciones Científicas de la Provincia de Buenos Aires (CIC) and the Consejo Nacional de Investigaciones Científicas y Técnicas (CONICET) for the sponsorship of this research. The authors also thank to Mr. R. R. Iasi for the atomic absorption measurements.

REFERENCES

[1] Meyer G.- **Farbe + Lack, 69** (7); 528-532 (1963).

[2] Meyer G.- **Farbe + Lack, 71** (2); 113-118 (1965).

[3] Gerhard A., Bittner A., Gawol M.- **European Supplement to Polymer Paint Colour Journal**; 62-68 (1981).

[4] Ruf J.- **Chimia, 27**; 496 (1973).

[5] Dean S.W.(Jr.), Derby R., Von Dem Bussche G. T.- **Material Performance, 20** (12); 47-51 (1981).

[6] Leidheiser H. (Jr.).- **J. Coat. Tech., 53** (678); 29-39 (1981).

[7] Pryor M. J., Cohen M.- **J. Electrochem. Soc., 100**; 203 (1953).

[8] Kozlowski W., Flis J.- **Corr. Sci., 32** (8); 861-875 (1991).

[9] Burkill J. A., Mayne J. E. O.- **J. Oil Colour Chem. Assoc., 71** (9); 273-285 (1988).

[10] Gerhard A., Bittner A.- **J. Coat. Tech., 58** (740); 59-65 (1986).

[11] Kresse P.- **Farbe + Lack, 80** (2); 85-95 (1977).

[12] Robu B. C., Orban N.,Varga G.- **Polymer Paint Col. J., 177** (4197); 566 and 569 (1987).

[13] Clay M. F., Cox J. H.- **J. Oil Colour Chem. Assoc., 56**; 13 (1973).

[14] Szklarska-Smialowska Z., Mankowsky J.- **Br. Corros. J., 4** (9); 271-275 (1969).

[15] Pfizer Pigments, Inc.- **Zinc Phosphate. Technical Specification** (1988).

[16] Barraclough J., Harrison J. B.- **J. Oil Col. Chem. Assoc., 48** (4); 341-355 (1965).

[17] Pietsch S.- **Plaste Kautschuk, 36** (7); 246 (1989).

[18] Fragata F. de L., Dopico J.- **J. Oil Col. Chem. Assoc., 74** (3); 82-97 (1991).

[19] Mishra U. S., Shukla M. C.- **Paint & Ink Internat., 5** (3); 23-26 (1992).

[20] Bittner A.- **J. Coat.Tech., 61** (777); 111-118 (1989).

[21] Hare C. H.- **J. Protect. Coat. & Linings, 7** (10); 61-67 (1990).

[22] Williams-Wynn D. E. A.- **J. Oil Colour Chem. Assoc., 60**; 263-267 (1977).

[23] Colores Hispania S. A.- **Actirox-Hispafos. Anticorrosive pigments. Technical Specifications.**

[24] Bittner A.- **J. Oil Colour Chem. Assoc., 71**; 97-102 (1988).

[25] Aubareda J., Leblanc O., Martorell C.- **Spanish Patent 8.702.407**.

[26] Bose S. K.- **Paintindia, 41** (2); 25-26 (1991).

[27] Hajas J.- **Europ. Coat. J., 3**; 116-127 (1993).

[28] Kukla J.,Tyrka E., Polen S.- **Hydrokorr-Organokorr '86 Seminar**, 42-51 (1986).

[29] Waardal O. (Jr.).- **Polym. Paint. Col. J., 182** (4302); 154-156 (1992).

[30] Garnaud M. H. L.- **Polym. Paint. Col. J., 174**; 268-270 (1984).

[31] Depireux J., Piens M.- **18th FATIPEC Congress, Vol. 3**; 183-201 (1987).

[32] Roland W. A., Gottwald K. H.- **Metalloberflaeche, 42** (6); 301-305 (1988).

[33] Chromy L., Kaminska E.- **Prog. Org. Coat. 18** (4); 319-324 (1990).

[34] Torriano G., Papo A.- **15th FATIPEC Congress, Vol. 3**; 223-239 (1980).

[35] Mazan P., Trojan M., Brandova D., Solc Z.- **Polym. Paint Color J., 180** (4270); 605 (1990).

[36] Gorecki G.- **J. Sci. Eng. Corros., 48** (7); 613-616 (1992).

[37] Takahashi M.- **Polym. Paint Colour J., 177** (4197); 554-556 (1987).

[38] Tang S. Q.- **Paint & Coatings Ind., 4**; 12-15 (1989).

[39] Tayca Corp.- **Japanese Unexamined Patent 03/146567**, 1991.

[40] Teikoku Kako, Co., **European Patent Application 389653**.

[41] Titov V. P., Pavlov A. V., Korchagin V. I., Sushko V., Yu. M. Ivanov, Yu. M.- **U.S.S.R. SU 1, 353, 788** (Cl. C09 c1/36, 23 M)1987, Appl 3, 980, 330. 26 Nov. 1985.

[42] Rozenfeld I. L., Zolotova S. A., Rubinshtejn F. I., Mamontova L. M.- **Lakokras Mater. Ikh. Primen., 1**; 27 (1975).

[43] Shtern M. A., Danjushevskaja N. E., Alelujeva O. V.- **Lakokras Mater. Ikh. Primen, 1**; 32 (1964).

[44] Austin M. J., Beland M.- **Polym. Paint Col. J., 181** (4280), 168-171 (1991).

[45] Beland M.- **Am. Paint J., 76** (15), 43-50 (1991).

[46] Austin M. J.- **Proc. PRA Second Asia-Pacific Conf. "Advances in Coatings, Inks and Adhesives Technology"**, Paper 15, Singapore (1992).

[47] Nippon Chemical Industry Co., **Japanese Patent 90/000384, Jap. Pat. Abs. 90** (2), Gp M, 3.

[48] Zovob E. V., Lugantseva L. N., Petrov L. V.- **Lakokras. Mater. Ikh. Primen, 5**, 27-29 (1987).

[49] Robertson J. A.- **Official DIGEST, 36**, 138 (1964).

[50] Brugarolas J., Rodellas F.- **Proc. 3rd Internat. Zinc Coated Sheet Conf.**, (EGGA/Asoc. Tec. Espan. de Galv.), Paper 7, Barcelona (1991).

[51] Hanumanth-Rao G.,Sivasabam M.- **Paint Manufacture, 49** (10), 26-28 (1979).

[52] Hanumanth-Rao G.- **Paint Manufacture, 37** (2), 70-75 (1967).

[53] Vetere V. F., Rozados E., Eugeni O. S.- **Rev. Iber. Corros. y Prot., 7** (5); 275-280 (1976).

[54] Brauer G.- **Química Inorgánica Preparativa**, Ed. Reverté, p. 646, Barcelona (1958).

[55] Leblanc O.- **J. Oil Col. Chem. Assoc., 73** (6), 231 (1990).

[56] Romagnoli R., Vetere V. F.- **CIDEPINT-Anales**, 121-132 (1993).

[57] Harris D. C.- **Quantitative Chemical Analysis**, Ed. W.H. Freeman and Company, New York (1987).

[58] Stern M., Geary M. A. L.- **J. Electrochem. Soc., 104**, 56 (1957).

[59] Callow L. M., Richardson J. A., Dawson J. L.- **Br. Corros. J., 11**, 123 (1976).

[60] Mansfeld F.- **Corrosion, 32**, 143 (1970).

[61] Heitz E., Schwenk W.- **Br. Corros. J., 11**, 74 (1976).

[62] Snell F. D., Snell C. T.- **Inorganic Colorimetric Methods of Analysis, Vol. I**, pp. 283-312, D. Van Nostrand Company Inc., New York (1941).

[63] Snell F. D., Snell C. T.- **Inorganic Colorimetric Methods of Analysis, Vol. I**, pp. 480-516, D. Van Nostrand Company Inc., New York (1941).

[64] Boltz D. F., Mellow M. G.- **Anal. Chem., 19** (11), 873-877 (1947).

[65] Wormwell J., Brasher A., **J. Iron Steel Inst., 162**, 129 (1949).

[66] Leblanc O.- **J. Oil Col. Chem. Assoc., 74** (8), 288 (1991).

[67] Kündig W., Bömmel H.- **Physical review, 142** (2), 327-333 (1966).

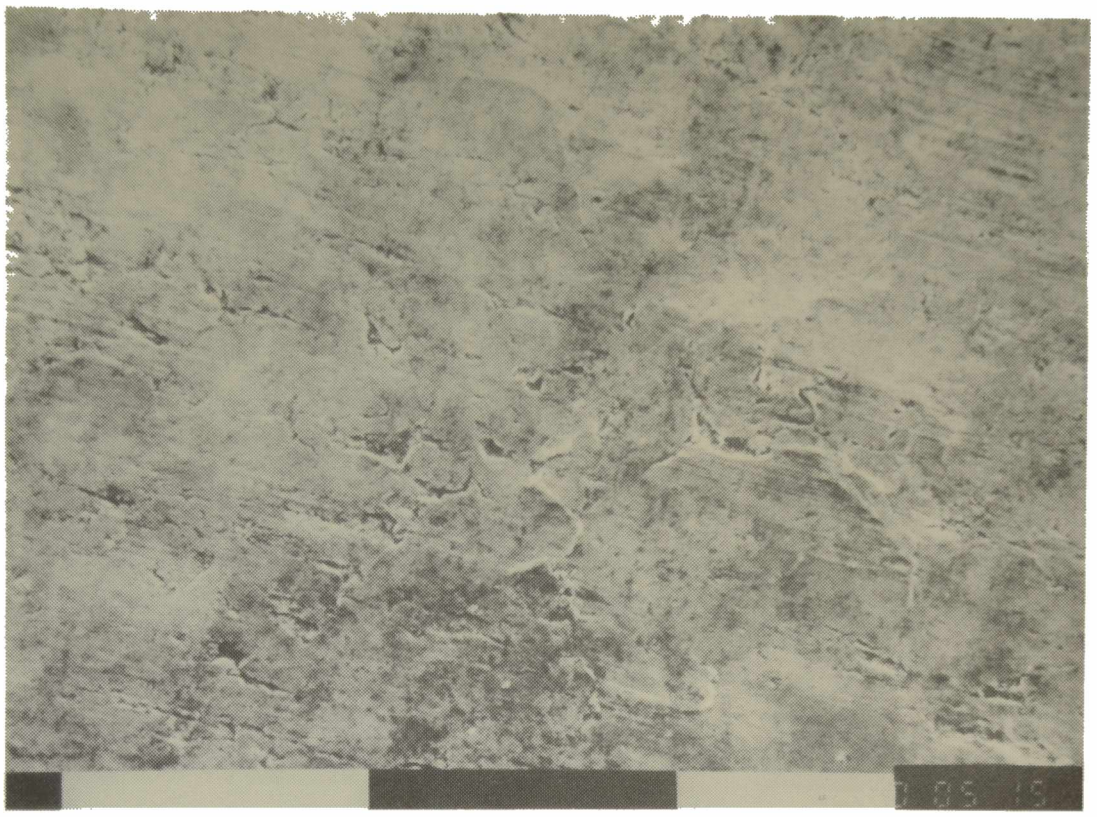

Fig. 7.- SEM micrograph of the steel surface after 72 hours immersion in a zinc phosphate suspension. Electrolyte: 0.5 M sodium perchlorate solution.

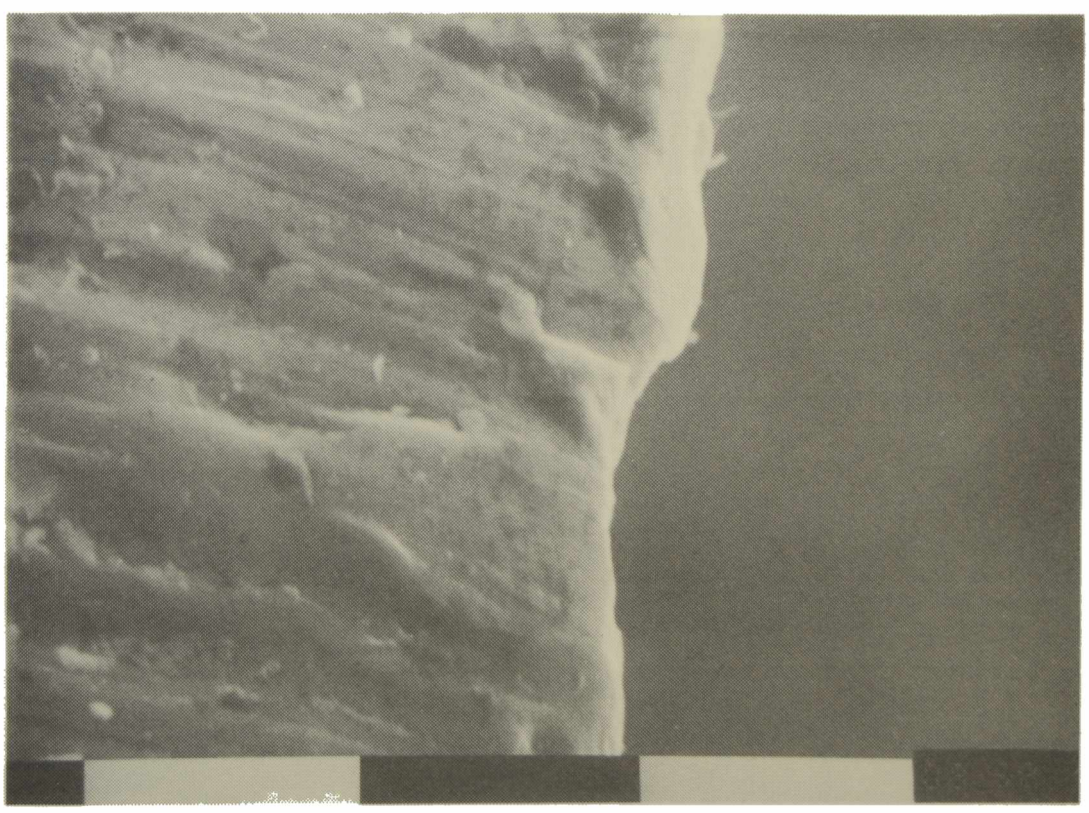

Fig. 8.- SEM micrograph of a cross-section view of a steel panel after 72 hours immersion in a zinc phosphate suspension.
Electrolyte: 0.5 M sodium perchlorate solutions

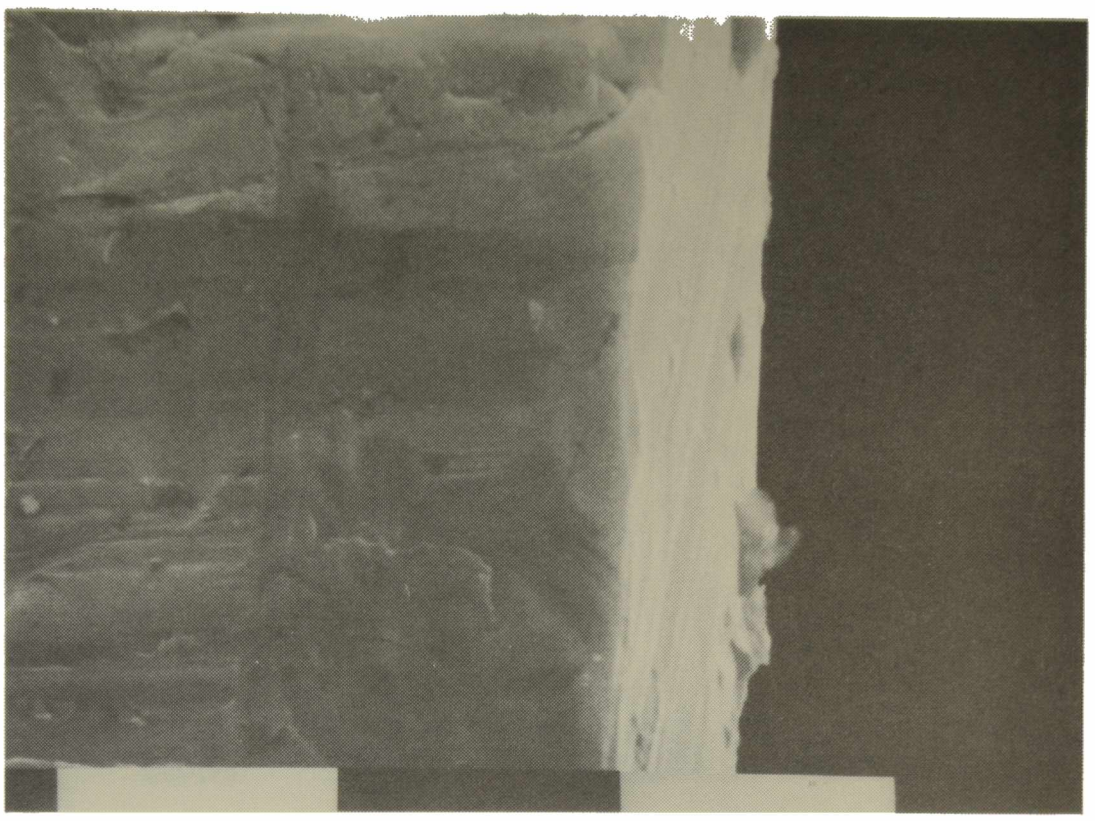

Fig. 9.- SEM micrograph of a cross-section view of a steel panel after 72 hours immersion in a calcium acid phosphate suspension.
Electrolyte: 0.5 M sodium perchlorate solution.

Fig. 10.- SEM micrograph of a cavity on the steel surface after 72 hours immersion in a zinc phosphate suspension. Electrolyte: 0.5 M sodium perchlorate solutions

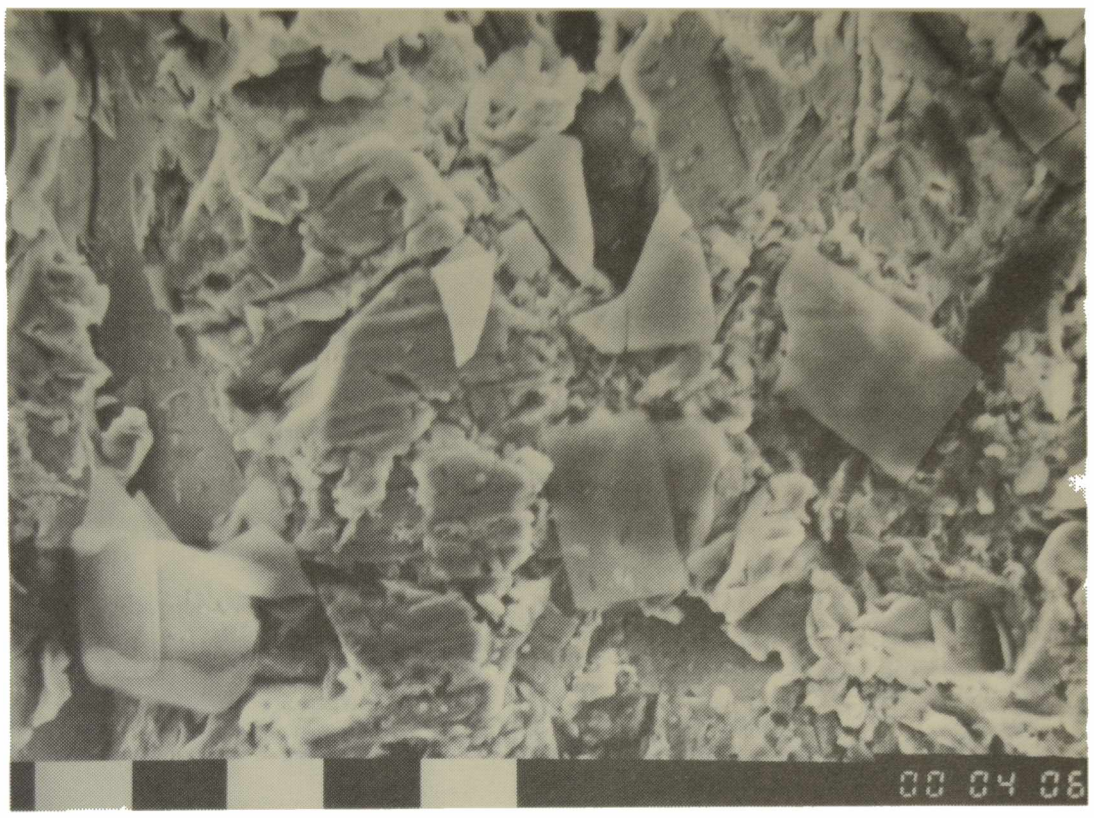

Fig. 11.- SEM micrograph of an uncoated steel surface obtained after removing the binder with triclorethylene. Immersion time of the coated specimen: 24 hours in 0.5 M sodium perchlorate solution.

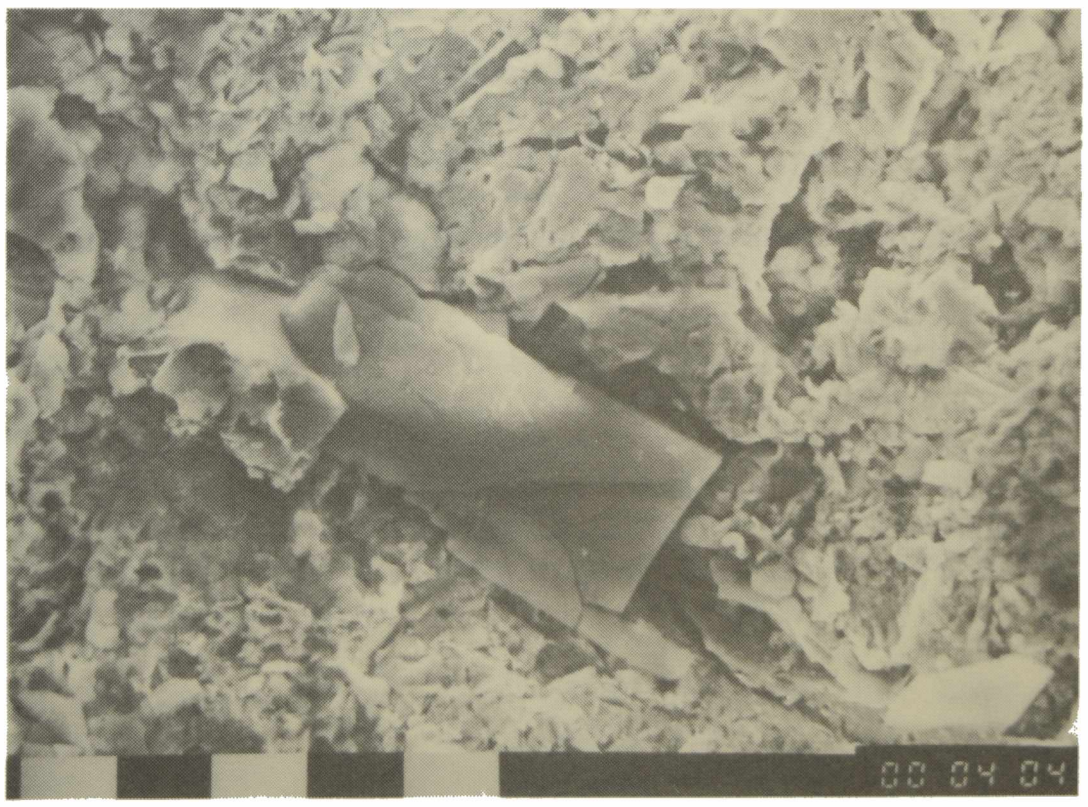

Fig. 12.- SEM micrograph of an uncoated steel surface obtained after removing the binder with triclorethylene. A big oxide plate could be seen with some detail. Immersion time of the coated specimen: 24 hours in 0.5 M sodium perchlorate solution.

Fig. 13.- SEM micrograph of an oxide layer built on an unprotected surface.

Note: This paper has been sent for publication to Corrosion (NACE).

HALOMETHANES IN TRI-n-OCTYLAMINE AND SQUALANE MIXTURES AT INFINITE DILUTION

HALOMETANOS A DILUCION INFINITA EN MEZCLAS DE TRI-n-OCTILAMINA Y ESCUALANO

R.C. Castells[1] , E.L. Arancibia[2] and A.M. Nardillo[1]

SUMMARY

The retention behavior of eight halomethanes and four saturated hydrocarbons was measured in gas chromatographic stationary phases consisting in tri-n-octylamine (TOA), squalane (SQ) and six TOA + SQ mixtures, at 55.0, 58.5, 62.5 and 65.0 °C. Equilibrium constants for complex formation were extracted from experimental data by using a lattice model developed by D.E.Martire (J.Phys.Chem. **87**, *2425 (1983)). The results may be interpreted in terms of the formation of weak hydrogen-bonded complexes, with "sociation" constants of about 0.13 L.mol^{-1} for haloforms and 0.07 L.mol^{-1} for dihalomethanes at 60 °C.*

KEYWORDS: *Tri-n-octylamine, Halomethanes, Molecular association, Hydrogen-bonded complexes, Nonrandom mixtures, Gas-liquid chromatography.*

INTRODUCTION

Gas chromatography is a highly advantageous option to study molecular complexation equilibria. Systems to be studied must fulfil the requirement that one of the partners in the association (the "additive") be a low vapor pressure liquid at the working temperature, while the other (the "solute") is volatile enough as to be eluted from a gas chromatographic column. Two experimental approaches have been used: 1) the two-columns method of Martire and Rideal **[1]**, where association constants are calculated from retention data of complexing and alkane solutes from columns containing the additive and an inert solvent, both in the pure state, as the stationary phases; 2) in Purnell's **[2]** many-columns method complexing solutes are eluted from a series of columns whose stationary phases are solutions of the additive in an inert solvent. Several combinations of both approaches have also been used **[3,4]**.

Unfortunately no solvent is actually "inert" and, on the other side, solute-additive interactions different from that responsible for the formation of the complex are also feasible. Therefore, to obtain meaningful thermodynamic association constants it is necessary to discriminate between deviations from the ideal solution behavior attributable to the formation of the complex and those stemming from other origins, as combinatorial and free volume contributions and "other-end-interactions". With this purpose it is unavoidable to resort to some kind of molecular model.

The simplest model is the one that assumes that the complexing interaction is

[1] CIDEPINT, Miembro de la Carrera del Investigador del CONICET

[2] Instituto de Ingeniería Química, Fac. Cs. Exactas y Tecnología, UN Tucumán

strong enough as to consider negligible all other types of nonidealities. This criterion, regularly applied in the early chromatographic complexation studies, is inappropriate for studying weak complexes. Ideally the model should be capable of dealing with interactions of different strength.

Several years ago the concept of degree of "sociation" was introduced by Guggenheim **[5]** as the excess in the degree of "association" in a given mixture over that based on probabilities in a totally random mixture. Scott **[6]** went further into this matter utilizing a lattice of monomeric donor, acceptor and inert solvent molecules; non-randomness was introduced by means of quasi-chemical calculations, considering that all interaction energies are equal except that between a given pair of "faces".

Scott's model was extended by Martire**[7]** to cover mixtures of heterogeneous molecules of different sizes: solute (a), inert solvent (b) and additive (c) molecules contain r_a, r_b and r_c segments, respectively; solute molecules are constituted by type 1 and type 2 segments, with fractions f_{1a} and f_{2a}, respectively; inert solvent molecules are chemically homogeneous, with all of their segments being of type 3 (paraffinic); additive molecules have a fraction f_{3c} of segments of type 3 and a fraction f_{4c} of type-4 segments. The formation of an i-j pair and a 3-3 pair from i-3 and j-3 pairs is characterized by the exchange energy $\Delta W_{ij} = (w_{ij} + w_{33}) - (w_{i3} + w_{j3})$. This definition makes $\Delta W_{13} = \Delta W_{23} = \Delta W_{34} = 0$; however, as a first order approximation it is assumed that $|\Delta W_{ij}| \ll kT$ for all the segment pairs except for the 2-4 pair. Martire applied this assumption together with quasi-chemical and conservation equations to correct the results for the different pair numbers deduced for random pairing and to obtain an expression for the partial molar excess configurational energy of the solute at infinite dilution. If it is further assumed that the free volume contributions are negligible (which shall be the case when additive and inert solvent thermal expansion coefficients are close enough) it can be shown that the solute infinite dilution vapor-liquid partition coefficient in a mixed solvent ($K^\circ_{a(m)}$) is related to that in the pure inert solvent ($K^\circ_{a(b)}$) by

$$\ln [K^\circ_{a(m)} / K^\circ_{a(b)}] = r_a(r_c^{-1} - r_b^{-1})\varphi_c - zr_a f_{1a}(\varphi_c f_{4c})(\Delta W_{14}/ kT) + + zr_a f_{2a} \ln [1 + K^\circ_{ac}\varphi_c / V^\circ_c] - zr_a (\varphi_c f_{4c})^2(\Delta W_{34}/ kT) \quad (1)$$

where z is the lattice coordination number, V°_c and φ_c represent the additive molar volume and volume fraction in the mixture, r_i is the ratio between the solute and a reference solute (methylene chloride in the present paper) molar volumes, $\Delta w_{34} = w_{34} - (1/2)(w_{33} + w_{44})$ is the usual interchange energy, and K°_{ac} is the thermodynamic solute-aditive excess or "sociation" constant, related to the corresponding "association" constant, K_{ac} , by

$$K^\circ_{ac} = K_{ac} - K^r_{ac} = f_{4c} V^\circ_c (\kappa - 1) \quad (2)$$

In this equation K^r_{ac} represents the equlibrium constant for random pairing and $\kappa \equiv \exp(-\Delta W_{24}/ kT)$.

Expressions pertinent to some particular cases of importance for the application of the model are deduced from eq (1). In the random mixing limit ($\kappa \longrightarrow 1$), for instance

$$\ln [K^\circ_{a(m)}/K^\circ_{a(b)}] = r_a (r_c^{-1} - r_b^{-1}) \varphi_c - zr_a f_{1a}(\varphi_c f_{4c})(\Delta W_{14} / kT) - zr_a f_{2a}(\varphi_c f_{4c})(\Delta W_{24} / kT) - zr_a(\varphi_c f_{4c})^2(\Delta w_{34} / kT) \quad (3)$$

and the equation for a chemically homogeneous solute is obtained by making $f_{1a}= 0$ in eq (3). For a paraffinic (p) solute,

$$\ln [K^{\circ}_{p(m)}/K^{\circ}_{p(b)}] = r_p (r_c^{-1} - r_b^{-1}) \phi_c - zr_a(\phi_c f_{4c})^2(\Delta w_{34} / kT) \quad (4)$$

Substracting eq. (4) from eq. (1):

$$Q + \varepsilon = zr_a f_{1a}(\phi_c f_{4c})(\Delta W_{14} / kT) + zr_a f_{2a} \ln [1 + K^{e}_{ac}\phi_c / V^{\circ}_c] \quad (5)$$

where

$$Q \equiv \ln [K^{\circ}_{a(m)} K^{\circ}_{p(b)} / K^{\circ}_{a(b)} K^{\circ}_{p(m)}] \quad (6)$$

and

$$\varepsilon \equiv (r_p - r_a)[(r_c^{-1} - r_b^{-1})\phi_c - z(\Delta w_{34}/ kT)(f_{4c}\phi_c)^2] \quad (7)$$

An important aspect of these equations is that only relative retention times need to be measured to calculate Q; ε is a correction term that takes into consideration molecular size differences between solutes a and p. When the measurements have been made at several temperatures eq [2] and the definition of κ can be introduced into eq (6) to give

$$Q + \varepsilon = A(\phi_c/T) + \ln \{1 + [\exp(C/T) - 1] f_{4c}\phi_c\} \quad (8)$$

where $A = -zr_a f_{1a} f_{4c}(\Delta W_{14}/k)$ and $C = -\Delta W_{24}/k$; the assignment $zr_a f_{2a} = 1$ has been made, implying that only one of the zr_a solute molecule sites participates in the strong interaction (which is fully justified for hydrogen-bonding). Nonlinear least-squares fit of experimental data to eq (8) yields the parameters A and C; from C not only the values of K°_{ac} at several temperatures can be obtained, but also ΔH°_{ac} and ΔS°_{ac}, the standard enthalpy and entropy of excess complex formation. Analogously, from eq (3) and eq (4), we have for the random mixing limit

$$Q + \varepsilon = D(\phi_c / T) \quad (9)$$

with

$$D = -zr_a f_{4c}(f_{1a}\Delta W_{14} + f_{2a}\Delta W_{24})/ k \quad (10)$$

Results for the systems halomethane (HM) + di-n-octyl ether (DOE) + n-octadecane **[9]** and HM + tri-n-octylphosphine oxide (TOPO) + squalane (SQ) **[10,11]** were analyzed by means of this model. HM + TOPO complexes are highly stable (K°_{ac} = 8.92 L.mol^{-1} for chloroform at 60 °C), the plots of Q + ε vs ϕ_c display a pronounced curvature and no linear contribution is necessary in the fit of eq (8) to experimental data, which may be imputed to large differences between the strengths of the 2-4 (X_3C-H...OPR_3, X halogen) and 1-4 (HX_2C-X...OPR_3) interactions that make the consideration of this last type of interaction unnecessary. Much less strong complexes are formed between HM and DOE (K°_{ac} =

0.308 L.mol^{-1} for chloroform at 30 °C), and the contribution of the lineal term in eq (8) is no negligible.

In the present paper the results obtained for eight HM plus tri-n-octylamine (TOA) at 55.0, 58.5,62.5 and 65.0 °C, using four saturated hydrocarbons as reference solutes, are reported. Earlier studies **[12-14]** indicate that when alkyl chains are of approximate sizes, tri-n-alkylamines + HM complexes are weaker than those formed between HM and di-n-alkylethers. TOA was expected to be a weak HM complexing agent, a good example to study both the lower limits of the method and the possibility of distinguishing between two types of interaction under these circumstances. Squalane was chosen as the inert solvent because its thermal expansion coefficient (8.15 x 10^{-4} K^{-1} at 20 °C) **[15]** is almost coincident with that of TOA (8.32 x 10^{-4} K^{-1} at 25 °C) **[16]**; on the other side, being SQ a branched paraffin, short range orientational order shall be absent from its mixtures.

EXPERIMENTAL

The glc apparatus consisted of a Perkin-Elmer Sigma 300 gas chromatograph, equipped with a thermal conductivity detector and an LCI-100 computing integrator, with modifications that were described in an earlier publication **[17]**; a Haake N3B water bath was used as column thermostat. Hydrogen, previously passed through a trap containing molecular sieve 5A, was used as the carrier gas. Columns were made from 0.53 cm i.d. stainless steel tubes, 0.6-1.0 m in length.

TOA (Aldrich Chemical Co.) was purified by destillation under reduced pressure; SQ (Hewlett-Packard) was used as received. Chromosorb W, AW DMCS treated 60/80 mesh, was used as the solid support; packings contained between 6 and 8% by weight of stationary phase. Retention data were obtained for pure SQ and the following weight fractions of TOA: 0.192, 0.335, 0.488, 0.695, 0.762, 0.891 and 1.000. Densities at five temperatures within the range 50-65 °C were measured for TOA, SQ and three mixtures using a 5-mL picnometer; since excess volumes were less than 0.1 %, volume fractions were computed from weight fractions and pure component densities at each temperature.

All the solutes were more than 99 moles per cent pure, and were used without further purification. n-Hexane, n-heptane, n-octane and cyclohexane were used as reference solutes. Solute vapors, together with one or two of the reference hydrocarbons and a small quantity of methane were injected by means of 100- and 250-μL Hamilton syringes. Relative retentions were computed from the HM and reference hydrocarbon peak maximum retention times in the same chromatogram, after dead volume corrections using the methane peak.

RESULTS AND DISCUSSION

There are several options to calculate the correction term ε. Martire **[9]** used a method based on the measurement of the retention time for a solute with the same functional group as the additive solvent; it could not be applied in the present work because amines tail severely in most chromatographic columns, thus precluding the obtention of thermodynamically meaningful retention data. For that purpose we applied the equation

$$\ln [K^{\circ}_{p(m)}K^{\circ}_{p'(b)}/K^{\circ}_{p(b)}K^{\circ}_{p'(m)}] - (r_p - r_{p'}) (r_c^{-1} - r_b^{-1}) \phi_c - \psi (r_p - r_{p'})^2\phi_c \quad (11)$$

where $\psi = zf^2_{4c}(\Delta w_{34}/kT)$, obtained by substracting from eq (4) the equation corresponding to a second hydrocarbon solute (p'). Eq (11) involves only relative retentions, and the value of ψ can be calculated from the slope of the straight line obtained by plotting the left-handside against ϕ_c^2. Choosing cyclohexane as the reference solute, the mean of the values of ψ obtained with the remainig hydrocarbons was 0.013 ± 0.001 at 55 °C; this result was introduced into eq (7) to calculate the values of ε. Solute molar volumes necessary for these and following calculations were obtained from the literature **[18, 19]**.

In **Fig. 1** can be found a plot of Q + ε against ϕ_c/T for bromotrichloromethane. A linear least-squares treatment indicates: slope 41.2 ± 0.77 K (± stands for standard deviation), intercept 0.002 ± 0.0015, correlation coefficient 0.998; the same treatment for carbon tetrachloride data results in: slope 20.0 ± 0.61 K, intercept -0.002 ± 0.0012, and correlation coefficient 0.993. The intercepts are very small and of poor statistical significance; with zero intercept assumed the slopes are 42.1 ± 0.37 K for bromotrichloromethane and 18.8 ± 0.31 K in the case of carbon tetrachloride. Data for both solutes seem to be satisfactorily accounted by eq (9) (*i.e.*, by the random pairing assumption).

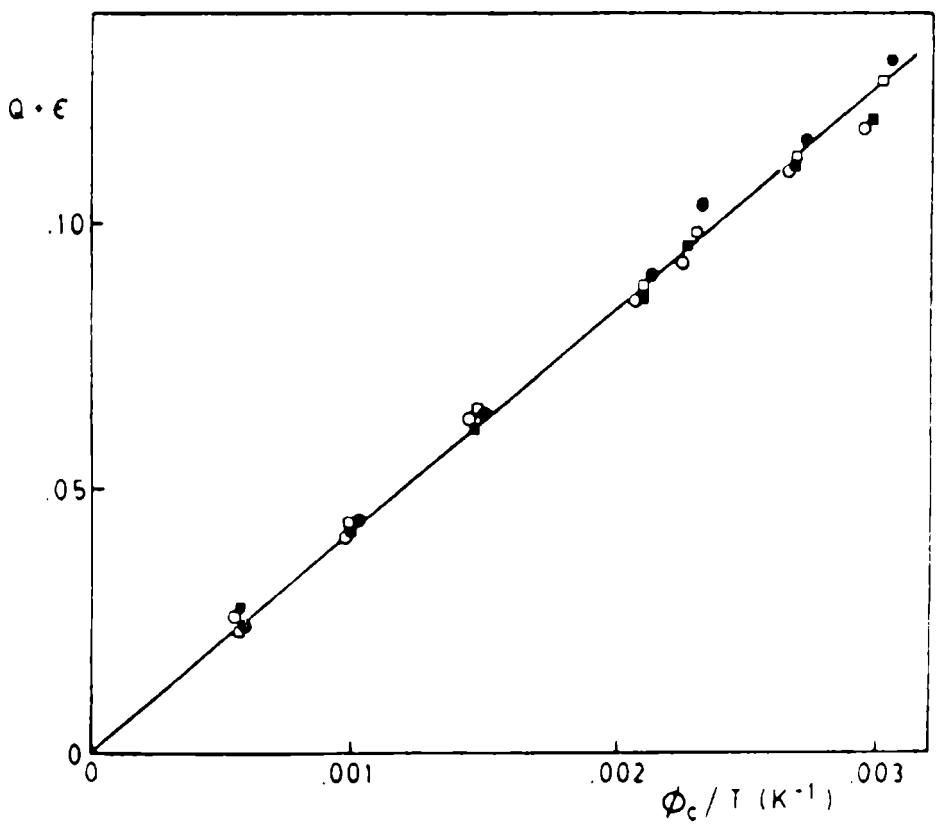

Fig. 1.- Plot of Q + ε vs. ϕ_c/T for the solute bromotrichloromethane: ° 45°C; □ 48.5°C; ■ 52.5°C; • 55°C.

The value of $\Delta W_{14}/k$ for the Cl-N interaction can be deduced from the carbon tetrachloride slope: $D = -zr_a f_{4c}(\Delta W_{14}/k)$. To this end $f_{4c} = 0.0166$ is estimated from Bondi's **[20]** compilation of van der Waals volumes; then the assignment $zr_a f_{1a} = 1$ with $f_{4c} = 0.0945$ **[20]** is made for chloroform, from which $zr_a = 13.1$ is deduced for carbon tetrachloride on the assumption that the total number of contacts is directly proportional to the molecular size. On these basis, $\Delta W_{14}/k$ = -87 K, a result considerably smaller than $\Delta W_{14}/k$ = -230 K obtained by Martire and collaborators for the system CCl_4+ DOE. Charge transfer (n⟶ σ* type) between an n-donor and an acceptor halogen atom,and dipole-induced dipole , are the most probable mechanisms of interaction for these systems **[12, 13, 21, 22]**; the

stronger interaction manifested by DOE could be explained on the basis of steric considerationes, its O atom being more accesible than the N atom in TOA. Bromotrichloromethane, a permanent dipole, constitutes a particular case that shall be discussed later.

Shown in **Fig. 2** is a plot of Q + ε against ϕ_c for chloroform at 55°C. The plots for the three haloforms studied are very much alike, their curvatures being markedly smaller than those shown by the plots obtained for the same solutes in TOPO or DOE; the plots for the dihalomethane solutes display the smallest curvatures. Nonlinear fits of Q + ε = $f(\phi_c,T)$ were performed by using the Marquardt-Levenberg algorithm **[23]**, as included in SigmaPlot 4.1 program (Jandel Scientific, San Rafael, CA). Attemps to fit eq (8) to experimental data resulted in A parameters of very small values and large standard deviations; C parameters were calculated with better precision. Parameter dependencies, however, were greater than 0.998, this suggesting that the model is overparameterized, and that a model with fewer parameters would be better (dependence ≡ 1 - (parameter variance other parameters held constant / parameter variance allowing other parameters to change in the usual way)). Overparameterization can mean that the model is inappropriate or else that the data are not adequate for estimating all the parameters. In our opinion there are neither inadequacies in the model nor low quality in the data; the fact is that the systems we are dealing with are characterized by very small A parameters, as indicated by the very weak Cl-N interactions detected during the work with carbon tetrachloride. Dificulties in separating both contributions to Q + ε have already been encountered by Martire et al **[9]** during their work with haloform + DOE systems, in spite of stronger other-end-interactions.

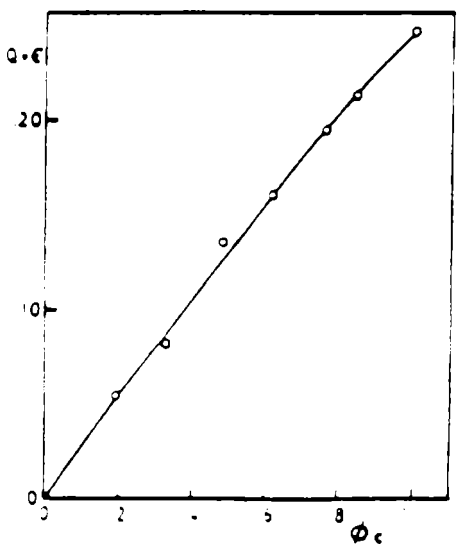

Fig. 2.- Plot of Q + ε vs. ϕ_c at 48.5°C for the solute chloroform.

On the basis of these findings, experimental data were fitted to eq [8] assuming A = 0. The results have been gathered in **Table I**, where the values of K°_{ac} at 60.0°C have also been included. The haloforms sociation constants reveal weak hydrogen-bonded complexes; as could be foreseen, dihalomethane complexes are still weaker. Although the K°_{ac} for the three haloforms are roughly the same within the error limits, it seems feasible to detect a trend to increase complex stability as Cl atoms are substituted for Br atoms in the solute molecule. No trend is detected within the dihalomethanes family. From eq (2), the expression for the standard enthalpy of excess complex formation is obtained:

$$\Delta H^\circ_{ac} = R\{\alpha T^2 - C/[1 - \exp(-C/T)]\} \qquad (12)$$

where α is the additive thermal expansion coefficient (9.0 x 10^{-4} K^{-1} at 60°C);

results obtained at 60°C can also be read in **Table I**. Since K^{e}_{ac} and ΔH°_{ac} are calculated from C, there is an obvious correlation between both sets of thermodynamic properties.

TABLE I

Results of analysis of chromatographic data according to Eq. 2, 8 and 12. T = 333.15 K

SOLUTE	C	K°_{ac}	$-\Delta H^{\circ}_{ac}$
$CHCl_3$	946 ± 30	0 121 ± 0.012	7.52 ± 0.22
$CHCl_2Br$	974 ± 50	0 132 ± 0.021	7.72 ± 0.37
$CHClBr_2$	992 ± 32	0 140 ± 0.014	7.85 ± 0.24
CH_2Cl_2	757 ± 29	0 065 ± 0.006	6.18 ± 0.20
CH_2ClBr	777 ± 40	0 070 ± 0.009	6.32 ± 0.28
CH_2Br_2	755 ± 55	0 065 ± 0.012	6.17 ± 0.36
UNITS	C: K^{-1}	K°_{ac} : $L.mol^{-1}$	ΔH°_{ac} : $KJ.mol^{-1}$

Bromotrichloromethane represents an intermediate case between that of carbon tetrachloride and those of the haloforms and dihalomethanes. $\Delta W_{24}/k$ can in principle be calculated from its relatively large D parameter by introducing into eq (10) zr_a, f_{4c}, f_{1a} and f_{2a} estimations from van der Waals volumes **[20]** and by assuming that $\Delta W_{14}/k$ retains the same value as in carbon tetrachloride (an assumption of dubious validity in the presence of a permanent dipole moment). Such a calculation leads to $\Delta W_{24}/k$ = -460 K, a result that by no means guarantees random mixing for CCl_3Br + TOA mixtures, which can be used in eq (2) to obtain $K^{e}_{ac} \cong 0.02$ $L.mol^{-1}$. This value is not large enough as to give rise to curved Q + ε vs φ_c plots, but it is debatable whether the interaction represents a collision interchange or if a labile complex is formed. Bromotrichloromethane is probably a border case where Martire's model is unable to give a definite answer.

ACKNOWLEDGEMENT

This work was sponsored by CONICET (Consejo Nacional de Investigaciones Científicas y Técnicas) and by CIC (Comisión de Investigaciones Científicas de la Provincia de Buenos Aires).

REFERENCES

[1] D. E. Martire, P. Riedl.- **J. Phys. Chem, 72**, 3478 (1968).

[2] D. F. Cadogan, J. H. Purnell.- **J. Chem. Soc. A**, 2133 (1968).

[3] R. J. Laub, R. L. Pecsok.- **Physicochemical Applications of Gas Chromatography** Wiley, New York, (1978).

[4] J. R. Conder, C. L. Young.- **Physicochemical Measurements by Gas Chromatography**, Wiley, New York, (1979).

[5] E. A. Guggenheim.- **Trans. Faraday Soc., 56**, 1159 (1960).

[6] R. L. Scott.- **J. Phys. Chem., 75**, 3843 (1971).

[7] D. E. Martire.- **J. Phys. Chem., 87**, 2425 (1983)

[8] P. J. Flory.- **Discuss. Faraday Soc., 49**, 7 (1970)

[9] T. J. Bruno, D. E. Martire, M. W. P. Harbison, A. Nicoli, C. F. Hammer.- **J. Phys. Chem., 87**, 2430 (1983).

[10] R. C. Castells, A. M. Nardillo.- **J. Solution Chem., 14**, 87 (1985).

[11] A. M. Nardillo, R. C. Castells, E. L. Arancibia.- **J. Chromatogr., 387**, 85 (1987).

[12] J. P. Sheridan, D. E. Martire, Y. B. Tewari.- **J. Am. Chem. Soc., 94**, 3294 (1972)

[13] J. P. Sheridan, D. E. Martire, F. P. Banda.- **J. Am. Chem. Soc., 95**, 4788 (1973)

[14] D. E. Martire, J. P. Sheridan, J. W. King, S. E. O'Donnell.- **J. Am. Chem. Soc., 98,** 3101 (1976).

[15] G. Gee, D. Mangaraj, D. Sims., G. J. Wilson.- **Polymer**, 1, 467 (1960).

[16] R. Philippe, G. Delmas, M. Couchon.- **Can. J. Chem., 56**, 370 (1978).

[17] R. C. Castells, E. L. Arancibia, A. M. Nardillo.- **J. Chromatogr., 504**, 45 (1990).

[18] R. R. Dreisbach.- **Adv. Chem. Ser., 15** (1955); **22** (1959); **29** (1961).

[19] J. A. Riddick, W. B. Bunger.- **Organic Solvents**, 3rd. edn. Wiley-Interscience, New York, (1970).

[20] A. Bondi.- **J. Phys. Chem., 68**, 441 (1964).

[21] D. P. Stevenson, G. M. Coppinger.- **J. Am. Chem Soc., 84**, 149 (1962).

[22] C. J. Biaselle, J. G. Miller.- **J. Am. Chem. Soc., 96**, 3813 (1962).

[23] D. W. Marquardt.- **J. Soc. Appl. Math., 2**, 431 (1963).

Note: This paper was published in Journal of Solution Chemistry, **22** *(1), 85-94 (1993).*

THE EXCESS ENTHALPIES OF (DINITROGEN OXIDE + TOLUENE) AT THE TEMPERATURE 313.15 K AND AT PRESSURES FROM 7.60 MPa TO 15.00 MPa

LAS ENTALPIAS DE EXCESO DE (OXIDO DE DINITROGENO + TOLUENO) A LA TEMPERATURA DE 313.15 K Y PRESIONES DESDE 7.60 MPa A 15.00 MPa

R.C. Castells[1] , C. Menduiña[2], C. Pando[2] and J.A.R. Renuncio[2]

SUMMARY

The excess molar enthalpies $H_m^E\{xN_2O + (1-x)C_6H_5CH_3\}$ were measured in the vicinity of the critical locus and in the supercritical region. Mixtures at the temperature T = 313.15 K and at the pressure p = 7.60 MPa show very exothermic mixing. Mixtures at T = 313.15 K and p = 9.49 MPa show moderately endothermic and exothermic mixing in the toluene-rich region and dinitrogen-oxide-rich region, respectively. The changes observed in the excess enthalpy with pressure are discussed in terms of (liquid + vapour) equilibrium and critical constants for (dinitrogen oxide + toluene).

Keywords: *Excess enthalpies, Nitrous oxide, Toluene, Critical conditions, Differential Calorimetry.*

INTRODUCTION

Thermodynamic properties such as the excess enthalpies H^E of mixtures formed by dinitrogen oxide have been very seldom studied. Machado et al. **[1]** reported H_m^E for $\{xN_2O + (1-x)Xe\}$ and Wormald and Eyears **[2]** reported H_m^E for $\{xN_2O + (1-x)CO_2\}$. Prior to this work, no H^E measurements of (nitroux oxide + a hydrocarbon) had been made. However, the excess enthalpy may play an important role in understanding the practical uses of N_2O. N_2O is often used in supercritical-fluid extraction and several authors have reported that N_2O is a better solvent than CO_2 for certain molecules **[3, 4]**. The present work reports values of H_m^E $\{xN_2O + (1-x)C_6H_5CH_3\}$ at the temperature 313.15 K and the pressures 7.60 MPa, 9.49 MPa, 12.27 MPa, and 15.00 MPa. The pressure and temperature conditions of the measurements were chosen in order to compare results for $\{xN_2O + (1-x)C_6H_5CH_3\}$ with those previously obtained for $\{xCO_2 + (1-x)C_6H_5CH_3\}$ **[5]**.

EXPERIMENTAL

The high-pressure flow calorimeter from Hart Scientific (model 7501) used for the experiments and the experimental procedure have been described elsewhere **[6-8]**. The chemicals were pumped into the calorimeter by two thermostatted ISCO pumps (model LC2600). The calorimeter cell was thermostatted in a silicon-oil bath

[1] CIDEPINT, Miembro de la Carrera del Investigador del CONICET

[2] Departamento de Química Física I, Universidad Complutense, Madrid, España

(± 0.0005 K) and the pressure was controlled by a back-pressure regulator. A manually controlled piston acted as a fine adjustment of the nitrogen pressure over the back-pressure regulator. Oscillations in pressure were smaller than ± 0.01 MPa.

The materials employed were N_2O (99.99 moles per cent pure) and $C_6H_5CH_3$ (Merck 99.5 moles per cent pure) previously dehydrated with sodium.

All runs were made in the steady-state fixed-composition mode. Flow rates were selected to cover the whole mole-fraction range. In most cases, the measurements were carried out at a total flow rate of 0.010 $cm^3.s^{-1}$. A few measurements were carried out at a total flow rate of 0.005 $cm^3.s^{-1}$. Reproducibility of results was estimated to be ± 1 per cent. The flow rates were converted to amount-of-substance rates and to mole fractions using the densities of the two materials estimated as follows. The densities of N_2O at the temperature of the pump and at pressures of 7.60 MPa, 9.49 MPa, 12.27 MPa, and 15.00 MPa were calculated by interpolation of the pressure (volume) isotherms of the liquid dinitrogen oxide measured by Couch et al. **[9]**. The densities of toluene at the temperature of the pump and at pressures of 7.60 MPa, 9.49 MPa, 12.27 MPa, and 15.00 MPa were calculated from the densities and isothermal compressibilities of Garbajosa et al. **[10]** and Aicart et al. **[11]**.

RESULTS AND DISCUSSION

Excess molar enthalpies were determined for $\{xN_2O + (1-x)C_6H_5CH_3\}$ over the entire composition range at the temperature T = 313.15 K and pressures p = 7.60 MPa, 9.49 MPa, 12.27 MPa, and 15.00 MPa. The results are given in **Table I**. Values for H_m^E at each pressure studied were fitted to the equation:

$$H_m^E/(J.mol^{-1}) = [x(1-x)/\{1 + k(2x-1)\}].\sum_{i=0}^{j} C_i(2x-1)^i \qquad (1)$$

The parameters C_i and k are given in **Table II** together with the standard deviations s between experimental and calculated H_m^E values.

Fig. 1 is a plot of H_m^E against x for the four isobars studied. **Fig. 2** is a plot of p against T for $\{xN_2O + (1-x)C_6H_5CH_3\}$ showing the vapour-pressure equilibrium curve of dinitrogen oxide **[9]**, the critical locus in the vicinity of its critical point, and the points at which experimental measurements of H_m^E have been made. For toluene T_c is 591.8 K and p_c is 4.10 MPa, while for dinitrogen oxide T_c is 309.6 K and p_c is 7.24 MPa **[12]**. Neither (vapour + liquid) equilibria nor the critical locus are available for $\{xN_2O + (1-x)C_6H_5CH_3\}$. The critical locus shown in **Fig. 2** has been estimated using the procedure developed by Heidemann and Khalil **[13]** and the Peng-Robinson equation of state **[14]**.

The densities of dinitrogen oxide and toluene at the conditions of temperature and pressure of the experiments are listed in **Table III**. Values for the densities of dinitrogen oxide were taken from Couch et al. **[9]** and from Langenfeld et al. **[15]**. Values for the densities of toluene were calculated from the parameters of the Tait equation given by Takagi **[16]**. The toluene enters the calorimeter as a liquid because the temperature is lower than the critical temperature of this component and the pressures are always higher than its critical pressure. The values for the density of toluene shown in **Table III** are those typical of a liquid and change very little with pressure. The dinitrogen oxide enters the calorimeter as a supercritical fluid because the temperature and pressures studied are always greater than those defining its critical point. However, this supercritical fluid may be a low-density (gas-like) fluid or a high-

density (liquid-like) fluid depending on the pressure. The values for the density of dinitrogen oxide shown in **Table III** change as the pressure increases from that typical of a gas at 7.60 MPa to that typical of a liquid at 15.00 MPa. The resulting $\{xN_2O + (1-x)C_6H_5CH_3\}$ may be liquid, gas-like fluid, or liquid-like fluid, depending on the critical temperature and pressure of the particular mixture. The critical locus predicted by the Peng-Robinson equation **[14]** for $\{xN_2O + (1-x)C_6H_5CH_3\}$ is similar to the critical locus for the $\{xCO_2 + (1-x)C_6H_5CH_3\}$ **[5]**. The critical line goes through a maximum at approximately p = 15.5 MPa and T = 435 K and it comes back to the toluene critical point (T_c = 591.8 K, p_c = 4.10 MPa). Since the temperatures and pressures studied are far away from those defining the critical point of toluene, $\{xN_2O + (1-x)C_6H_5CH_3\}$ is liquid from x = 0 to approximately x = 0.95, and is fluid only in a narrow composition range in the N_2O-rich region. Due to the transition from a liquid to a fluid mixture, there is also a two-phase region between the liquid and the fluid-mixture regions. this is detected by a high-slope linear section in the 7-60 MPa isobar of **Fig. 1**. When the pressure increases, the linear section becomes narrower. Unfortunately, the vapour and liquid equilibrium-phase compositions cannot be determined from **Fig. 1**. When the states and densities of the pure components and the mixture are similar (liquid-like fluid dinitrogen oxide and liquid toluene forming a liquid or liquid-like fluid mixture), the values of H^E are negative or slightly positive. This is so for isobars at 12.27 MPa and 15.00 MPa when the values of density are similar for dinitrogen oxide and toluene. When the states and densities of the pure components differ (gas-like fluid dinitrogen oxide and liquid toluene), and the resulting mixture is a liquid, large negative values of H^E are observed. This is so for the isobar at 7.60 MPa when the density of dinitrogen oxide is much lower than that of toluene. The isobar at 9.49 MPa presents an intermediate situation between those shown at 7.60 MPa and 12.27 MPa.

The shape of the isobars in **Fig. 1** denotes a behaviour similar to that previously reported fro $\{xCO_2 + (1-x)C_6H_5CH_3\}$ **[5]**. The critical point of carbon dioxide **[17]** (T_c = 304.21 K; p_c = 7.38 MPa) is very close to that of dinitrogen oxide and the $\{xCO_2 + (1-x)C_6H_5CH_3\}$ and $\{xN_2O + (1-x)C_6H_5CH_3\}$ critical loci are very similar. The temperature and pressures at which experimental measurements have been made for $\{xCO_2 + (1-x)C_6H_5CH_3\}$ and $\{xN_2O + (1-x)C_6H_5CH_3\}$ have a similar position with respect to the critical locus in the p against T plot. This may be seen by comparing the plot of **Fig. 2** with a similar one shown for $\{xCO_2 + (1-x)C_6H_5CH_3\}$ in figure 3 of reference 5.

ACKNOWLEDGEMENT

This work was funded by the Spanish Ministry of Education (DGICYT) Research Project PB-91-0392. We appreciate the aid given to us in estimating the critical locus by Dr. R. A. Heidemann. R. C. Castells wishes to acknowledge the Universidad Complutense of Madrid for a vising research professorship at the Department of Physical Chemistry.

REFERENCES

[1] Machado, J. R. S., Gubbins, K. E., Lobo, L. Q., Staveley, L. A. K.- **J. Chem. Soc. Faraday Trans. I, 76**, 2496 (1980).

[2] Wormald, C. J., Eyears, J. M.- **J. Chem. Soc. Faraday Trans. I, 84**, 3097 (1988).

[3] Sakaki, K.- **J. Chem. Eng. Data, 37**, 249 (1992).

[4] Alexandrou, N., Lawrence, M. J., Pawliszyn J.- **Anal. Chemistry, 64**, 301

(1992).
[5] Pando, C., Renuncio, J. A. R., Schofield, R. S., Izatt, R. M., Christensen, J. J.- **J. Chem. Thermodynamics**, **15**, 747 (1983).

[6] Christensen, J. J., Izatt, R. M.- **Thermochim. Acta**, **73**, 117 (1984).

[7] Christensen, J. J., Hansen, L. D., Izatt, R. M., Eatough, D. J., Hart, R. M.- **Rev. Sci. Instrum.**, **52**, 1226 (1981).

[8] Gmehling, J.- **J. Chem. Eng. Data**, **38**, 143 (1993).

[9] Couch, E. J., Hirth, L. J., Kobe, K. A.- **J. Chem. Eng. Data**, **6**, 229 (1962).

[10] Garbajosa, G., Tardajos, G., Aicart, E., Diaz Peña, M.- **J. Chem. Thermodynamics**, **14**, 671 (1982).
[11] Aicart, E., Tardajos, G., Diaz Peña, M.- **J. Solution Chem.**, **11**, 557 (1982).

[12] Reid, R. C., Prausnitz, J. M., Poling, B. E.- **The properties of Gases and Liquids**, McGraw-Hill, Singapore (1988).

[13] Heidemann, R. A., Khalil, A. M.- **AIChE J.**, **26**, 769 (1980).

[14] Peng, D. Y., Robinson, D. B.- **Ind. Eng. Chem. Fundam.**, **15**, 59 (1976).

[15] Langenfeld, J. J., Hawthorne, S. B., Miller, D. J.- **Anal. Chem.**, **64**, 2263 (1992).

[16] Takagi, T.- **Rev. Phys. Chem. Japan**, **48**, 17 (1978).

[17] **Carbon Dioxide, IUPAC Thermodynamic Tables of the Fluid State**. Angus, S., Armstrong, B., Renck, K. M. de, editors, Pergamon, Oxford (1976).

Note: This paper was published in J. Chem. Thermodynamics, **26**, *641-646 (1994).*

TABLE I

Experimental and calculated excess enthalpies H_m^E for $\{xN_2O + (1-x)C_6H_5CH_3\}$

x	H_m^E/(J.mol^{-1}) expt	calc.	x	H_m^E/(J.mol^{-1}) expt	calc.	x	H_m^E/(J.mol^{-1}) expt	calc.
			T = 313.15 K, p = 7.60 MPa					
0.097	-206	-274	0.337	-988	-960	0.738	-2129	-2082
0.142	-402	-402	0.390	-1047	-1110	0.840	-2319	-2320
0.189	-451	-535	0.430	-1249	-1225	0.892	-2318	-2396
0.240	-630	-681	0.530	-1610	-1511	0.946	-2293	-2334
0.289	-739	-822	0.634	-1895	-1802	0.990	-1466	-1435
			T = 313.15 K, p = 9.49 MPa					
0.049	-21	-17	0.442	-289	-295	0.824	-646	-646
0.097	-46	-38	0.489	-336	-343	0.843	-659	-648
0.122	-50	-50	0.542	-386	-399	0.869	-627	-639
0.147	-69	-64	0.592	-456	-452	0.894	-619	-616
0.196	-104	-93	0.640	-517	-503	0.901	-602	-606
0.246	-124	-127	0.694	-564	-557	0.930	-540	-541
0.246	-130	-127	0.743	-602	-601	0.947	-473	-474
0.294	-168	-163	0.750	-608	-607	0.969	-340	-345
0.346	-198	-206	0.796	-635	-637	0.990	-155	-144
0.393	-243	-248	0.816	-643	-645	0.995	-82	-76
			T = 313.15 K, p = 12.27 MPa					
0.050	6.3	6.0	0.347	-27	-27	0.708	-243	-240
0.050	7.5	6.0	0.400	-47	-48	0.749	-265	-266
0.099	11.0	9.1	0.450	-73	-71	0.801	-296	-294
0.126	11.0	9.5	0.450	-70	-71	0.821	-301	-300
0.149	11.0	9.0	0.497	-99	-96	0.873	-302	-301
0.199	4.1	5.5	0.545	-126	-126	0.897	-282	-288
0.252	0.25	-2.2	0.600	-160	-162	0.932	-254	-247
0.252	-4.6	-2.3	0.647	-191	-196	0.970	-145	-147
0.303	-17.0	-14.0	0.700	-233	-234	0.990	-52	-57
			T = 313.15 K, p = 15.00 MPa					
0.051	19.0	20.0	0.405	55	60	0.857	-133	-134
0.101	42.0	36.0	0.456	53	50	0.882	-143	-137
0.152	53.0	50.0	0.503	42	36	0.906	-135	-135
0.202	60.0	60.0	0.559	21	19	0.929	-125	-125
0.256	65.0	66.0	0.605	-8.5	-5.6	0.950	-104	-105
0.307	65.0	68.0	0.713	-64.	-64	0.971	-769	-76
0.351	65.0	67.0	0.804	-111.	-114	0.990	-27	-30

TABLE II

Parameters and standard deviations s for least-squares representation of H_m^E/(J.mol^{-1}) for $\{xN_2O + (1-x)C_6H_5CH_3\}$ by equation 1

p/MPa	7.60	9.49	12.27	15.00
C_0	-5932.6	-1399.8	-392.42	148.81
C_1	-904.67	-905.57	-860.69	-766.30
C_2	1875.8	-78.751	-207.28	-177.83
C_3	709.53	265.54	--	--
C_4	-1205.8	--	--	--
k	-0.98066	-0.87088	-0.77261	-0.77149
s	49	6.5	2.9	3.2

TABLE III

Densities of dinitrogen oxide and toluene at the conditions of temperature (T = 313.15 K) and pressure p of the experiments

p/MPa	p/(kg.m^{-3})	
	dinitrogen oxide	toluene
7.60	326	855
9.49	672	857
12.27	743	859
15.00	786	861

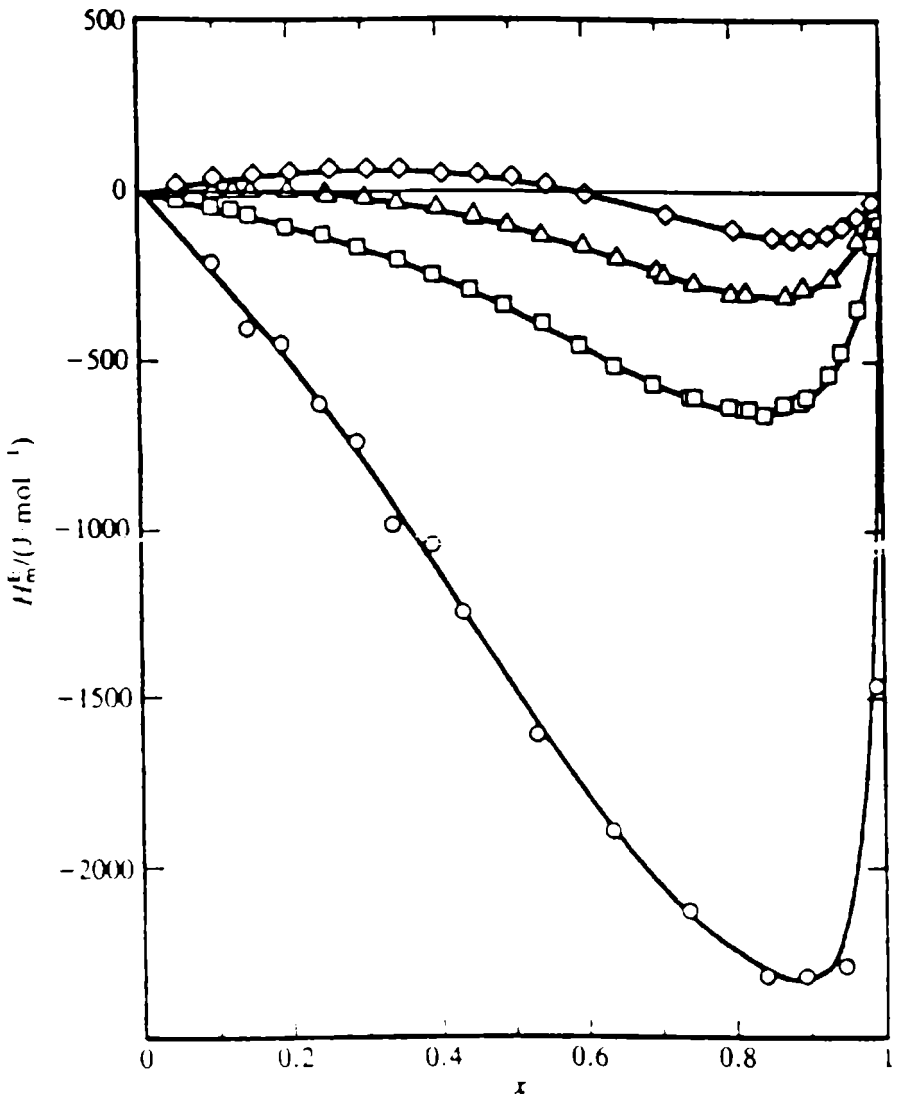

Fig. 1.- Plot of H_m^E against x for $\{xN_2O + (1\text{-}x)C_6H_5CH_3\}$ at T = 313.15 K as a function of pressure: O 7.60 MPa; □ 9.49 MPa; Δ 12.27 MPa; ◇ 15.00 MPa; —— calculated from equation (1).

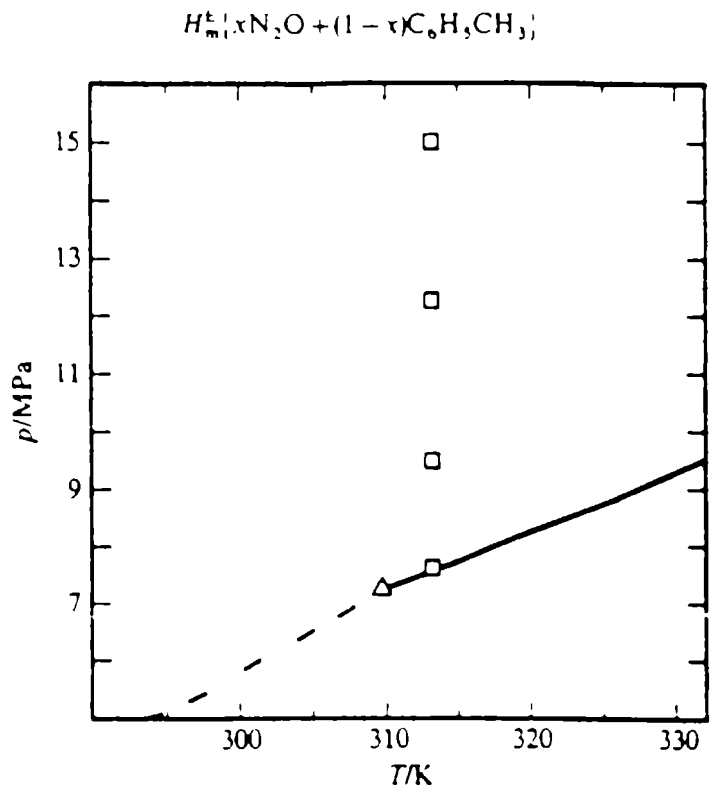

Fig. 2.- Plot of p against T for $\{xN_2O + (1\text{-}x)C_6H_5CH_3\}$ showing ---, the (vapour + liquid) equilibrium curve; Δ, the critical point of dinitrogen oxide; ——, the critical locus; and □, the (T,p) coordinates where experimental measurements were made.

PROPUESTA DE UN METODO PARA LA DETERMINACION DE TENSION DE ADHESION Y COHESION DE MATERIALES TERMOPLASTICOS PARA LA DEMARCACION DE PAVIMENTOS

PROPOSAL FOR A METHOD TO DETERMINE THE COHESIVE OR ADHESIVE BOND STRENGTH OF TRAFFIC MARKING THERMOPLASTIC MATERIALS

A. C. Aznar[1]

SUMMARY

A new method to determine the cohesive or adhesive bond strength of thermoplastic materials employed for traffic marking is proposed. The obtained results were more precise than those provided by ASTM D-4796-88 and IRAM specifications currently used.

Different reflective thermoplastic materials were prepared in laboratory scale using different pigment volume concentrations (PVC) to verify the accuracy of the method. Higher values of bond strength and cohesion were obtained at lower PVC values. A progressive decrease of those values were obtained when PVC increases.

Keywords: *bond strength (tensión de adhesión), cohesion (cohesión), thermoplastic reflective material (material termoplástico reflectante), traffic demarcation (demarcación de franjas de tránsito).*

Definiciones

Para la determinación de las fuerzas de adhesión al hormigón y de cohesión del material termoplástico (que son dos medidas realizadas simultaneamente en el mismo ensayo), el procedimiento tiene en cuenta los siguientes factores:

a) Lograr, como condición prioritaria, que el esfuerzo de tensión de tracción, **se distribuya uniformemente** en la totalidad del área de contacto tal como se representa en la **Fig. 1**.

b) Reducir la influencia de los efectos no deseables que se **localizan en forma axial** y que producen tensiones no deseadas para el ensayo, tales como:

Cizallamiento: se inicia en el momento en que la fuerza actúa paralelamente al plano de la junta **(Fig. 2)**.

Desgarramiento: a pesar de tratarse de una situación similar a la tracción, ya que el esfuerzo se aplica en forma perpendicular, actúa sólo en uno de los lados de la unión, mientras que el resto permanece sin tensión **(Fig. 3)**.

---

[1] Personal de Apoyo del CONICET y Planta Permanente CIC

Peladura o escoriación: que se restringe a una línea delgada en el borde de la unión **(Fig. 4)**.

En consecuencia, las cualidades exigibles para la preparación de las probetas para ensayo para el desarrollo del método son las siguientes:

- Lograr la distribución uniforme de los esfuerzos en la totalidad del área de contacto.

- Lograr una menor influencia de los efectos no deseables.

Preparación de las probetas de hormigón para la realización del ensayo

Se prepararon probetas de hormigón en moldes de acero, utilizando una mezcla de arena-cemento, en relación volumétrica 2,5:1. Se introdujo un alambre de acero galvanizado flexible de 1,5 mm de espesor y 400 kg de resistencia a la tracción, de la forma, dimensiones y posición que se indica en la **Fig. 5**.

Las probetas se sometieron a curado en un ambiente saturado de humedad y a temperatura ambiente durante 20 días.

Imprimación de las probetas de hormigón

A las probetas secas, se les aplicó con pincel una capa de imprimación de la siguiente composición:

Resina acrílica 50 % de sólidos (g)	30,0
Resina alquídica 50 % de sólidos (g)	7,0
Aditivos (g)	0,7
Tolueno (g)	62,3

El tiempo de secado duro de la película aplicada fue de 20 minutos.

Preparación de las muestras de material termoplástico

Se prepararon las muestras de material termoplástico por calentamiento en baño de aceite hasta 190 °C, mezclando manualmente sus componentes durante la operación de fundido. La composición de los mismos y el PVC de cada muestra se consignan en la **Tabla I**.

Procedimiento para la aplicación del material termoplástico a las probetas de hormigón para la realización de los ensayos

A las probetas de hormigón imprimadas se las precalentó a 40 - 45 °C en estufa. Este procedimiento trata de reproducir el calentamiento del pavimento que se realiza antes de la aplicación del material termoplástico, a fin de asegurar

que la masa fundida penetre en las irregularidades existentes.

El material se fundió en baño de aceite a 190 °C y se agregó sobre una probeta de hormigón (colocada en posición horizontal). Inmediatamente se colocó la segunda probeta, apoyándola sobre el material fundido. Luego se invirtió la posición de ambas probetas de manera de asegurar la distribución uniforme del termoplástico.

Seguidamente se retiró con una espátula filosa el exceso de material de los bordes. El espesor de termoplástico entre ambas probetas de hormigón es de 3 mm.

Realización del ensayo de tracción de las probetas

Las probetas preparadas se mantuvieron en ambiente de laboratorio 24 horas; luego se colocaron en un dinamómetro de 200 kg de carga máxima, tomando los alambres en las mordazas de la forma indicada en la **Fig.6**. Se aplicó el esfuerzo de tracción empleando una velocidad de 20 $cm.min^{-1}$, hasta el momento de la rotura y se tomó la lectura en kg. En la **Tabla II** se expresan los valores obtenidos.

Consideraciones

1.- Graficados los valores obtenidos en el ensayo de resistencia a la tracción (**Fig. 7**), se observa buena correlación entre los mismos y el PVC de las muestras preparadas; a mayor cantidad de ligante el valor de la resistencia a la tracción es mayor.

2.- Se observa una correlación prácticamente lineal de los valores de tensión de adhesión y cohesión en función de los distintos PVC de las muestras ensayadas; la excepción está constituída por la correspondiente a los PVC entre 55 y 60 %. La inflexión podría deberse a que se ha alcanzado la concentración crítica de pigmento en volumen (CPVC)

3.- Resulta importante la observación de la dispersión que se produce para una misma muestra (**Figs. 8 y 9**). Se determinó que a medida que aumenta el PVC (menor cantidad de ligante) esta dispersión se hace más significativa. Esto indica que el número de ensayos que se deberá realizar será mayor a medida que los valores de tracción sean inferiores.

4.- El método propuesto es rápido, de fácil realización y las probetas pueden ser utilizadas en más de una determinación. Para ello se deberá eliminar previamente el material que quede adherido a la base del hormigón por calentamiento, limpiando finalmente con disolventes orgánicos.

5.- Por lo expresado en el punto 3, se estima que deben realizarse como mínimo 10 ensayos de tracción en cada muestra, para evaluar un material termoplástico para demarcación de pavimentos.

6.- Para valores de PVC bajo (mayor relación ligante/carga inerte), los valores de tracción obtenidos son altos y uniformes. A medida que el PVC aumenta, los valores de tracción se reducen significativamente con mayor dispersión de los resultados.

7.- El valor mínimo establecido en las Normas IRAM y en especificaciones particulares para el ensayo de tracción de este tipo de materiales es de 10 $kg.cm^{-2}$, lo que coincide con el obtenido para la muestra N° 4 (PVC 62,3). En este caso no existe gran dispersión de resultados y a partir de ahí la dispersión

resulta menor. En las Normas ASTM e IRAM se establecen cantidades mínimas de aglutinante entre 18 y 25 % en peso.

8.- La carga de despegue, resulta muy similar a la de cohesión del material.

REFERENCIAS

[1] ASTM D 4796 - **Standard Test Method for Bond Strength of Thermoplastic Traffic Marking Materials**, Vol. 06.01, 846-849 **(1988).**

[2] Castells, R., Meda, J., Caprari, J. J. y Damia, M. – **Particle Packing Analisis of Coatings Above the Critical Pigment Volume Concentration, J. Coat. Techn., 55** (707), 53-59 (1983).

[3] Liesa, F. y Bilurbina L. - **Adhesivos Industriales**. Marcombo S.A., Barcelona, España, 17-26 (1990).

[4] Lindberg, B. - **Painting Concrete. J. Oil col. Chem. Assoc., 57**, 100-113 (1974).

[5] Norma IRAM 1212 - **Recubrimientos Termoplásticos Reflectantes para Demarcación de Pavimentos**. Diciembre 1971.

[6] Nutt, N. O. - **Concrete as a Substrate for Paint, J. Oil col. Chem. Assoc., 51**, 702-709 (1968).

[7] Oosterbroek, A.M., Boerman, A. E. y Bosma, M. - **A Cuantitative Method for Determining the Adhesion of Coatings to Plastics. J. Oil col. Chem. Assoc., 75**, 53-58 (1992).

[8] Payne, H. F. - **Organic Coating Technology**, Vol. II, John Wiley & Sons, EE.UU. (1961).

TABLA I

Composición de los materiales termoplásticos experimentales

	Muestra N° 1	Muestra N° 2
Aglutinante (g)	22,0	19,8
Plastificante (g)	3,3	3,0
Pigmento (Materiales de carga)(g)	54,7	57,2
Esferas de vidrio (g)	20,0	20,0
PVC (conc. de pigmento en volumen)	51,1	54,6

	Muestra N° 3	Muestra N° 4
Aglutinante (g)	17,6	15,4
Plastificante (g)	2,6	2,3
Pigmento (Materiales de carga)(g)	59,8	62,3
Esferas de vidrio (g)	20,0	20,0
PVC (conc. de pigmento en volumen)	58,4	62,3

	Muestra N° 5	Muestra N° 6
Aglutinante (g)	13,2	11,0
Plastificante (g)	2,0	1,7
Pigmento (Materiales de carga)(g)	64,8	67,3
Esferas de vidrio (g)	20,0	20,0
PVC (conc. de pigmento en volumen)	66,5	71,0

TABLA II

Valores obtenidos en los ensayos de tracción

Determinaciones (kg)	Muestra N°					
	1	2	3	4	5	6
1	200	179	143	140	151	110
2	200	183	148	140	143	110
3	200	179	151	161	146	100
4	190	173	170	141	130	129
5	200	196	175	135	125	63
6	200	190	180	132	120	131
7	200	158	156	135	121	105
8	200	166	146	130	132	58
9	200	191	163	151	131	133
10	200	180	160	145	135	105
11	200	190	155	140	128	141
12	200	160	163	138	126	130
13	200	180	163	136	121	120
14	200	196	165	169	126	115
15	183	181	151	162	136	111
16	200	185	143	141	123	126
17	191	180	155	153	149	112
18	200	185	143	141	119	109
19	200	190	156	134	120	92
20	200	180	163	141	113	90

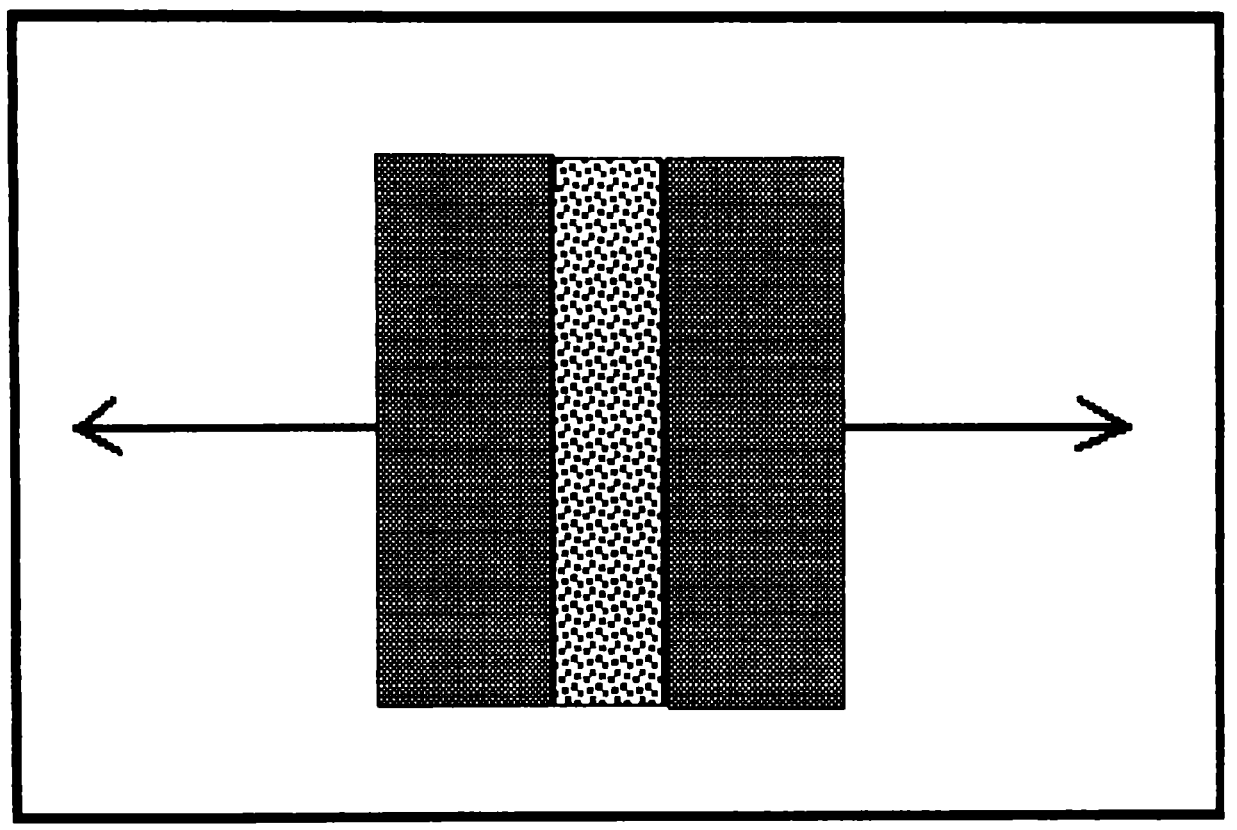

Fig. 1.- Representación del esfuerzo de tracción.

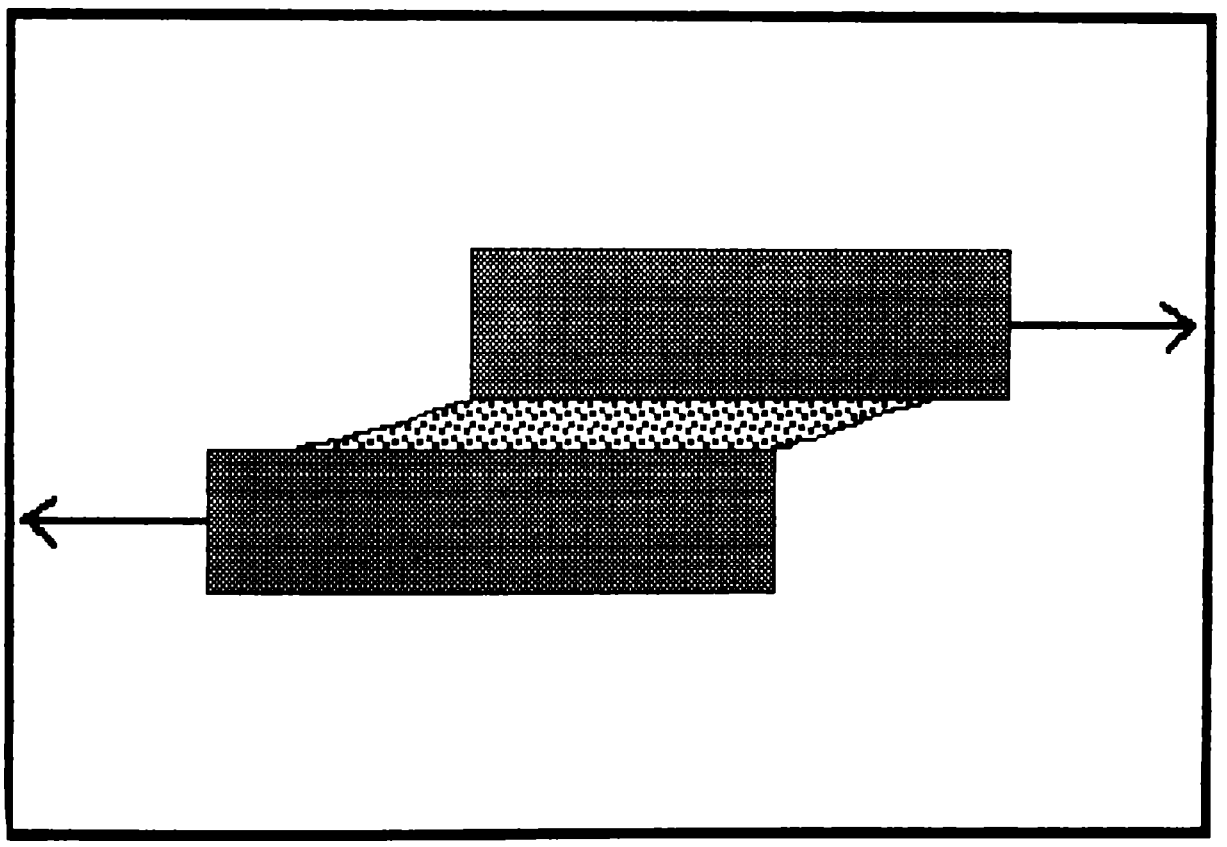

Fig. 2.- Representación del esfuerzo de cizallamiento.

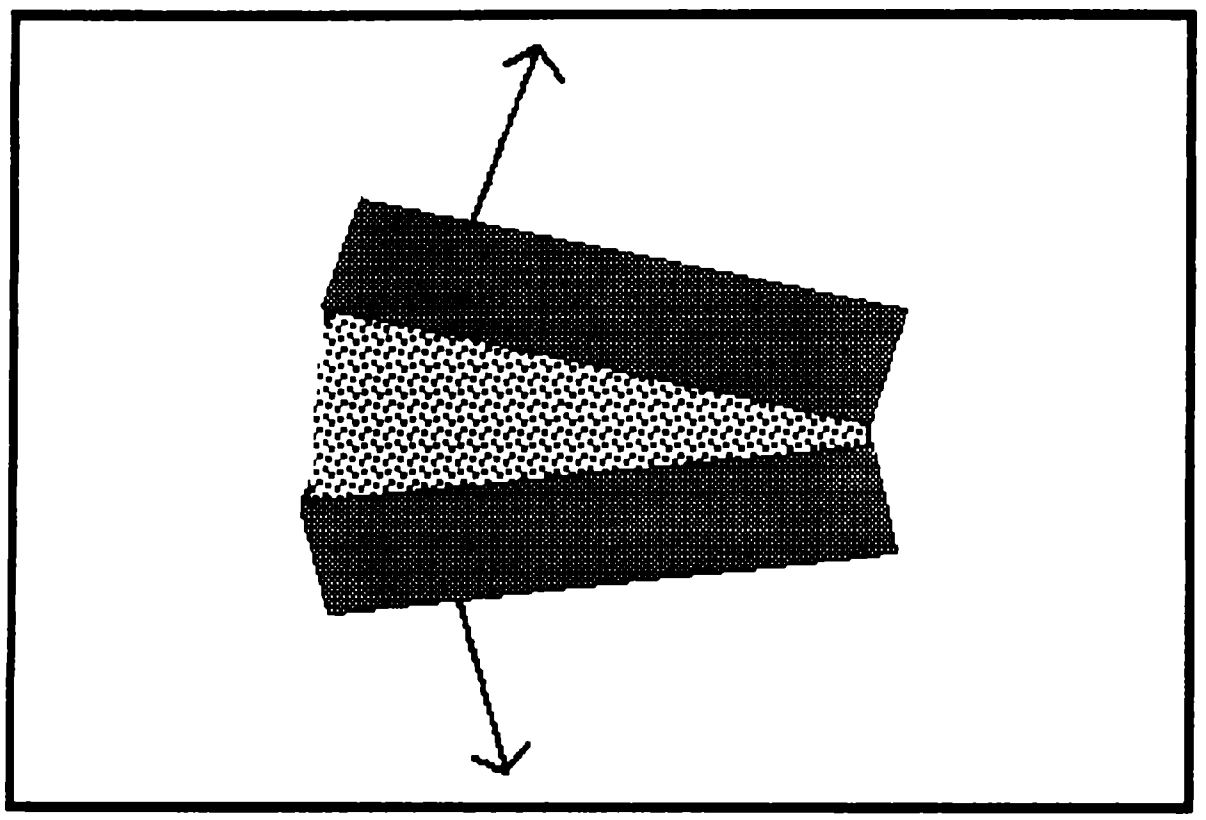

Fig. 3.- Representación del esfuerzo de desgarramiento.

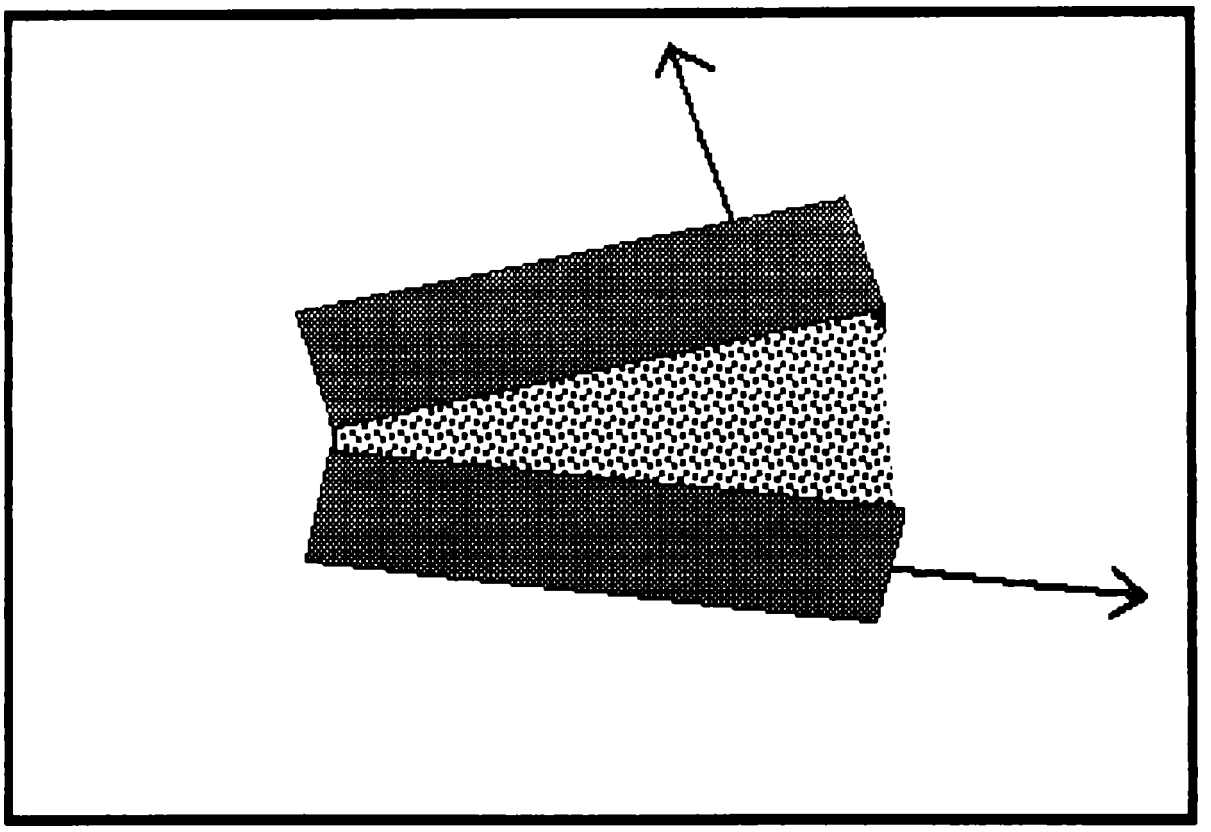

Fig. 4.- Representación del esfuerzo de peladura o escoriación.

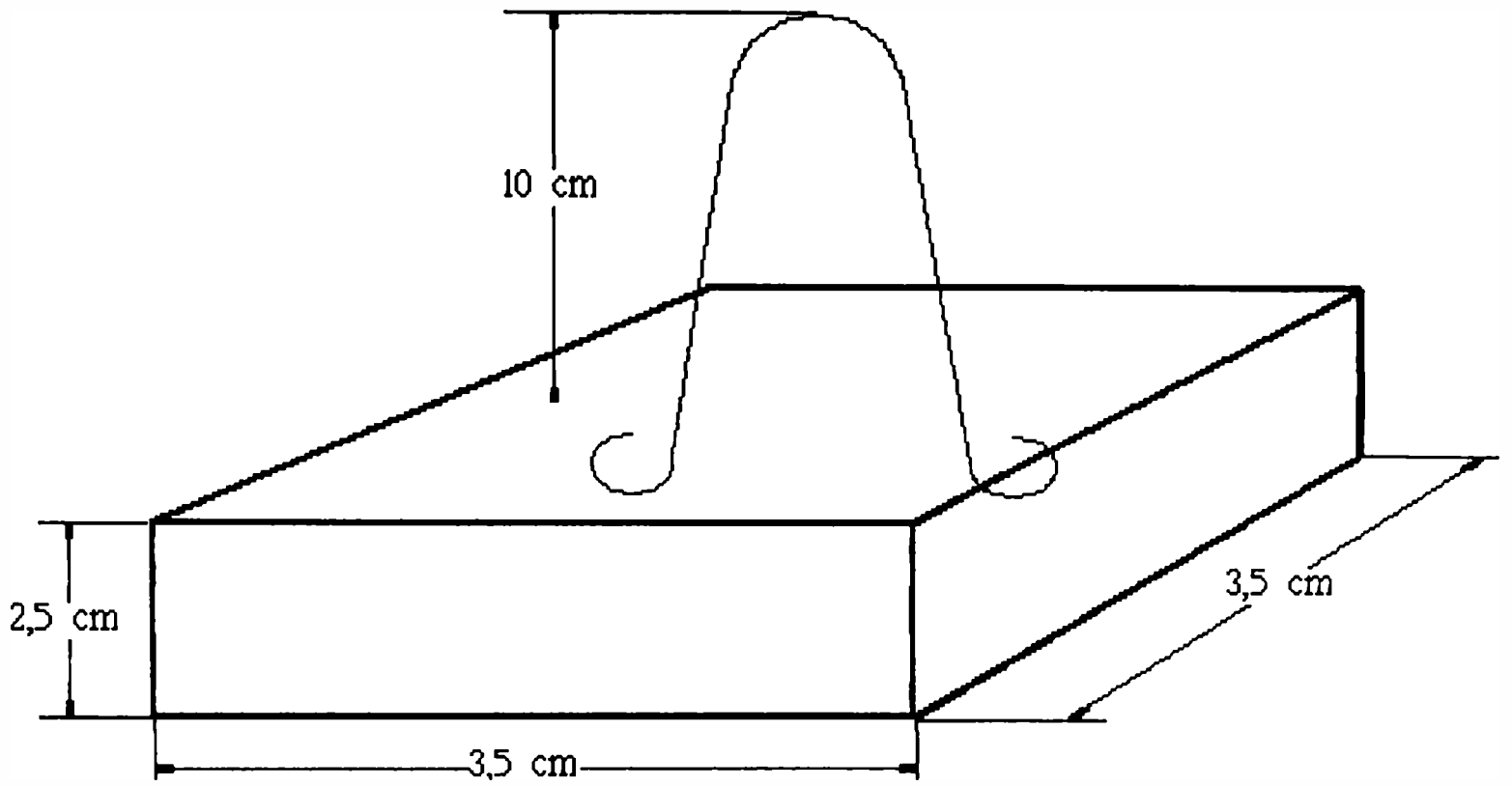

Fig. 5.- Esquema para la confección de las probetas de hormigón utilizadas en el ensayo de tensión de adhesión y cohesión con el alambre galvanizado incluido en la posición que se indicó.

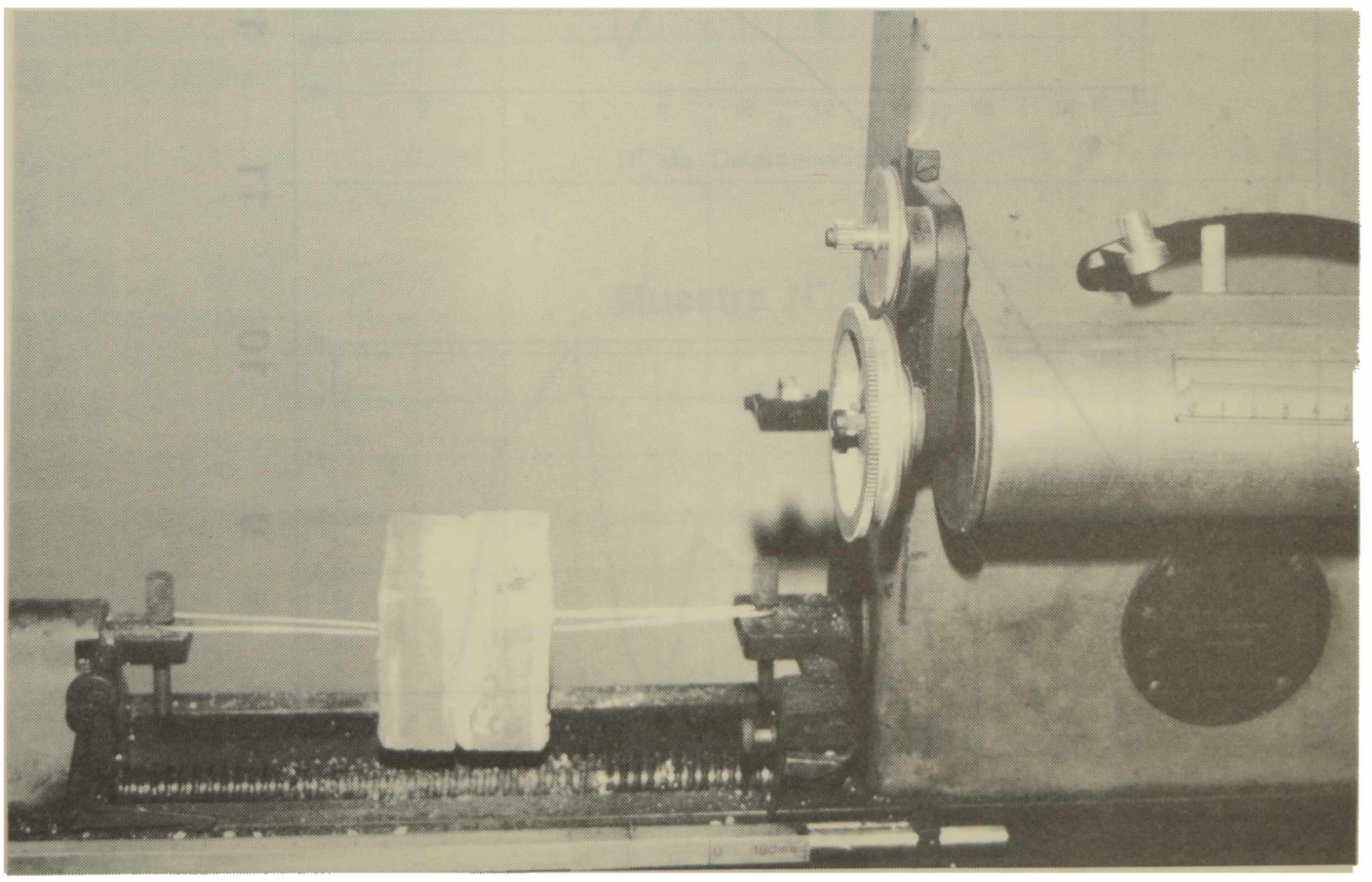

Fig. 6.- Ejecución del ensayo de tensión de adhesión y cohesión por tracción empleando un dinamómetro de 200 kg de carga máxima.

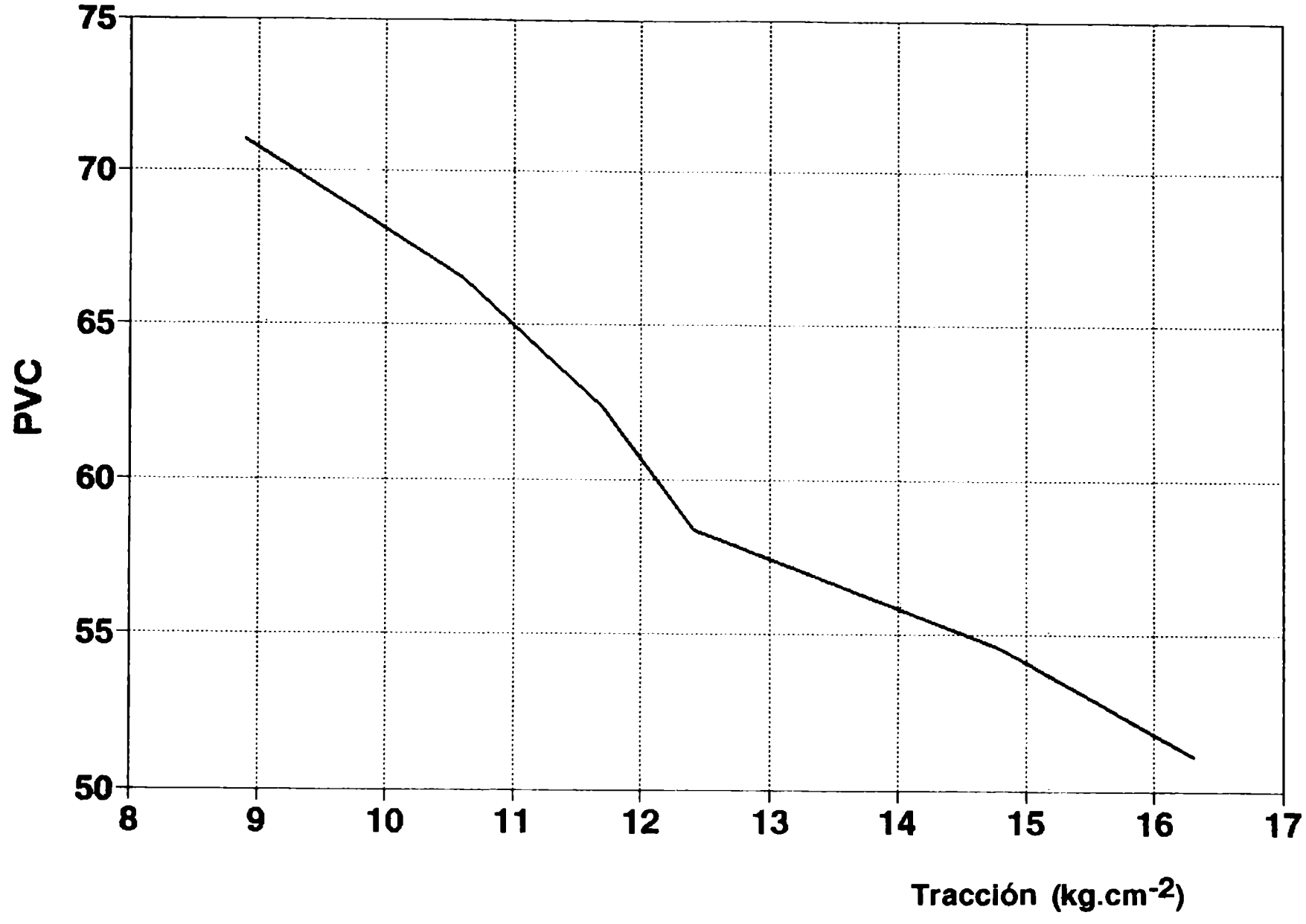

Fig. 7.- Representación de los valores de tensión de adhesión y cohesión en función de los distintos PVC de las muestras ensayadas.

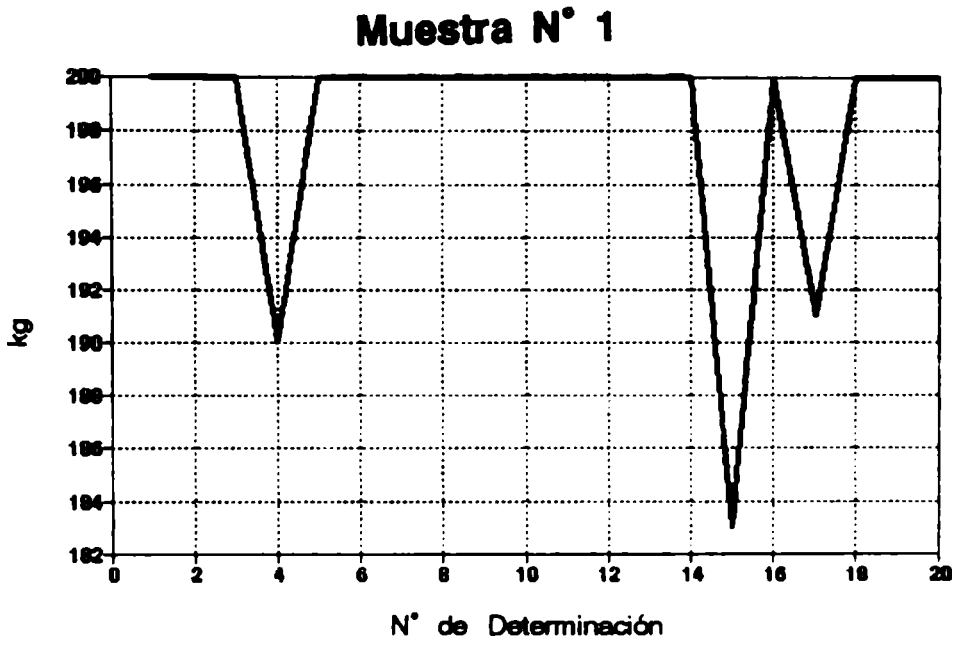

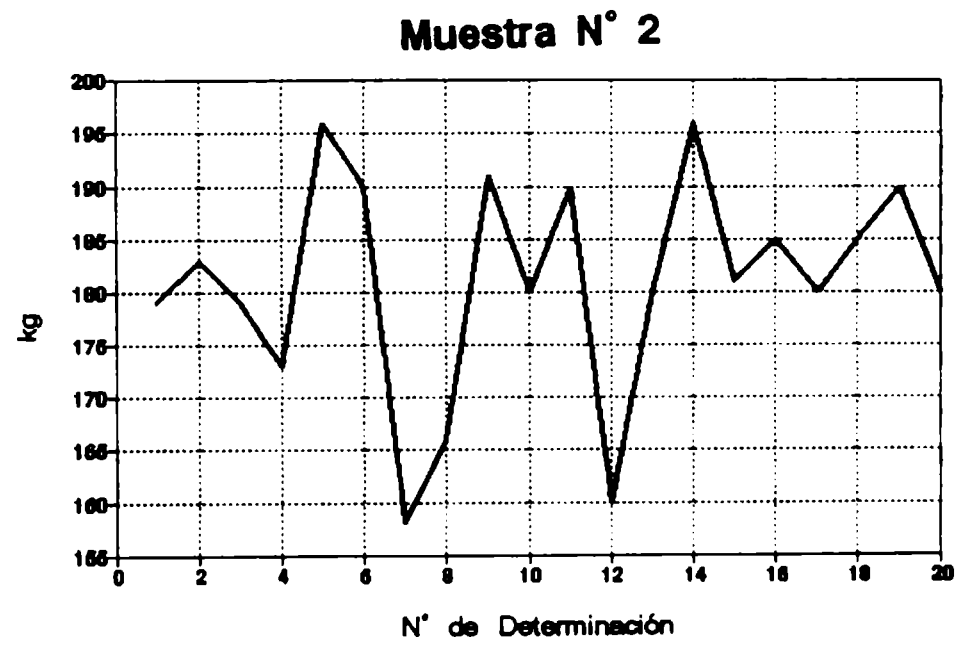

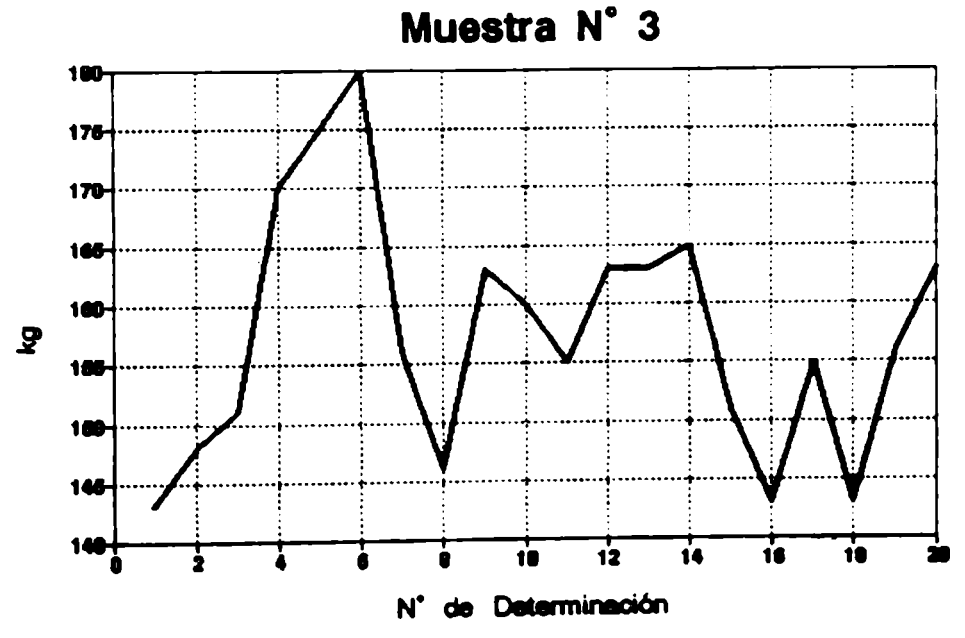

Fig. 8.- Dispersión de los valores de tensión de adhesión y cohesión de las muestras N° 1, 2 y 3.

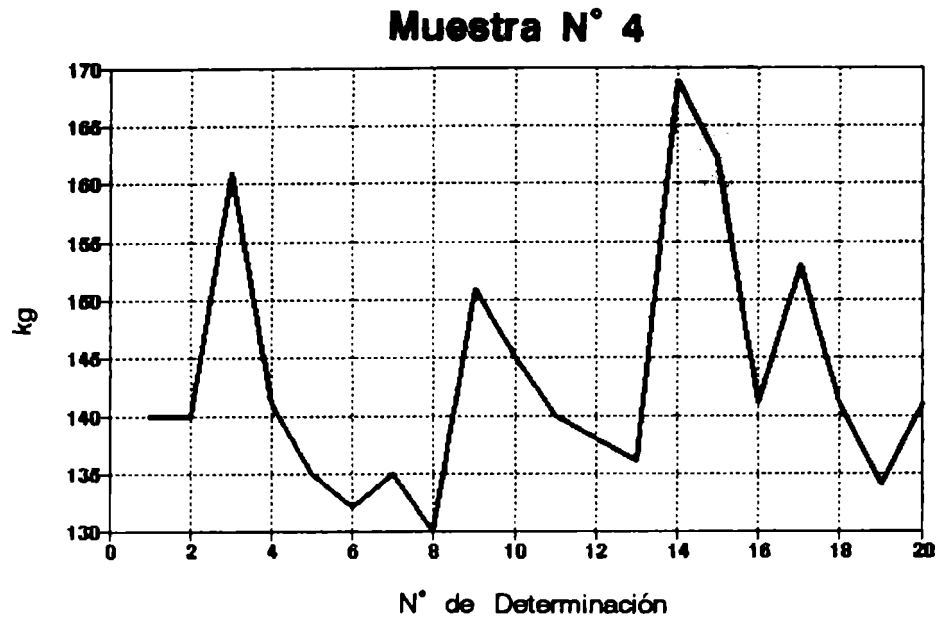

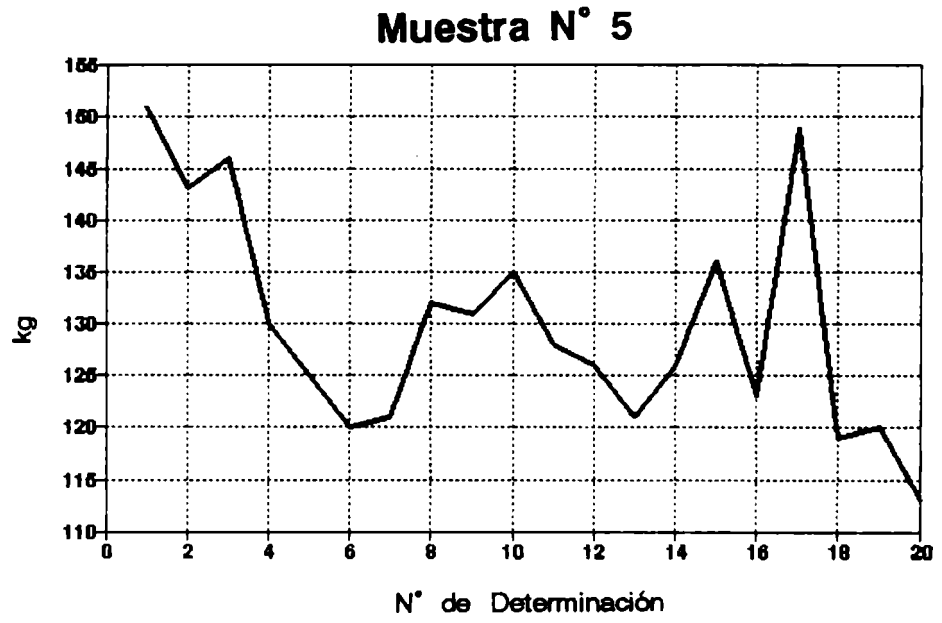

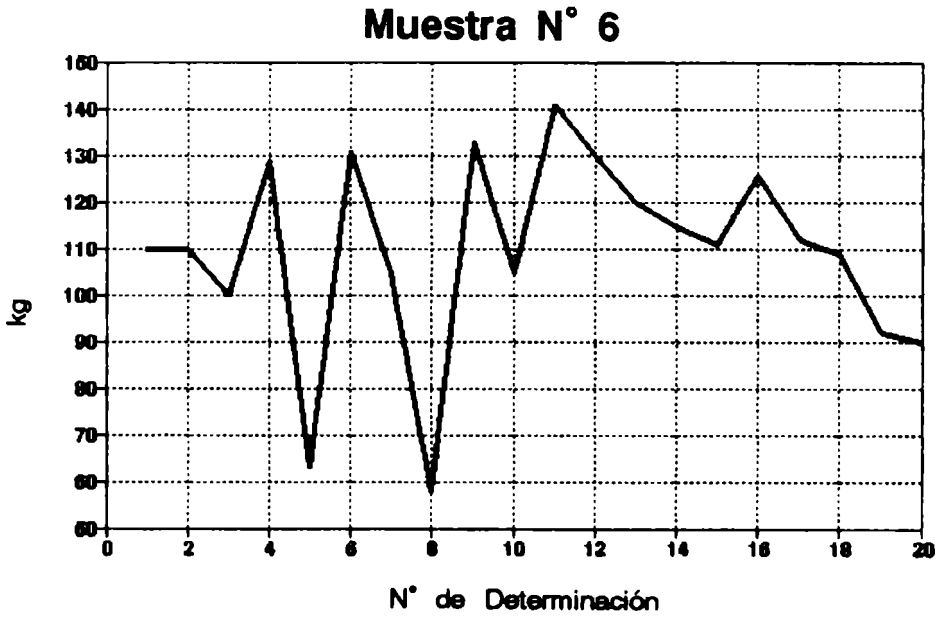

Fig. 9.- Dispersión de los valores de tensión de adhesión y cohesión de las muestras N° 4, 5 y 6.

PINTURAS. ASPECTOS ECOLOGICOS RELACIONADOS CON SU EMPLEO. IMPACTO AMBIENTAL PRODUCIDO POR LOS DISOLVENTES, COMPONENTES DEL LIGANTE Y ADITIVOS[1]

PAINTS. ECOLOGICAL ASPECTS RELATED TO ITS USAGE. ENVIRONMENTAL IMPACT PRODUCED BY SOLVENTS, BINDER COMPONENTS AND ADDITIVES

J. J. Caprari[2]

ABSTRACT

This paper deals with the ecological impact produced by the elaboration and application of paints. This trend has induced the governments of different countries to establish legal regulations in order to limit the environmental effect of solvents.

The possible pollution sources are briefly described but those derived from the different paint formulations are specially studied. A particular interest has been also devoted to the application stage when a drastic volatile solvent liberation takes place. Such effect is afterwards less severe along the useful life-time of the paint system.

The Volatile Organic Compound (VOC) concept and its numerical value, detemined according to ASTM standards, together with the effects of different emission sources on the environment (heat retention and the action on water, flora and fauna) are also reported.

Likewise, the indexes used to establish the contamination degree as well as the discrepancies among the different values obtained are described.

Finally, a brief reference to the new products appearing in the market to create a "Green Technology in Paints" is made.

Keywords: *VOCs, Volatile Organic Compouds; BOD5, Biological Oxygen Demand 5 Days; POCP factor, Photochemical Oxidant Creation Potential Factor; UV curing paints; solvent free paints; emulsion based paints.*

INTRODUCCION

La constante evolución tecnológica permite la realización de estudios científicos cada vez más profundos sobre el impacto que la actividad industrial produce sobre el medio ambiente, en especial por la generación de residuos no reciclables y los daños que los mismos causan sobre el ecosistema. Por consiguiente, los considerables progresos alcanzados en las técnicas de operación, procesos e instalación de plantas químicas contribuyen a una mayor protección

---

[1] Conferencia dictada en la Asociación Argentina de Corrosión, Rosario, octubre 1993

[2] Miembro de la Carrera del Investigador del CONICET

ambiental. Dentro de estas plantas se encuentran las dedicadas a la elaboración de pinturas y sus derivados, fabricación de resinas, pigmentos y aditivos.

La emisión de contaminantes producidos por las pinturas reconoce al menos cinco fuentes básicas:

a) Operaciones de obtención de materias primas y del producto final. Pueden afectar la salud del trabajador, por la carencia o el uso inadecuado de elementos de seguridad.

b) Alteración del medio ambiente. Por la emisión de polvo proveniente de pigmentos contaminantes (derivados del plomo, cromatos, polvos metálicos, etc.) y/o por la producción de residuos provenientes de la limpieza de equipos, que son reciclados en gran proporción pero que siempre conducen a la formación de un producto residual último, no aprovechable (aún cuando sea en cantidad mínima), que debe ser dispuesto y retirado de la planta. Durante todas las operaciones mencionadas se produce, inevitablemente, la emisión de compuestos volátiles orgánicos (VOCs) que para no contaminar el ambiente de trabajo son eliminados por extractores pero afectan la atmósfera a nivel de estratósfera y tropósfera.

c) Operaciones de preparación y pretratamiento de superficies. Durante la preparación y el pretratamiento de superficies por proyección de abrasivos, la composición del polvo atmosférico puede ser alterada por la emisión de materiales silíceos (arenas), metales agresivos (escorias de fundición de cobre o bronce) y también de aquéllos provenientes del material removido, en especial de sistemas anticorrosivos aplicados muchos años atrás y cuyos principales pigmentos estaban constituídos por minio, cromatos y tetroxicromatos de cinc, sulfato básico de plomo, etc. Estos afectan directamente a los operarios que intervienen en ellas por el ingreso al organismo de componentes acumulativos como el plomo de los pigmentos y secantes que contiene o puede contener la pintura y/o la sílice de la arena y/o por la alteración del medio ambiente en el lugar de trabajo, en los lugares cercanos de la planta o en lugares residenciales hacia donde son transportados por los vientos predominantes del lugar. Hay residuos que aparecen como consecuencia de otras operaciones de preparación de superficie, cuyos volúmenes generan problemas de disposición del efluente. Así, durante el decapado del acero con ácido clorhídrico se producen dos efluentes: uno líquido, que contiene cloruros de hierro en un medio de alta acidez, proveniente del ácido sin reaccionar, que debe ser al menos neutralizado antes de su eliminación y el otro sólido, compuesto mayoritariamente por una mezcla de óxidos de hierro que, convenientemente tratados, constituyen una fuente importante de esta materia prima para la industria de la pintura.

d) Procedimientos de aplicación de las pinturas. Dependiendo del tipo de pintura empleada (convencional o de bajos sólidos, de altos sólidos o de base acuosa), del método de aplicación y del espesor de película requerido, el medio ambiente puede ser afectado antes de la aplicación de la pintura por la emisión de vapores de disolventes volátiles a la atmósfera cuando se ajusta la viscosidad del producto (dilución). Durante la aplicación, parte de los disolventes que se evaporan y de los sólidos que no llegan a la superficie a proteger (caso de la aplicación a soplete) son transportados a los alrededores por las corrientes de aire, afectando a las personas que, por no estar involucradas en la operación, no tienen los elementos de protección necesarios.

e) Emisiones que pueden producirse durante el tiempo de vida útil del producto aplicado. La película de pintura emite permanentemente pequeñas cantidades de contaminantes a la atmósfera, ya que dentro de su composición se incluyen aditivos, plastificantes y disolventes que, en forma total o parcial, son retenidos por el material constituyente del ligante o por los disolventes

incorporados al producto para dotarlo de características de secado y de nivelado adecuados. Estas sustancias producen dicha retención por las fuerzas eléctricas de diferente polaridad existentes entre los constituyentes de la pintura, y que pueden difundir o migrar hacia la superficie, evaporándose.

La contaminación producida durante la elaboración y la aplicación es un aspecto específico que afecta a los que participan en estas operaciones. Sin embargo, desde el punto de vista ecológico, deben considerarse también aquellos aspectos relacionados con el uso cotidiano de estos productos, información que debe ser difundida entre los profesionales y técnicos que planifican y supervisan las operaciones de mantenimiento y también entre los usuarios.

FORMULACION, MATERIAS PRIMAS UTILIZADAS Y CONTAMINACION

Los problemas de contaminación provienen de los conceptos de formulación manejados actualmente y que tienden a lograr un buen comportamiento en servicio y buena ecuación económica para el proveedor del producto. De ello se infiere la gran importancia que tiene una adecuada selección de las materias primas a fin de reducir la emisión de compuestos orgánicos volátiles (VOCs), en parte responsables del deterioro observado en las distintas capas de la atmósfera.

¿Qué se define como Compuesto Orgánico Volátil y cuáles son sus principales fuentes de emisión? Después de aplicada, una pintura se transforma en una película sólida compuesta por resinas, plastificantes, pigmentos, extendedores inertes, aditivos y secantes, que recubre la superficie a proteger. Algunos de estos componentes quedan retenidos durante toda la vida útil del recubrimiento mientras que otros se van eliminando gradualmente. Durante el proceso de formación de la película se produce la emisión de gran cantidad de componentes orgánicos volátiles, tales como tolueno, benceno, xileno, cloruro de metileno, tricloro-etano, etc.

Según las normas ASTM se considera compuesto orgánico volátil (VOC) a todo aquel disolvente hidrocarbonado emitido que es susceptible de participar en reacciones fotoquímicas atmosféricas, produciendo lo que se conoce con el nombre de "smog" fotoquímico.

Los niveles de VOC se expresan en gramos de disolvente por litro de pintura, y es posible calcularlos mediante la expresión:

$$VOC\ (g.l^{-1}) = \frac{A \times (B-C-D)}{100 - \frac{A.C}{D_w} - \frac{A.D}{D_{ex}}}$$

donde:

A, densidad de la pintura ($g.l^{-1}$).

B, contenido de volátiles en peso (incluida el agua) en la pintura (g).

C, contenido de agua en peso en la pintura (g).

D, contenido de disolventes excluidos en la pintura (g).

D_w, densidad del agua ($g.l^{-1}$).

D_{ex}, densidad de los disolventes excluidos ($g.l^{-1}$).

Se entiende por disolventes excluidos (D) los que participan de la fórmula pero se consideran ecológicamente inactivos, razón por la cual es necesario descontarlos junto con el contenido de agua de la formulación.

Cuando se expresa que el contenido de VOCs en una laca convencional es de 720 $g.l^{-1}$ equivale a decir que cuando un litro de laca se aplica sobre una superficie, 720 g de VOCs se evaporan y contribuyen a la polución atmosférica. Esta sola mención podría parecer en principio de escasa relevancia; sin embargo, en 1991 Munn estimaba que en el área de Los Angeles, California, se emitían 360 toneladas por día de solventes hidrocarbonados debido solamente a la actividad de la industria de la pintura y a su utilización con fines decorativos o protectores.

Es tal la importancia asignada a este factor que en los países desarrollados se han tomado medidas cuya rigurosidad aumenta permanentemente. Luego de años de estudio y en función de los resultados obtenidos en numerosas determinaciones y teniendo en cuenta la composición de los disolventes utilizados y comercializados en el área, las comisiones de regulación de New York y New Jersey han determinado los límites VOCs para los diferentes revestimientos empleados en el pintado y mantenimiento arquitectónico de ambas ciudades (**Tabla I**).

Las diferencias que pueden apreciarse en las distintas regulaciones se deben a los diversos criterios que adoptan los responsables de la especificación, aunque la tendencia es que dichos valores sean más restrictivos y se tomen en "boca de lata". Esta posición es razonable dado que el límite VOC establece los valores máximos permitidos en el producto, pero no tienen en cuenta las posteriores operaciones de ajuste de viscosidad que difieren según el método de aplicación que se emplean. Fundamentalmente se trata de mantener dichos valores en los mínimos permitidos incluyendo la dilución.

Es así que los VOCs mencionados en la Tabla I, con variaciones entre 450-680 para New York y entre 350-600 para New Jersey, se reducen en las especificaciones militares (MIL) a valores límite entre 133 y 420 $g.l^{-1}$ (**Tabla II**).

En la **Tabla III** se indican nuevos materiales definidos como peligrosos (año 1990).

En un simposio realizado en marzo de 1994 entre expertos de Marketing de diferentes compañías de la Comunidad Económica Europea, Sykes propuso a la Comisión Europea de Protección del Medio Ambiente una disminución de los VOCs para pinturas al agua de uso arquitectónico, partiendo de los valores de 1992 con un punto de referencia en 1996 y el final en el año 2000 (**Tabla IV**).

Estos límites están basados en la comprobación de los efectos ecológicos producidos por la emisión de contaminantes que, además de lo expresado en la definición ASTM mencionada precedentemente, alteran otros mecanismos naturales, al verificarse una disminución de espesor y extensión de la capa de ozono, un aumento del efecto invernadero, la producción de lluvias ácidas y el deterioro de las fuentes de agua (subterránea, de lagos, ríos y arroyos), lo que afecta la flora y la fauna.

Cinética de producción del "smog" fotoquímico

El "smog" fotoquímico es el principal fenómeno donde los disolventes hidrocarbonados empleados tienen gran influencia. Se desarrolla en la baja atmósfera, en especial en áreas densamente pobladas y de gran actividad industrial; su composición depende fundamentalmente de la emisión de óxidos de nitrógeno generados por la actividad humana. Un estudio realizado en el año 1985

TABLA I

Límites VOC de pinturas para obras civiles en New York y New Jersey

Tipo de recubrimiento	VOC (máximo), $g.l^{-1}$	
	New York	New Jersey
Barniz	450	350
Imprimaciones, selladores y pinturas de fondo	550	350
Selladores para inmersión	550	400
Entonadores	550	400
Lacas	680	600

TABLA II

Especificaciones VOC para pinturas de uso militar

Tipo de pintura	VOCs en el momento de la aplicación $g.l^{-1}$
IMPRIMACIONES	
Pinturas epoxídicas libres de compuestos de plomo y cromatos	420
Pinturas epoxídicas reducibles con agua libres de plomo y cromatos	340
Pintura para electrodeposición catódica, resistente a agentes químicos	144
PINTURAS DE TERMINACION	
Pinturas a base de poliuretano alifático, de dos componentes, resistente a agentes químicos	420
Pinturas a base de poliuretano alifático, de un componente, resistente a agentes químicos	420
Pintura epoxídica resistente a agentes químicos	420

TABLA III

Nuevos materiales definidos como peligrosos (año 1990)

Acrilonitrilo	Hexacloroetano
Benceno	Isobutinol
Bis(2 cloroetil)eter	Cloruro de metileno
Disulfuro de carbono	Metil etil cetona
Tetracloruro de carbono	Nitrobenceno
Chlordane	Pentaclorofenol
Clorobenceno	Fenol
Cloroformo	Piridina
O-Cresol	1-1-1-2 Tetracloroetano
M-Cresol	1-1-2-2 Tetracloroetano
P-Cresol	Tetracloroetileno
1-2 Diclorobenceno	2-3-4-6 Tetraclorofenol
1-4 Diclorobenceno	Tolueno
1-2 Dicloroetano	1-1-1 Tricloroetano
1-1 Dicloroetileno	1-1-2 Tricloroetano
Heptacloro	Tricloroetileno
Hexaclorobenceno	2-4-5 Triclorofenol
Hexaclorobutadieno	2-4-6 Triclorofenol
Cloruro de vinilo	

TABLA IV

Máximo contenido de VOCs propuesto para la Comunidad Económica Europea (en $g.l^{-1}$, excluyendo el agua y los entonadores)

Tipo de pintura	Contenido máximo de VOC, $g.l^{-1}$		
	1992	1996	2000
Látex interior, paredes y cielorrasos	10	1	1
Látex exterior, paredes	50	10	1
Estucado, interior	250	150	5
Estucado, exterior	250	150	5

sobre las fuentes de producción de nitrógeno en la ciudad de París **(Fig. 1)** permitió determinar que el 73,5 % correspondía a emisiones de automóviles, autobuses, camiones livianos, etc., el 6,1 % a las estaciones generadoras de energía eléctrica, el 12,2 % a la actividad residencial y servicios auxiliares menores o de tercer orden (tintorerías, panaderías, lavaderos) y el 8,2 % a la actividad industrial, donde se encuentra incluida la industria de la pintura en todos sus aspectos.

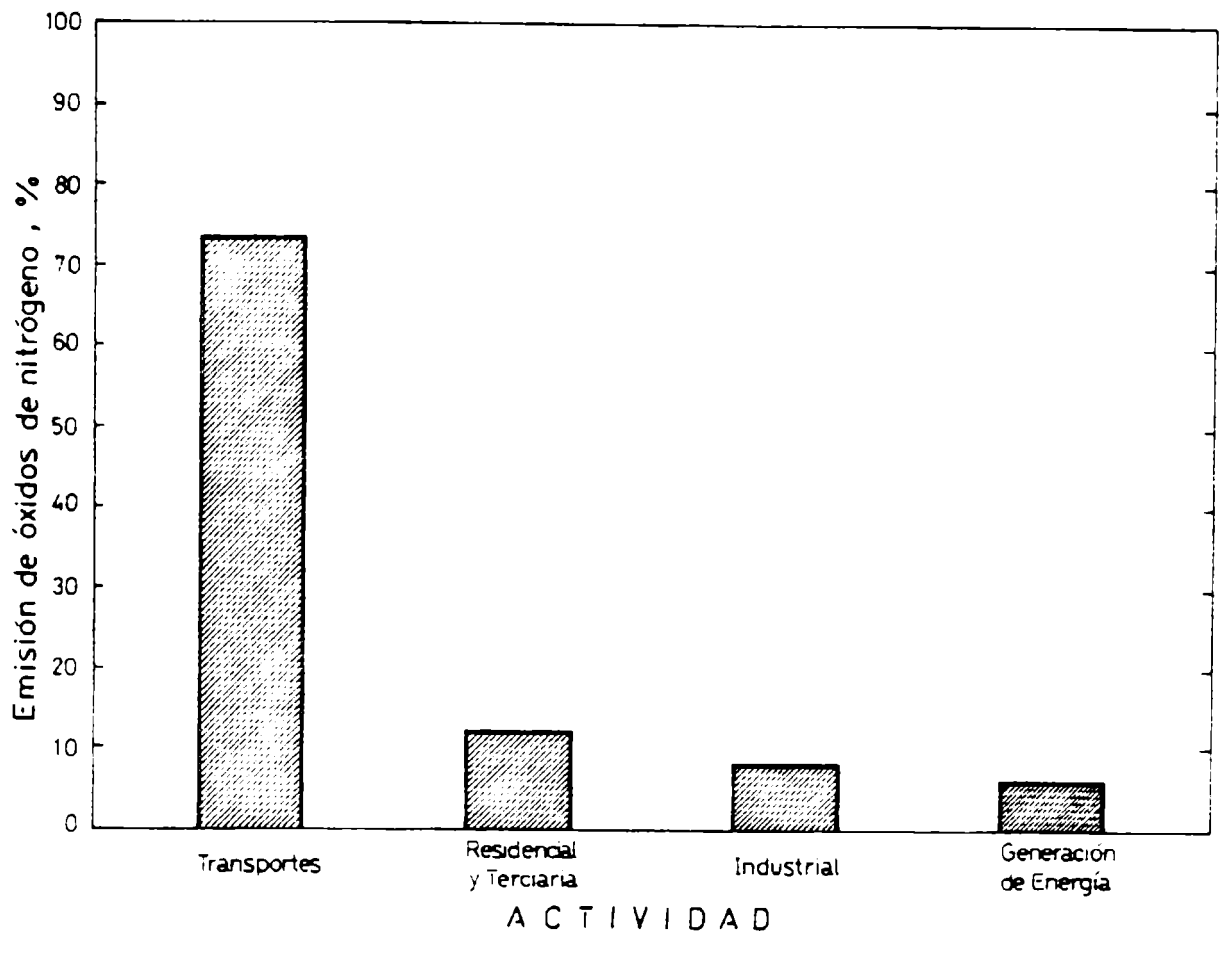

Fig. 1.- Fuentes de emisión (París, 1985).

En presencia de luz ultravioleta e hidrocarburos, el óxido de nitrógeno reacciona según se indica en la **Fig. 2.** Todos los productos de reacción son compuestos susceptibles de producir irritaciones agudas en ojos, sistema respiratorio o reacciones alérgicas de mayor o menor magnitud, en especial por un aumento de la concentración de ozono.

A la presencia de hidrocarburos debida a la mala combustión de motores y evaporación de combustibles en estaciones de servicio, se suma la evaporación de disolventes provenientes de operaciones de limpieza, emitidos durante la formación de la película en la operación de pintado, manteniendo constante la alta concentración de ozono en una región atmosférica donde naturalmente no existe y donde participa cíclicamente en otras reacciones y en su propia regeneración.

Una alta concentración de ozono en zonas bajas de la atmósfera es perjudicial, tanto como el efecto deteriorante de ciertos solventes sobre la capa de ozono en la atmósfera superior. Esto es así porque en la atmósfera inferior afecta la salud del ser humano mientras que su destrucción en la capa superior anula el efecto regulador de la intensidad de radiación UV que llega a la superficie terrestre.

El problema es particularmente importante en aquellas zonas donde, por la ubicación geográfica, los altos niveles de radiación UV, el poco viento y las altas temperaturas se produce una inversión atmosférica evitando que los

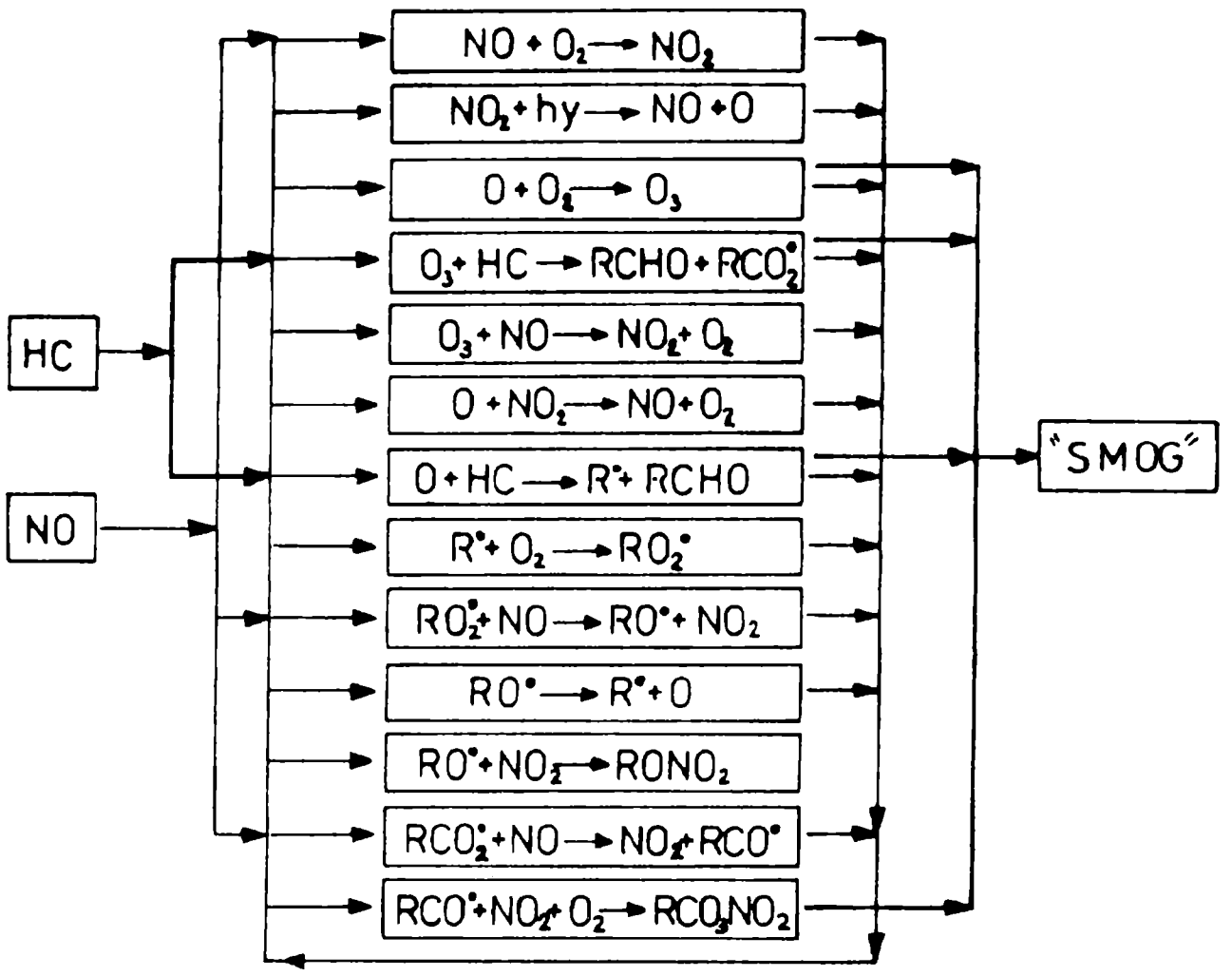

- NO Oxido nítrico
- HC Hidrocarburo
- NO_2 Dióxido de nitrógeno
- O_2 Oxígeno
- hy Energía solar
- O Oxígeno atómico
- O_3 Ozono
- $R^{\bullet}$ Radical alquílico
- $RO^{\bullet}$ Radical oxialquílico
- $RO_2^{\bullet}$ Radical peroxialquílico
- $RCO^{\bullet}$ Radical acilo
- $RCO_2^{\bullet}$ Radical oxiacilo
- $RONO_2$ Nitrato de alquilo
- RCO_3NO_2 Cpd X-Peroxinitrato de acilo
- RCHO Aldehido

Fig. 2.- Reacciones que tienen lugar durante la producción de "smog" fotoquímico.

contaminantes escapen rápidamente de la zona donde se originan. Aún cuando los períodos críticos tienen lugar en lapsos relativamente cortos, la velocidad de reacción de los hidrocarburos es el factor más importante en el aumento de la concentración de sustancias irritantes. Por ello, una adecuada elección de la mezcla disolvente contribuye no sólo a lograr una película final de buenas características y resistencia sino también a evitar los daños que se podrían causar al ecosistema. En este sentido, los disolventes isoparafínicos son de menor agresividad que los aromáticos.

Deterioro de la capa de ozono

El deterioro de la capa de ozono, es decir, su disminución en espesor y extensión comienza en la estratósfera, sobre los polos (entre los 20-30 km de altura). Se debe, en especial, a la acción de los compuestos clorofluorcarbonados sometidos a la fracción UV de la radiación solar, formándose radicales catalizadores de la descomposición del ozono y, en consecuencia, del deterioro atmosférico.

Este problema se ve agravado porque los compuestos mencionados, con una vida media relativamente larga (1 a 2 años), tienen tiempo suficiente para alcanzar y actuar en la alta atmósfera. Tanto los disolventes aromáticos como los isoparafínicos poseen una vida media menor de 24 horas y no actúan sobre la capa de ozono.

Efecto invernadero

En este aspecto, las opiniones de diversos investigadores son controvertidas. Según la teoría más difundida ciertos gases provenientes de sustancias de alto peso molecular contribuyen a evitar que los rayos infrarrojos de la luz solar, que llegan a la tierra, puedan ser reflejados o irradiados al espacio; al quedar atrapados al nivel de la tierra elevan paulatinamente su temperatura media, algo que se supone continuará, debido al incremento de la concentración de gases en la atmósfera (**Fig. 3**). En este aspecto se considera que uno de los principales factores es la concentración de dióxido de carbono (60 %) y metano (20 %); el primero proveniente de la actividad humana e industrial y el segundo de la actividad biológica (humana, animal y bacteriológica). Otro factor importante está constituido por los compuestos halogenados (15 %); sin embargo, su control y paulatina eliminación reducirá su influencia en los próximos años.

La industria de la pintura emplea disolventes agresivos en algunas pinturas horneables, en operaciones de desengrasado y en la elaboración de removedores orgánicos. En este último caso, la aparición de una nueva generación de productos con igual costo, baja toxicidad, baja solubilidad en agua, alto punto de ebullición y de autoignición, baja presión de vapor y excelente poder disolvente, a los que se une como factor importante el de ser biodegradables, posibilitarán su reemplazo en un corto lapso. Dichos productos son una mezcla refinada de ésteres dimetílicos derivados de los ácidos adípico, glutárico y succínico.

Hay evidencias que los disolventes aromáticos y alifáticos no producen metano pero si dióxido de carbono, aún cuando en proporciones extremadamente bajas en relación con las cantidades que aparecen como consecuencia de la actividad humana.

Producción de lluvia ácida

La lluvia ácida es causada por la emisión a la atmósfera de dióxido de azufre

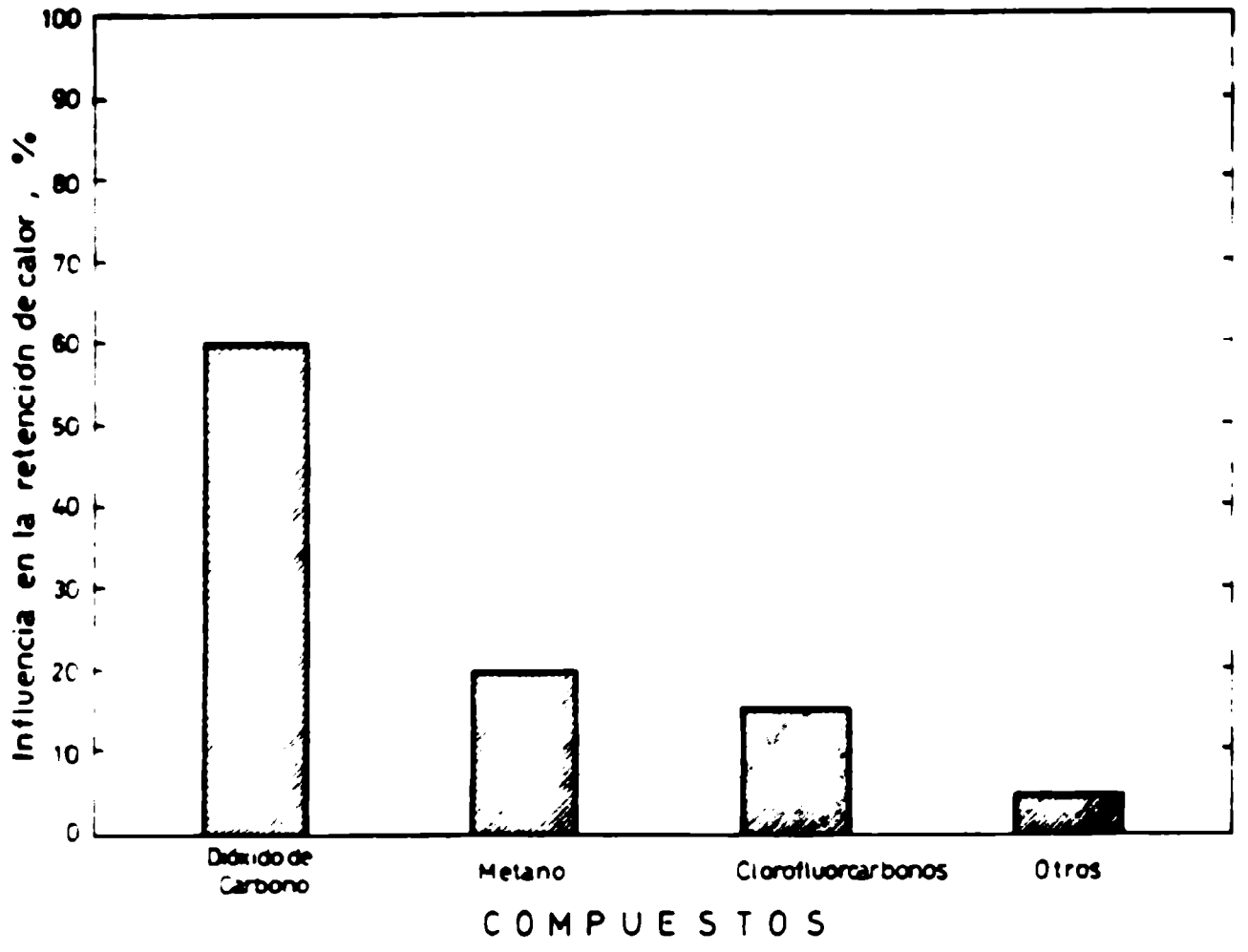

Fig. 3.- Influencia de diferentes compuestos en la retención del calor.

y óxidos de nitrógeno, provenientes de la combustión de naftas, diesel oil, gas oil, fuel oil, gas natural y envasado, carbón de madera y de piedra y de la deforestación. En este último caso, la operación se realiza quemando bosques y en otros casos rastrojos en campos ya cosechados. No existe evidencia de acción alguna relacionada con la emisión de disolventes provenientes de las pinturas.

Acción sobre el agua, la flora y la fauna

Los disolventes orgánicos empleados tienen diferente solubilidad en agua y su presencia tiene distintos efectos sobre el agua de ríos, napas freáticas, océanos y constituye un problema tan serio como la polución atmosférica. En algunos casos, la contaminación de los ríos subterráneos que en muchos casos proveen agua potable a la población, se transforma en un problema crítico debido a que es potencialmente irreversible.

Una forma de clasificar los efectos de estas sustancias en agua es determinando su toxicidad y su biodegradabilidad.

Todas las sustancias orgánicas expuestas a ambientes naturales se degradan por mecanismos físicos, químicos y/o biológicos. Los mecanismos químicos y biológicos usan como fuente de energía el oxígeno disuelto en agua; por lo tanto, si la cantidad de contaminante aportada proviene de sustancias cuya descomposición se produce con una demanda muy alta de oxígeno, sus niveles pueden disminuir hasta valores incompatibles con la vida dentro del cauce receptor. En consecuencia, es muy importante determinar parámetros que indiquen los requerimientos de oxígeno del mismo (**Fig. 4**), los que se expresan mediante dos valores:

a) La Demanda Química de Oxígeno, DQO (o Chemical Oxygen Demand, COD) que informa sobre el consumo de oxígeno necesario para la oxidación de casi todas las

sustancias orgánicas solubles en el medio, a excepción de una serie de compuestos nitrogenados y de algunos hidrocarburos casi insolubles en aguà. Constituye un parámetro importante para el control de la contaminación de cursos de agua producida por desechos industriales y/o plantas de tratamiento de efluentes con funcionamiento deficiente. Si los desechos incorporados al curso de agua son de alta toxicidad es casi el único valor que permite determinar la carga orgánica de la corriente y tomar medidas para su tratamiento.

b) La demanda bioquímica de oxígeno, DBO (o Biochemical Oxygen Demand, BOD), que informa sobre el consumo de oxígeno que se necesita para producir la degradación microbiana aeróbica de las sustancias orgánicas presentes en el cauce receptor. Como el proceso de descomposición biológica tarda varios meses en completarse y su velocidad depende de la temperatura, en la práctica se toma la DBO correspondiente a 5 días, a 20°C (de allí la expresión DBO_5).

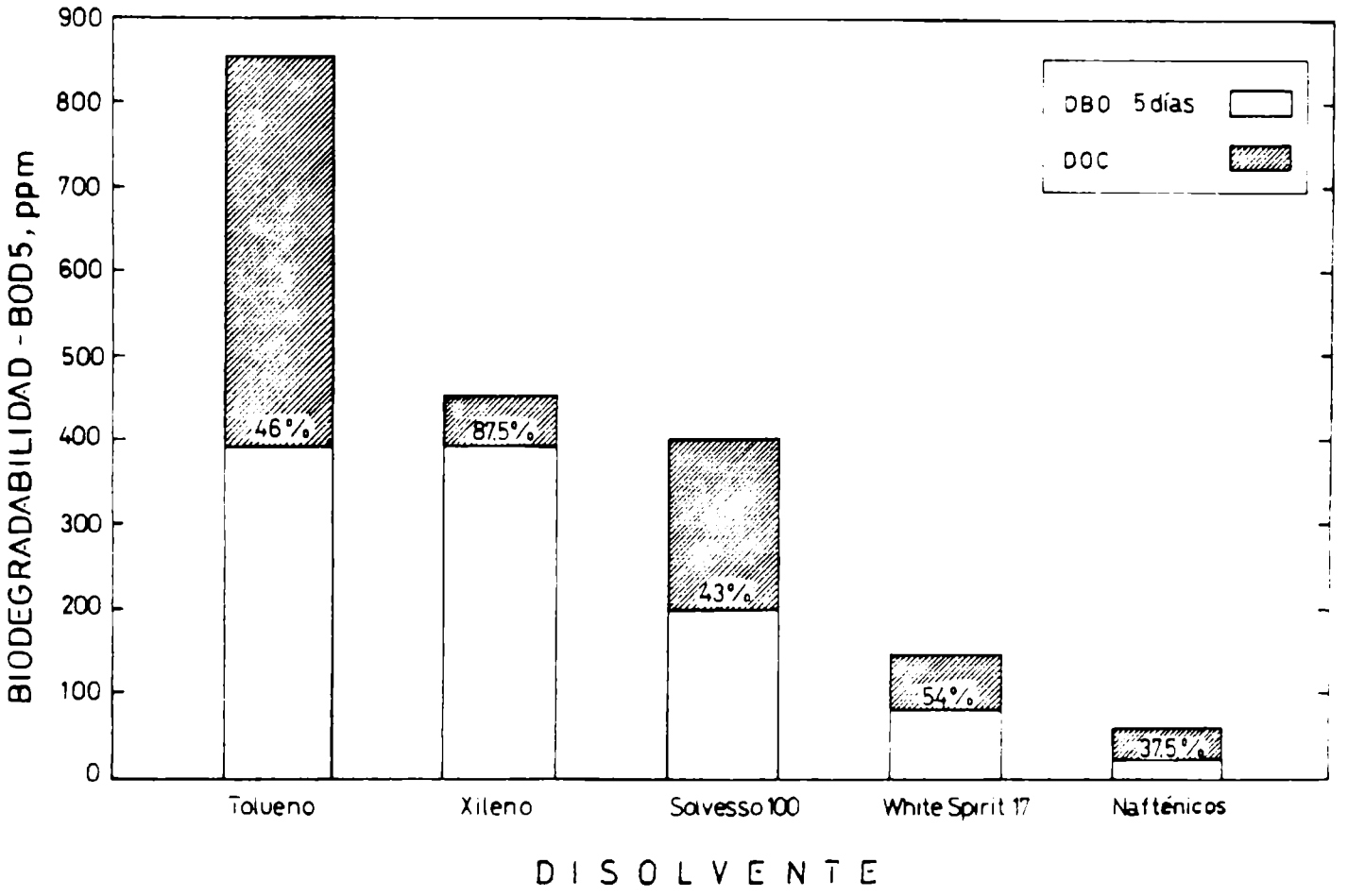

Fig. 4.- Valores típicos de DBO_5 y DOC para diferentes disolventes empleados en pinturas.

La correcta medida del valor de la DBO requiere la presencia simultánea de materia orgánica sobre la cual opera la descomposición, de microorganismos aeróbicos o facultativos que produzcan la descomposición y de oxígeno disuelto para que el proceso pueda realizarse en medio aeróbico. En casos especiales puede también determinarse este valor a los 20 días y a 20°C, lo que se expresa como DBO_{20}. Los requerimientos totales de oxígeno que generan ambos casos pueden llevar la concentración a límites incompatibles con las necesidades biológicas, determinando la extinción de vida en el curso receptor. La formación de una película disolvente sobre la superficie del agua debido a su menor densidad anula, además, la llegada de oxígeno e impide la aireación normal del fluido.

Los efectos tóxicos de los disolventes se evalúan sobre peces por la Concentración Límite CL_{50} (o en inglés Limit Concentration, LC_{50}) para 96 horas de exposición. El método permite establecer los límites inferior y superior de la dosis letal de tóxico capaz de matar el 50 % de la población en estudio en 96

horas a 20°C **(Tabla V)**. Cuanto menor sea este valor en ppm, mayor será la toxicidad del disolvente ensayado.

TABLA V

Toxicidad acuática CL_{50} para peces (96 horas)

Disolvente	Concentración (ppm)
Tolueno	24
Xileno	13,5
White Spirit 17	11,0
Nafténicos	> 1000
Isoparafínicos	> 1000

La clasificación alemana para contaminantes tóxicos no tiene en cuenta la demanda química o bioquímica de oxígeno sino la acción directa sobre ratas, bacterias y peces. Los coeficientes obtenidos para cada categoría determinan un intervalo de valores del índice WGZ (en alemán Wassergefährdungzahlen) o WEN (en inglés water endangering number) estableciéndose clases denominadas WGK (en alemán Wassergefährdungsklasse) o WEC (en inglés water endangering class), que indica el valor de las concentraciones límites de la sustancia considerada, clasificándola desde no peligrosas hasta muy peligrosas **(Tabla VI)**.

TABLA VI

Relación entre el índice WGZ y su clasificación WGK

WGZ*	WGK	
0 - 1,9	0	Concentración no peligrosa
2 - 3,9	1	Concentración poco peligrosa
4 - 5,9	2	Concentración peligrosa
> 6	3	Concentración muy peligrosa

* Calculado en base a la acción aguda sobre ratas, bacterias y peces.

Indice combinado

De acuerdo a esta clasificación, puede observarse que los aromáticos son más peligrosos que sus mezclas (solvesso 100) o que los alifáticos con cantidad reducida de aromáticos (Withe Spirit 17). Los nafténicos e isoparafínicos no son considerados peligrosos. No se encontraron valores para ésteres de dimetilo **(Tabla VII)**.

Se han resumido hasta aquí dos estrategias de control: el monitoreo de los VOCs producidos por cada etapa (producción, dilución y aplicación) y el listado de disolventes clasificados como peligrosos por los organismos de regulación establecidos por cada país, provincia, estado o comunidad.

TABLA VII

Clasificación WGK para disolventes derivados del petróleo

Disolvente	Indice WGK
Tolueno	2
Xileno	2
Aromático pesado 100	1
White Spirit 17	1
Nafténicos	0
Isoparafínicos	0

El tercer sistema es distinguir entre los diferentes tipos de disolventes tomando en cuenta el factor potencial de creación de oxidantes fotoquímicos, en inglés POCP, **(Tabla VIII)**, que se evalúa considerando: a) peso molecular (cuanto mayor sea el peso molecular mayor es el factor POCP); b) cantidad emitida (cuanto mayor emisión mayor factor POCP); c) estructura química (los más inestables tienen mayor factor POCP); y d) reacción con OH (cuanto mayor sea la reacción con este grupo mayor será el factor POCP).

TABLA VIII

Valores del factor POCP* para diferentes disolventes

Disolventes	Factor POCP
Alquenos	83,9
Aromáticos	76,1
Aldehidos	44,3
Alifáticos	41,6
Cetonas	41,1
Esteres	22,3
Alcoholes	19,6
Hidrocarburos clorados	2,0

* Photochemical oxidant creation potential factor
(Factor potencial de creación de oxidantes fotoquímicos)

El factor POCP varía ampliamente con valores mayores para los alquenos y aromáticos y menores para los disolventes clorados. Es posible entonces reducir los VOCs tomando en cuenta el factor POCP, la relación entre ambos se muestra en la **Tabla IX.**

De acuerdo con ello, las operaciones de desengrasado realizadas con disolventes clorados son menos contaminantes que las tintas de imprenta, circunstancia que debería ser estudiada cuidadosamente pues indicaría la necesidad de un único índice que reuna todos los factores hasta aquí enumerados o que se estudie una combinación de ellos capaz de definir el grado de agresividad de un disolvente.

TABLA IX

Valores de emisión VOC y POCP en Gran Bretaña (Año 1991)

Industria	VOC	POCP
Pintura	278,0	56
Adhesivos	58,0	48
Limpieza y desengrasado	46,4	13
Tintas de imprenta	41,4	34

Pinturas con bajo contenido de compuestos orgánicos volátiles

La mayor parte de los VOCs son disolventes de diferente agresividad para el medio ambiente, por lo que las regulaciones internacionales acotan cada vez con mayor rigidez su contenido en las pinturas comerciales.

La respuesta tecnológica al planteo de esta nueva situación reconoce al menos dos alternativas: para el trabajo en taller emplear pinturas en polvo, electrostáticas o de curado UV; en trabajos en obra pinturas convencionales de alto espesor y pinturas libres de disolventes. Para ambos usos, se puede aplicar pinturas de alto contenido de sólidos y pinturas de base acuosa.

Las pinturas en polvo, productos totalmente libres de disolventes, aplicadas por procedimientos electrostáticos en locales cerrados y con mecanismos de recuperación y clasificación del polvo no depositado sobre el objeto a pintar, permiten el reciclado casi total del producto. En general, su uso está limitado a trabajos en taller (electrodomésticos, equipos para la industria de la alimentación, etc.) debido a que la formación de película y su curado se realiza por calor (150-200°C). Sin embargo, como un ejemplo de su empleo en grandes obras puede mencionarse el pintado de caños para gasoductos y oleoductos. El grado de contaminación que producen es mínimo ya que no contienen VOCs en su composición y el polvo de pequeño tamaño de partícula, que puede escapar del sistema, es fácilmente controlado por los equipos purificadores.

Las pinturas de curado UV son productos usados en la formulación de tintas de

imprenta, lacas para madera, para papel, para protección de circuitos impresos y para el pintado de plásticos. Desde el punto de vista ecológico, el problema de estas formulaciones reside en que contienen mezclas de monómeros, oligómeros y fotoiniciadores. Se aplican por el sistema de rodillos o por inmersión (sólo en muy contadas ocasiones a soplete) en películas muy delgadas y sus composiciones contienen sólo pequeñas cantidades de disolventes orgánicos. Por lo expuesto sus emisiones son perfectamente controlables por los circuitos purificadores modernos.

Desde el paulatino retiro de los cauchos clorados y algunas resinas vinílicas del mercado internacional por cuestiones ecológicas, el empleo de las pinturas convencionales de alto espesor (muy utilizadas hasta 5 años atrás) se ha reducido a las pinturas alquídicas de alto espesor.

El caucho clorado se elabora en solución de tetracloruro de carbono y retiene, luego de su transformación en polvo, alrededor de 3 a 5 % de dicho disolvente, el que luego es paulatinamente liberado a la atmósfera a lo largo de la vida útil del recubrimiento. Su baja temperatura de descomposición (60-70°C) con liberación de cloruro de hidrógeno produce ácido clorhídrico en ambientes con alta humedad afectando el ecosistema. Las pinturas vinílicas de alto espesor también retienen disolventes, los que son liberados lentamente y alteran la atmósfera de trabajo en lugares cerrados **(Fig. 5)**. Las resinas alquídicas, en cambio, son solubles en hidrocarburos alifáticos y en los nuevos disolventes ecológicos por lo que aparentan ser una buena solución para ambientes o condiciones de servicio normales y de baja o media agresividad, pudiendo aumentar su resistencia por mezclas con resinas fenólicas o cauchos puros sintéticos ecológicamente aceptables.

Las pinturas libres de disolventes ("solvent free-paints"), productos de dos componentes elaborados a base de resinas epoxídicas líquidas, son usadas intensivamente en industrias de la fermentación (vasijas vinareas), de la alimentación (equipos), en la potabilización de agua (piletas de tratamientos y cisternas de almacenaje), etc. Su empleo se encuentra acotado por: a) sus características de aplicación que se realiza en general por medio de espatulas y menos frecuentemente con equipos sofisticados de alta presión lo cual limita su utilización a aquellos casos en que la superficie sea de reducida extensión o permita el solapado entre áreas mostrando escasas propiedades decorativas; y b) por la baja resistencia a la emisión ultravioleta, aunque las resinas empleadas poseen alta resistencia a agentes químicos.

Las pinturas con alto contenido de sólidos han sido desarrolladas en los últimos 10 años con mayor rapidez debido también a la presión ecológica. La ventaja relativa con respecto a las otras pinturas se debe a su gran resistencia a los ambientes altamente agresivos. Los productos con altos sólidos se definen en base a dos parámetros fundamentales: su contenido relativo de sólidos, respecto a los otros revestimientos y su nivel de sólidos por volúmen en términos de emisión de VOCs **(Fig. 6)**.

Se considera con 100 % de sólidos a las pinturas en polvo (con 0 % de VOCs) y se espera obtener pinturas líquidas de similar contenido sin las limitaciones explicadas precedentemente para las libres de disolventes **(Tabla X)**. Antes del planteo ecológico y por razones económicas y de mercado, el desarrollo de pinturas de altos sólidos horneables se ha realizado con mayor rapidez que las de altos sólidos de secado al aire. Esto se debe al esfuerzo conjunto de los fabricantes de resinas y de equipos de aplicación que proveyeron productos de menor viscosidad, solubles en solventes ecológicos y máquinas de mayor potencia y velocidad de aplicación, respectivamente.

La obtención de productos con altos sólidos de buenas características de

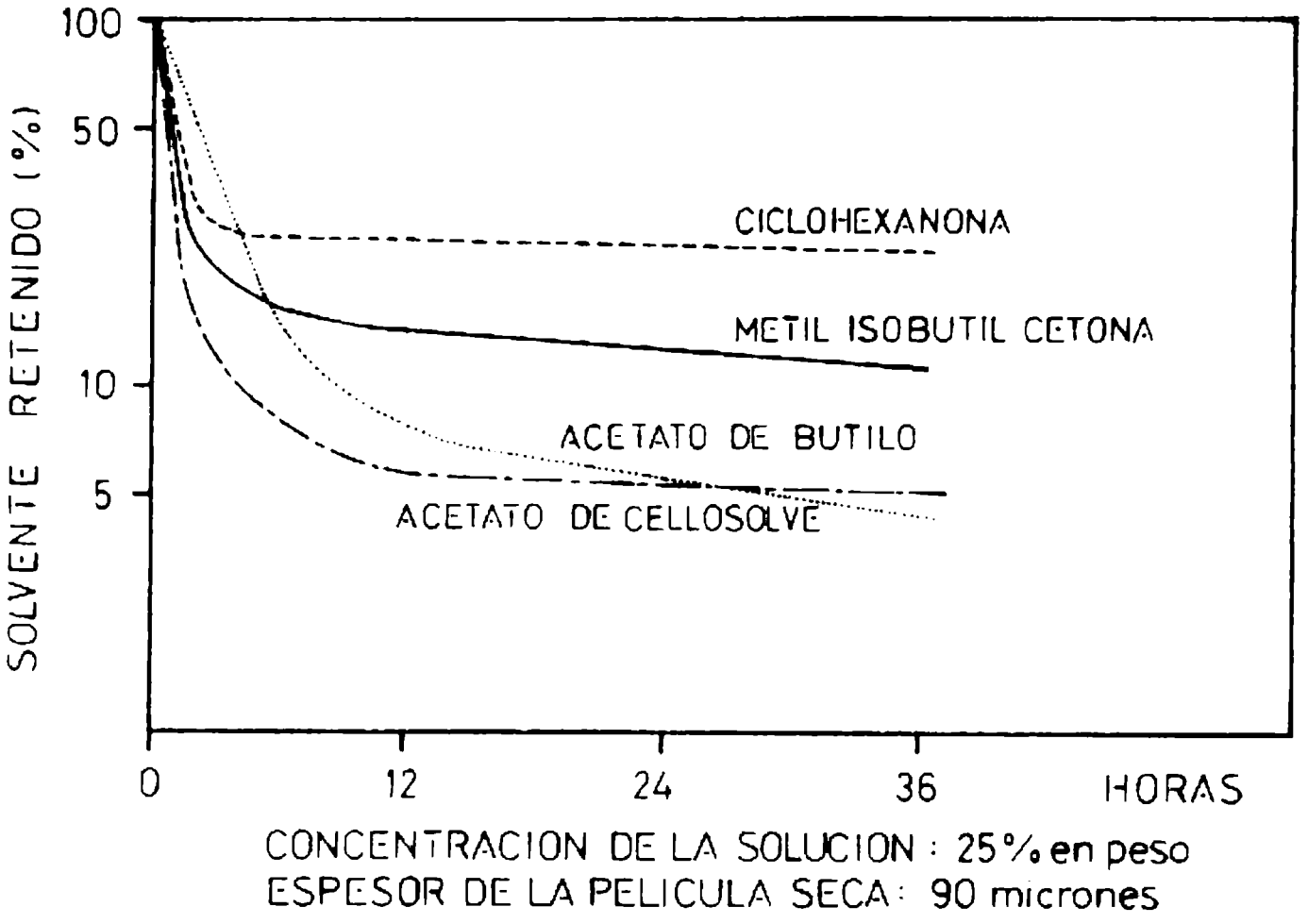

Fig. 5.- Tendencia a la retención de disolventes por parte de una resina vinílica.

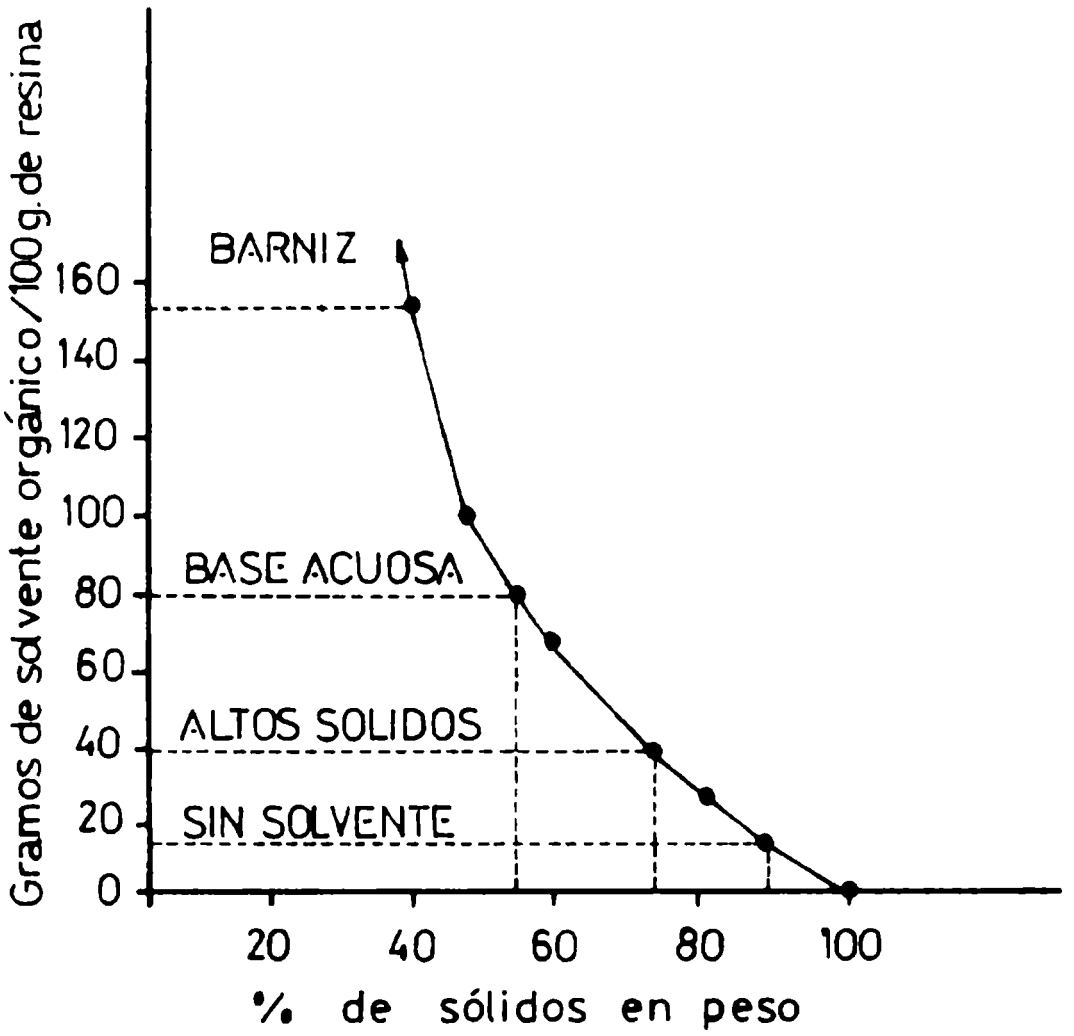

Fig. 6.- Contenido relativo de sólidos en diferentes recubrimientos.

aplicación, de curado al aire o a menores temperaturas en los horneables y de buena resistencia a medios agresivos significó resolver diversos problemas en función de las propiedades que se detallan en la **Tabla XI**. En la actualidad, los productos horneables se basan en resinas epoxídicas, poliésteres, acrílicas de contenido de sólido medio y alquídicas de alto espesor mientras que en los de secado al aire se emplean resinas epoxídicas, alquídicas, acrílicas modificadas con alquídicas, acrílicas y uretanos de dos componentes. También se trabaja en disminuir la viscosidad por modificación con diluyentes reactivos.

TABLA X

Relación entre contenido de sólidos por volumen y emisión de VOCs

Tipo de pintura	Volumen de sólidos, %	VOC, $g.l^{-1}$
Altos sólidos	100-65	0-340
Sólidos medios	65-40	340-720
Bajos sólidos	15-40	720-1800

TABLA XI

Principales propiedades de las pinturas de alto contenido de sólidos

Secado por efecto térmico	Secado al aire
- Resistencia al escurrimiento	- Resistencia al escurrimiento en altos espesores de película
- Compatibilidad con otras pinturas de bajo y alto contenido de sólidos empleadas en la línea	- Entrecruzamiento
- Control del brillo	- Tiempo crítico de repintado
- Conductividad adecuada para aplicación electrostática	- Durabilidad al exterior
- Buenas propiedades de "mojado" de la superficie	- Tiempo de secado rápido
- Compatibilidad con diferentes tratamientos de superficie	- Sensibilidad a metales sin preparación de superficies

Las pinturas de base acuosa de uso práctico pueden ser reducibles con agua, es decir un producto de base solvente al que se diluye por el agregado de agua, y las emulsiones propiamente dichas. En cualquiera de los dos casos, contienen una

fase orgánica que es por naturaleza incompatible con el agua. Tanto para mantener estable la emulsión como para lograr la formación de película se emplean productos químicos activos como agentes humectantes, aminas, agentes coalescentes (o formadores de película), espesantes, biocidas para obtener estabilidad en el envase y resistencia a hongos en la película seca y aditivos antioxidantes para evitar la corrosión del envase y el "flash rust" de las superficies metálicas arenadas. Todos estos aditivos son solubles en agua y pueden constituirse en potenciales contaminantes ya que, al final de la operación, los equipos se lavan con agua y a pesar que buena parte de ella se recicla, el resto resulta de difícil disposición final.

Es por ello que algunos componentes orgánicos del tipo amina usados como emulsionantes y ayudas de emulsión son clasificados por el índice WGK **(Tabla XII)**, eliminándose los más agresivos y limitándose la utilización del resto. De cualquier forma, los mismos son menos agresivos que otros componentes de la formulación y su concentración nunca supera un contenido del 4 % sobre sólidos, es decir, un 2 % sobre pintura total.

TABLA XII

Indice WGK para algunas aminas utilizadas como emulsionantes

Compuesto	Valor índice WGK
Trietanolamina	1
Etanolamina	1
Dietanolamina	1
Etilendiamina	2
Amoníaco	2

Como consecuencia del empleo de agua varía el mecanismo de secado y de formación de la película ya que, en las pinturas convencionales, las cadenas del material polimérico están rodeadas por una solución de disolvente y plastificante que las mantiene separadas al estado líquido. Luego de la aplicación, la evaporación del disolvente produce una contracción lenta del sistema, acercando las cadenas del polímero entre sí, transformándolo en una película compacta.

El mecanismo de formación de la película es de mayor complejidad en el caso de las emulsiones porque la dispersión del ligante oleorresinoso está formada por una fase polimérica en forma de microesferas dispersas en un medio líquido, lo cual lo transforma en un sistema molecularmente heterogéneo. Cuando dicho sistema comienza a perder agua, sea por evaporación o por evaporación-absorción en el caso de sustratos porosos, las micropartículas esféricas del polímero oleorresinoso se van acercando hasta tocarse.

Para alcanzar una película continua y uniforme, libre de huecos y de baja porosidad, la necesaria deformación de las microesferas implica la existencia de una fuerza de suficiente magnitud como para superar la resistencia al cambio de forma que ellas oponen, dado que los cuerpos adoptan la forma esférica como estado de mínima energía. La naturaleza del polímero determina la magnitud de la fuerza necesaria para que ocurra la transformación en una película continua ya que ésta

depende de su tendencia a la deformación. Si dicha tendencia es mínima, la deformación no tiene lugar y al final del proceso de evaporación se obtiene una estructura porosa.

El agua ejerce una fuerza capilar que tiende a juntar las microesferas dispersas, desarrollando una presión de gran magnitud respecto del tamaño de las partículas que constituyen el sistema. A medida que el agua se evapora, las microesferas se acercan cada vez más aumentando el valor de esa fuerza capilar hasta el momento en que se tocan. Es importante entonces la presencia de agentes coalescentes, que ayudan a vencer las fuerzas internas de las microesferas deformándolas y transformando el conjunto en una película continua. Es decir, los agentes coalescentes (usualmente glicoles e hidrocarburos alifáticos) logran que, en el período final, la película se comporte como la correspondiente a una pintura base solvente. Esto puede comprobarse comparando las curvas de evaporación (**Fig. 7**), de una mezcla diluyente de pinturas base solvente (aguarrás mineral 50 % - tolueno 50 %) con respecto a la fase líquida típica de una pintura de base acuosa (agua 95 % - hidrocarburos aromáticos de C_9 4 % - propilen glicol 1 %) y de un barniz oleorresinoso base solvente (curva 3) y otro de similar composición empleado en la formulación de un ligante de base acuosa (curva 31). La secuencia de microfotografías del secado de una película de ligante emulsionado fue obtenida en el CIDEPINT (**Fig. 8**) y se corresponden con las 6 etapas que se pueden observar en dicha figura.

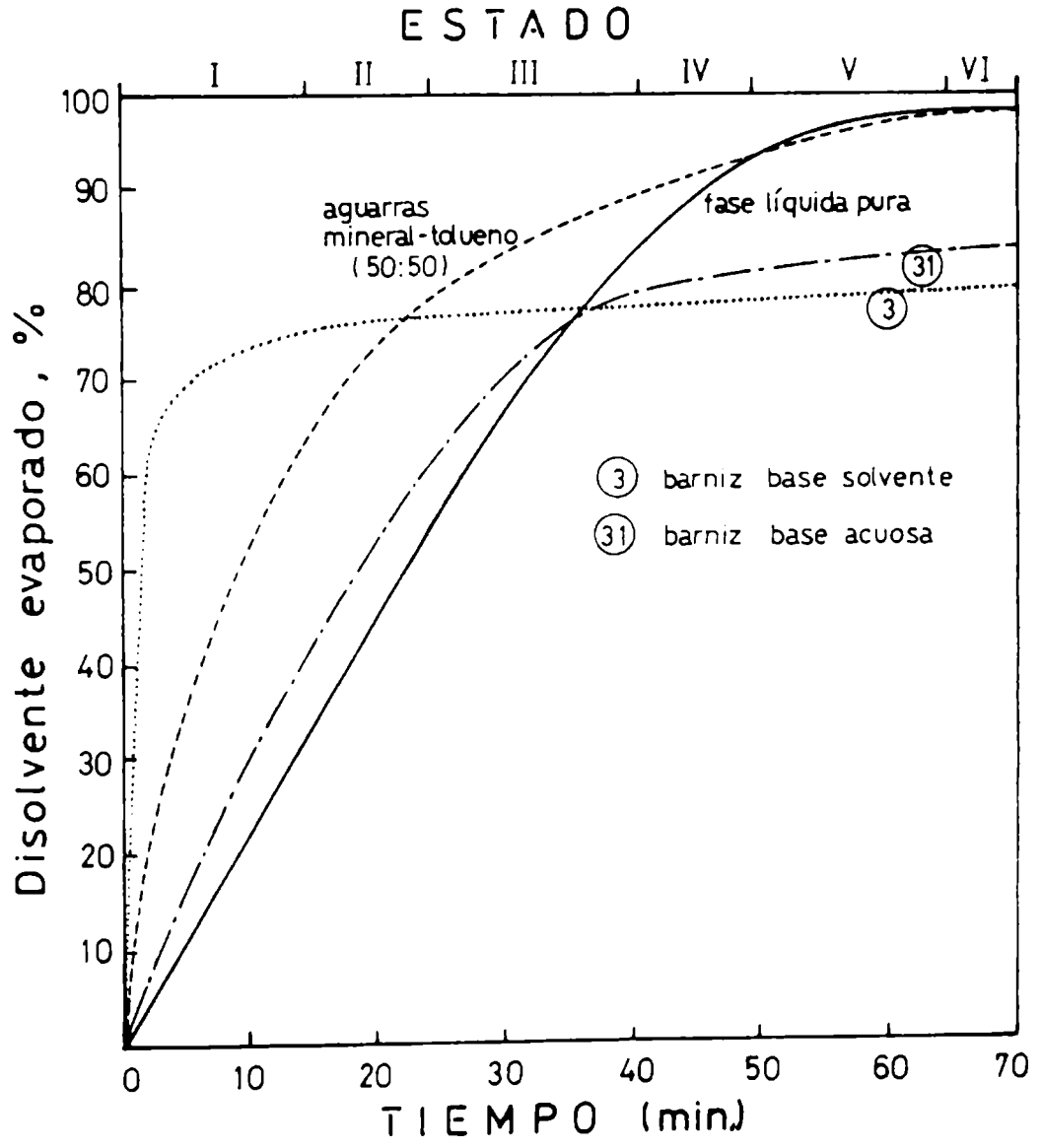

Fig. 7.- Curvas de evaporación para mezclas de diluyentes y emulsiones.

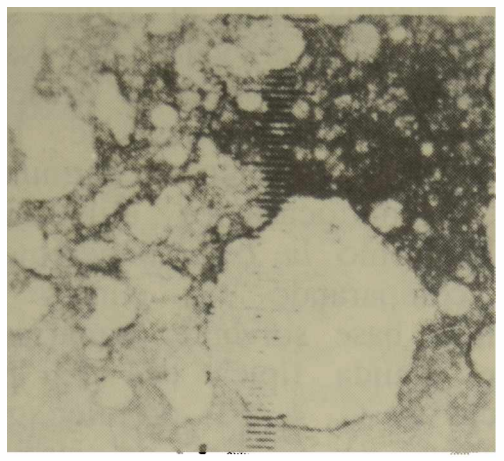

STAGE I

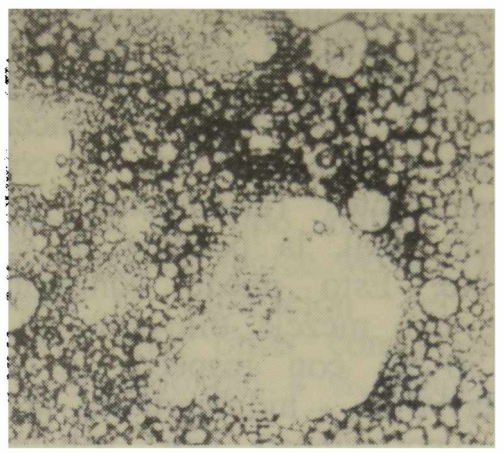

STAGE II

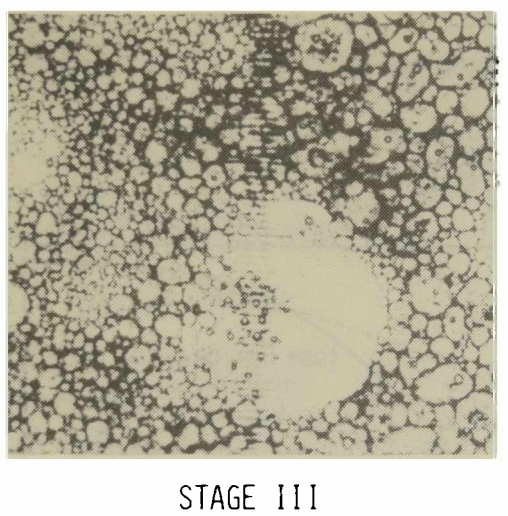

STAGE III

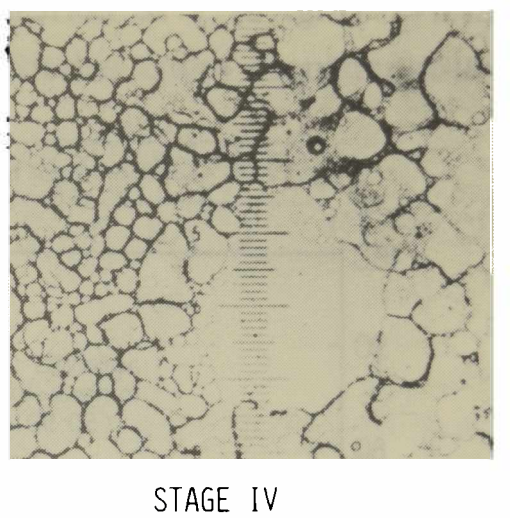

STAGE IV

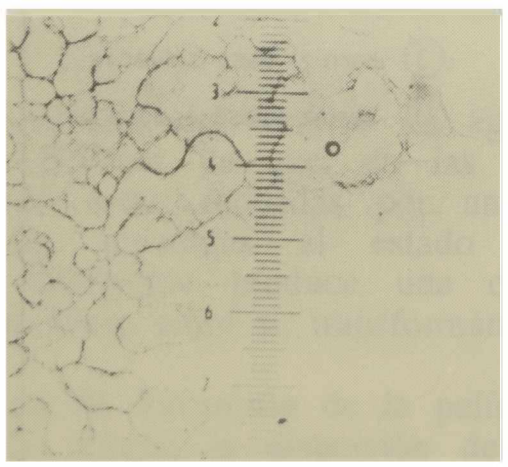

STAGE V

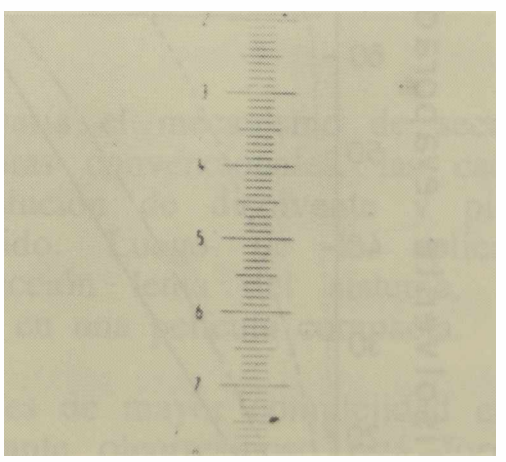

STAGE VI

Fig. 8.- Secuencia de secado de una emulsión oleorresinosa

Estos coalescentes conforman los VOCs de las pinturas en emulsión y están siendo objeto de constantes investigaciones para encontrar productos eficientes y de menor agresividad.

Es así que se puede hablar en estos momentos del desarrollo de las primeras pinturas decorativas de base acuosa sin contenido de compuestos orgánicos volátiles (Zero-VOCs), que por pertenecer a un intervalo limitado de colores y niveles de brillo no se consideran comercialmente atractivos.

CONSIDERACIONES FINALES

1. La creciente tendencia de los países desarrollados a acotar los límites de emisión de VOCs a valores cada vez menores conducirá a la desaparición de las pinturas convencionales (que emplean disolventes) en el mediano plazo y su reemplazo por sistemas ecológicamente aceptables.

2. Hasta el presente se han logrado grandes avances en materia de control ambiental debido al esfuerzo de fabricantes de resinas, productores de pintura y fabricantes de equipos, que ha promovido el empleo de pinturas aceptables ecológicamente (pinturas en polvo, de curado UV, convencionales de alto espesor, libres de disolventes y alto contenido de sólidos) que ha contribuido a disminuir la polución ambiental.

3. Es imprescindible un desarrollo acelerado de pinturas de base acuosa de alta resistencia, lo que también ayudará a disminuir la contaminación atmosférica por efecto de disolventes. Un proyecto vinculado con este tema se encuentra en ejecución actualmente en el CIDEPINT.

4. El contenido de otros aditivos en la formulación debe ser acotado, ya que muchos de ellos son de larga permanencia en agua por su baja biodegradabilidad. Un esfuerzo en ese sentido está siendo realizado por los fabricantes de aditivos y permite presumir que en los próximos años se obtendrán aditivos biodegradables de buenas propiedades.

5. Sería conveniente que los países que marcan el rumbo en protección ambiental propiciaran una **Reunión Internacional** destinada a establecer las bases que permitan no sólo normalizar los valores máximos admitidos (Maximum Allowable Concentration o MAC) para la emisión de VOCs sino también determinar qué factores serán válidos y qué métodos de evaluación indirectos (monitoreo de VOCs y clasificación de disolventes peligrosos) o directos (acción aguda sobre ratas, bacterias y peces) deberían ser empleados. Se evitarían así las discrepancias actuales entre los valores VOC y POCP para determinados rubros potencialmente peligrosos.

AGRADECIMIENTOS

El autor agradece a la Comisión de Investigaciones Científicas de la Provincia de Buenos Aires (CIC) y al Consejo Nacional de Investigaciones Científicas y Técnicas (CONICET), el apoyo económico que posibilitó la realización del presente trabajo.

BIBLIOGRAFIA

Akkerman, J.- **Progress in Organic Coatings**, **17**, 53-68 (1989).

ASTM Annual Book of ASTM St. 06.01.1992.- Standard D-3960-91, 606-610.

Bernard, D.- **High Solid Coatings**, 15-16 (1982).

Bishton, W.- Buyer's Guide. **High Solid Coatings**, 18-19 (1982).

Chemoxy International. Estasol. Product and Safety Information, 5° Edición, diciembre 1992.

Cobbs, W., Rehman, W. and Kirchner J.- **High Solid Coatings**, 7-11 (1983).

De Woody, B.- **J. of Protective Coatings and Linings**. SSPC Applicator Training Bulletin, **6** (4), 1-4 (1989).

Exxon Chemicals.- **A practical guide for protecting man and environment. I. Basics of Toxicology**, 1-8 (1988).

Exxon Chemicals.- **A practical guide for protecting man and environment. II. Environmental toxicology definitions**, 1-5 (1988).

Fiero, G.W.- **Journal of Paint Technology**, **40**, 222-228 (1968).

Ginsler, V. and Bigelow E.- Buyer's Guide. **High Solid Coatings**, 7-12 (1982).

Good Year Chemical Europe.- **Plioway Handbook**.

Juffermans, J.- **Progress in Organic Coatings**, **17**, 15-26 (1989).

Klein, D.- **Anales 3er Congreso Internacional de Tintas**, 319-337 (1993).

Noomen.- **Progress in Organic Coatings**, **17**, 27-39 (1989).

O'Neill, L.- **J. Oil and Colour Chemists Association**, **70** (3), 79-81 (1987).

Paint Research Association.- **Notes to Industry N° 8**, junio 1980.

Paint Research Association.- **Notes to Industry N° 9**, setiembre 1980.

Regulation News.- **Journal of Protective Coatings and Linings**, **9** (10), 21-43 (1992)

Schultheis, H.- **Reportaje Bayer**, **62**, 11-19 (1990).

Sharma, M.- **High Solid Coatings**, 17-18 (1982).

Sykes, D.- **Proceedings West Coatings Symposium**, 1-6, marzo 1993.

Telles de Oliveira, E.- **Anales 3er Congreso Internacional de Tintas**, 902-913 (1993).

Tonini, I.- Eastbourne Conference Paper, **J. Oil and Colour Chemists Association**, **70** (12), 365-368 (1987).

US Environmental Protection Agency.- **J. of Protective Coatings and Linings**, **10** (6), 39-41 (1993).

Whitesell, M.- **Materials Protection**, **26** (12), 17-20 (1989).

Yee, A. and Fry, J.- **American Paint Journal Reprint**, junio 23, 1986.

NON-POLLUTANT CORROSION INHIBITIVE PIGMENTS: ZINC PHOSPHATE. A REVIEW

PIGMENTOS NO CONTAMINANTES INHIBIDORES DE LA CORROSION: FOSFATO DE CINC. Revisión bibliográfica.

R. Romagnoli[1] and V. F. Vetere[2]

SUMMARY

The study of organic coatings applied to protect metals against corrosion is of great importance. Anticorrosive paints containing lead or hexavalent chromium compounds as pigments are particularly hazardous. Zinc phosphate was proposed as an alternative non pollutant one. However, results obtained with this pigment are very contradictory.

The aim of this paper is to give a state-of-the-art-report about the pigment performance in order to clarify the causes of such contradictory and, sometimes, discouraging behaviour.

INTRODUCTION

In the present world, corrosion phenomena are observed everywhere on cars, metallic structures, equipments, etc. In recent years, the environmental pollution has led to enhanced corrosion processes. Thus, the application of organic coatings to protect metals against detrimental effects of corrosion is of great importance. Anticorrosive paints containing lead or hexavalent chromium compounds as pigments are particularly hazardous and contribute to the mentioned pollution.

Due to the toxicity of conventional pigments and legal restrictions imposed on their use, pigments manufacturers have accorded to undertake extensive research and development programms about new, non-toxic and corrosion inhibitive compounds.

The present world trends for changing the toxic anticorrosive pigments are mainly focused on their substitution by different phosphates or ferrites. Other compounds such as borates, molybdates, silicates or ion exchanging inorganic compounds have also been proposed to a lesser extent. Barrier pigments with lamellar structure were found to be effective for restraining the steel corrosion of painted specimens.

Zinc phosphate (ZP) has reached a great diffusion as anticorrosive pigment. However, very different experimental results were obtained with this pigment, therefore, new phosphates based pigments have been developed to replace it.

Ferrites constitutes a novel group of corrosion inhibitive pigments; the main difficulty being its high cost of production due to the fact that they are obtained by heating at 1000°C. Its anticorrosive mechanism is not still fully

---

[1] Miembro de la Carrera del Investigador del CONICET

[2] Profesional de Apoyo del CONICET y Planta Permanente CIC

understood but it was suggested that their action could be improved by adding zinc phosphate to the paint formulation.

The aim of this paper is to carry out a literature reviewing about ZP specifying its advantages, the most important characteristics, the available techniques to prepare it and a detailed description of its anticorrosive effect, in order to give the reader a state-of-the-art-report on this field. Likewise, an extended list of other phosphates is included. Alternative pigments such as modified zinc phosphates, together with its anticorrosive performance compared with that of ZP, are also described. Different formulations performance, when subjected to laboratory accelerated and/or outdoor tests, are included too.

THE IMPORTANCE OF ZINC PHOSPHATE AS ANTICORROSIVE PIGMENT. ADVANTAGES AND DISADVANTAGES

For environmentally compatible anticorrosive priming formulations, the raw materials producers often recommend using ZP together with adequate binders and metallic substrates to form adhesive and inhibitive complex substances (henceforth referred as "complexes") assisting the phosphatizing of the metal base. It results particularly effective in anodic areas where protective layers are formed.

ZP is:

a) A white pigment, therefore, primers of all colours may be obtained.
b) Less sensitive to corrosion stimulating ions (such as chloride and sulphate) than chromates **[1, 2]**.
c) Weldable without producing toxic fumes.
d) Able to be used with all types of binders; when added to resins it improves both the drying and the adhesion to the metal substrate **[2]**.
e) Particularly effective when coatings are exposed to SO_2 polluted environments; therefore, it is a valuable product for the most industrial atmospheres **[3-5]**.

Hydrated ZP proved to be a very effective way to incorporate water and phosphoric acid to wash primer paints, which uptake small amounts of phosphoric acid or are almost incompatible with water. The low acidity of the system allows the binder being modified with phenolic and polyester resins, improving coating hardness and adhesion **[2]**.

Meyer **[2]** stated that in order to protect a painted metal for longer exposure times, ZP could not be employed as the only anticorrosive pigment but it must be accompanied by another one. This is due to the fact that ZP hydrolyzes itself and its content diminishes continuously in the paint film. Besides improving the anticorrosive coating performance, ZP has additional effects on brushing and flow characteristics promoting an excellent topcoat adhesion **[6]**.

Kukla et al **[7]** pointed out that inorganic phosphates did not give a suitable anticorrosive protection. On steel panels covered with a porous epoxy polyamide coating and exposed for 100 days, the electrochemical impedance spectroscopy proved that chromates were more effective than ZP **[8]**. However, Pietsch **[9]** found that the anticorrosive properties afforded by chlorinated rubber paints pigmented with ZP at 25 wt % were equivalent to those using zinc chromate.

ZP coatings showed certain susceptibility to attack by fungi **[10]**. This is due to the nutritious properties of the phosphate. The main difficulty concerning ZP seems to be related with its low solubility **[11]**, which originates a small phosphate concentration to protect the metallic base.

TECHNICAL SPECIFICATIONS

Table I summarizes some technical data about ZP. Two types, differing in the percentage of fine particles, were recognized, one having 94.59 %, the other 98.48 % of particles finer than the DIN 130 sieve, respectively.

TABLE I

Determination of technical specifications for zinc phosphate

Assay	Specification	Reference
Zinc ion (Zn^{2+}, %)	approx. 51	[3]
Phosphate ion (PO_4^{3-}, %)	approx. 49	[3]
Ignition loss (%)	approx. 10-14	[3,25]
Oil absorption (g/100 g)	20 - 23	[3,4]
Water soluble chloride (% Cl^-)	< 0.01	[3]
Water soluble sulphate (% SO_4^{2-})	< 0.01	[3]
Water solubility, 20°C (%)	0.05 - 0.08	[25]
Water solubility, 23°C (g/100 ml)	0.0155	[3]
Specific density	3.0 - 3.25	[4,25]

THE ELABORATION PROCESS OF ZINC PHOSPHATE

ZP can be prepared either by mixing disodium phosphate and zinc sulfate solutions or saturating a 68 % phosphoric acid solution with zinc oxide, both methods at the boiling temperature **[12]**. In each case, the resulting precipitate must be adequately treated to yield a product having the composition $Zn_3(PO_4)_2.4\ H_2O$, which loses two water molecules at temperatures up to 200°C. Water free ZP can only be obtained by heating it to a temperature of 800°C **[13]**. Compared with zinc chromate, ZP has an extremely coarse crystalline structure. By further grinding or sifting it is possible either to break down or remove coarser particles or aggregates improving pigment characteristics such as dispersibility, settling and/or anticorrosive behaviour. Primary particles with an average diameter comparable to that of the zinc chromate could not be obtained with these methods. Controlling reaction conditions during the production process it would be possible to make metal phosphates with the desired particle size distribution **[14]**.

Micronized ZP has acquired increasing significance since it disperses better, sediments less and its content in the paint formulation may be reduced. This is probably due to the smaller particle size and the surface changes produced during the micronization process.

Pigments with particle size < 5 μm and a core containing titanium white, iron pigments, zinc oxide, lithopone, barium sulfate, silica, alumina, kaolin, mica, talc, alkaline earth carbonates, or magnesium carbonate, coated with 5-30 % ZP, were prepared precipitating this last one on the pigment particles in aqueous suspensions. In this form ZP consumption in anticorrosive paints is reducted to < 90 % **[15]**.

MODIFIED ZINC PHOSPHATES

Gerhard and Bittner **[16]** sustained that the protective characteristics of

zinc chromate are not achieved by ZP, therefore, modified zinc phosphates were proposed. The most important modifications are concerned with one or more of the following properties:

a) adequate particle size distribution;
b) addition of Al, Mo, Mn, etc.;
c) addition of basic groups; and
d) an organic pretreatment.

Conventional ZP consists of large (12-20 μm) lamellar particles. As it was mentioned previously, metal phosphates with enhanced particle size distribution may be obtained **[14, 16, 17]**. A technique to attain small spherical ZP particles was recently developed **[18]**.

Zinc aluminium phosphate (ZPA), obtained from the ZP and aluminium phosphate combination in wet phase, appeared interesting because it exhibited a higher phosphate content than ZP **[16, 17]**. The acidity generated by the hydrolysis of aluminium ions cause an increasing phosphate concentration **(Table II)**.

In binders containing aliphatic acids the addition of basic groups is important with regard to metal soap formation **[14]**. Furthermore, adhesion is also improved when the reaction between the basic and acid groups from the binder takes place.

The zinc molybdenum phosphate basic hydrate (ZMP) produces molybdate anion (MoO_4^{2-}) which is an anodic inhibitor with a passivating capacity only slightly lesser than that of chromate anion.

A manganese modified ZP coating for the automobile industry was reported **[19]** as improving the anticorrosive performance of low content ZP coatings.

MIXING OF ZP WITH OTHER PIGMENTS. ACTIVATION

Meyer **[2]** distinguished three phases in the anticorrosive protection process. A complete anticorrosive primer must be formulated containing pigments for every phase. ZP would only be useful for the initial and prolongation ones due to a leaching process through the paint film. For the late phase, consequently, another pigment such as lead phosphate ($Pb_3(PO_4)_2$), iron phosphate ($FePO_4$) or chromates must be added to achieve a protective action for at least 6 years. Likewise, addition of very small concentrations of organic chromates such as guanidine chromate or cyclohexylamine chromate when ZP is used as anticorrosive pigment was suggested **[7]**. These organic compounds reduce chromate level in the mixture when acting on the micropores of the paint film.

Accelerated tests have shown that activated and modified basic zinc phosphates are corrosion inhibitors as effective as ZP plus a mixture of pigments containing water soluble chromates **[20]**.

The anticorrosive performance of a pigment mixture such as **[21]**:

alkaline red oxide from bauxite 45-60 %
zinc chromate 18-25 %
ZP 5-10 %
zinc ferrite 18-25 %

was similar to the red lead one. The mixture proportion was 34-40 % in binder; talc as the filling material and 30 μm the suggested average particle diameter.

TABLE II

Relative solubilities in water of zinc phosphate and modified zinc phosphate pigments

Pigment	Water soluble matter ($mg.l^{-1}$) (ASTM D 2448-73, 10 g pigment in 90 ml water)				
	Total	Zn^{2+}	PO_4^{3-}	MoO_4^{2-}	CrO_4^{2-}
Hydrated zinc phosphate	40	5	1	--	--
Hydrated organic modified zinc phosphate	300	80	1	--	--
Hydrated aluminum zinc phosphate	400	80	250	--	--
Hydrated zinc molybdenum phosphate	200	40	0.3	17	--
Zinc potassium chromate	1500	--	--	--	1000

Note: These data were taken from reference [25]

ZP was employed with borates **[5, 22]**, molybdates **[23]** and zinc nitrophtalate **[5]**. Alquil acid phosphates could be added to ZP in order to improve adhesion **[2]**.

Multiphase pigments are also produced depositing an active chromate-phosphate together with lead on a silicate core. A multiphase ZP anticorrosive pigment containing $Ti_3(PO_4)_3$ having a good hiding power was also prepared **[24]**.

In acid media, phosphates solubility increases due to the development of species like $PO_4H_2^-$ and PO_4H^-, whose relative amounts depend on the pH **[25]**.

BINDERS

ZP can be used with all types of binders. The recommend level is 40 % in the paint or 25 % in the coat film. Binders include vegetable oils, alkyd resins, phenolic resins, phenolic resins modified with tung oil, vinyl chloride copolymers, chlorinated rubber, epoxy and urethane resins and acrylic emulsions **[2, 4, 6]**. The employment of mixed binders was also reported **[14]**.

FORMULATIONS PERFORMANCE

The misleading nature of the conventional salt spray and, in lesser scale, the humidity cabinet tests to assess the anticorrosive primers performance was noticed early in the 60th's decade. The accelerated tests of ZP gave bad results but outdoor long exposure tests were encouraging **[5, 6]**. It was assumed that differences in evaluating paints performance arose because sometimes accelerated but other the outdoor exposures tests were the criterion employed to monitor them.

Several researchers **[26, 27]** established that during accelerated test, the behaviour of a paint system is mainly governed by the binder. If the binder fails, the influence of the inhibitive pigment can be observed. For instance, there were not important differences among the anticorrosive pigments when epoxy and polyurethane were employed as binders. With chlorinated rubber ones, ZP led to good results.

Moreover, variables which are relevant to paint formulation are not always controlled during its evaluation. All these factors make difficult a reliable assessment of the ZP effectiveness as anticorrosive pigment.

During 1961, steel structures were painted and examined 3 years later. ZP pointed out the same protective properties than any conventional anticorrosive pigment with binders based on vegetable oils and alkyd resins. It offered better protection than similar paints pigmented with red oxide, red oxide/zinc chromate or zinc chromate. Furthermore, it showed advantages over red lead since maintained a tightly bound film, whereas the lead-based primer show chalking after one year exposure **[6]**. In the multicoat system (two primer coats and aluminium or micaceous iron pigmented alkyd gloss topcoat paint), ZP in oil and alkyd paints took as excellent performance as those containing lead pigments. When aluminium paints were applied on the phosphate based primer there was not apparent erosion of the topcoats such as occurs when these paints are applied on the red lead pigmented primer **[6]**.

In more recent studies, painted specimens with alkyd and epoxy water based formulations were tested using accelerated (salt spray, humidity, SO_2) and outdoor exposure tests (natural and industrial environments) **[3, 28]**. Two coats, 35-40 μm dry film thickness each one, were applied on sandblasted panels with 24 hours

drying between each coat. Compared with the red lead or zinc chromate pigmented alkyd or epoxy paints, those using ZP showed a lower poorer anticorrosive performance in almost all the tests. However, when exposed to an industrial atmosphere these paints behaved similarly in areas far from the scratch and better than those pigmented with iron oxide.

For moderate outdoor exposure conditions, modern specifications **[29]** recommended a maximum content of ZP of about 20 % by volume in the dry film when a standardization fineness was used. When spherical optimized particle size distributions are employed, the ZP content can be lowered to 10 % and the painted panel is able to withstand more severe exposures.

The performance of ZP pigmented coatings could be improved through an adequated surface preparation. Better results in the humidity test were obtained with grit blasted steel panels **[30]**. The corrosion resistance of paints with ZP is enhanced using wetting and dispersing agents. These additives have similar chemical composition, which invariably contain a low molecular weight polycarboxylic acid polymer with multifunctional structure (carboxyl groups as well as C=C bonds, amide structure, amino groups, etc.). They do not only contain groups with pigment affinity but also reactive ones which facilitate the crosslinking reactions in the paint system. The maximum level of these additions is 1.5-2.5 % of the pigment content. Higher contents would produce blistering and drying problems **[31]**.

Bose **[32]** reported the employment of an anticorrosive epoxy-ZP primer modified with organosilanes. Five methoxysilanes were used in order to improve adhesion as well as hardness and corrosion resistance.

Results obtained by Williams-Wynn **[33]** reflect the differences between outdoor exposure and accelerated tests. ZP-iron oxide pigmented paints showed good anticorrosive performance for 270 days outdoor exposure while a fair behaviour was observed for a 1000 hours salt spray test. ZP alone led to fair and poor results in both conditions, respectively. However, a formulation based on yellow (10 %) and red (9.2 %) iron oxides, talc (8 %) and ZP (25 %) as anticorrosive pigment in an alkyd binder (38 %) was reported as giving promising results **[34]**.

Compared with other anticorrosive pigments, ZP in conjunction with chlorinated rubber binder showed a very good performance in protecting steel sheets under cathodic polarization. The initial current requirement was 1.2 $mA.m^{-2}$ but increased up to 7.8 $mA.m^{-2}$ after 24 weeks exposure. With other pigments, the final current requirements were near to 30 $mA.m^{-2}$ **[35]**.

The anticorrosive behaviour of modified zinc phosphates was studied by several researchers **[14, 16]**. The anticorrosive pigment was 40 % by volume and the PVC/CPVC ratio (Q) was maintained in the range 0.7-0.8. The paints were applied by means of a spraying technique on pickled or sandblasted panels. The coating thickness was 50 ± 5 μm. The coated specimens were subjected to the salt spray (DIN 50021) and the Kesternich tests (DIN 500181.0.5).

ZPA and the zinc basic phosphate with an organic pretreatment (ZPO) proved to be superior to the traditional ZP with respect to the anticorrosive behaviour. In salt spray test, they exhibited better adhesion characteristics, lower blister formation and higher anticorrosive properties. Furthermore, ZPA and ZPO produced equivalent or superior results to zinc chromate in both standardized test. ZMP showed an acceptable behaviour too. The protective action of modified zinc phosphates depends on the Q value; if Q lied between 0.8 and 1.0, the loss of adherence as well as the oxidation increased after 400 hours exposure to the salt spray chamber. If Q equals 1, considerable blistering and oxidation may occur. The optimum Q value must lie between 0.7 and 0.8 [16]; in these cases, the best

protective effect was obtained with a PVC of about 33 % .

The protection obtained with ZP was remarkably inferior to the other phosphates; a PVC of about 33 % produced a protective effect equal than 11 % by volume of ZPA, ZMP or ZPO **[16]**.

The anticorrosive behaviour of these pigments was also influenced by filler. ZPA led to good results with fillers like magnesium silicate or titanium dioxide; the same occurred with ZMP and ZPO assocciated with magnesium or aluminium silicate, titanium dioxide, calcium carbonate, etc. Other fillers produced either poorer or bad results **[14, 16, 33]**. The filler particle size was not important **[16]**.

The surface preparation also influenced the pigments response, ZPA was the most suitable. Results obtained with ZPA in accelerated tests were similar to the zinc chromate ones **[30]**.

The anticorrosive behaviour of ZP and modified zinc phosphate was studied in low solvent content or water thinnable systems **[25, 30]**. High solids alkyds, water reducible coatings based on acrylic emulsions and water borne epoxy paints were chosen and tested due to the fact that they are environmentally acceptable.

In high solids primers, ZP provided the poorest anticorrosive properties compared with other anticorrosive pigments **[25]**. ZMP and ZPO led to low rusting of underlying metal surfaces covered with water reducible coatings based on acrylic emulsions. The emulsifiers enhance both the water resistance and the corrosion protection after film formation.

According with salt spray tests, ZPA is the most suitable pigment for water based epoxy coatings. As a general rule, it can be said that ZPA is the most effective anticorrosive pigment, but ZMP and ZPO led to good results too. ZP showed good results in the humidity test when grit blasted steel was employed. The performance of these coatings may be improved through changes of extenders and/or adequated surface preparation **[36, 37]**.

In the case of water borne coatings, the salt spray test exposure produces in some cases a total destruction of the paint film. Further information could be obtained from the humidity and water immersion tests and also from that proposed by Kossman **[38]**.

ZINC PHOSPHATE ANTICORROSIVE ACTION MECHANISM

The aqueous extract of ZP produces the same corrosion that water. The pigment is sufficiently insoluble to act as an inhibitor. ZP slurry instead of the aqueous extract must be employed if lower weight losses are to be obtained **[25]**. However, the differences are not significant.

Weight losses of steel specimens are smaller in aqueous extracts from ZP ground in linseed oil than the original in water; likewise, they were only slightly smaller than in the extracts obtained from linseed oil alone. The ZP-linseed oil extracts contained ten times more phosphate than the aqueous ones, those prepared with water, and had a pH 4.4 value which was similar to that attained with a zinc soap. Therefore, it was concluded that ZP in linseed oil forms soaps which may yield inhibitive degradation products. ZP soaps are not as efficient inhibitors as lead ones **[39]**.

Regardless of the linseed oil binder, the protective effect of phosphate

pigments is due to the humidity penetrating through the pores of the coating; this causes slight hydrolysis giving rise to secondary phosphate ions. These ions affect the anodic corrosion process through the formation of a protective passive layer **[14, 40]**. The layer build up to a thickness enough to provide apparent passivity **[41]**. Porosity of phosphate coatings (which is closely related to the coating protective performance) was measured by electrochemical impedance spectroscopy **[42]**. Poor phosphate coating coverage leads to flash rusting **[43]**.

Compounds such as mixed zinc and iron phosphates were supposed to be formed on protected steel surfaces **[21]**, but the proposed formulas are incorrect from a stoichiometric point of view.

Because of the slight solubility of ferrous phosphate, the corrosion reaction is not totally controlled, but is reduced to an acceptable degree. Pryor and other researchers **[44, 45]** stated that the inhibition was due to a protective film of γ-Fe_2O_3, maintained in constant repair by dissolved oxygen. Such film was proposed as being formed by adsorption of oxygen, followed by heterogeneous reaction and thickening until reaching an equilibrium value of 20 nm, from which the outward diffusion of iron is prevented. It is assumed that phosphate ions do not participate directly in the oxide film formation. Their function is confined to discontinuities in the oxide film. The pore plugging of deffective areas of the ferric oxide is provided by the anion precipitation. Fe(II) react with dissolved oxygen to give more insoluble Fe(III) ions. Pryor's results were obtained employing soluble phosphates, and probably they could not be extrapolated directly to very insoluble phosphates as those employed in paint formulations.

Phosphate based pigments provide corrosion inhibition in aerated solutions but they are ineffective in deaerated ones. The corrosion potential becomes more noble in aerated solutions, and sometimes reaches the characteristic value of passivated steel is reached.

Corrosion inhibition by phosphates takes place only when the anion concentration is higher than 10^{-3} M in a salt solution, which pH value ranges between 5.5-7.0 **[44]**.

More recent studies confirmed both the presence of increased amounts of oxyhydroxides and the incorporation of iron phosphates in the protective film **[46]**.

Clay and Cox **[47]** have suggested that the protection mechanism involved the polarization of cathodic areas caused by the formation of scarcely soluble basic salts adhered to the metal surface. These salts may contain the anion. The layer is claimed to be effective by limiting the access of dissolved oxygen to the metal surface. This statement was confirmed by the work of Szklarska-Smialowsaka et al **[48]**.

Meyer **[49]** sustained that the major utility of ZP in paints may be found in the mixtures with other less soluble inhibitive pigments in order to avoid underfilm corrosion during the initial stage of the protective period. According to this author, ZP protective action includes the phosphatizing of the metal substrate and the formation of "complexes" products through reactions with the binder components. Then, these "complexes" can react with corrosion products yielding a layer strongly adhered to the metallic substrate. Such "complexes", due to reactions between carboxylic acids and hydroxyl groups of the binder, and of these with the corrosion products, are possibly caused by the dissociation of hydrated zinc phosphate into various intermediate compounds. According to Meyer **[2, 49]**, the following theoretical reaction path is proposed to interpret the inhibitive action of zinc phosphate:

$$Zn_3(PO_4)_2.4\ H_2O \Leftrightarrow (H^+)_4[Zn_3(PO_4)_2(OH)_4]$$

$$H_4[Zn_3(PO_4)_2(OH)_4] + 12\ RCOOH \Leftrightarrow H_4[Zn_3(PO_4)_2(RCOO)_4] + 12\ H_2O$$

$$3\ H_4[Zn_3(PO_4)_2(OH)_4] + 4\ Fe^{3+} \Leftrightarrow Fe_4[Zn_3(PO_4)_2(OH)_4]_3 + 12\ H^+$$

Basic complex inhibitive substance

$$3\ H_4[Zn_3(PO_4)_2(RCOO)_4] + 4\ Fe^{3+} \Leftrightarrow Fe_4[Zn_3(PO_4)_2\ (RCOO)_4]_3 + 12\ H^+$$

Complex inhibitive and adhesive substance

$$Fe_4[Zn_3(PO_4)_2(OH)_4]_3 + 12\ RCOOH \Leftrightarrow Fe_4[Zn_3(PO_4)_2\ (RCOO)_4]_3 + 12\ H_2O$$

$$Fe_4[Zn_3(PO_4)_2(OH)_4]_3 + 6\ H_2CO_3 \Leftrightarrow Fe_4[Zn_3(PO_4)_2(CO_3)_2]_3 + 12\ H_2O$$

Slightly soluble complex inhibitive substance

$$Fe_4[Zn_3(PO_4)_2(OH)_4]_3 + 4\ H_3PO_4 \Leftrightarrow 3\ FeZn_3(PO_4)_3 + FePO_4 + 12\ H_2O$$

Complex inhibitive substance

Species responding to the general formula $[Zn_3(PO_4)_2(OH)_x.n\ H_2O]$, being $n + x = 4$ and $x = 1\text{-}4$, are generated by hydrolysis. There is a slight formation of inhibitive substances on the base metal. The system becomes hydrophobic because of the fatty acids from the binder. This fact improves the stability of both the inhibitive and adhesion promoting substances by minimizing their hydrolysis.

The incorporation of alquil acid phosphates to certain binders improves adhesion by promoting the formation of certain "adhesion complexes". The following reaction path shows the effect of adding 3 % of butyl phosphoric acid:

$$H_4[Zn_3(PO_4)_2(OH)_4] + 2\ H_2(C_4H_9PO_4) \Leftrightarrow$$

Butyl phosphoric acid

$$\Leftrightarrow H_4[Zn_3(PO_4)_2(C_4H_9PO_4)_2] + 4\ H_2O$$

$$3\ H_4[Zn_3(PO_4)_2(C_4H_9PO_4)_2] + 4\ Fe^{3+} \Leftrightarrow$$
$$\Leftrightarrow Fe_4[Zn_3(PO_4)_2(C_4H_9PO_4)_2]_3 + 12\ H^+$$

Complex inhibitive and adhesive substance

Considering that equilibrium may occur:

$$Zn_2(PO_4)_2 + 6\ H_2O \Leftrightarrow 2H_3PO_4 + 3\ Zn(OH)_2$$

the following inhibitive compounds may be formed on the metal surface:

$$Zn_3(PO_4)_2.4\ H_2O \Leftrightarrow 4\ H^+ + [Zn_3(PO_4)_2(OH)_4]^{4-}$$

$$[Zn_3(PO_4)_2(OH)_4]^{4-} + 4\ H_3PO_4 \Leftrightarrow$$
$$\Leftrightarrow [Zn_3(PO_4)_4]^{6-} + 2\ [Zn_3(PO_4)_3]^{3-} + 12\ H_2O$$
$$[Zn_3(PO_4)_4]^{6-} + 3\ Fe^{2+} \Leftrightarrow Fe_3Zn_3(PO_4)_4$$
Complex inhibitive substance

$$[Zn_3(PO_4)_3]^{3-} + Fe^{3+} \Leftrightarrow FeZn_3(PO_4)_3$$
Complex inhibitive substance

Meyer established that it is necessary to take into account these theoretical reactions to make a proper selection of the binders and the pigments which lead to the formation of adhesion and inhibition promoting substances.

OTHER PHOSPHATES AS INHIBITIVE PIGMENTS

Because of the discouraging and contradictory results obtained with ZP, other phosphates, apart from modified zinc phosphates, were introduced to replace current toxic anticorrosive pigments.

Phosphate pigments capable of inhibiting corrosion processes, may be divided into two groups **[20]**. The first one includes phosphates and hydroxyphosphates of metals such as Fe, Ba, Cr, Ca Mg and Zn; but only $FePO_4.2\ H_2O$, $Ca_3(PO_4)_2.1/2\ H_2O$, $Ba_3(PO_4)_2$, $BaHPO_4$ and $FeNH_4PO_4.2\ H_2O$ are of some importance. The use of a $CaZn_2(PO_4)_2.2\ H_2O$ was also reported **[21]**.

The anticorrosive performance of iron phosphate was studied with some detail **[27, 50]**. When used alone, it gave poor results in accelerated tests but mixtures with ZPO are promising. The employment of reaction accelerators such as sodium molybdate, sodium chlorate and sodium m-nitrobenzenesulphonate improved the corrosion resistance of coatings containing this pigment **[51]**.

The second group comprises compounds based on dihydrogen aluminium triphosphate ($AlH_2P_3O_{10}.2\ H_2O$), which is an acid with a pK_a 1.5-1.6. The $P_3O_{10}^{5-}$ anion reacts with anodic iron to yield an insoluble layer consisting mainly of ferric triphosphate. It exhibits a higher corrosion inhibiting power and may be used with alkyd, phenolic, epoxies, epoxy-polyester, acrylic melamine resins, water-thinnable, air drying and stoving binders. Likewise its anticorrosive properties can be improved adding other pigments **[52, 53, 54, 55]**. A freely tonable aluminium metaphosphate employed in conjunction with a zinc compound, preferably zinc oxide and/or an alkaline earth compound, was patented **[54]**. A titanium phosphate with good hiding powder was also prepared **[56]**.

Inorganic pigments such as titanium and zinc white, iron pigments, lithopone, hematite, barium sulphate, silica, alumina, bentonite, talc, chalk, mica, etc., coated with manganese phosphate ($Mn_3(PO_4)_2.3\ H_2O$), were used as anticorrosive ones **[57]**.

Chromic phosphate is not an efficient anticorrosive pigment due to its slight solubility and slow hydrolysis rate. However, it may be used together with other pigments such as strontium chromate and zinc tetroxychromate, in order to improve their inhibiting properties. Chromic phosphate is also used in the so-called one component wash primers **[13, 41, 58, 59]**.

The employment of a strontium zinc phosphosilicate in solvent and water borne paints was reported **[60, 61]**. Austin **[62]** introduced a calcium strontium zinc phosphosilicate showing a performance and versatility similar to zinc chromate.

Zinc hydroxiphosphite **[63, 64]** is claimed to be an effective non-toxic anticorrosive primer. It has small particle size, low oil absorption, minimizes the tendency of latex paints to flush rust, etc.

A japanese patent recorded the employment of a hydrated basic potassium zinc phosphate-phosphite as non toxic anti-rusting pigment **[65]**.

Polyphosphate pigments such as calcium hexamethaphosphate, calcium tripolyphosphate and zinc tripolyphosphate were found adequated for protecting steel against corrosion under typical conditions of the food industry **[66]**.

Tetramethaphosphates of bivalent metals such as zinc, manganese, cobalt, calcium and magnesium were prepared by thermal dehydration of dihydrogen phosphates or from phosphoric acid and metal oxides, hydroxides and carbonates mixtures. Single and double tetramethaphosphates were tested as anticorrosive pigments in alkyd resins based formulations. Some of them, such as calcium and cobalt containing pigments, showed better corrosion resistance than ZP when subjected to accelerated and natural weathering **[67, 68]**.

Surface steel conversion with an organic film barrier were combined in a single corrosion resistance coating utilizing a phosphated polyepoxide coating with good results **[69]**. Phosphated polymers and related treatments were successfully employed in zinc and zinc alloy coatings **[70]**.

Neutral organic phosphates (triphenilphosphate) were used as corrosion inhibitors in engines using lubricant oil containing these phosphates. Their effectiveness depended on the easeness to hydrolyze forming acid phosphates on the metal surface. More readily it hydrolyzes better its performance **[71]**.

FINAL CONSIDERATIONS

In spite of the contradictory data appearing in the reviewed literature it may be seen that the employment of ZP could become successful in moderate outdoor exposures and in industrial atmospheres although poor or bad results were obtained in accelerated tests **[72, 73]**. This fact can be explained considering the very low solubility of ZP. Thus, the penetrating rate of aggressive agents occurring in accelerated tests, largely exceeds the protective action of both the phosphate anion and the formation of a thick iron oxides layers on the metal substrate.

The research work carried out by the authors **[74]** showed that: a) the concentration of phosphate anion is low enough as to impede the metal base oxidation **[45, 75]**, and b) the dissolved oxygen in solution causes the steel dissolution reaction giving ferrous and ferric ions. A compact layer of iron oxyhydroxides (having certain protective characteristics) being formed on the metal surface and the zinc hydroxide precipitated in the cathodic area help to inhibit the oxygen reduction reaction. ZP produces non-adherent ferric phosphate. Further oxygen penetrating leads to the ferric oxide formation

Experimental results and conclusions emanated from different researchers may be not always compared because:

a) Experimental variables such as particle diameter, PVC, types of pigments, additives and binders must be carefully controlled in order to use equivalent experimental conditions. These variables are not always specified in the reviewed literature.

b) ZP does not withstand accelerated tests although it can perform well in moderate outdoor environments and in acid environments because it activates in

such media.

c) Anticorrosive paints behaviour is highly dependent on the type of binder employed, and only after its barrier effect fails the pigment action becomes important. Modified zinc phosphates have a better anticorrosive performance and they can have good performance in accelerated tests.

In order to improve the ZP anticorrosive action it is recommended:

a) optimize both the shape and the particle size distribution;
b) increase the soluble phosphate anion concentration;
c) introduce other inhibitive species; and
d) increase coating adhesion.

Spherical shaped particles are preferred to lamellar ones in order to improve the coating packaging. Modifying the specific surface area, the phosphate leaching from the pigment is enhanced.

When binders with carboxylic acids are to be employed, the addition of basic groups improved their adhesion properties.

ZP could be employed with most binders.

ZP anticorrosive mechanism is not still fully understood yet. It was believed that the phosphate anion is an anodic inhibitor producing a protective layer on ferrous substances. The building up of this layer depends on the phosphate concentration. Some researchers have found that the cathodic areas were also polarized by the sparingly soluble salts appearing on them.

Adhesion promoting substances would also enhance the anticorrosive properties of zinc phosphates.

ZPA is more acidic because of the hydrolysis of aluminium ion and gives rise to a higher soluble phosphate concentration.

ZMP incorporates molybdates as anodic inhibitors. Neverthless, the mixtures with other toxic pigmentes, although useful, is not recommended due to the environmental pollution.

The authors of this review think that ZP could be employed in the terms described in the paper. At present, modified zinc phosphate is a convenient alternative pigment; however, from now on other phosphates with enhanced solubility in water must be ascertained. The anticorrosive mechanism needs to be clarified in order to find the adequated phosphate for each kind of exposure (rural, industrial, etc.) be chosen.

ACKNOWLEDGEMENTS

The authors are grateful to CIC (Comisión de Investigaciones Científicas de la Provincia de Buenos Aires) and CONICET (Consejo Nacional de Investigaciones Científicas y Técnicas) for their sponsorship to write this review.

REFERENCES

[1] Reichle, P., Funke W.- **J. Protect. Coat. & Linings, 4 (9)**, 6 (1987).

[2] Meyer, G.- **Farbe+Lack, 69** (7), 528-532 (1963).

[3] Fragata, F. de L., Dopico, J. E.- **J. Oil Col. Chem. Assoc., 74 (3)**, 92-97 (1991).

[4] Pfizer, Pigments, Inc.- **Zinc Phosphate. Technical Specification.**

[5] Hare, C. H.- **J. Protect. Coat. & Linings, 7 (10)**, 61-67 (1990).

[6] Barraclough, J., Harrison, J. B.- **J. Oil Col. Chem. Assoc.,** 341-355 (1965).

[7] Kukla, J., Tyrka, E., Polen, S.- **Hydrokorr-Organokorr '86 Seminar**, 42-51 (1986).

[8] Depireux, J., Piens, M.- **18th FATIPEC Congress, vol. 3**, 183-201 (1987).

[9] Pietsch, S.- **Plaste Kautschufk, 36 (7)**, 246 (1989).

[10] Stranger-Johannessen, M.- **18th Congress FATIPEC, vol 3**, 1-3 (1987).

[11] Burkill, J. A., Mayne, J. E. O.- **J. Oil Colour Chem. Assoc., (9)**, 273-285 (1988).

[12] Brauer, G.- **Química Inorgánica Preparativa.** Ed. Reverté, p 646, Barcelona (1958).

[13] Svoboda, M.- **Prog. Org. Coat. 12**, 251-297 (1984).

[14] Gerhard, A., Bittner, A., Gawol, M.- **European Supplement to Polymer Paint Colour Journal**, 62-68 (1981).

[15] Nedorost, M., Svoboda, M., Braun, S., Palffy, A., Halamova, K., Jirakova, D., Knapek, B., Donat F.- **Czech. CS 235.770 (CI. C09 C3/00)**, 1 Dec 1986, Appl 82/5, 514, 19 Jul 1982.

[16] Gerhard, A., Bittner, A.- **J. Coat. Tech. 58(740)**, 59-65 (1986).

[17] Kresse, P.- **Farbe+Lack 80(2)**, 85-95 (1977).

[18] Aubareda, J., Leblanc, O., Martorell C.- **Spanish Patent 8.702.407**.

[19] Roland, W. A., Gottwald, K. H.- **Metalloberflaeche 42(6)**, 301-305 (1988).

[20] Chromy, L., Kaminska, E.- **Prog. Org. Coat. 18(4)**, 319-324 (1990).

[21] Robu, B. C., Orban, N., Varga, G.- **Polymer Paint Col. J. 177(4197)**, 566 y 569 (1987).

[22] Waardal, O.(Jr.)- **Polym. Paint. Col. J. 182 (4302)**, 154-156 (1992).

[23] Garnaud, M. H. L.- **Polym. Paint. Col. J. 174**, 268-270 (1984).

[24] Nedorost, M., Svoboda, M., Mlcoch, AA., Palffy, A., Braun, S., Jirakova, D., Halamova, K., Knapek, B., Donat, F.- **Czech.CS 237,475** (Cl, C 09 C 1/36), 15 Jan 1987, Appl 84 11,023, 14 Feb 1984.

[25] Bittner, A.- **J. Coat.Tech., 61 (777)**, 111-118 (1989).

[26] Koopmans, A.- **XIV FATIPEC Congress, Congress Book**, 321-328 (1978).

[27] Torriano, G., Papo, A.- **XV FATIPEC Congress, Vol. III**, 223-239 (1980).

[28] Mishra, U. S., Shukla, M. C.- **Paint & Ink Internat., 5 (3)**, 23 (1992).

[29] Colores Hispania S.A.- Actirox-Hispafos. Anticorrosive pigments. Technical Specifications.

[30] Bittner, A.- **J. Oil Colour Chem. Assoc., 71**, 97-102 (1988).

[31] Hajas, J.- **Europ. Coat. J. 3**, 116-127 (1993).

[32] Bose, S. K.- **Paintindia, 41(2)**, 25-26 (1991).

[33] Williams-Wynn, D. E. A.- **J. Oil Colour Chem. Assoc., 60**, 263-267 (1977).

[34] Gomaa, A. Z. and Gad, H. A.- **J. Oil and Colour Chem. Assoc., 71**, 50-55 (1988).

[35] Nirvan, Y. P. S., Kumar, D., Yagannath, J. H.- **J. Coat. Tech., 59 (745)**, 43-47 (1987).

[36] Schroeder, H., Froemming, I., Schwingeweitzen, G., Hertel, R.- **Ger. (East) DD 245, 892** (Cl. C09D5/08), 20 May 1987, Appl. 286,424, 23 Jan. 1986.

[37] Boxall, J.- **Polym. Paint Col. J., 181**, 443-444 (1991).

[38] Kossmann, H., Witsuba, E.- **XVIII FATIPEC Congress, vol. 1/A**, 291-310 (1986).

[39] Mayne, J. E. O.- **Br. Corros. J., 5 (5)**, 106-111 (1970).

[40] Ruf, J.- **Chimia, 27**, 496 (1973).

[41] Dean, Jr. S. W, Derby, R., Von Dem Bussche, G. T.- **Mat. Perf., (12)**, 47-51 (1981).

[42] Wang, Y., Radovic, D.- **Proc. "Corrosion '91",** Paper 491, Cincinnati 1991.

[43] Menke, J. T.- **Metal Fin. 90(8)** 51-57 (1992).

[44] Leidheiser, H., Jr.- **J. Coat. Tech., 53 (678)**, 29-39 (1981).

[45] Pryor, M. J. Cohen, M.- **J. Electrochem. Soc., 100**, 203 (1953).

[46] Kozlowski, W., Flis, J.- **Corr. Sci., 32(8)**, 861-75 (1991).

[47] Clay, M. F., Cox, J. H.- **J. Oil Colour Chem. Assoc., 56**, 13 (1973).

[48] Szklarska-Smialowska, Z., Mankowsky, J.- **Br. Corros. J., 4 (9)**, 271-275 (1969).

[49] Meyer, G.- **Farbe+Lack, 71(2)**, 113-118 (1965).

[50] Gorecki, G.- **Metal Fin., 90(8)**, 27-29 (1992).

[51] Gorecki, G.- **J. Sci. Eng. Corros., 48(7)**, 613-16 (1992).

[52] Takahashi, M.- **Polym. Paint Colour, J., 177 (4197)**, 554-556 (1987).

[53] Tang, S. Q.- **Paint & Coatings Ind., 4**, 12-15 (1989).

[54] Tayca Corp.- **Japanese Unexamined Patent 03/146567** (1991).

[55] Teikoku Kako, Co.- **European Patent Application 389653.**

[56] Titov, V. P., Pavlov, A. V., Korchagin, V. I., Sushko, V., Ivanov, Yu. M.- **U.S.S.R. SU 1, 353, 788** (Cl. C09 c1/36, 23 M)1987, Appl 3, 980, 330. 26 Nov. 1985.

[57] Nedorost, M., Svoboda, M., Chaloupka, V., Braun, S., Halamova K., Jirakova, D., Knapek, B., Donat, F.- **Czech. C. S. 235, 851** (Cl. C09C3/00), 01 Mar 1987, Appl. 82/ 8, 261, 19 nov 1982.

[58] Rozenfeld, I. L., Zolotova, S. A., Rubinshtejn, F. I., Mamontova, L. M.- **Lakokras Mat. Ikh. Primen., 1**, 27 (1975).

[59] Shtern, M. A., Danjushevskaja, N. E., Alelujeva, O. V.- **Lakokras Mater. Ikh. Primen, 1**, 32 (1964).

[60] Austin, M. J., Beland, M.- **Polym. Paint Col. J., 181**, 168-171 (1991).

[61] Beland, M.- **Am. Paint J., 76(15)**, 43-50 (1991).

[62] Austin, L. - **Proc. PRA Second Asia-Pacific Conf. "Advances in Coatings, Inks amd Adhesives Technology"**, Paper 15, Singapore 1992.

[63] N. L. Chemicals.- **Nalzin 2. Corrosion inhibitive pigment.** Technical report.

[64] Frechette, E., Compere, C., Ghali, E.- **Corr. Sci., 33(7)**, 1067-81 (1992).

[65] Nippon Chemical Industry Co.- **Japanese Patent 90/000384, Jap. Pat. Abs. 90 (2)**, Gp M, 3.

[66] Zovob, E. V., Lugantseva, L. N., Petrov, L. V.- **Lakokras. Mater. Ikh. Primen, 5**, 27-29 (1987).

[67] Mazan, P., Trojan, M., Brandova, D., Solc, Z.- **Polym. Paint Col. J., 180**, 605-606 (1990).

[68] Trojan, M.- **Dyes & Pigments, 12 (1)**, 35-47 (1990).

[69] Robertson, J. A.- **Official Digest,** 138-150 (Feb. 1964).

[70] Brugarolas, J., Rodellas, F.- **Proc. 3rd Internat. Zinc Coated Sheet Conf.** (EGGA/Assoc. Tec. Espan. de Galv.), Paper 7, Barcelona 1991.

[71] Barcroft, F. T., Daniel, S. G.- **Transactions of the ASME, J. of Basic Engeneering,** paper N° 64, pp 1-7 (1964).

[72] Leblanc, O.- **J. Oil. Chem. Assoc., 73 (6)**, 231 (1990).

[73] Leblanc, O.- **J. Oil. Chem. Assoc., 74 (8)**, 288 (1991).

[74] Romagnoli, R., Vetere, V. F.- **CIDEPINT-Anales**, 177-197 (1994).

[75] Rozados, E., Vetere, V. F., Carbonari, R.- **Rev. Iber. Corros. y Prot., IX (3-4)**, 3 (1978).

Nota: This Review has been accepted for publication in Corrosion Reviews.

HIGH BUILD ANTIFOULING PAINTS BASED ON DISPROPORTIONATED CALCIUM RESINATE

PINTURAS ANTIINCRUSTANTES TIPO ALTO ESPESOR BASADAS EN RESINATO DE CALCIO DESPROPORCIONADO

C. A. Giúdice[1] and J. C. Benítez[2]

SUMMARY

Disproportionated calcium resinate was manufactured from disproportionated WW rosin and its fundamental characteristics were determined in laboratory tests.

Some experimental binders were elaborated with disproportionated calcium resinate as soluble film forming material and also with WW rosin, disproportionated WW rosin and calcium resinate which were used as reference.

Then high build soluble antifouling paints based on above mentioned binders and red cuprous oxide as main toxicant were manufactured and tested in raft trials for 33 months: a series of painted panels was exposed to air for 24 hours and another one for 30 days previous to seawater immersion.

Some antifouling paints based on disproportionated calcium resinate displayed good bioactivity at the end of the test being their behaviour unaffected by the exposure to air previous testing.

Keywords: *antifouling paint, binder, cobinder, soluble matrix, high build, dissolution rate, bioactivity, raft trial.*

INTRODUCTION

New products and raw materials applied to antifouling paints manufacture are developed by the constant technological research. One of the advantages of this fact, from a chemical and a biological point of view, is that it obliges to modify the formulations with the aim to attain a higher efficiency and simultaneously to decrease the marine environment pollution.

In this paper, a disproportionated calcium resinate was prepared with the aim to study the influence of different variables of composition of antifouling paints based on this resinous material, using samples formulated with WW rosin **[1]**, disproportionated WW rosin **[2]** and calcium resinate **[3]** as references.

DISPROPORTIONATED CALCIUM RESINATE ELABORATION

Starting from WW rosin as raw material, a disproportionated WW rosin was firstly elaborated by adding iodine at 260 °C and then furfural at 70 °C, according to a method described in a previous paper **[2]**.

---

[1] Miembro de la Carrera del Investigador del CONICET

[2] Miembro de la Carrera del Investigador de la CIC

Employing finely divided disproportionated WW rosin, a disproportionated calcium resinate was prepared adding an aqueous solution of sodium hydroxide, heating at 80 °C up to its complete solubilization. In the same conditions a solution of calcium chloride was added, forming after five minutes with intense stirring a yellow, homogeneous and consistent paste. It was repeatedly washed with distilled water in order to eliminate the sodium chloride formed.

After approximately 10 hours at 45 °C a white powder of small diameter particles of disproportionated calcium resinate was obtained.

FORMULATION VARIABLES

Paints composition is shown in **Table I**. Several variables were considered:

Soluble resinous materials type. WW rosin, disproportionated WW rosin, calcium resinate and disproportionated calcium resinate were selected as film formers.

With the object to evaluate the characteristics of the resinous materials, fusion point (capillary method), melting point (ball and ring method, ASTM E 28-92) and acid number (inside indicator method, ASTM D 465-92) were determined.

The color of transparent solutions based on above mentioned resins and an adequate solvent through the comparison with Gardner standards according to ASTM D 1544-80 and density of the samples at 20 °C, were also determined.

Infrared spectra of the resins were made by applying the method of the solid phase; each material was dissolved in toluene and then was extended on a mounting which is transparent to the infrared radiation (potassium bromide). After the solvent was evaporated in vacuum, film was lifted off the substrate and fixed in the frame to fit it in the rays path.

Soluble resinous material/cobinder ratio. In order to study the influence of this variable on the dissolution rate of the different paints, two resinous material/cobinder ratios were established (1/1 and 2/1 by volume) giving the second one a binder of higher dissolution rate.

Cobinder employed was a non-modified copolymer of medium molecular weight, consisting of 86 % vinyl chloride-14 % vinyl acetate, which offers an adequate balance of the following characteristics: it shows an easy dissolution in cellosolve acetate/xylene/methyl isobutyl ketone mixture (60/30/10 ratio by weight) **[4]** and also leads to films with good physical properties.

42 per cent clorinated paraffin was used as plasticizer since it improves binder flexibility and reduces solvent retention.

Employing a high rate impeller, 8 binders (4 soluble resins x 2 soluble resin/cobinder ratios) were elaborated.

Toxicant content. Cuprous oxide was selected as fundamental toxicant **[5-8]**, zinc oxide as reinforcing pigment (10 % by volume respect to the mentioned toxicant) and calcium carbonate (chalk) as extender.

Two levels of cuprous oxide were considered: 10.0 % and 12.7 %, expressed as solids by volume on paint. With the aim to dispose high pigment contents but without affecting seriously the film characteristics, only one volume pigment concentration (PVC 39.4 %) was selected in all the cases.

EXPERIMENTAL PAINTS ELABORATION

Sample manufacture was made by employing a ball mill of 3.3 liters capacity **[9, 10]**. The four series of paints based on WW rosin, disproportionated WW rosin, calcium resinate and disproportionated calcium resinate were prepared by dispersing firstly the zinc oxide and the calcium carbonate and then, the cuprous oxide. After the last one was added, the process went on for 3 hours.

Finally the rheological additive was incorporated to each sample by employing the before mentioned high rate impeller: a gel of amorphous silicic acid with 5 % by weight was used, selecting a level of 2.0 % by weight on the total paint in order to achieve good rheological properties and easy airless spray application.

A similar set of paints was prepared but using only 1.0 % of thixotropic additive in order to have conventional products which were colored with blue, red or yellow pigments in order to facilitate the visual observation to estimate film thickness decreasing on service.

RAFT TESTING VARIABLES

Antifouling paints performance was evaluated on the experimental raft anchored at Puerto Belgrano (38°54'S; 62°06'W), area whose hydrological and biological conditions were studied **[11, 12]**.

Steel panels SAE 1010 were sandblasted to the grade ASa 2 1/2, washed with xylene and covered with an anticorrosive coating (two coats, 120-150 μm of dry film thickness) and a sealer (one coat, 50-60 μm). This scheme showed a successful behaviour in previous trials.

After 24 hours, the experimental antifouling samples were applied. Panels were covered with three coats of the formulated thixotropic products (approximately 300 μm of total dry film thickness). Other series of panels with 6 coats of conventional colored products were prepared, reaching also about 300 μm of total dry film thickness.

In all cases the time between coats was 24 hours, retouching by brush the panels edge. A series of panels was exposed to air for 24 hours and a similar one for 30 days for weathering previous to seawater immersion.

RESULTS AND DISCUSSION

Characteristics of the soluble resinous material

Table II shows the values of fusion and melting points for WW rosin and disproportionated WW rosin measured at laboratory; both materials have perfectly defined values which allow the characterization of the resins. However these methods could not be applied to both calcium resinates since at low temperatures they did not display any modification and besides when they were heated over 200 °C showed clear signs of decomposition.

Acid number determination was also very useful; this value decreased from 160 to 139 through the disproportionating process of the original rosin giving a mixture of dehydro, dihydro and tetrahydroabietic acids. The acid value of the disproportionated calcium resinate was as expected (lower in relation to the natural WW rosin and disproportionated WW rosin).

TABLE I

Composition of the antifouling paints (solids by volume, %)

Composition	A	B	C	D
Cuprous oxide	10.0	10.0	12.7	12.7
Zinc oxide	1.0	1.0	1.3	1.3
Calcium carbonate	28.4	28.4	25.4	25.4
Soluble resin*	24.4	34.0	24.4	34.0
Cobinder	24.4	17.0	24.4	17.0
Plasticizer	7.0	4.8	7.0	4.8
Additives	4.8	4.8	4.8	4.8
Soluble resin/cobinder ratio by volume	1/1	2/1	1/1	2/1

* Each one of the experimental samples was prepared by employing WW rosin, disproportionated WW rosin, calcium resinate or disproportionated calcium resinate

TABLE II

Characterization of the resinous materials

Test	WW rosin	Disproportinated WW rosin	Calcium resinate	Disproportionated calcium resinate
Fusion point, °C	75	68	---	---
Melting point, °C	57	50	---	---
Acid number	160	139	29	25
Color Gardner	7	4	3	2
Density (20°C), g/ml	1.08	1.11	1.13	1.18

Color comparison of the resins solutions according to ASTM D 1544-80 also was a method of easy application; it showed a color decreasing according to the transformation of the original resin (disproportion in a first stage and after this partial neutralization).

Infrared spectra of both calcium resinates **(Fig. 1 and 2)** display in the zone of wave number 3400-3250 cm^{-1} , the overtone of the present peaks at 1720 cm^{-1} corresponding to the carbonyl group of esters. In the zone of wave number 3200-2800 cm^{-1} both calcium resinates show a significant thinning of the resinates peak respect to both rosins, according to an important decreasing of the acid dimers. Also, it is confirmed due to the disappearance of the peaks in the zone 1300-1100 cm^{-1} of the disproportionated WW rosin spectrum which is also attributable to the stretching of the C-O bond at 1475 cm^{-1} and 1180 cm^{-1} in the carboxyl group of the acids. Finally at 1560-1540 cm^{-1} appeared a peak that corresponds to the stretching of the acid group

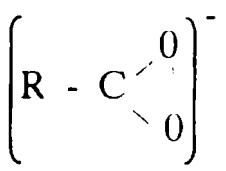

which is characteristic of salts.

Immersion trial. Bioactivity

Raft trials were programmed in order to observe periodically the painted panels and to record the fouling settlement after 4, 16, 28, and 33 months of immersion; the last one includes three periods of intense biological activity of the fouling organisms (spring-summer).

Sandblasted non-toxic acrylic panels submerged at the same depth than the mentioned ones were employed as reference of fouling fixation.

Fouling settlement evaluation, which allows the judging of the performance or bioactivity degree of each sample, was made by applying the scale mentioned in previous papers **[13, 14]**. Value 0 (100 % of efficiency) corresponds to a panel without settlement and 5 (0 % of efficiency) to the one totally fouled; value 1 , which corresponds to 80 % of efficiency, was fixed as the maximum limit to accept a paint from the antifouling point of view.

In all the cases the observations were complemented by means of color prints which allowed to compare the results obtained in the different observations and to have a homogeneous evaluating criterion.

The conclusions of the inspections are included in **Tables III and IV** (24 hours and 30 days of exposure to air previous testing respectively). To a minimum biocidal efficiency of 80 % (settlement 1, little), the useful life of each paint and also the film thickness required to achieve the before mentioned behaviour are pointed out.

A great influence of the several variables considered (soluble resinous material type, soluble resinous material/cobinder ratio, toxicant content and exposure time to air after painting and before seawater immersion) was observed. The analysis of results corresponding to experiments carried out in the present study and some conclusions previously attained allow to set a series of advantages and disadvantages that the several resinous materials studied present.

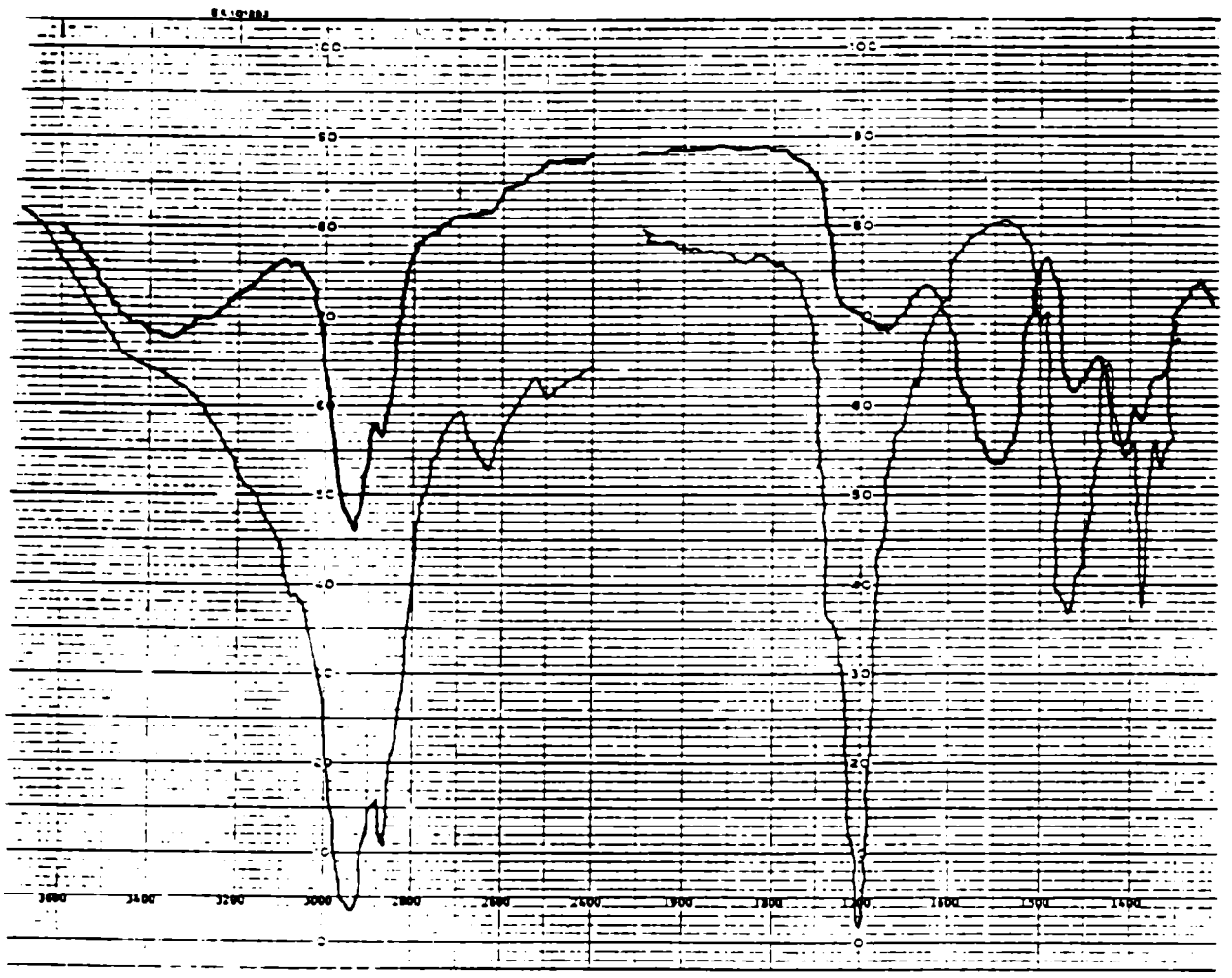

Fig. 1.- Infrared spectra of the WW rosin resin (fine stroke) and calcium resinate (thick stroke).

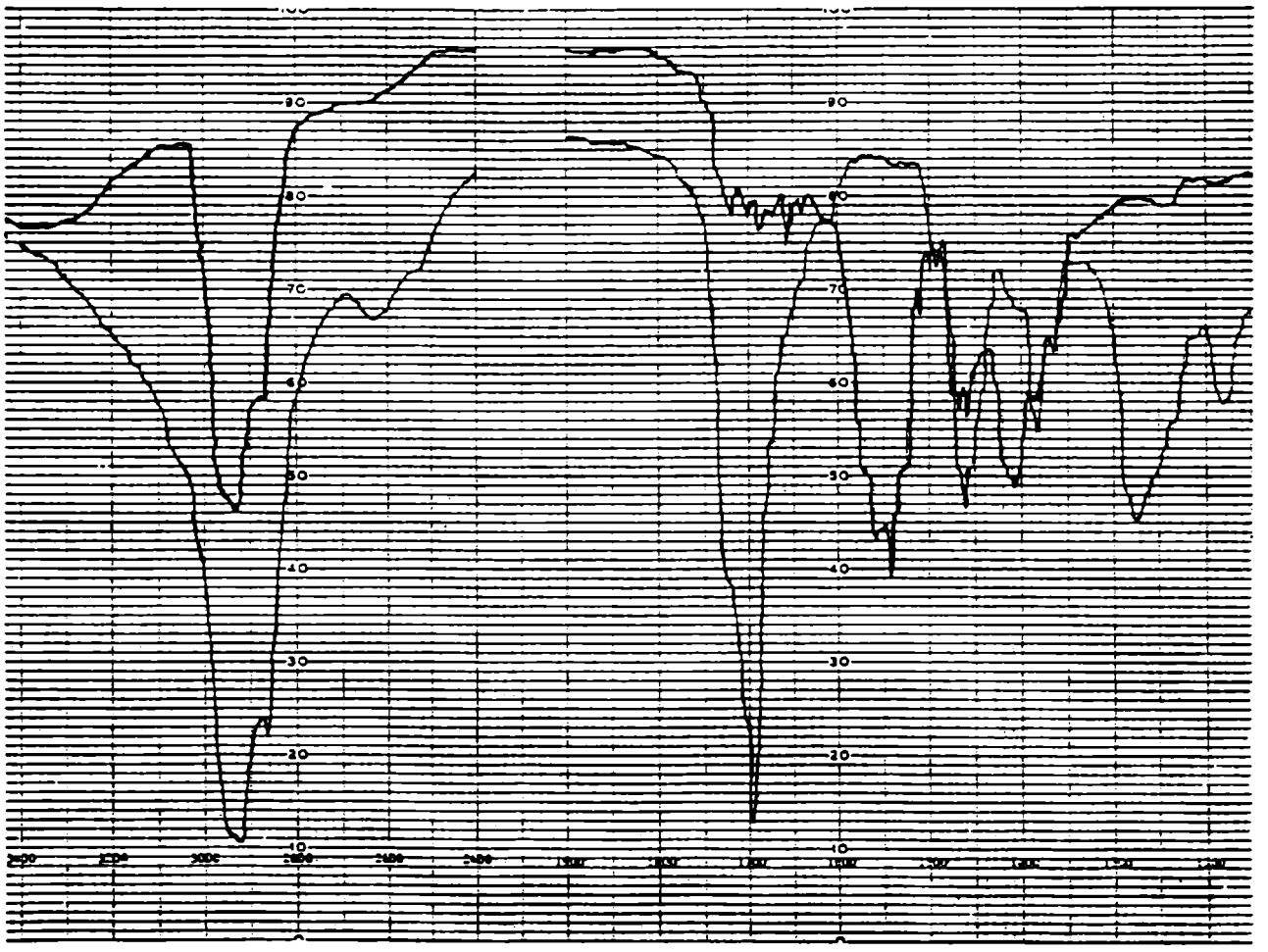

Fig. 2.- Infrared spectra of disproportionated WW rosin (fine stroke) and disproportionated calcium resinate (thick stroke).

TABLE III

Biocide behaviour of the paints
24 hours of air exposure before immersion

Formulation	Soluble resin	Efficient time, months	Fixation grade, %	Required film thickness (minimum), μm
A	Original WW rosin	16	80	150
B		28	80	250
C		16	90	150
D		33	100	250
A	Disproportionated WW rosin	16	80	150
B		28	90	250
C		16	90	150
D		33	90	250
A	Calcium resinate	16	80	100
B		28	90	200
C		16	80	100
D		33	90	200
A	Disproportionated calcium resinate	16	80	100
B		28	90	200
C		16	90	100
D		33	100	200

TABLE IV

Biocide behaviour of the paints
30 days of air exposure before immersion

Formulation	Soluble resin	Efficient time, months	Fixation grade, %	Required film thickness (minimum), μm
A	Original WW rosin	28	80	250
B		33	100	>300
C		33	100	250
D		33	100	>300
A	Disproportionated WW rosin	16	80	150
B		28	80	250
C		16	90	150
D		33	100	250
A	Calcium resinate	16	80	150
B		28	100	250
C		28	90	200
D		33	100	300
A	Disproportionated calcium resinate	16	80	100
B		28	90	200
C		16	80	100
D		33	100	200

CONCLUSIONS

Original WW rosin

Advantages. Due to its physical and chemical properties, rosin is a natural resin widely used in the paint industry. It consists of nearly 85 per cent of resinic acids (abietic acid and its isomers) and the rest are complex esters of those acids with unsaponifiable materials. Due to its acid nature, rosin is the main binder component in soluble antifouling paints since it regulates the leaching rate of the toxic pigments. Toxicant content can be ranged between extensive limits if binder dissolution rate is selected to have in film/seawater interface the adequate toxicant concentration to prevent fouling settlement. Efficient antifouling paints were developed worldover for long immersion time using WW rosin. Paints based on binders with the 2/1 WW rosin/cobinder ratio showed a higher seawater dissolution rate (less remainder dry film thickness) as well as a longer useful life than the paints formulated with 1/1 ratio binders. **Fig. 3.1** displays the excellent behaviour (100 % of efficiency) corresponding to the paint D (original WW rosin, 24 hours of air exposure before seawater immersion) for 33 months on raft.

Disadvantages. The molecule of abietic acid has a carboxyl group which is responsible during immersion for the reaction with sodium and potassium ions to give a rapid initial dry film decrease and a high undesirable toxicant release; the reaction with calcium and magnesium ions reduces the dissolution rate. The mentioned reaction with divalent cations also takes place during paint manufacture, particularly when cuprous oxide and calcium carbonate are employed in the formulations. Cuprous oxide generates cupric oxide and metallic cooper **[15]** forming cupric resinates, which diminishes the binder dissolution rate and therefore the toxicant leaching rate **[8, 9]**. The pigment-binder reaction, which significantly depends on cuprous oxide dispersion time, modifies the composition of the paint and reduces the film bioactivity. However, when before mentioned toxicant dispersion takes place in the absence of WW rosin, or when it is adequately controlled, paint bioactivity remains practically unmodified.

Other important disadvantage is given by the fact that when paint films based on WW rosin are exposed to air previously seawater immersion, oxidation takes place and as a consequence, binder dissolution rate increases according to the exposure time and then a higher dry film thickness is required. This is not convenient from a technical, economical and ecological viewpoint since a higher toxicant leaching rate than the critical value takes place. **Fig. 4.1** shows the very good biocidal capacity (100 % of efficiency) of sample D (original WW rosin, 30 days of air exposure before seawater immersion) for 33 months in raft trial, which was attained with a high dry film thickness (300 μm as minimum).

Disproportionated WW rosin

Advantages. This resin shows some important modifications in relation with original WW rosin. As before mentioned, the last one is mainly formed by abietic acid and its isomers (levopimaric and isodextropimaric acids) while after its exposure to air the presence of dihydroxiabietic acid is firstly observed and when the exposure time increases (higher oxidation degree) the main component is the tetrahydroxiabietic acid **[2]**.

Disproportionated WW rosin is basically constituted by some rest of original resin and mainly by a mixture of dehydroabietic (three double bonds), dihydroabietic (only one double bond) and tetrahydroabietic acid (without double bonds). As a consequence, the steady state dissolution rate of binders based on disproportionated WW rosin becomes practically independent of exposure time to air previous seawater immersion, which is a very important fact from a technical and

economical viewpoint to establish drydock programs. **Fig. 3.2 and 4.2** show a similar bioactivity of paint D both for 24 hours and 30 days of exposure to air previous seawater immersion (90 % and 100 % of efficiency, respectively); both paints had the same dry film thickness requirement at the end of the test (33 months on experimental raft).

Disadvantages. Antifouling paints based on both WW rosin and disproportionated WW rosin as film forming resins, show a high initial dissolution rate. In a first stage, the reaction between acid components of the resin and sodium and potassium ions present in seawater, is responsible for the significant dry film reduction **[8]** and then for the high toxicant content lixiviated **[16]**.

Calcium resinate

Advantages. Antifouling paints based on WW rosin show a fast reduction of resinic acids content in the outlayers of the film and slower in the interior ones after seawater immersion. In general, these films display an important increase of metallic resinates concentration and a marked reduction after reaching a maximum level **[16]**. After long immersion time, results indicate that acid materials are not practically present in the film; consequently it is possible to deduce that the film dissolution rate takes place by the solubilization of metallic resinates when the steady state is reached.

The employ of calcium resinate instead of WW rosin leads to paints which attain on service a faster dissolution steady state **[8]**; thus, it decreases significantly the disadvantages showing films based on WW rosin at the begining of seawater immersion (high dry film thickness reduction and consequently an excessive toxicant lixiviation).

Besides, when calcium resinate is selected as soluble resin in antifouling paints, films show on service a similar efficiency than those based on WW rosin and cuprous oxide dispersed in absence of the quoted acid resin **[3]**. Now, both toxicant dispersion in absence or in presence of calcium resinate and the time selected for pigment processing do not have a significant influence on the paint bioactivity. However, it simplifies markedly the paint manufacture (no exhaustive control of cuprous oxide dispersion is necessary).

Disadvantages. Films formulated with calcium resinate as soluble resin show an increase in the binder dissolution rate similar to films based on WW rosin when are exposed to air previous seawater immersion, originating consequently a similar damage (economical loss and unnecessary marine pollution), **Tables III and IV**. **Fig. 3.3 and 4.3** display the biocidal capacity of sample D for 24 hours and 30 days of air exposure previous seawater immersion, respectively; dry film thickness required as minimum for 33 months on raft is significantly higher when painted panel was exposed to air for 30 days.

Disproportionated calcium resinate

Advantages. This resinous material combines the good properties which characterize WW rosin, disproportionated WW rosin and calcium resinate as soluble film former. Thus, antifouling paints formulated with disproportionated calcium resinate achieve a fast dissolution steady state without lixiviating unnecessary toxicant for the first stage of immersion. Binder dissolution rate (dry film thickness diminution) becomes practically independent of exposure time to air before immersion and the reaction between divalent ions and some acid components of binder during paint manufacture, which modifies the paint composition and then the film bioactivity on service, is negligible. **Fig. 3.4 and 4.4** show the excellent biocidal behaviour (100 % of efficiency in both cases) corresponding to paint D, with 24 hours and 30 days of air exposure before seawater immersion, for

33 months on raft. Paints manufactured with this resinous material are the most convenient from technical, economical and ecological viewpoints.

Disadvantages. Disproportionated calcium resinate does not show relative disadvantages according to variables considered in this study.

ACKNOWLEDGEMENTS

The authors are grateful to CIC (Comisión de Investigaciones Científicas) and to CONICET (Consejo Nacional de Investigacines Científicas y Técnicas) for their sponsorship for this research, to Puerto Belgrano Naval Shipyard and Control Laboratory for the assistance given during the observations and to Lic. R. Perez Duprat and Chem. Eng. S. Zicarelli (CIDEPINT) for the infrared spectra interpretation.

REFERENCES

[1] Giúdice, C. A., del Amo, B., Rascio, V.- **Proc. 9th International Congress on Metallic Corrosion**, Toronto, Canada, **2**, 510-514 (1984).

[2] Giúdice, C. A., Benítez, J. C.- **Anales 4to. Congreso Iberoamericano de Corrosión y Protección**, Mar del Plata, Argentina, **Vol.II**, 653 (1992).

[3] Giúdice, C. A., del Amo, B., Rascio, V. - **Progress in Organic Coatings, 16** (2), 165 (1988).

[4] del Amo, B., Giúdice, C. A., Sindoni, O. - **Progress in Organic Coatings, 17**, 287 (1989).

[5] Abd el-Malek, M., Ghanem, N. A. - **Proc. 4th Int. Congress on Marine Corrosion and Fouling**, Antibes, France, 33 (1976)

[6] Jhonsen, S., Rendbaek, V. - **Proc. 4th Int. Congress on Marine Corrosion and Fouling**, Antibes, France, 271, (1976).

[7] de la Court, F. M. - **J. Oil Col. Chem. Assoc., 63** (9) 241 (1986).

[8] Giúdice, C. A., Rascio, V.- **Proc. 11th Int. Corrosion Congress**, Milano, Italia, **Vol.2**, 2335 (1990).

[9] Giúdice, C. A., del Amo, B., Rascio, V., Sanchez, R.- **J.Coat.Technol., 55** (697), 23 (1983).

[10] Giúdice, C. A., Benítez, J. C., Rascio, V., Presta, M.- **J. Oil Col. Chem. Assoc., 63** (4) 153 (1980).

[11] Bastida, R. et al.- **Corrosión y Protección, 8** (8-9), 11 (1977).

[12] Bastida, R., Lichtschein, V.- **Corrosión y Protección, 10** (3-4),7 (1979).

[13] Bastida, R.- **Proc. 3rd Int. Congress on Marine Corrosion and Fouling,** Gaithersburg, Maryland, 847 (1972).

[14] Fletcher, R. L.- **Bulletin de Liaison du COIPM** N° 8, 5 (1980).

[15] Hurd, L. C., Clark, A. R.- **Industrial and Enginnering Chemistry, Analytical Ed., 8** (5), 380 (1936).

[16] Giúdice, C. A., del Amo, B., Rascio, V., Sindoni, O.- **J. of Coat.Technol., 58** (733), 45 (1986).

3.1. WW rosin resin
Dry film thickness
required, minimum 250 µm
Efficiency, 100 %

3.2. Disproportionated WW rosin
Dry film thickness
required, minimum 250 µm
Efficiency, 90 %

3.3. Calcium resinate
Dry film thickness
required, minimum 200 µm
Efficiency, 90 %

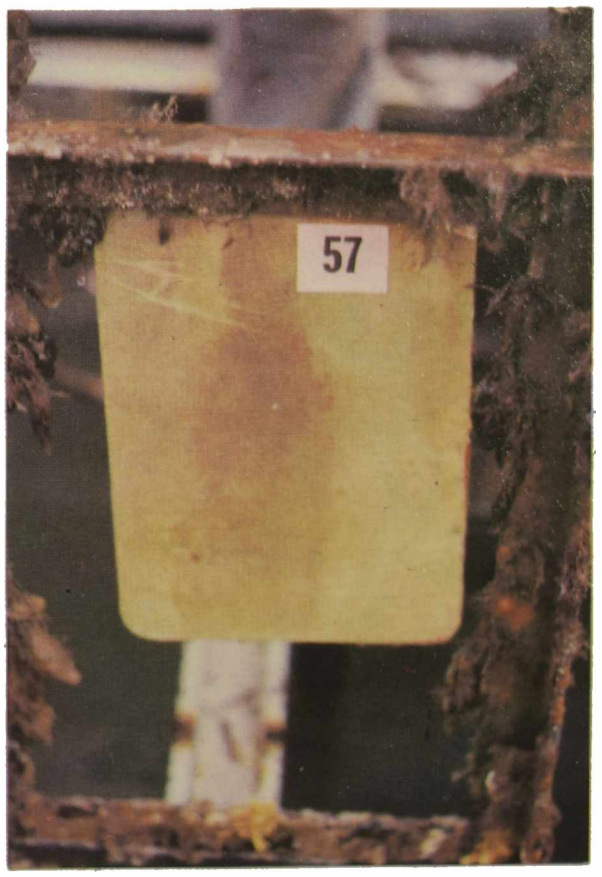

3.4. Disproportionated calcium resinate
Dry film thickness
required, minimum 200 µm
Efficiency, 100 %

Fig. 3.- Behaviour of sample D (24 hours of air exposure before immersion) in raft trial after 33 months of immersion.

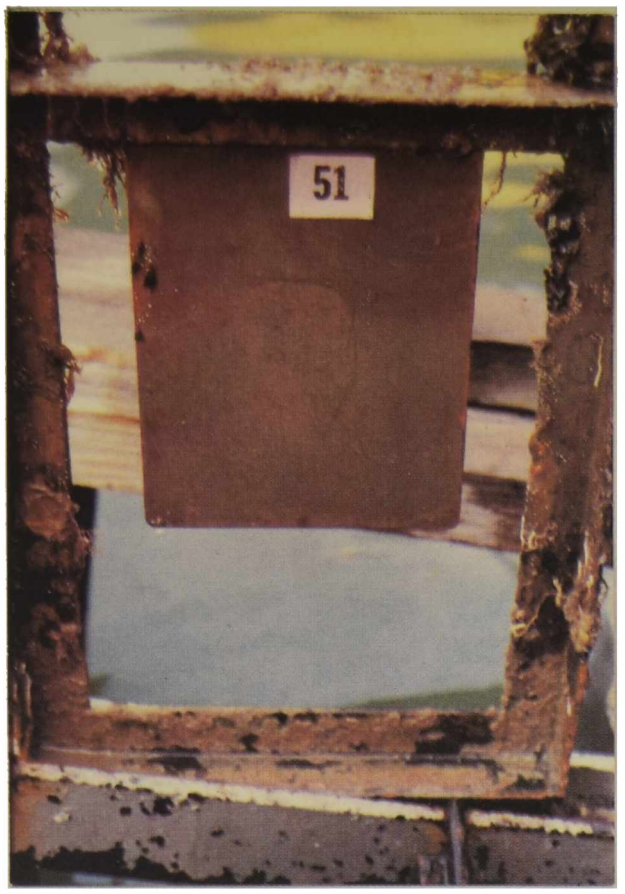

4.1. WW rosin resin
Dry film thickness
required, minimum 300 µm
Efficiency, 100 %

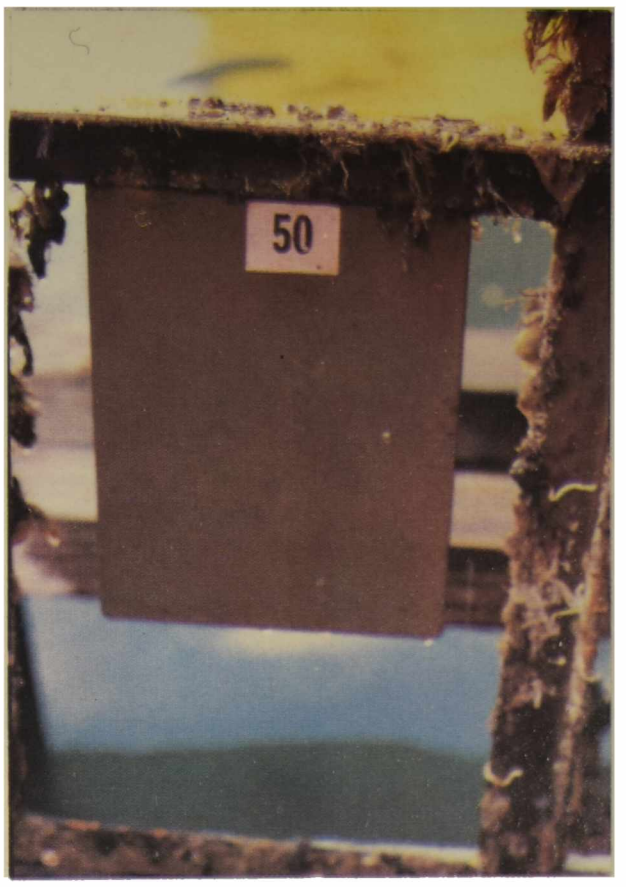

4.2. Disproportionated WW rosin
Dry film thickness
required, minimum 250 µm
Efficiency, 100 %

4.3. Calcium resinate
Dry film thickness
required, minimum 300 µm
Efficiency, 100 %

4.4. Disproportionated calcium resinate
Dry film thickness
required, minimum 200 µm
Efficiency, 100 %

Fig. 4.- Behaviour of sample D (30 days of air exposure before immersion) in raft trial after 33 months of immersion.

CYTED - SUBPROGRAMA XV

CORROSION: IMPACTO AMBIENTAL SOBRE LOS MATERIALES

REUNION CONSTITUTIVA DE LA RED TEMATICA XV:
Red Iberoamericana de Corrosión Microbiológica
y Biofouling en Sistemas Industriales

La primera Reunión Constitutiva de la Red se realizó en La Plata en el Centro de Investigación y Desarrollo en Tecnología de Pinturas (CIDEPINT), durante los días 1, 2 y 3 de diciembre de 1993. Las tareas de organización de la misma estuvieron a cargo del Dr. Héctor Videla y la Dra. Mónica F. L. de Mele.

En el inicio de la reunión se sometió a votación la propuesta realizada por el Dr. Leonardo Üller, Coordinador Internacional del Subprograma XV, de designar al Dr. Héctor A. Videla como Coordinador Internacional de la Red. Dicha propuesta fue aprobada por unanimidad por los participantes de la reunión.

Los participantes de la reunión fueron:

Coordinador Internacional del Subprograma XV: Dr. Leonardo Üller
Coordinador Internacional de la Red Temática XV: Dr. Héctor A. Videla

y los delegados de los siguientes países (en orden alfabético):

Argentina: Dra. Mónica F. L. de Mele y Dr. Vicente Rascio, Director del CIDEPINT, sede de la reunión y miembro de la Red.

Brasil: Dra. Christine Gaylarde.

España: Dr. Carlos Ranninger.

México: Dr. Guillermo Hernández.

Portugal: Dra. Ana Rosa Leal Lino

Venezuela: Ing. Cilene Boscán de González

En forma extraoficial, el último día de la reunión, participó también la Ing. Susana Rivero, representando a Uruguay.

El programa de la reunión fue el siguiente:

Miércoles 1 de diciembre
Apertura (Dr. Videla - Dr. Rascio)
Contenido General del Plan CYTED (Dr. Üller)
Exposición por países:
- Argentina (Dra. Mele)
- Brasil (Dra. Gaylarde)
- España (Dr. Ranninger)
- México (Dr. Hernández)

Comentarios generales de cierre

Jueves 2 de diciembre
Exposición por países:
Portugal (Dra. Lino)
Venezuela (Dra. Boscán)
Resumen general y comentarios
Presentación de propuesta del Coordinador de la Red (Dr. Videla)
Discusión general, propuestas y comentarios generales de cierre

Viernes 3 de diciembre
Visita al CIDEPINT
Propuestas del Coordinador (Dr. Üller)
Discusión sobre la incorporación de nuevos países
Plan de actividades para 1994 y Sede de la próxima reunión
Conclusiones. Discusión. Aprobación del plan de actividades y publicaciones

De acuerdo con lo expuesto precedentemente la apertura de la reunión estuvo a cargo del Dr. Videla, que se refirió a la organización de la misma. Seguidamente el Dr. Rascio dió la bienvenida a coordinadores y delegados destacando la trascendencia del evento.

El Dr. Üller se refirió posteriormente a la organización del CYTED en lo referente a su historia, objetivos, países y organismos signatarios, mecanismos de gestión y explicación de la génesis y desarrollo de un proyecto precompetitivo dentro del programa CYTED. También se describieron las modalidades de actuación y los proyectos y redes actualmente existentes dentro del Subprograma XV.

A continuación se inició la exposición por parte de los representantes de cada país sobre el estado actual de desarrollo del tema de la Red en su grupo de investigación así como en los centros e instituciones relacionadas a la temática en dicho país. Se enumeraron las publicaciones, congresos y actividades relacionadas, poniéndose especial énfasis, en los problemas de corrosión y biofouling que afectan a la industria y destacándose aquéllas que serían potencialmente indicadas para apoyar la iniciativa. Expusieron sucesivamente:

Dra. Mónica F. L. de Mele, Sección Bioelectroquímica, Instituto de Investigaciones Fisicoquímicas Teóricas y Aplicadas (INIFTA), Argentina.

Dra. Christine Gaylarde, Dept. de Solos, Universidad Federal de Río Grande do Sul, Brasil.

Dr. Guillermo Hernández-Duque, Universidad Autónoma de Campeche, México.

Dr. Carlos Ranninger, Dept. Ingeniería y Ciencia de Materiales, Escuela Técnica Superior de Ingenieros Industriales, España.

En la segunda jornada hicieron lo propio los siguientes expositores:

Dra. Ana Rosa Leal Lino, Instituto de Tecnología Química y Biológica, Portugal.

Ing. Cilene Boscán de González, Centro de Investigación y Apoyo Tecnológico Filial Petróleos de Venezuela, INTEVEP, S.A., Venezuela.

A continuación el coordinador internacional de la Red, Dr. Üller, presentó a consideración de los delegados la propuesta de objetivos que se enumeran a continuación:

Creación de un banco de datos

Realización de una reunión de trabajo de frecuencia anual
Desarrollo de sistemas de monitoreo
Estudio de mecanismos, microorganismos, colección de cultivos, biocidas, cubiertas, etc.
Evaluación del impacto ambiental
Publicación de un manual práctico para la industria
Organización de cursos y seminarios

Posteriormente se enunció el contenido temático de la Red, en base a una descripción de los siguientes puntos:

Definición conceptual del proceso
Complementación interdisciplinaria e interinstitucional
Detección, identificación y diagnóstico del problema
Evaluación de la incidencia en el sector industrial
Implementación de sistemas de seguimiento, prevención y protección

El plan de actividades para el año 1994 quedó formulado de la siguiente manera:

Diagramación definitiva de las unidades participantes
Propuesta de nuevas unidades
Detección de industrias afectadas en cada país
Elaboración del cronograma de reuniones
Congresos y seminarios
Relación interinstitucional
Complementación con otros proyectos o redes CYTED

Por último el coordinador internacional de la Red enumeró los países participantes de la Red y propuso a Cuba y Uruguay como países a incorporar en forma inmediata.

A continuación de dicha presentación se discutieron las propuestas y se realizaron comentarios respecto a las mismas por parte de los distintos delegados de la Red y del coordinador del Subprograma XV. Fue así como, a iniciativa del representante de España se incorporó un nuevo objetivo prioritario: Apoyar y promover en cada país los programas y proyectos nacionales de investigación sobre "Corrosión Microbiológica y Biofouling en Sistemas Industriales".

A propuesta del Dr. Üller, coordinador del Subprograma XV, se discutió el orden de prioridad de los objetivos. Se decidió que durante 1994 se elaboraría un banco de datos en coordinación con la Red RICORR que determinaría la forma de presentar y procesar los datos.

Se sometieron a consideración de los participantes distintos nombres abreviados para la red, eligiéndose por votación la sigla BIOCORR y se eligió a Venezuela como país sede de la próxima reunión que se realizaría en la ciudad de Maracaibo en una fecha próxima a la de la convocatoria para el Primer Congreso de Corrosión NACE - Región Latinoamericana (noviembre de 1994).

Se consideró además que debería realizarse la evaluación del impacto ambiental de los problemas de Biocorrosión y Biofouling a fin de poder sentar los precedentes que diera lugar al establecimiento de normativas al respecto y también se consideraron como posibles temas para la elaboración de otros subproyectos que en un futuro podrían proponerse a consideración del CYTED. Se consideró adecuada la realización de cursos y seminarios en fechas próximas a la reunión anual del CYTED, para el aprovechamiento por parte del país sede de la presencia de los especialistas extranjeros.

En cuanto al cronograma de actividades para 1994 se establecieron las posibles fechas límite para la realización de las tareas:

	Fecha tentativa
Información sobre Banco de Datos (últimos 5 años) (Area temática, Instituciones, Empresas, productos y servicios, Tesis y monografías, Simposios, reuniones y asociaciones relacionadas)	30 de abril
Normativas sobre impacto ambiental	
Preliminar	30 de abril
Final	30 de agosto
Capítulos del manual I.- Introducción II.- Casos históricos III.- Identificación de casos de corrosión microbiológica IV.- Sistemas de seguimiento, evaluación y estudio V.- Prevención y control	30 de agosto
Próxima Reunión de la Red, realización de cursos y seminarios	30 de agosto

De izquierda a derecha. Primera fila, Ing. C. B. de González (Venezuela), Dra. M. F. L. de Mele (Argentina), Dra. A. R. Leal Lino (Portugal), Dra. C. Gaylarde (Brasil) e Ing. S. Rivero (Uruguay); segunda fila, Dr. V. Rascio (Argentina), Dr. H. A. Videla (Argentina), Dr. L. Üller (Brasil), Dr. C. Ranninger (España) y Dr. G. Hernández (México).

**ESTE EJEMPLAR SE TERMINO
DE IMPRIMIR EL DIA 30 DE
AGOSTO DE 1994 EN LA
EMPRESA COPIAS 55**

SERVICIOS CALIFICADOS QUE PRESTA EL CENTRO

Estudios y asesoramiento sobre problemas de corrosión de materiales en contacto con medios agresivos.
Estudios y asesoramiento sobre protección de los mencionados materiales por medio de cubiertas orgánicas (pinturas), inorgánicas (silicatos) o metálicas (galvanizado, cromado, niquelado).
Estudios sobre protección de metales, maderas, hormigones, plásticos, etc., empleados en estructuras de edificios, puentes, diques, instalaciones industriales, instalaciones navales, etc.
Estudio de medios agresivos.
Asesoramiento sobre diseño de estructuras y selección de los materiales a utilizar.
Diseño de esquemas de protección de acuerdo a las diferentes condiciones de servicio.
Formulación de recubrimientos para protección de superficies y estructuras.
Suministro de información sobre tecnología de preparación de superficies metálicas y no metálicas.
Estudio de operaciones y procesos involucrados en la preparación de pinturas y revestimientos protectores.
Preparación, a requerimiento de usuarios, de pinturas en escala de laboratorio o de planta piloto.
Normalización, en casos especiales no cubiertos por IRAM.
Formación y perfeccionamiento de personal científico calificado.
Transferencia de conocimientos a la industria, organismos estatales, universidades, etc., a través del dictado de conferencias, cursos, etc.

SERVICIOS NO CALIFICADOS

Control de calidad para la industria de pinturas (pigmentos, aceites, resinas, aditivos, etc.).
Control de calidad de pinturas, barnices y materiales para revestimiento, a requerimiento de fabricantes o usuarios.
Ensayos de resistencia a agentes corrosivos o de envejecimiento acelerado.
Control de calidad de materiales para señalización vial.
Suministro de documentación a través del servicio de repropgrafía del Centro.
Análisis de metales, cementos, cales y materiales para edificios, materiales refractarios y arcillas, minerales, etc.

ci
de
pint

Centro de Investigación y Desarrollo en Tecnología de Pinturas (CIC-CONICET)

52 entre 121 y 122
1900 La Plata (Argentina)
Teléfonos (021) 3-1141/44
(021) 21-6214
Télex: CESLA 31216 AR
FAX: 54-21-250471

Investigación y Desarrollo de pinturas anticorrosivas, antiincrustantes y productos especiales para protección industrial, en escala de laboratorio y planta piloto; estudios electroquímicos aplicados a problemas de corrosión de materiales y estructuras.

Control de calidad para la industria de pinturas y materiales afines, asesoramientos, peritajes, etc.